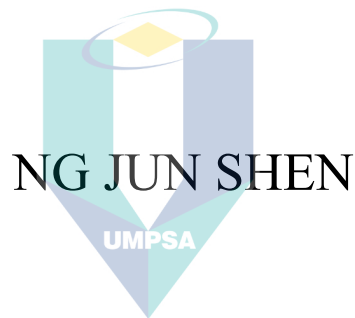


SHEAR STRENGTH OF SOFT CLAY REINFORCED WITH POLYETHYLENE TEREPHTHALATE (PET) COLUMN



اونيفرسيتي مليسيا قهغ السلطان عبدالله
UNIVERSITI MALAYSIA PAHANG
AL-SULTAN ABDULLAH

MASTER OF SCIENCE

UNIVERSITI MALAYSIA PAHANG
AL-SULTAN ABDULLAH

UNIVERSITI MALAYSIA PAHANG AL-SULTAN ABDULLAH

DECLARATION OF THESIS AND COPYRIGHT

Author's Full Name : NG JUN SHEN
Date of Birth : 17 JULY 1998
Title : SHEAR STRENGTH OF SOFT CLAY REINFORCED
WITH POLYETHYLENE TEREPHTHALATE (PET)
COLUMN
Academic Session : SEMESTER II 2023/2024

I declare that this thesis is classified as:

- ☐ CONFIDENTIAL (Contains confidential information under the Official Secret Act 1997)*
☐ RESTRICTED (Contains restricted information as specified by the organization where research was done)*
☒ OPEN ACCESS I agree that my thesis to be published as online open access (Full Text)

I acknowledge that Universiti Malaysia Pahang Al-Sultan Abdullah reserves the following rights:

1. The Thesis is the Property of Universiti Malaysia Pahang Al-Sultan Abdullah
2. The Library of Universiti Malaysia Pahang Al-Sultan Abdullah has the right to make copies of the thesis for the purpose of research only.
3. The Library has the right to make copies of the thesis for academic exchange.

Certified by:



(Student's Signature)



(Supervisor's Signature)

New IC/Passport
Number Date: 5/8/2024


Assoc. Prof. Ts. Dr Muzamir Hasan
Name of Supervisor
Date: 5/8/2024

NOTE : * If the thesis is CONFIDENTIAL or RESTRICTED, please attach a thesis declaration letter.



SUPERVISOR'S DECLARATION

I hereby declare that I have checked this thesis and in my opinion, this thesis is adequate in terms of scope and quality for the award of the degree of Master of Science.


(Supervisor's Signature)

Full Name : TS. DR. MUZAMIR BIN HASAN

Position : ASSOCIATE PROFESSOR

Date : 5/8/2024



اونيورسيتي مليسيا قهغ السلطان عبد الله
UNIVERSITI MALAYSIA PAHANG
AL-SULTAN ABDULLAH



STUDENT'S DECLARATION

I hereby declare that the work in this thesis is based on my original work except for quotations and citations which have been duly acknowledged. I also declare that it has not been previously or concurrently submitted for any other degree at Universiti Malaysia Pahang Al-Sultan Abdullah or any other institutions.

(Student's Signature)

Full Name : NG JUN SHEN

ID Number : MAG 22003

Date : 5/8/2024



اونيورسيتي مليسيا قهغ السلطان عبد الله
UNIVERSITI MALAYSIA PAHANG
AL-SULTAN ABDULLAH

SHEAR STRENGTH OF SOFT CLAY REINFORCED WITH POLYETHYLENE
TEREPHTHALATE (PET) COLUMN



Thesis submitted in fulfillment of the requirements

اونيفورسيتي مليسيا پاهانج
for the award of the degree of
Master of Science

UNIVERSITI MALAYSIA PAHANG
AL-SULTAN ABDULLAH

Faculty of Civil Engineering Technology

UNIVERSITI MALAYSIA PAHANG AL-SULTAN ABDULLAH

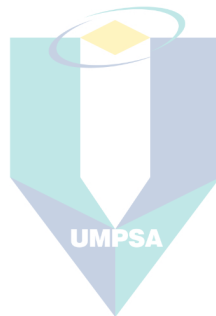
AUGUST 2024

ACKNOWLEDGEMENTS

Firstly, I would like to express my highest sincere appreciation to my supervisor, Associate Professor Ts. Dr. Muzamir Hasan for his professional guidance, evaluation, advice, comments and encouragement throughout my research. With his guidance, I was able to overcome all the encountered problems, which further enhanced my geotechnical knowledge.

Furthermore, I would like to express my gratitude to the head and lab assistant of Soil Mechanics & Geotechnics Laboratory, Mr. Ziunizan, Mr. Azmi and Mr. Haliman for assisting and providing support during my master study. Besides the lab assistance, I would also like to thank Mr. Ikramul and Mr Syamsul, PhD students who assisted me in my laboratory work and thesis.

Last but not least, I thank my family and friends who always supported me by giving encouragement and blessings throughout my study.



اونيفرسيتي مليسيا قهغ السلطان عبدالله
UNIVERSITI MALAYSIA PAHANG
AL-SULTAN ABDULLAH

ABSTRAK

Penggunaan sumber asli yang tidak terkawal dari tahun ke tahun dengan penjana sisa telah membawa kesan yang ketara kepada Bumi. Salah satu bahan kitar semula, Plastik Polietilena Tereftalat (PET) yang boeh mengakibatkan pencemaran alam sekitar telah meningkat disebabkan oleh kadar penggunaan yang banyak oleh manusia. Salah satu kaedah mampan untuk mengatasi masalah tersebut adalah menggunakan plastik PET dalam peningkatan sifat geoteknik tanah liat kaolin S300, di mana tanah liat ini lemah dari segi ciri-ciri kejuruteraan. Untuk penyelidikan ini, tujuannya adalah menyiasat penggunaan plastik PET sebagai tiang berbutir yang bertindak sebagai tetulang di bawah tanah liat kaolin lembut untuk penambahbaikan pengeksploatan tanah, pecutan pelepasan airliang dan peningkatan keupayaan galas tanah. Pembinaan tiang berbutir dipisahkan kepada dua kumpulan, kumpulan-kumpulan ini ialah lajur PET tunggal dan juga berkumpulan (terdiri daripada 3 lajur). Spesimen-spesimen ini diuji dalam model makmal yang berskala kecil. Secara khususnya, setiap kumpulan tiang PET yang terdiri daripada dua diameter yang dicadangkan iaitu 10 mm dan 16 mm. Sebelum menjalankan ujian Ujikaji Mampatan Tak Berkurung (UCT) dan Tidak Disatukan Tidak Salir (UU), parameter-parameter lajur ini telah ditentukan terlebih dahulu termasuklah Nisbah Penggantian Kawasan (A_c/A_s), Nisbah Penembusan Lajur (H_c/H_s), Nisbah Ketinggian Lajur kepada Diameter Lajur (H_c/D_c) dan Nisbah Penggantian Isipadu (V_c/V_s). Daripada jumlah 52 spesimen bertetulang PET tanah liat kaolin, setiap spesimen mempunyai diameter 50 mm dan ketinggian 100 mm dengan reka bentuk lajur PET yang berbeza manakala spesimen tidak bertetulang adalah sebagai sampel kawalan. Daripada keputusan UCT, lajur PET tunggal yang mempunyai diameter 16 mm dan 1.0 H_c/H_s atau 10.24 A_c/A_s telah mencatatkan peningkatan kekuatan ricih terbesar, 56.53%. Bagi lajur PET berkumpulan, peningkatan kekuatan ricih terbesar dicatatkan ialah 48.24% yang mempunyai 12.00 A_c/A_s dan 1.0 H_c/H_s . Keputusan ujian UU yang dijalankan dalam tekanan kurungan bebezanya dengan 100kPa, 200kPa dan 400kPa telah menunjukkan bahawa 200kPa mencatatkan peningkatan tegasan penyimpang maksimum tertinggi untuk kategori tunggal dan kumpulan, 94.48% dan 86.21%. Semua spesimen ini mempunyai 0.8 H_c/H_s . Untuk peningkatan kohesi, trend adalah sama dengan parameter kekuatan ricih, iaitu 0.8 H_c/H_s bagi kedua-dua kategorinya yang menunjukkan peningkatan terbesar, mencatatkan 21.80% dan 35.78% manakala bagi peningkatan sudut geseran, julatnya dalam lingkungan 3.33 – 13.33% untuk lajur PET tunggal dan 4 – 10.67% untuk lajur PET berkumpulan. Selaras dengan itu, penggunaan bahan PET telah berjaya membuktikan bahawa bahan kitar semula ini merupakan bahan yang berpotensi untuk menggantikan tanah yang tidak boleh diperbaharui. Pembinaan PET tunggal dan berkumpulan memperbetulkan sifat kejuruteraan tanah liat kaolin dengan menambah baik parameter kekuatan ricih yang telah direkodkan dalam tekanan mampatan tak berkurung, kohesi dan sudut geseran tanah. Pendek kata, peningkatan tanah liat kaolin menghasilkan keupayaan untuk menahan kenakan beban yang lebih besar.

ABSTRACT

The unregulated usage of natural resources from years to years with the generation of waste has brought significant adverse effects on the Earth. One of the recycling materials, Polyethylene Terephthalate (PET) plastic which can lead to environmental pollution has been seen increasing due to the large consumption of this material by humans. One of the sustainable methods to overcome the problem is to utilize the PET plastic in the geotechnical property enhancement of kaolin clay S300, where this soil is weak in terms of its engineering characteristic. For this research, the aim was to investigate the use of PET plastic as granular columns beneath the soft kaolin clay acting as a reinforcement for the improvement of soil settlement, acceleration of pore water dissipation and increase of soil bearing capacity. The granular column construction was separated into two groups, which were single and group PET columns (consist of 3 columns). The specimens were tested in a small-scale laboratory model. Specifically, each group of PET column consists of two proposed diameters which are 10 mm and 16 mm. Before conducting the Unconfined Compression Test (UCT) and Unconsolidated Undrained (UU), the column parameters included the Area Replacement Ratio (A_c/A_s), Column Penetrating Ratio (H_c/H_s), Column Height to Column Diameter Ratio (H_c/D_c) and Volume Replacement Ratio (V_c/V_s) were first identified. From the total of 52 kaolin clay PET-reinforced specimens, each of the specimens had 50 mm diameter and 100 mm height with different PET column design while the unreinforced specimen was treated as a control sample. From the UCT results, the single PET column, the column with 16 mm diameter and 1.0 H_c/H_s or 10.24 A_c/A_s showed the largest shear strength improvement, which recorded 56.53%. For group PET columns, the largest shear strength improvement recorded was 48.42% which had 12.00 A_c/A_s and 1.0 H_c/H_s . The UU test results which obtained from different confining pressures with 100kPa, 200kPa and 400kPa had shown that the 200kPa recorded the maximum deviator stress improvement for single and group category, recorded 94.48% and 86.21% respectively and these specimens were all had 0.8 H_c/H_s . For cohesion improvement, the trend was the same to previous shear strength parameters, 0.8 H_c/H_s for both single and group category showed the largest improvement, recorded 21.80% and 35.78% respectively while for friction angle improvement, the range was within 3.33 – 13.33% for single PET column and 4 – 10.67% for group PET columns. Coherent to that, the use of PET material had successfully proven this recycling material was a potential material for the substitution of non-renewable soil. The installation of single and group PET columns rectified the engineering properties of the kaolin clay soil by improving the shear strength parameters which was recorded in its unconfined compression stress, cohesion and soil friction angle. In short, the strength improvement of the kaolin clay soil resulted for the capability in withstanding the larger applied loads.

TABLE OF CONTENT

DECLARATION

TITLE PAGE

ACKNOWLEDGEMENTS ii

ABSTRAK iii

ABSTRACT iv

TABLE OF CONTENT v

LIST OF TABLES x

LIST OF FIGURES xi

LIST OF SYMBOLS xiv

LIST OF ABBREVIATIONS xvi

CHAPTER 1 INTRODUCTION 1

1.1 Background of Research 1

1.2 Problem Statement 3

1.3 Research Objectives 5

1.4 Scope of Research 5

1.5 Research Significance 6

1.6 Thesis Organisation 7

CHAPTER 2 LITERATURE REVIEW 8

2.1 Introduction 8

2.2 Sustainable Construction 8

2.3 Soft Clay Soil 11

2.3.1 Compressibility and Compression 13

2.3.2 Undrained Shear Strength 17

2.4 Kaolinite 19

| | | |
|------------------------------|---|-----------|
| 2.5 | Plastic Industry | 19 |
| 2.5.1 | Polyethylene Terephthalate (PET) Plastic | 23 |
| 2.5.2 | Polyethylene Terephthalate (PET) Utilization | 26 |
| 2.5.3 | Physical Properties of Polyethylene Terephthalate (PET) | 29 |
| 2.5.4 | Mechanical Properties of Polyethylene Terephthalate (PET) | 38 |
| 2.5.5 | Morphological Characteristics of Polyethylene Terephthalate (PET) | 43 |
| 2.6 | Ground Improvement | 45 |
| 2.7 | Stone Column | 47 |
| 2.7.1 | Physical Modelling of Stone Columns | 51 |
| 2.7.2 | Failure Mechanism of Stone Column | 53 |
| 2.7.3 | Undrained Shear Strength of Reinforced Clay | 59 |
| 2.7.4 | Critical Column Length | 61 |
| 2.8 | The Use of Correlation Technique in Shear Strength Parameters | 62 |
| 2.9 | Research Gap | 62 |
| CHAPTER 3 METHODOLOGY | | 64 |
| 3.1 | Introduction | 64 |
| 3.2 | Selection of Ground Improvement Technique | 66 |
| 3.3 | Selection of Materials | 67 |
| 3.4 | Determination of Physical, Mechanical and Morphological Properties of the Materials | 68 |
| 3.4.1 | Atterberg Limit | 69 |
| 3.4.2 | Particle Size Distribution | 70 |
| 3.4.3 | Compaction Test | 72 |
| 3.4.4 | Specific Gravity | 73 |
| 3.4.5 | Permeability | 74 |

| | | |
|---|--|-----------|
| 3.4.6 | One Dimensional Consolidation Test | 74 |
| 3.4.7 | Direct Shear Test | 75 |
| 3.4.8 | Relative Density | 76 |
| 3.4.9 | Scanning Electron Microscope (SEM) | 77 |
| 3.5 | Determination of Shear Strength Parameters of the Material | 77 |
| 3.5.1 | Unconfined Compression Test (UCT) | 78 |
| 3.5.2 | Unconsolidated Undrained (UU) Triaxial Test | 79 |
| 3.6 | Design of Polyethylene Terephthalate Column Model | 82 |
| 3.6.1 | Sample Preparation | 82 |
| 3.6.2 | Polyethylene Terephthalate Column Installation | 83 |
| 3.6.3 | Detailed Arrangement for PET Column | 85 |
| 3.7 | Summary of Methodology | 87 |
| CHAPTER 4 RESULTS AND DISCUSSION | | 88 |
| 4.1 | Introduction | 88 |
| 4.2 | Engineering Properties of Materials | 88 |
| 4.2.1 | Particle Size Distribution | 90 |
| 4.2.2 | Atterberg Limit | 92 |
| 4.2.3 | Relative Density | 93 |
| 4.2.4 | Specific Gravity | 94 |
| 4.3 | Mechanical Properties | 95 |
| 4.3.1 | Compaction | 95 |
| 4.3.2 | Permeability | 97 |
| 4.3.3 | One Dimensional Consolidation Test | 99 |
| 4.4 | Undrained Shear Strength | 100 |
| 4.4.1 | Direct Shear Test | 100 |

| | | |
|-------------------|---|------------|
| 4.5 | Morphological Characteristics | 101 |
| 4.6 | Soft Kaolin Clay Reinforced with Single and Group PET Column | 103 |
| 4.6.1 | Unconfined Compression Test (UCT) | 103 |
| 4.6.2 | Effect of Area Replacement Ratio | 106 |
| 4.6.3 | Effect of Column Penetration Ratio | 108 |
| 4.6.4 | Effect of Volume Replacement Ratio | 110 |
| 4.6.5 | Unconsolidated Undrained (UU) Triaxial Test | 111 |
| 4.6.6 | Correlation of Cohesion and Friction Angle with Column Parameters | 119 |
| 4.7 | Summary of Results and Discussion | 132 |
| CHAPTER 5 | CONCLUSIONS | 133 |
| 5.1 | Introduction | 133 |
| 5.2 | Conclusion | 133 |
| 5.3 | Recommendation for Future Study | 135 |
| REFERENCES | | 137 |
| APPENDIX A | SIEVE ANALYSIS RESULT | 153 |
| APPENDIX B | HYDROMETER TEST RESULT | 154 |
| APPENDIX C | ATTEBERG LIMIT TEST RESULT | 155 |
| APPENDIX D | RELATIVE DENSITY TEST RESULT | 156 |
| APPENDIX E | SPECIFIC GRAVITY TEST RESULT | 158 |
| APPENDIX F | STANDARD COMPACTION TEST RESULT | 159 |
| APPENDIX G | FALLING HEAD TEST RESULT | 161 |
| APPENDIX H | CONSTANT HEAD TEST RESULT | 162 |
| APPENDIX I | ONE CONSOLIDATION DIMENSIONAL TEST RESULT | 163 |
| APPENDIX J | DIRECT SHEAR TEST | 167 |

| | |
|--|------------|
| APPENDIX K UNCONFINED COMPRESSION TEST | 170 |
| APPENDIX L UNCONSOLIDATED UNDRAINED TRIAXIAL TEST | 172 |



اونيفرسيتي مليسيا قهغ السلطان عبدالله
UNIVERSITI MALAYSIA PAHANG
AL-SULTAN ABDULLAH

LIST OF TABLES

| | | |
|------------|--|-----|
| Table 2.1 | Typical values for the coefficient of volume compressibility | 13 |
| Table 2.2 | Typical values of the coefficient of consolidation (C_v) | 16 |
| Table 2.3 | Typical values of the soil's undrained shear strength (C_u) | 17 |
| Table 2.4 | Categories of plastic | 21 |
| Table 2.5 | Key data of Malaysia's plastic industry | 22 |
| Table 2.6 | The properties of PET plastic | 24 |
| Table 2.7 | Plastic Production by Plastic Category in Malaysia | 25 |
| Table 2.8 | Sieve analysis of various PET aggregates Error! Bookmark not defined. | |
| Table 2.9 | Specific gravity of PET plastic from previous works | 36 |
| Table 2.10 | Geotechnical properties of PET plastic blends | 37 |
| Table 2.11 | Optimum moisture content and maximum dry density of mixture of PET plastic with subbase soil from compaction test | 39 |
| Table 2.12 | Results of permeability of PET plastic from previous research works | 42 |
| Table 2.13 | Comparison of porosity and water contact angle of the membrane from PET bottle and those from PET resin without additive | 44 |
| Table 2.14 | Ground improvement techniques, functions and methods | 45 |
| Table 2.15 | Classification of ground improvement techniques based on type of soils | 46 |
| Table 3.1 | Test standard with methods for the kaolin clay S300 and PET | 68 |
| Table 3.2 | Sample of coding and testing programme of UU triaxial tests for unreinforced clay and clay reinforced with PET column | 81 |
| Table 3.3 | Density of various dimensions of PET columns installed in kaolin specimens | 85 |
| Table 4.1 | Engineering properties of PET and kaolin clay S300 | 89 |
| Table 4.2 | Comparison between the PET specific gravity by different researchers | 94 |
| Table 4.3 | Comparison between maximum dry density and optimum moisture content by different researchers | 96 |
| Table 4.4 | The permeability result of PET by constant heat test | 97 |
| Table 4.5 | The permeability result of kaolin clay S300 by falling heat test | 98 |
| Table 4.6 | Effect of fully penetrating column towards the clay undrained shear strength | 108 |
| Table 4.7 | The cohesion and friction angle value with their improvement rate | 112 |

LIST OF FIGURES

| | | |
|-------------|---|----|
| Figure 1.1 | Waste and plastic waste statistics at the national level in 2014 | 2 |
| Figure 2.1 | The aspects of sustainable development in the construction industry | 11 |
| Figure 2.2 | Flow chart of plastic recycling in Malaysia | 20 |
| Figure 2.3 | Annual global plastic production, 1950 – 2015 (million tonnes) | 21 |
| Figure 2.4 | Global use of PET packaging in 2010 (excluding fibre) | 27 |
| Figure 2.5 | PET recycling and PET material utilization ratio | 27 |
| Figure 2.6 | Recycled plastic used in different field | 28 |
| Figure 2.7 | Particle size distribution of PET plastic | 30 |
| Figure 2.9 | Grain size distribution curves PET fragments and fine sand | 32 |
| Figure 2.9 | Variation of friction angle with percentage of PET waste for sand | 34 |
| Figure 2.10 | Variation of cohesion with percentage of PET waste for sand | 35 |
| Figure 2.11 | Standard and Modified Proctor compaction curves of the soil | 41 |
| Figure 2.12 | SEM photomicrograph of the cross section of the PET membranes bottle and PET resin with magnification of 1000 | 44 |
| Figure 2.13 | SEM photomicrograph of the cross section of the PET membranes bottle and PET resin with magnification of 5000 | 44 |
| Figure 2.14 | Effectiveness of Ordinary Stone Column (OSC) and Encased Stone Column (ESC) on underlying foundation soil | 48 |
| Figure 2.15 | Schematic diagram of installing vibro stone column using dry bottom-feed method | 50 |
| Figure 2.16 | Single and group stone columns under different type of situation | 54 |
| Figure 2.17 | Failure mechanism of single stone column in a homogeneous soft layer | 55 |
| Figure 2.18 | Modes of failure mechanism develop in group of stone columns | 56 |
| Figure 2.19 | Photographs of deformed sand columns exhumed at the end of the footing penetration | 57 |
| Figure 2.20 | Photographs of group of sand columns beneath the strip footings | 58 |
| Figure 2.21 | Typical loading configurations for single and group columns in clay | 58 |
| Figure 2.22 | Design chart for stone columns | 59 |
| Figure 3.1 | Flow chart for methodology process | 65 |
| Figure 3.2 | The raw materials for geotechnical testing | 67 |
| Figure 3.3 | Cone penetrometer test | 70 |
| Figure 3.4 | Hydrometer Apparatus | 72 |

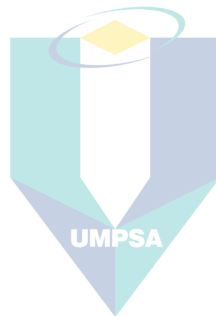
| | | |
|-------------|--|-----|
| Figure 3.5 | Standard Proctor compaction test | 73 |
| Figure 3.6 | One dimensional consolidation test equipment | 75 |
| Figure 3.7 | Direct shear test equipment | 76 |
| Figure 3.8 | Scanning Electron Microscope model ZEISS EVO 50 | 77 |
| Figure 3.9 | Unconfined compression test (UCT) on kaolin specimen | 79 |
| Figure 3.10 | Specimen was placed on the platform carefully | 80 |
| Figure 3.11 | Soil specimens inside the triaxial chamber | 81 |
| Figure 3.12 | Soft kaolin clay preparation process | 83 |
| Figure 3.13 | Preparation of PET column | 84 |
| Figure 3.14 | Reinforced kaolin sample with PET | 86 |
| Figure 3.15 | Detailed column arrangement for single and group PET column installed in clay specimens | 87 |
| Figure 4.1 | Particle distribution of PET plastic | 91 |
| Figure 4.2 | Particle distribution of kaolin clay 300 | 91 |
| Figure 4.3 | Penetration against moisture content | 92 |
| Figure 4.4 | Location of kaolin clay based on the USCS chart | 93 |
| Figure 4.5 | Relationship between dry density and moisture content of kaolin S300 | 97 |
| Figure 4.6 | Void ratio against the applied pressure of kaolin S300 | 100 |
| Figure 4.7 | Maximum shear stress against the normal stress | 101 |
| Figure 4.8 | PET plastic at 35 X magnification | 102 |
| Figure 4.9 | PET plastic at 1000 X magnification | 103 |
| Figure 4.10 | PET plastic at 2000 X magnification | 103 |
| Figure 4.11 | Result of Unconfined Compression Test | 104 |
| Figure 4.12 | Maximum deviator stress and the axial strain values obtained from UCT | 105 |
| Figure 4.13 | Shear strength improvement versus area replacement ratio | 107 |
| Figure 4.14 | Effect of height over column diameter towards the shear strength improvement | 109 |
| Figure 4.15 | Shear strength improvement against height penetration ratio for single and group PET column | 110 |
| Figure 4.16 | Shear strength improvement against volume replacement ratio for single and group PET column | 111 |
| Figure 4.17 | Maximum deviator stress and axial strain recorded at failure mode | 115 |
| Figure 4.18 | Maximum deviator stress versus average axial strain for single PET column with 10 mm and 16 mm diameter at 100kPa confining pressure | 116 |

| | | |
|-------------|--|-----|
| Figure 4.19 | Maximum deviator stress versus average axial strain for single PET column with 10 mm and 16 mm diameter at 200kPa confining pressure | 116 |
| Figure 4.20 | Maximum deviator stress versus average axial strain for single PET column with 10 mm and 16 mm diameter at 400kPa confining pressure | 117 |
| Figure 4.21 | Maximum deviator stress versus average axial strain for group PET columns with 10 mm and 16 mm diameter at 100kPa confining pressure | 118 |
| Figure 4.22 | Maximum deviator stress versus average axial strain for group PET columns with 10 mm and 16 mm diameter at 200kPa confining pressure | 118 |
| Figure 4.23 | Maximum deviator stress versus average axial strain for group PET columns with 10 mm and 16 mm diameter at 400kPa confining pressure | 119 |
| Figure 4.24 | Correlation of cohesion improvement versus column penetrating ratio for single PET column | 121 |
| Figure 4.25 | Correlation of cohesion improvement versus column penetrating ratio for group PET columns | 122 |
| Figure 4.26 | Correlation of friction angle improvement versus column penetrating ratio for single PET column | 123 |
| Figure 4.27 | Correlation of friction angle improvement versus column penetrating ratio for group PET columns | 124 |
| Figure 4.28 | Correlation of cohesion improvement versus column height over column diameter ratio for single PET column | 125 |
| Figure 4.29 | Correlation of cohesion improvement versus column height over column diameter ratio for group PET columns | 126 |
| Figure 4.30 | Correlation of friction angle improvement versus column height over column diameter ratio for single PET column | 127 |
| Figure 4.31 | Correlation of friction angle improvement versus column height over column diameter ratio for group PET columns | 128 |
| Figure 4.32 | Correlation of cohesion improvement versus volume replacement ratio for single PET column | 129 |
| Figure 4.33 | Correlation of cohesion improvement versus volume replacement ratio for group PET columns | 130 |
| Figure 4.34 | Correlation of friction angle improvement versus volume replacement ratio for single PET column | 131 |
| Figure 4.35 | Correlation of friction angle improvement versus volume replacement ratio for group PET columns | 132 |

LIST OF SYMBOLS

| | |
|----------|---|
| A_c | Area of polyethylene terephthalate column |
| A_s | Area of kaolin clay sample |
| α | Alpha |
| a_v | Compression factor |
| c | Cohesion |
| C_u | Undrained shear strength |
| C_v | Coefficient of consolidation |
| D_r | Relative density |
| e | Void ratio |
| g/cm^3 | Gram per cubic centimetre |
| G_s | Specific gravity |
| H_c | Height of polyethylene terephthalate column |
| H_s | Height of kaolin clay sample |
| I_p | Plasticity index |
| k | Permeability |
| kJ/m^2 | Kilojoule per square metre |
| kN | Kilo Newton |
| kN/m^2 | Kilo Newton per square metre |
| kN/m^3 | Kilo Newton per cubic metre |
| kPa | Kilo Pascal |
| L | Length of column |
| mm | Millimetre |
| μm | Micrometre |
| MPa | Mega Pascal |
| m_v | Coefficient of volume compressibility |
| q_u | Unconfined compressive strength |
| S_t | Sensitivity |
| S_u | Undrained shear strength |
| V_c | Volume of polyethylene terephthalate column |
| V_s | Volume of kaolin clay sample |
| w | Moisture content |
| w_L | Liquid limit |
| w_P | Plastic limit |
| S_u | Undrained shear strength |

| | |
|-----------------|------------------------------|
| ρ_d | Dry density |
| $\rho_{d(max)}$ | Maximum dry density |
| γ | Gamma |
| γ | Unit weight |
| γ_{min} | Minimum unit weight |
| γ_{max} | Maximum unit weight |
| ϕ | Angle of shearing resistance |
| % | Percent |
| ° | Degree |
| °C | Degree Celsius |



اونيفرسيتي مليسيا قهغ السلطان عبدالله
UNIVERSITI MALAYSIA PAHANG
AL-SULTAN ABDULLAH

LIST OF ABBREVIATIONS

| | |
|--------|--|
| AASHTO | American Association of State Highway and Transportation Officials |
| ABS | Acrylonitrile butadiene-styrene |
| ASTM | American Society for Testing and Material |
| BAC | Bituminous Asphaltic Concrete |
| BS | British Standards |
| ESC | Encased Stone Column |
| GDP | Gross Domestic Product |
| GGBS | Ground Granulated Blast-furnace Slag |
| HDPE | High Density Polyethylene |
| ISO | International Organization for Standardization |
| IUSS | International Organization for Standardization |
| LL | Liquid Limit |
| MDD | Maximum Dry Density |
| MPMA | Malaysian Plastic Manufacturers Association |
| MPW | Mismanaged Plastic Waste |
| OECD | Organisation for Economic Co-operation and Development |
| OMC | Optimum Moisture Content |
| OSC | Ordinary Stone Column |
| PC | Polycarbonate |
| PCA | Plastic Concrete Aggregate |
| PET | Polyethylene Terephthalate |
| PI | Plasticity Index |
| PL | Plastic Limit |
| PP | Polypropylene |
| PS | Polystyrene |
| PVC | Polyvinyl Chloride |
| SEM | Scanning Electron Microscope |
| SRR | Settlement Reduction Ratio |
| UCT | Unconfined Compression Test |
| USCS | Unified Soil Classification System |
| USDA | United States Department of Agriculture |

CHAPTER 1

INTRODUCTION

1.1 Background of Research

The world population has always been an issue to be discussed as the increase in population will increase the demand for land for human activities especially the rapid urban expansion and population growth since the 1970s (Jun Shen et al., 2024; Zhang et al., 2023). Population growth is a sign that the productivity of work will continue to proceed as usual, particularly playing an important role for a developing country to transform to a developed country for instance Germany. The practice of sustainable development is one of the considerations to cater the outburst of population growth around the world since the last century, and it reduces the negative impact to the environment at the same time fulfilling the human needs (Hasan et al., 2021; Zhang et al., 2023). The land demand for human activities always have the dire consequences on the natural resources and environment, which have caused the destruction of flora and fauna, disposal of waste from the construction site, and other potential environmental issues. (Zhang et al., 2023). Clearing of forest to obtain a bare land to meet the needs of humans that speeds up the deforestation process has caused global warming to get serious from year to year. The issue of global warming is seen as a huge challenge, and it is also a potential risk to kill humanity from the Earth (Rehman et al., 2021).

Since the invention of plastic, it has become one of the most abundant disposal items around the world as its advantages have caused humans to dispose of plastic easily. Malaysia is seen to be a country with a higher amount of plastic usage, and this can be noticed through the usage of plastic-made items like plastic bottles with bags. Plastic is the third highest waste generated in Malaysia and other developing countries (Hoornweg & Bhada-Tata, 2015; Letcher & Vallero, 2019). Plastic production is a famous business in Malaysia, and 24 listed companies on Bursa Malaysia with related business to packaging material, while the overall plastic companies available in our country have approximately 750 members registered in the Malaysian Plastic Manufacturers Association (MPMA). Some famous plastic producers available in Malaysia like Lam Seng Industries Sdn Bhd, Nam Keong Sdn Bhd, and Sonyu Plastic Industries Sdn Bhd manufacturers are famous for making quality plastic that are catered

for commercial purpose including PP plastic in kitchenware, PET plastic in beverage bottle, and others different type of plastic being produced from these manufactures. Generally, these plastic-made items are to be used once and will be either recycled or disposed directly. From Figure 1.1(a), the plastic waste generated in Malaysia had reached an amount of 1.9 million tonnes, while the municipalsolid waste generated recorded 13.0 million tonnes in 2014 while Figure 1.1(b) shows the way in managing the plastic disposal wastes. Although the plastic generation is only 1.9 million tonnes or 12.75% generated, however, this issue has caught global attention regarding plastic pollution (Hasan et al., 2021). Thus, it plays a crucial role in utilizing these plastics again, as the unspecified percentage has occupied more than 50% signifying that the final location of these plastics remains unknown.

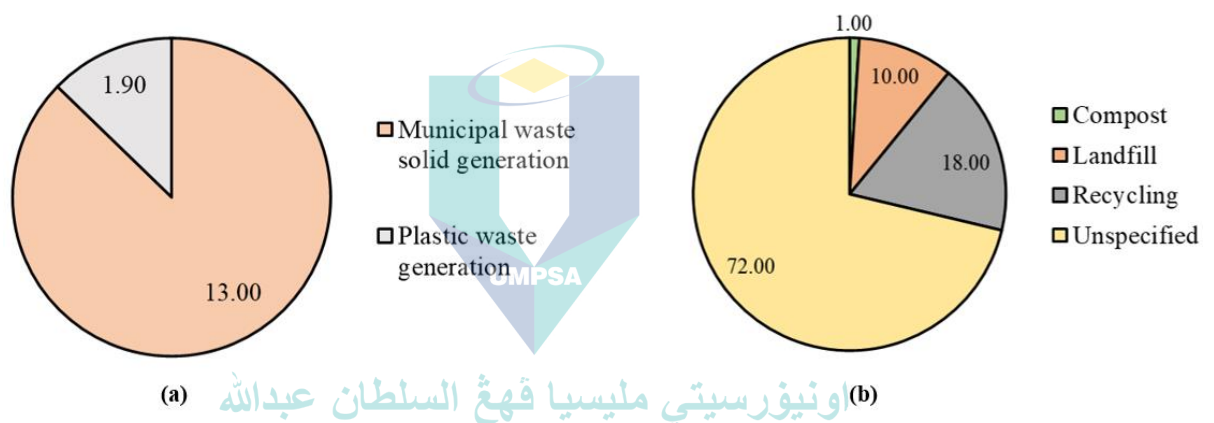


Figure 1.1 Waste and plastic waste statistics at the national level in 2014
 (a)Municipal and plastic waste generation (in million tonnes) (b)Method of plastic waste management (in percentage)

Source: Organisation for Economic Co-operation and Development (2022)

In recent years, the 3R concept, recycling, reuse and reduce, and sustainability construction have been the hot issues to be debated when dealing with environmental considerations. According to the Green Technology Master Plan Malaysia by the

Ministry of Energy, Green Technology and Water in 2017, the existing initiative to evaluate the greenery of a structure includes Green Building Design such as Green Building Rating Tools, Sustainable Construction Practices, and Green Building Design KeTTHA (2017).

In regard to the above issue, professional teams have started to conduct their study according to relevant issues to become more conscious especially when constructing a building, clearing land, and replanting of plants, and different measures have continuously appeared on the news to raise the awareness of humans. According to Cai & Waldmann (2019), “Sustainability” is one of the most concerning words to human society worldwide at present, which significantly affects human activities and the earth's environment. Previous studies had also concluded that plastic is appropriate for construction civil engineering fields such as geotechnical engineering to treat the problematic clay soil issue. PET fibre had been replaced for coarse aggregate and recorded to have increased the soil friction angle and cohesion of soil (Hernández & Botero, 2020) and the Polypropylene (PP) plastic material as a sustainable material for the substitution of sand and gravel (Hasan et al., 2021). Hence, the utilization of plastic such as PET by replacing the conventional coarse aggregate such as sand has the potential to enhance the engineering properties of soil. Through the analysis of shear strength parameters that include the shear strength, soil cohesion, and friction angle value, and coherently, the PET expects to assist the soil in raising the strength value.

1.2 Problem Statement

Kaolin clay is a problematic soil and from its general properties, it is a type of soil having high porous water pressure and is highly compressible (Zaini & Hasan, 2023). The engineering properties of kaolin clay is interpreted as when the force is applied to the soil, water will be drained out from the soil and deform from its original shape. While in Malaysia, the soft clay soil which comprises of clayey silts which have higher moisture content and undrained shear strength of 8 to 11kPa (Aljanabi et al.,

2013). Due to the adverse nature of the clay, researchers have been continuously inventing new technologies and methods to get rid of these properties so that the problematic soil can be used by improving its strength.

Besides, over the past few decades, PET plastic consumption has recorded a faster growth trend due to the increase of PET plastic bottles in the market (Esfandiari et al., 2012), which are linked to human activities which include construction, industrialization, and urbanization process. As Malaysia keeps on developing, the demand for land has been increasing after independence for various purposes. According to the 10th and 11th Malaysia Plans between 2011-2015 and 2016-2020, the plans emphasized providing affordable houses to our people from poor to middle-income households by practicing sustainable concepts in development and hence, the land demand is expected to increase though for the land which contains a higher proportion of clay. Thus, these activities are expected to generate plastic which will then settle in the recycling centre and provide more opportunities for the researchers to utilize it for civil engineering applications like the enhancement of soil and concrete strength, meanwhile reducing the plastic waste as discussed in Figure 1.1.

In regard to that, the physical mechanical and morphological properties of soft clay are required to determine. In regard to the sustainable construction concept in catering the land that contains a high proportion of clay, the replacement of conventional coarse aggregates with other materials such as PET and PP plastic to treat the kaolin clay is appropriate and coherent with the engineering properties (Ferreira et al., 2021; Murthi et al., 2020). Referring to the previous data about the substitution of coarse aggregate using sustainable materials in enhancing the engineering properties of kaolin clay. Therefore, it is now drawing the attention from the related parties such as developers and researchers to design the buildings by using the appropriate ground improvement and soil stabilization techniques to strengthen the shear strength parameters of soil. Through the execution of relevant testing such as Unconfined Compression Test (UCT) and Unconsolidated Undrained (UU) test, the values are

accessed in terms of shear strength, soil cohesion, and soil friction angle with the assistance of correlation technique to streamline the complexity of data (Hasan et al., 2021; Syamsul et al., 2023). Coherent to that, it can be incorporated with the relevant techniques such as stone column method to improve the soft clay properties.

1.3 Research Objectives

The research is aimed to investigate the performance of the PET columns through the improvement of its shear strength and compressibility of the soft reconstituted kaolin clay. Hence, the objectives for the study are to be carried out accordingly and they are as follows.

1. To identify the kaolin clay and polyethylene terephthalate (PET) plastic in terms of its physical, mechanical and morphological characteristic.
2. To access the shear strength parameters of kaolin clay with kaolin clay reinforced with single and group polyethylene terephthalate (PET) column.
3. To correlate shear strength parameters of soft clay reinforced with various dimensions of single and group polyethylene terephthalate (PET) column at different effective confining pressure

1.4 Scope of Research

In this research, it was focused on improving the shear strength of kaolin clay by using the PET sand. Prior to assessing the shear strength parameters of kaolin clay reinforced with single and group PET columns, the engineering properties of both materials were analysed through necessary testing. Furthermore, the use of stone column technique in small-scale model tests which is practical and appropriate were performed to determine the undrained shear strength and effective shear strength parameters of soft clays from the relevant geotechnical tests by altering the variables such as the applied load and effective confining pressure. The research considered the diameter of the PET column, the height of the column, area replacement ratio, height

penetrating ratio, and the ratio of height to diameter of the column.

All the related required works were carried out in the Soil Mechanic and Geotechnical Laboratory, Faculty of Civil Engineering Technology (FTKA), Universiti Malaysia Pahang Al-Sultan Abdullah (UMPSA) by following the American Society for Testing and Materials (ASTM) and British Standard (BS). The details of the laboratory works were referred to Chapter 3.

1.5 Research Significance

This study was carried out to understand the properties of soft clay like bearing capacity and compressibility, and the use of PET plastic as a substituent in stone columns to prevent the failure of the foundation system. Substituting unwanted plastic such as PET plastic can also reduce the unwanted disposal of plastic that can further cause pollution to the environment. The stabilization of expansive soft clay with PET bottle strips is a reliable method for the improvement of the volume fluctuation issue of clay and the protection of the environment from the disposal of PET plastic (Kassa et al., 2020).

The use of PET plastic that substituted in the design of the column increased the cohesion of pure clay from 5 kN/m^2 to 17.5 kN/m^2 at the same time increasing the angle of internal friction, ϕ from 3° to 19° (Manuel & Joseph, 2014). By applying the ground improvement technique, the stone columns that were constructed with PET plastic can lead to the increment of shear strength of the soft clay. Geotechnical engineers can further improve the design of a foundation system when having construction on soft clayey land by mixing a certain percentage of PET plastic as a substituent material. This study presented the results with the effect of reinforced PET columns of its strength towards the highly compressible soft clayey soil where it reviews the performance of this design. Furthermore, the confining pressure is one of the considered parameters to be analysed as its effect on the PET columns, shear strength, and the compressibility of soft clay was important to analyse the performance of the overall design. The relevant

chart, figure and table were created to support the analysis of the PET plastic in improving the shear strength of the soft clay soil.

1.6 Thesis Organisation

Chapter 1 discussed the research background with the issue of soft clay for construction purposes. It leads to the research objectives, scope and experimental problems of the study.

Chapter 2 focused on literature review of the study background, the previous research conducted by previous researchers about the ground improvement techniques, properties of clay and PET plastic, and their applications toward the construction industry.

Chapter 3 presented the research methodology where it mainly comprised the laboratory experiment setups with its procedures. The installation of soft clay reinforced with PET columns were presented in terms of its detailed columns arrangement where they separated into single and group columns and the size of designed geometries were analysed to determine their shear strength and compressibility in this chapter.

Chapter 4 comprised the results obtained from the laboratory works. Discussion with related diagrams, tables, and graphs were shown in this chapter.

Chapter 5 presented the conclusions of the research and the recommendation for future related field research as well as the expected outcomes that were obtained during the entire study.

CHAPTER 2

LITERATURE REVIEW

2.1 Introduction

This chapter reviewed the importance of sustainable development in the construction industry, and it was followed by the review of soft clay soil and the plastic industry within Malaysia and international. Specifically, the physical and mechanical of the soft clay soil and PET plastic were reviewed, and the morphological characteristic was only reviewed for the PET plastic. Apart from that, the shear strength parameters were being reviewed such as the undrained shear strength, using the conventional and sustainable materials in the ground improvement technique. Furthermore, the review of the technique was focused on the utilization of single and group granular columns beneath the soft clay soil, and the effect of the column parameters such as the critical column length in affecting the entire performance of the installed granular columns.

2.2 Sustainable Construction

The slow improvement in the ground improvement technique has successfully brought up the use of different materials to be substituted in stone columns such as bottom ash and plastic material to achieve a better sustainable construction based on the concept as shown in Figure 2.1. Using either bottom ash or other possible disposal waste is particularly saving the Earth through the utilization of this unwanted waste to an improvement field in civil engineering. Choosing the right ground improvement method is important for construction activities in heavily populated areas that cover a large part of the surface of the earth. Referring to Figure 2.1, while enhancing the buildability of a structure, sustainability which comprises environmental protection, social well-being,

and economic prosperity are important issues to be practiced for the entire construction process, even after the construction process. It is very important to know the condition of the soil when bringing the aspect of sustainability, so that a good improvement technique can be appropriately applied by mixing the selected material with the soil to achieve the target of increasing ground-bearing capacity, improving the stability of ground and the most important aspect is to reduce the ground settlement. Considering pollution control, material selection, safety issues, legislation, and so on as mentioned in Figure 2.1 can also increase the Green Building Index during the evaluation process.

From the scope of engineering studies, constructing a safe structure is the most fundamental idea that covers the ability to provide shelter to the residents of that building, and thus, the basic concept of the soil below the structure plays a critical part since it determines the structure is safe or dangerous towards the resident upon the completion of the project. Before a construction project begins, the engineering properties of the soil should be known by obtaining the soil from the respective site so that further analysis can be carried out then only bringing in the concept of sustainability, choosing the best material to use for the structure. From the concept of sustainability links with construction, improving the quality of life within the earth's carrying capacity to ensure equity within the current generation and between the present and future generations is the main focus of sustainability (Zhang et al., 2023).

The accumulation of mismanaged plastic waste (MPW) in the environment is a global growing concern (Lebreton & Andrady, 2019). Different types of plastics and where they are commonly found in the disposal waste include PET, High-Density Polyethylene (HDPE or 2 HDPE), and Polypropylene (PP or 5 PP). PET plastic products are commonly seen from the PET plastic bottles and by using them, this waste can be converted to an effective application where it achieves the cost-effective target with an environmental-friendly concept having a great impact on the environment. Using PET plastic can potentially show a better improvement from its properties in substituting it as a material in the stone column when it's inserted in a soft clayey ground. While for

PET application especially in concrete and adobe walls, PET bottles are frequently used as filler, as in the Philippines, San Salvador, Nigeria, Honduras, Guatemala, and other places (Nováková et al., 2013).

Generally, lighter, more durable, and less expensive plastics have replaced metal and even wood in building applications that account for about 20% of global production (Baierl & Bogner, 2021). From Figure 2.1, the sustainability diagram elaborates the importance of sustainability especially for those developing country for instance Malaysia, as the sustainable development emphasizes on the Environment (E), Social (S) and Governance (G) which concern all aspects as reported by the previous researchers (Li et al., 2021; Nazirah Zainul Abidin, 2010). Besides, the effective of the association of the sustainable development with the ESG concept can boost up the greenery index of a structure which is in conformity with the policy of Malaysia (KeTTHA, 2017), which is in line with the environmental protection, social well-being, and economic prosperity that intend to bring advantages to all the parties as shown in Figure 2.1. The aspect of environmental protection, which comprises biodiversity and ecology, must have the social involvement as stated in the social well-being, which links to the legislation compliance. Coherent to that, the ESG concept which is environmental, social, and governance is to be implemented simultaneously, regardless of the existing policy.

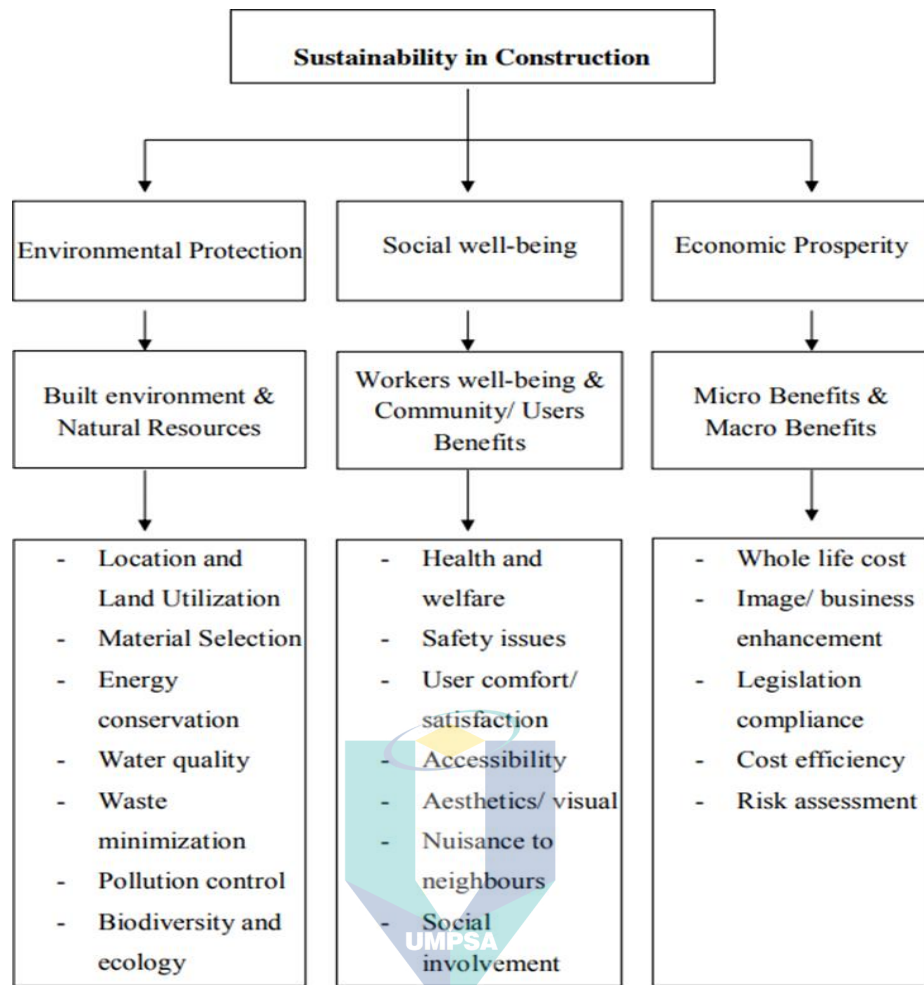


Figure 2.1 The aspects of sustainable development in the construction industry

Source: Nazirah Zainul Abidin (2010)

2.3 Soft Clay Soil

Clay soil is a natural mineral that is available on Earth where it is formed through the erosion of rock and using the geological weathering process. Clay minerals including kaolinite, smectite, chlorite, and micas are the primary raw elements for making clay and form when water is present (Cheng et al., 2016). Soft clay soil is always defined as having high pores pressure and void ratio because it contains minerals within itself. The minerals can also be either decayed organic matter, aggregates even the liquid that is being flown to the clay and occupying the empty spaces between the soil particles. The clay is considered to have high pores water pressure where the liquid limit

is lower than the water content. Referring to that, coarse-grained soil which is typically sand and gravel while fine-grained soils are known as the soils have more than 50% of the total weight passing the 0.075 mm or in No. 200 sieve.

Minerals that are naturally available on Earth have different textures, sizes, shapes, and physical and chemical properties. A soil mineral has a unique chemical formulation and crystal structure, though its chemical composition is not always fixed (Cheng et al., 2016). Some common clay that is available such as kaolinite, montmorillonite, and illite exhibit the properties of clay. The mineralogical composition of clays ranges from kaolinite to illite and montmorillonites, as well as other non-sheet- clay minerals (Syamsul et al. 2023).

Soil can be defined as a surface material that is brown covers most land on Earth, consisting of inorganic and organic matter. The mixture of organic matter fraction with mineral fractions such as gravel, clay, silt, and sand particles become the focus on determining the texture of the soil. Compared to other mineral fractions found on Earth, clay is a type of soil with a large surface area, and from this characteristic, clay is found to be chemically active and can store nutrients on its surface. Clay has low bearing capacity from its nature as it is due to it containing high organic matter within itself. Geotechnical engineers have been researching different techniques such as ground improvement to improve the bearing capacity of the soil typically maintaining stability of the structure, reducing the shrinkage and swelling of soil at the same time minimizing the uneven settlement of the ground surface.

Based on the Unified Soil Classification System (USCS), the clay has an organic content of approximately 20% - 75% of its overall percentage. The range of clay particle size detected is ranges within 0.1–300 μm by scanning electron microscopy (SEM) images as stated by Birmipilis et al. (2022), and it can notify that the soft clay soil is very sensitive to variation of the water content inside the clay as the increase of volume of the clay can result in the expansion of soil.

2.3.1 Compressibility and Compression

From the typical value of the liquid limit of soft clay soils, it is identified as disturbed cohesive soils because the liquid limit is less than its water content. Referring to that, the change in the water content of soft clay may be due to external factors that have altered its natural condition. Through the effect of weather, soft clay is easily affected when additional water flows in it causing the soil to be highly compressible. Highly compressible soil generally has poor shear strength. The details of the volume compressibility for different soils are tabulated in Table 2.1. Cohesive soils are structures, aggregates, and particles that are tightly held together, and not easily separated. When they are subjected to force, it will induce overburden pressure when they are being compressed, which will further deform if the imposing load is larger than the soil can withstand. The deformation mechanism is further analysed as the soil may not withstand it as the load imposed is almost equal to its original shear strength, then the entire structure with the soil can collapse, and a landslide will occur.

Table 2.1 Typical values for the coefficient of volume compressibility

| m_v (m^2/MN) | Soil type |
|--------------------|--|
| 10.0 – 2.0 | Peat |
| 2.0 – 0.25 | Plastic clay (normally consolidated alluvial clay) |
| 0.25 – 0.125 | Stiff clay |
| 0.125 – 0.0625 | Hard clay (boulder clay) |

Note: m_v = Coefficient of volume compressibility

Source: John Wiley & Sons (2014)

Generally, soils, especially soft clays are highly compressible due to their low value of shear strength because of disturbed conditions mainly due to the change in water content within itself. In the design process of a construction project, other than designing a safety structure by complying with respective codes and standards, the properties of soil from the specific site must be known and analysed. The properties of soil include angle of internal friction, capillarity, permeability, elasticity, cohesion, and compressibility. When dealing with soil in construction material, several properties of soil need to be considered such as cohesion, capillarity, angle of internal friction, permeability, elasticity, and compressibility. To obtain these data sets, an appropriate approach by the geotechnical engineers to resolve the issue of problematic soft clay is necessary to implement.

Regardless of the type of soil, when the soil mass is exposed to imposed loading, compressive force is created and subsequently exerted on the soil mass, which will then lead to the change in volume of that soil mass. Besides, rearrangement of the soil following the compressive force takes place as the change in volume. This situation is defined as the compressibility of soil upon receiving compressive force due to external loading. The phenomena of soil compression alter the soil's porosity, water drainage, and particle arrangement, which also disrupts the soil's overall structure (Bayat et al., 2018). Settlement of soil naturally is termed as consolidation where it is the compression of saturated soil under static pressure, and the water content within itself is expelled from the voids. Some typical fine-grained soils, silts, and clays are frequently associated with the consolidation process. To understand the consolidation process clearly, typical tests such as. Permeability of soil can be determined using classical tests such as the constant head permeability test which is suitable for granular soils including sand or gravel while the falling head test is appropriate for determining the hydraulic conductivity of fine-grained soils like silt and clay. These values are crucial together with the rate of compression so then it can further determine the entire consolidation process of the soil.

Immediate settlement occurs when a load is exerted on a soil profile and leads to the reduction of air voids between the particle arrangement due to the change in the volumetric of the soil. For clays, the elastic deformation or volume distortion of the area affected by the foundation load is known as immediate settlement without any drastic loss of excess pore water pressures. When the expulsion of the pore water pressure happens, which has initially occupied the void spaces of the soil and subsequently changed the volume that leads to the water expulsion, this process is called primary consolidation settlement. Referring to what has been mentioned in Terzaghi's effective stress principle, primary consolidation is defined as the time-dependent compression process connected to the dissipation of pore pressure (Zeng & Hong, 2015).

The stone column installation that causes the permeability reduction which is known by smear effects affects the consolidation of unsaturated composite ground (Zhang et al., 2021). Elastic settlement either known as initial compression due to the preloading, is the first stage of settlement of soil, followed by primary consolidation where at this stage the change in volume and excess pore water pressure is expelled. Settlement of soil continues by secondary consolidation where at this stage the behavior of plastic deformation occurs at the same time the soil particles tend to move after completing the primary consolidation where the excess pore water pressure has dissipated.

Secondary consolidation of soils has gained much importance as a major contributor to the long-term settlements of soft clays (Azad Sahib & Robinson, 2020). The typical values of the coefficient of consolidation of the soil's hardness is tabulated in Table 2.2. This process is much more complex as compared to the initial stages of soil consolidation as it involves many aspects to be considered to understand the entire process. Besides, the effect of creeping in soft soil makes the secondary consolidation process more complicated. This process is a continuation process from primary consolidation when the excess pore pressure dissipates. The results of the consolidation

test are used to determine the compression index, and the fluctuation in the void ratio with changing effective stress is shown on a semilogarithmic scale.

Table 2.2 Typical values of the coefficient of consolidation (C_v)

| C_v Range cm^2/s | Category | Typical material | Soil classification (USCS) |
|------------------------------------|-----------|------------------|---|
| <0.000032 | Very low | - | - |
| $0.000032 - 0.00032$ | Low | $>25\%$ clay | Medium plasticity clays (CL-CH), and volcanic silt (MH) |
| $0.00032 - 0.0032$ | Medium | $15 - 25\%$ clay | Low plasticity clay/mud (CL) |
| $0.0032 - 0.032$ | High | $<15\%$ silt | Organic silt (OL) |
| >0.032 | Very high | - | - |

Source: Acidri Samuel (2019).

Generally, clay has low bearing capacity as it is highly compressible as compared to other minerals like gravel and sand. For construction purposes, clay enhancement procedures can be used to reinforce soft clay's negative qualities, such as its excessive compressibility and low shear strength (Yoobanpot et al. 2017). Typical consolidation, Standard Oedometer test, or One-dimensional compression test is implemented to determine the rate and magnitude of consolidation of the soil when the soil is in the condition of laterally restrained and being loaded axially. The result obtained from the test can be used for estimating the magnitude of settlement of that structure. The variation of the coefficients of consolidation (C_v) was insignificant for low organic content and significant for high organic content (Rabbee et al., 2012).

2.3.2 Undrained Shear Strength

In engineering practice, the undrained shear strength denoted as C_u is regarded as one of the most fundamental parameters in describing soils. Parameter C_u is particularly important when dealing with clayey soil as this type of soil mostly blocks the movement of water by flowing in and out of the soil. According to the ISO standard, this characteristic also serves as the foundation for the classification of soil. To determine the value, common tests that are used for analysis are the unconfined compression test, triaxial compression test, and standard penetration test known as the cone penetration test.

Soil foundation is the most basic element that should be clearly understood by knowing its properties including the bearing capacity, lateral earth pressure in either passive or active on the retaining wall, and slope stability if the structure is inclined. Referring to the Mohr-Coulomb approach, French mechanical engineer Henri Tresca proposed his idea in the Tresca model for predicting equal undrained shear strengths in triaxial compression and triaxial extension (Krabbenhøft et al., 2019). According to Dhianty & Mochtar (2018), the undrained shear strength of soil which has the dominant of clay and silt is presented in Table 2.3.

Table 2.3 Typical values of the soil's undrained shear strength (C_u)

| Soil Consistencies | Undrained Shear Strength, C_u | |
|--------------------|---------------------------------|--------------------|
| | kPa | ton/m ² |
| Very Soft | 0 – 12.5 | 0 – 1.25 |
| Soft | 12.5 – 25 | 1.25 – 2.5 |
| Medium | 25 – 50 | 2.5 – 5 |
| Stiff | 50 – 100 | 5.0 – 10 |
| Very Stiff | 100 – 200 | 10 – 20 |
| Hard | > 200 | >20.0 |

Source: Dhianty & Mochtar (2018)

Parameter undrained shear strength is particularly important when a

construction project is involved in the analysis of embankment stability because the figure will be taken to further study whether the structure will fail under different circumstances such as overturning. While evaluating the foundation, the bearing capacity of soil mainly plays an important role if the soil on the site is clayey. Referring to the study by Dhianty & Mochtar (2018), the value of undrained shear strength for the hardness of soil from very soft to medium ranges from 0-50kPa where these categories of soil are mostly loose sandy soils including silty or clayey sands. This range of soil is potentially required for ground improvement such as the insertion of stone columns beneath the ground to achieve the commercial development purpose. The magnitude of undrained shear strength depends on soil types, composition, fabrics and structures, depositional environment, stress history, and physical and mechanical properties, which are taken to further study whether the structure will fail under different circumstances such as overturning (Rabbee et al., 2012). While evaluating the foundation, the bearing capacity of soil mainly plays an important role if the soil on the site is clayey. Referring to the study by Dhianty & Mochtar (2018), the value of undrained shear strength for the hardness of soil from very soft to medium ranges from 0-50kPa where these categories of soil are mostly loose sandy soils including silty or clayey sands. This range of soil is potentially required for ground improvement such as the insertion of stone columns beneath the ground to achieve the commercial development purpose. The magnitude of undrained shear strength depends on soil types, composition, fabrics and structures, depositional environment, stress history, and physical and mechanical properties (Rabbee et al., 2012).

Due to its natural clayey properties, clayey soil is not suitable for construction. Because of the low shear strength and high compressibility of this soil, many engineering problems such as slope stability, bearing capacity failure and excessive settlement could occur either during or after the construction phase (El Gendy et al., 2019). Some soils are simply unable to support the weight by the loading of either dead or live load on the foundation structure and subsequently causing damage to footings that will eventually lead to settlement.

2.4 Kaolinite

The word kaolinite or kaolin derives from Gaoling or High Hill located in Jingling Town, Jiangxi, China. It is also referred to as “China Clay” because of the discovery location, of Kao-Ling, China in 1867 (Syamsul et al., 2023). Kaolin is one of the most common minerals of a group of hydrous aluminum silicate, which results from the breaking of aluminum-rich silicate rock, such as feldspar and nepheline syenite, either through weathering or hydrothermal activity (Syamsul et al., 2023). When this type of mineral is exposed to water it becomes a wet compound, it can be easily broken and shaped accordingly. Kaolinite mineral is found abundantly in clay, and some of the clay might have an almost entirely kaolinite composition on itself. A rock is considered kaolin when the amount of kaolinitic is more than 50% (Turan et al., 2020). Others are formed in rocks such as granites and pegmatites when feldspars are altered by hot solutions. Furthermore, kaolinite is a type of mineral that has low moisture content and low shrinkage properties. A low shrink-swell capacity can be found in different colours such as white when it has higher purity, yellow, brown, or even red following the conditions of the kaolinite.

2.5 Plastic Industry

Plastics are readily moulded into a variety of goods with a wide range of applications. They are affordable, lightweight, and durable materials, and primarily highly polymerized carbon and hydrogen compounds generated from materials like petroleum and natural gas. Plastics are made from the crude gasoline left over after crude oil is refined. The behaviour of plastics when heated separates them into two primary categories: thermoplastics and thermosetting plastics (Mwanza & Mbohwa, 2017). Both thermoplastics and thermosetting plastics are polymer substances, but they react differently when exposed to heat the major distinction between them is thermoplastics melt in the presence of heat after curing, but thermosetting plastics maintain their original shape or remain in as solid state. Since thermoplastics are more practical than

thermosetting plastics based on their properties, thermoplastics are widely used as their commercial value where typical types of plastic are available in the market including PET or PETE, HDPE, and PP.

The life cycle of plastic is then divided into 4 main stages where there is a selection of materials in either recycled plastics or virgin material, followed by the production of plastic products this stage will define the grade of plastic and its types, which will send out to the consumers according to their needs. Figure 2.2 shows the flow chart of plastic recycling in Malaysia. As time passes, the plastic production rate has sharply increased from time to time due to the high demand for plastic that humans can benefit from.

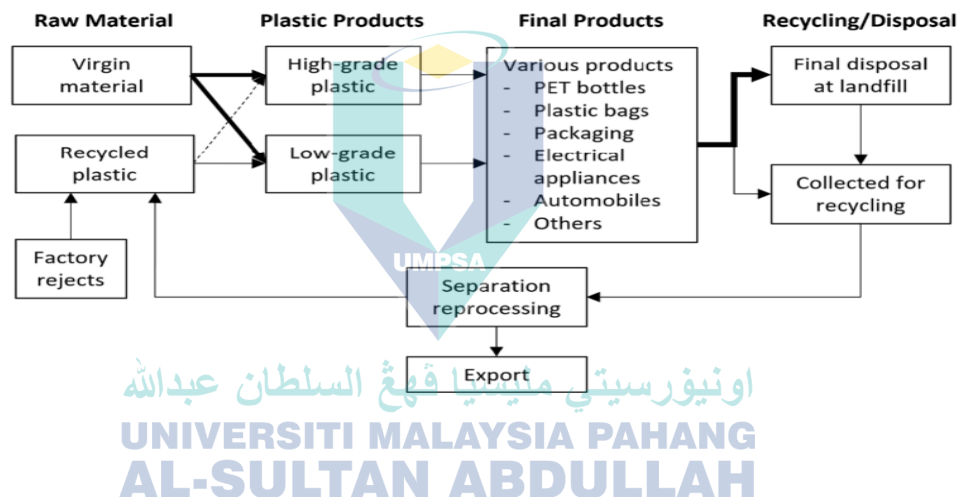


Figure 2.2 Flow chart of plastic recycling in Malaysia

Source: Solid Waste and Public Cleansing Department (2018)

The annual global plastic production increased from a mere 2 million (m) tonnes in 1950 to 381m tonnes in 2015 (Baierl & Bogner, 2021). Figure 2.3 shows the annual global plastic production from 1950 – 2015. The large production of plastics within the 100 years times has caused serious environmental issues as some of the plastics can be either recycled or reused after disposal. Preservation of the environment from preventing causing too many disposals of plastic has recently raised and hence, some of the plastics

are recyclable. Some common plastics that are not recyclable include Polyvinyl Chloride (PVC), LDPE, and Polystyrene due to its chemical properties. Table 2.4 presented the categories of plastic which can or cannot be recycled. The production of various types of plastics showed a trend of increasing due to their convenience for packaging purposes, different types of thermoplastic resin capacity are showing different proportions of percentages following the global demand. The polyethylene resin occupied the biggest part of thermoplastic resin production with a percentage of 29.1% as compared to other types of plastic in 2008 (Nkwachukwu et al., 2013).

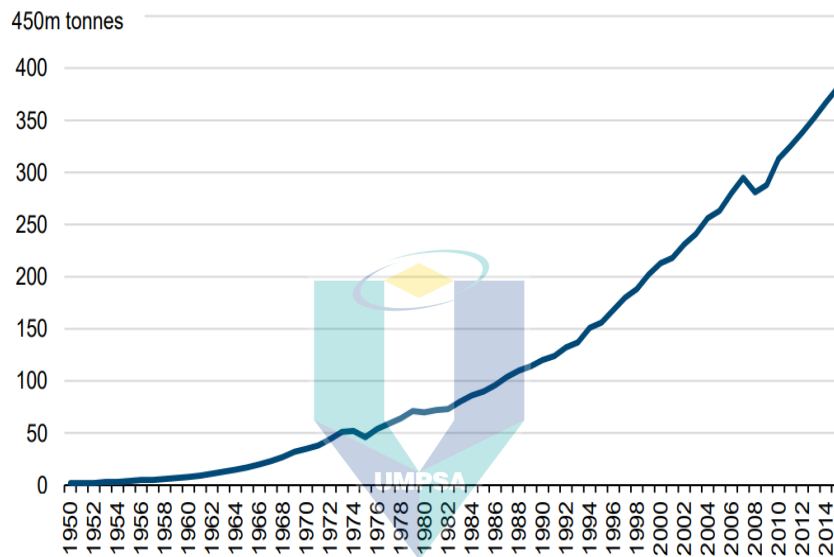


Figure 2.3 Annual global plastic production, 1950 – 2015 (million tonnes)

Source: Baierl & Bogner (2021)

Table 2.4 Categories of plastic

| No. | Category | Product of Uses | Recyclable in Malaysia |
|-----|---------------------------------------|---|------------------------|
| 1. | Polyethylene Terephthalate (PET/PETE) | Mineral water bottles, cookie jars | Yes |
| 2. | High-Density Polyethylene (HDPE) | Milk containers, buckets, shampoo bottles | Yes |

Table 2.4 Continued

| No. | Category | Product of Uses | Recyclable in Malaysia |
|-----|---------------------------------|---|------------------------|
| 3. | Polyvinyl Chloride (PVC) | Pipes, synthetic leather | No |
| 4. | Low-Density Polyethylene (LDPE) | Bubble wrap, plastic bags | No |
| 5. | Polypropylene (PP) | Disposable food containers, bottle caps | Yes |
| 6. | Polystyrene (PS) | Disposable cups, plates, cutlery | No |
| 7. | Others | Miscellaneous plastic, nylon | No |

Source: National Solid Waste Management Department (2011)

Table 2.5 Key data of Malaysia's plastic industry

| | 2014 | 2015 | 2016 | 2017 | 2018 |
|--|-------|-------|-------|-------|-------|
| Malaysia's Gross Domestic Product (GDP) Growth | 6.0% | 5.0% | 4.2% | 5.9% | 4.7% |
| Number of Plastic Manufactures | 1,300 | 1,300 | 1,300 | 1,300 | 1,300 |

Table 2.5 Continued

| | 2014 | 2015 | 2016 | 2017 | 2018 |
|--------------------------|-----------------------|----------------------|----------------------|-----------------------|-----------------------|
| Turnover (RM Billion) | RM19.46b (+7.3%) | RM24.77b (+27.3%) | RM27.32b (+10.3%) | RM29.80b (+9.1%) | RM30.98b (+4%) |
| Export (RM Billion) | RM11.94 b (+11.5%) | RM12.96 b (+8.5%) | RM13.11 b (+1.2%) | RM14.58 b (+11.2%) | RM14.60 b (+0.14%) |

Source: Malaysian Plastic Manufactures Association (2019)

Meanwhile in Malaysia, the production and consumption of plastic industry is seen to have a positive growth in the future and hence, the disposal of plastic is expected to increase. Plastic waste disposal is commonly disposed of, recycled, and used in research studies. According Cui et al. (2010), the best strategy for addressing the issue of environmental contamination brought on by plastic film and realizing resource utilization is recycling plastic waste. Plastic products or disposal of unwanted plastic products has been used in many studies such as cement, road base improvement, structural fills, and geotechnical applications. Table 2.5 presents the key data of Malaysia's plastic industry and from the report by Malaysian Plastic Manufactures Association (2019), it showed that the resin consumption (metric tonne) increased from 2.15 metric tonne to 2.45 metric tonne between year 2014 to 2018 or a total of 13.95 increments, the number of plastic manufacturers showed no changes between the years which recorded 1,300. The increment of plastic production causes plastic disposal to increase directly.

2.5.1 Polyethylene Terephthalate (PET) Plastic

PET plastic is a long-chain polymer that falls under the generic group of polyesters. Terephthalic acid and ethylene glycol are both substances generated from oil feedstock acting as an intermediate for the creation of PET plastic. PET has a similar appearance when it is ground and particle size distribution of the natural aggregate is similar to river sand. Referring to that, PET plastic has the potential as a substituent

material in stone columns as a ground improvement technique to improve the shear strength of soil. PET products are tough, especially the unfilled materials that show no breaks in unnotched impact strength test at low temperatures which is approximately 40°C (Archna et al., 2015). Although the tensile strength and flexural modulus are dropped when the temperature is increased, they are still available to use in many applications. Excellent performance under static and dynamic loads and dimensional stability even at high temperatures are the characteristics of PET plastic. When PET plastic is moulded, its surface becomes hard, and glassy, low coefficient of friction, and its surface turns abrasion resistant. The properties of PET plastic are shown in Table 2.6.

PET plastic which is under the polyester group is made through the reaction of bifunctional acids with alcohols using metal as a catalyst in this reaction. A condensation reaction will occur followed by a second polymerization reaction where this step the product has turned into a solid phase. The intermediates needed to make PET come from crude oil, where the first product is a monomer called bis-hydroxyethyl terephthalate, or BHET, which is then heated with oligomers to join with low molecular weight polymers. The liquid then undergoes further reaction, separating extra ethylene glycol to form PET. After all these steps, the PET is now a molten liquid, it is then extruded and quenched in the water. An amorphous material, the glasslike substance will form. Different manufacturing technologies using dimethyl esters of terephthalic acid may be applied to produce PET, but the properties of PET do not vary much. In 2002, the annual use of plastic material in the world amounted to 204 million tons, but in 2013 it increased to 300 million tons (Sulyman et al., 2016). The figure is expected to grow from year to year using the data collected in 2002 and 2013 as the reference for plastic usage.

Table 2.6 The properties of PET plastic

| Properties | Values |
|-------------------|--------------------|
| Molecular formula | $(C_{10}H_8O_4)_n$ |
| Molar mass | Variable |

Table 2.6 Continued

| Properties | Values |
|---------------------|--|
| Density | 1.38 g/cm ³ (20 °C), amorphous: 1.370 g/cm ³ , single crystal: 1.455 g/cm ³ |
| Melting point | >250 °C |
| Boiling point | >350 °C (decompose) |
| Solubility in water | Practically insoluble |

Source: Sinha et al. (2010)

In 2011, plastic production was categorized into 10 parts which include HDPE, LDPE, PET, PVC, PP, PS, Polycarbonate (PC), Acrylonitrile butadiene-styrene (ABS), Polymethyl Methacrylate (PMMA) and Others (acrylic nylon and epoxy resin). In 2014, the share of energy input in power stations was divided into 6 parts which are natural gas, coal, hydropower, diesel, fuel oil, and renewable. Table 2.7 shows the plastic production by category in Malaysia. The highest plastic production percentage was recorded at 24% by HDPE and LDPE, followed by PET and PP (13%), then PVC and PS (10%), ABS (4%), PC (3%), and lastly PMMA and others (2%).

Table 2.7 Plastic Production by Plastic Category in Malaysia

| Type of plastic | Plastic production (%) |
|--|------------------------|
| High Density Polyethylene (HDPE) | 24 |
| Low Density Polyethylene (LDPE) | 24 |
| Polyethylene Terephthalate (PET, PETE) | 13 |
| Polyvinyl Chloride (PVC) | 10 |
| Polypropylene (PP) | 13 |
| Polystyrene (PS) | 10 |
| Polycarbonate (PC) | 3 |
| Acrylonitrile butadiene-styrene (ABS) | 4 |

Source: Hasan et al. (2019)

2.5.2 Polyethylene Terephthalate (PET) Utilization

PET was successfully manufactured to use as the film in the late 1950s, extensive studies were done in the early 1970s and created the first oriented three-dimensional structures through blow moulding techniques. This invention has led to further development that finally creates lightweight PET products like PET plastic bottles. In 2008, the production capacity of only PET plastic around the world recorded a huge figure, 64,400 kilotons per year (kt/year). As reported Al-Salem et al. (2009), the recycled polyester (R-PET), which is made from PET, has received attention and is said to offer an alternative to the high-impact fibres on which the industry depends, such as polyester and cotton, which, as of 2015, market shares of 55% and 27% respectively.

The demand for PET recycled plastic has increased over the years due to its various advantages. Figure 2.4 shows the global use of PET packaging in 2010. Based on the study, it is noted that approximately 70% of the bottles supplied with soft drinks around the world were supplied in PET bottles, amounting to a total of 11.5 million metric tonnes. In recent years, the percentage of recycling rate compared to the utilization rate of PET plastic has shown signs of increase, where the ratio of recycling rate to utilization rate has always been bigger than 1 since 2003. Figure 2.5 shows the comparison between the recycling rate to the utilization rate of PET plastic from 2003 – 2013. It presents the recycling rate had increased sharply from about 17% to almost 30% from year 2002 to 2013, which was almost double the value of the utilisation rate. Hence, the previous data proved that the recycling rate was also higher than the utilisation rate, and the trend data was expected to follow the previous values based on the Figure 2.5.

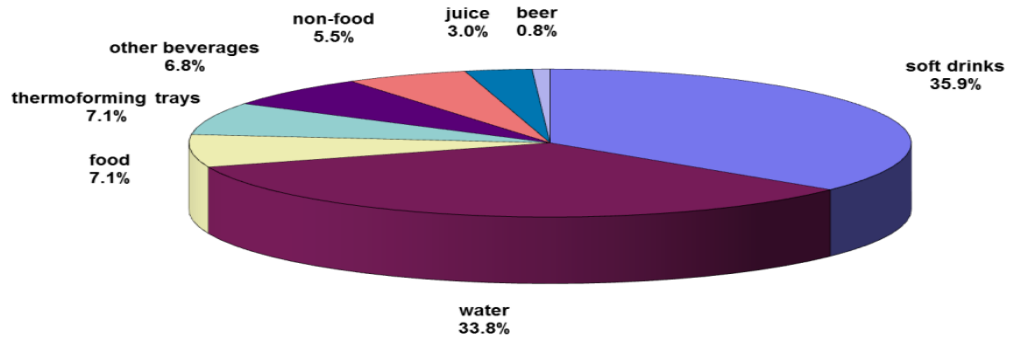


Figure 2.4 Global use of PET packaging in 2010 (excluding fibre)

Source: Welle (2011)

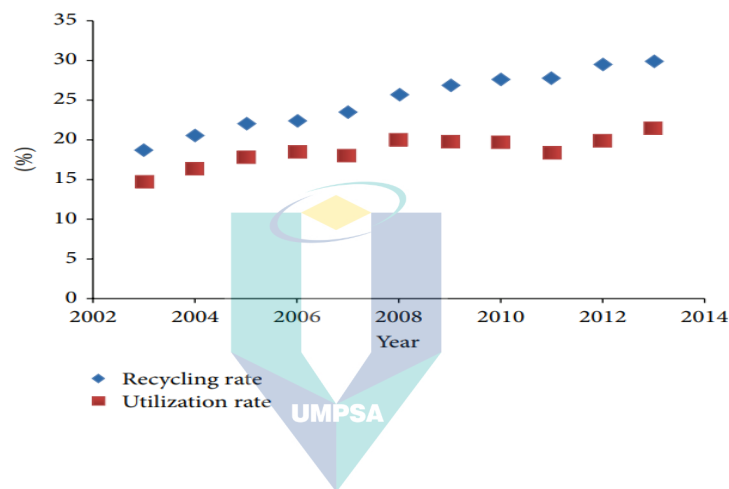


Figure 2.5 PET recycling and PET material utilization ratio

Source: Plastic and Chemicals Industries Association (2006)

Every year, the production of different types of plastic has increased and produced a huge number of plastics to the world, supplying the demand to humans. Therefore, analysis of PET plastic is necessary and required to carry out regarding its physical, chemical, and mechanical properties before they are used in different applications. The PET plastic makes up around 18% of all polymers manufactured globally, and more than 60% of it is generated for synthetic fibres and bottles, which account for about 30% of the world's PET consumption (Sulyman et al., 2016).

Various methods of handling the used PET plastic are seen in landfills, ponds, and drainage, harming the environment which destroys the flora and fauna easily. The composition of plastic regardless of its type is mostly non-biodegradable, however, it is classified as almost an inert packaging material and will not chemically react with the organic compounds in the soil (Later et al., 2015). Previously, the utilisation of PET plastic in construction with different particle shapes and surface texture will have different results in terms of the stability of the earthworks. As reported by Sojobi et al. (2016), the BAC that modified with PET plastic has found to increase the concrete strength and the durability. Thus, it is expected the modified material's lifespan with PET is longer than the conventional coarse aggregate since the nature properties are mostly non-biodegradable.

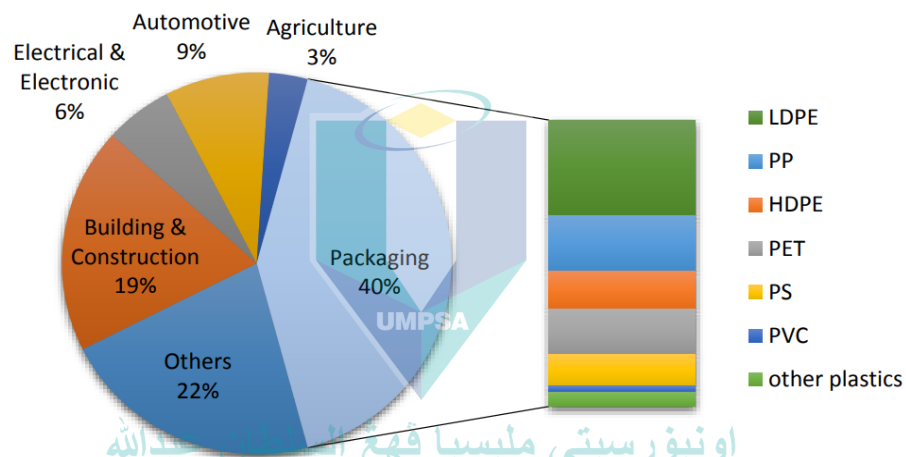


Figure 2.6 Recycled plastic used in different field

Source: Kaiser et al. (2018)

Referring to Figure 2.6 showing PET plastic compounding its market size, by product in the year of 2015, and it shows that the utilization of PET plastic in the construction industry is predicted to increase from year to year. Different types of plastics like PET plastic can be beneficial in the civil engineering industry, especially in the geotechnical field. Besides, the high demand for PET plastic around the world in producing different types of products, particularly in manufacturing items. The usage of

PET plastic for geotechnical fields is applied in such a way that it combines the concept of ground improvement where it can either encapsulate or non-encapsulate the PET column reinforcement. Coherent to that, plastic has been drawing attention from researchers, especially in the construction industry.

2.5.3 Physical Properties of Polyethylene Terephthalate (PET)

2.5.3.1 Particle Size Distribution

An analytical method called sieve analysis or gradation test is used to determine the particle size distribution of granular material where the analysis technique involves several layers of sieves with different grades of sieve opening sizes. Non-organic and organic granular materials are also available to know the particle size distribution comprising sands, clays, granite, and so on. When determining the particle size of a granular material, it is crucial to carry out sieve analysis since the particle size distribution can have an impact on the characteristic of the structure after being mixed where it can affect the strength of concrete, solubility, and the surface area property. In earlier work done by Saxena et al. (2018), at all PET percentages, coarse PET particles typically produced larger bulk densities than fine ones; consequently, finer PET particles are found to produce higher air void values, which equates to relatively lower bulk densities reached with this size.

Figure 2.7 shows the grain size distributions for pulverized PET according to ASTM C136 (2014) obtained from Umasabor & Daniel (2020). The grain size distribution showed the pulverized PET as a coarse-grained material, while the particle size ranged between 0.05 mm and 1.0 mm. The majority size lies within the sand region containing fine and coarse sand sizes. Referring to the grain size distribution, the PET plastic is categorized in sand size and able to pass through the 4.75 mm or No.4 sieve for approximately 50% - 90% of its overall size. This gradation test was carried out to analyse the particle size in bulk with its relative proportion for a maximum size up to 0.063mm while a hydrometer test was conducted for particles size which is finer than 0.063mm.

To increase the accuracy of the soil classification either clay, silt, sand, or even gravel, both of the tests were carried out.

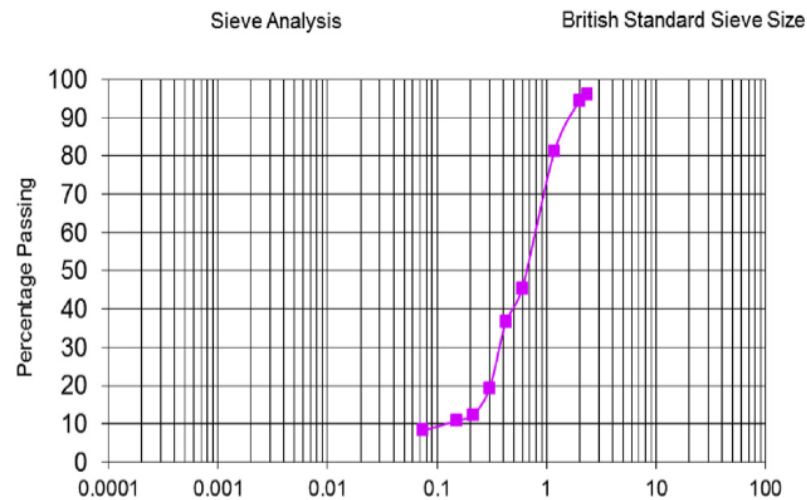


Figure 2.7 Particle size distribution of PET plastic

Source: Umasabor & Daniel (2020)

According to the USCS, PET is categorized as uniform-graded sand while referring to the classification by the AASHTO system, polyethylene terephthalate falls in the A-1 group and is classified as A-1-a. Cut waste PET bottles into fractions in the range of 5 – 15mm and coat them in ground granulated blast-furnace slag (GGBS) to solidify the surface of the aggregate (Choi et al., 2005). Generally, the feature of PET has a smooth surface with a low coefficient of friction with high flexural modulus, however its properties might alter due to several factors including the different manufacturing processes used to manufacture the PET plastic. The average coefficient of curvature for PET is relatively about 1.27 whereas the average coefficient of uniformity of PET is approximately 6.67. Table 2.8 shows the sieve analysis of various PET aggregates.

Table 2.8 Sieve analysis of various PET aggregates

| Sieve size (mm) | Cumulative amount passed (%) | | |
|-----------------|------------------------------|--------|--------|
| | PC | PF | PP |
| 16.0 | 100.00 | 100.00 | 100.00 |
| 11.2 | 99.96 | 100.00 | 100.00 |
| 8.0 | 97.69 | 100.00 | 100.00 |
| 5.6 | 49.24 | 100.00 | 100.00 |
| 4.0 | 20.59 | 99.99 | 99.46 |
| 2.0 | 0.89 | 45.65 | 7.93 |
| 1.0 | 0.02 | 0.94 | 0.04 |
| 0.5 | 0.00 | 0.01 | 0.02 |
| 0.25 | 0.00 | 0.00 | 0.00 |
| 0.125 | 0.00 | 0.00 | 0.00 |
| 0.063 | 0.00 | 0.00 | 0.00 |
| Residue | 0.00 | 0.00 | 0.00 |

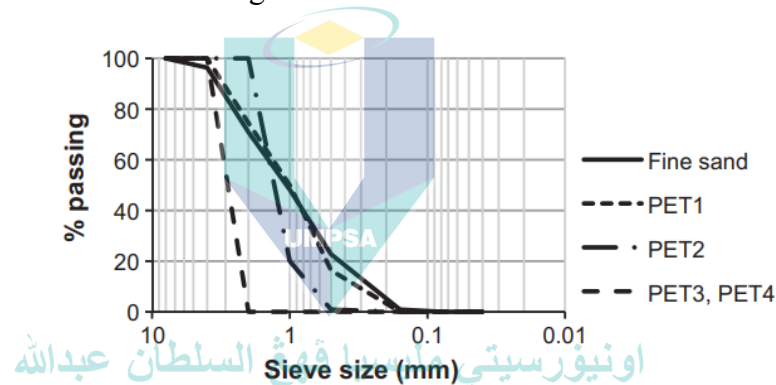
Note: PC – Coarse flakes; PF– Fine fraction; PP – Plastic pellets

Source: Saikia & De Brito (2013)

Besides, the particles of shredded PET plastic used for research purposes are mostly between 0.5 – 4mm. The use of smaller particles of PET appears to minimize the loss of compressive strength in comparison to large particles but including some small and some large can be equally effective as more efficient packing of the particles can be achieved (Thorneycroft et al., 2018). Furthermore, PET plastic particles practically have a higher water absorption ratio as it's sensitive to being exposed to water content because part of the shredded PET particles absorbs internally while the amount of water present

on the surface will then decrease the lubricant effect of internal particles. Thorneycroft et al. (2018) reported that grain size distribution of shredded PET particles ranging between 0.5 up to 4 mm in size could feasibly be used in structural concrete as they show identical performance in compression.

According to Ahmed et al. (2011), when the surfaces of two or more PET pieces come in contact with one another, the excessive PET content may cause slippage and a smaller size of PET produces a higher shear strength value while a larger PET generates a lower value. This is due to the PET pieces interacting with the shear plan of the soil and leading to an improvement in shear strength. For large PET pieces (i.e., 1.0 cm²) are favourable for fine-grained residual soil, while small PET pieces (i.e., 0.5 cm²) are favourable for coarse-grained residual soil (Zhao et al., 2015). Figure 2.9 shows the grain size distribution curves for PET fragments and fine sand.



form. When compared to other semi-crystalline polymers, it crystallises more slowly (Sudakov et al., 2019). It can be processed further to produce either amorphous or crystalline products, depending on the processing condition such as the solution used and environmental factors. The usage of lightweight and possess high flexural strength PET plastic material in concrete will influence the toughness behaviour of the product.

2.5.3.3 Shear Strength of Soil

The shear strength of soils is defined as the ability of a soil to sustain the shear stress being exerted in terms of the effective internal friction angle and effective cohesion, c' (Najjar, 2013). This parameter plays an important role it can affect the stability of the overall project. The strength of PET can decrease upon saturation after compaction. Depending on the water contents, the characteristic of strength may alter. In geotechnical engineering, the shear strength of soil can derive the bearing capacity parameter, applying the value for other design structures such as retaining walls, embankments and the analysis of slope stability (Syamsul et al., 2023).

The shear strength of soil varies based on the angle of friction, where it relates to the friction shear resistance and normal effective shear stress, deriving from the Mohr-Coulomb failure criterion (Syamsul et al., 2023). The friction angle increases as the content of polyethylene terephthalate increases because the friction between the particles is increased. This is due to the resistance of particle arrangement has increased as the content increases. Coarse-grained soils are cohesionless soils where the property of internal friction mainly affects it while internal friction is absent or the value is approximately zero from fine-grained soils, for this situation the shear strength of the soil is affected by cohesion. For coarse and fine-grained mixed soil, both factors for internal friction and cohesion influence the characteristics of the soil. Moreover, the particle size is increased due to the pozzolanic reaction, and hence more particles within itself tend to increase when the number of irregular shapes of particles is increased. Previous work by

Maharaj et al. (2015) reported that higher values of complicated shear moduli were noted when a larger size of PET was used.

Interaction between the solid, liquid, and gas particles is the fundamental that determines the shear strength of a soil. Composition of the soil particles, the amount of water present in the soil with the degree of compaction of the soil that further derives the soil shear strength. It is found that many factors that can affect the shear strength of granular soil include the particle size distribution, mineralogy of the size particles, angularity, degree of compaction, and the moisture content present. The soil particles regardless of the type of soil will be held tightly when they are being pressed or compacted, leading to the increment of its relative density together with effective stress. The installation of stone columns can increase the shear strength of soil by providing additional support beneath the ground. According to Suriya et al. (2020), by substituting aggregate columns for waste plastic, the load carried by clay soil properties is enhanced, lowering the plasticity index. The angle of shearing resistance, ϕ increased exponentially with that of the addition of PET waste but cohesion, C was noted to slightly decrease and then increase with further addition of PET (Meenakshi & Mohini, 2020) Figure 2.9 shows the variation of friction angle with the percentage of PET waste for sand and Figure 2.10 shows the variation of cohesion with the percentage of PET waste for sand.

اونيفرسيتي مليسيا فهد السلطان عبدالله
UNIVERSITI MALAYSIA PAHANG
AL-SULTAN ABDULLAH

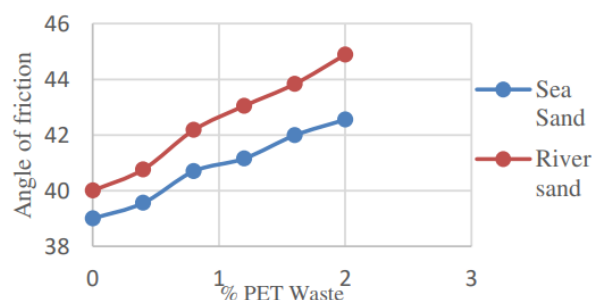


Figure 2.9 Variation of friction angle with percentage of PET waste for sand

Source: Meenakshi & Mohini (2020)

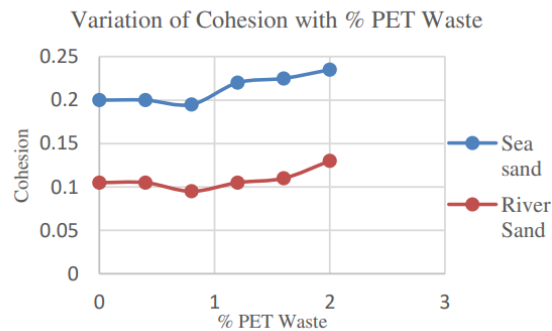


Figure 2.10 Variation of cohesion with percentage of PET waste for sand

Source: Meenakshi & Mohini (2020)

2.5.3.4 Specific Gravity

A soil mineral is classified as a three-phase material where it has solid particles with voids, filling with water and air. The specific gravity (GS) of soil is the ratio of the unit weight of the solid particles to the unit weight of water. The specific gravity of PET material is found to be more than 1, signifying that it's heavier than water, and will eventually sink if it is placed in the water. Theoretically, the increase of PET content in a mixture will cause an increase in the particle phase. Ogundipe (2019) investigated the use of plastic in a PET-modified asphalt concrete application, its density will increase as the content of PET plastic increases and could be attributed to the lower specific gravity of PET. Deraman et al. (2021) found that the lower value of specific gravity as compared to sand shows that it is lighter than sand and is classified as an organic material. The specific gravity of PET is influenced by particle porosity, and it has higher specific gravity than other plastic materials such as polystyrene and polyamide due to its arrangement of particles and weight. The ashes that have solid structures will be denser than the porous and hollow particles that tend to have the corresponding high specific gravity too. Besides, bigger sizes of shredded PET particles have the potential to be used as a partial replacement in the construction industry because dense particles may have a higher specific gravity. This leads to a low absorption rate as compared to the same

materials but having a smaller size of particle. Haque (2021) reported that bigger size of shredded PET plastic with 19 mm * 19mm size of plastic fibre shows better workability than 10 mm * 10mm in green concrete applications. Table 2.9 shows the specific gravity of various PET plastics being investigated from previous works.

Table 2.9 Specific gravity of PET plastic from previous works

| Researchers | Specific gravity |
|-------------------------|------------------|
| Peddaiah et al. (2018) | 1.37 |
| Choudhary et al. (2018) | 1.30 |
| Bozyigit et al. (2021) | 1.38 |
| Deraman et al. (2021) | 1.38 |

2.5.3.5 Compressibility

Compression of soil causes the rearrangement of soil particles, compressing and deforming of solid particles excluding air or water from the void spaces. It also relates to the compression of the liquid and gas within the voids of the soil. Furthermore, granular and non-granular material shows different reactions towards compression where granular material deforms in a shorter time compared to non-granular material. According to Singh & Noor (2012), the compressibility of soil mass is susceptibility to decrease in volume under pressure and is indicated by soil characteristics like the coefficient of compressibility, compression index, and coefficient of consolidation. While for embankments structure, the concept of compressibility is applied to analyse the magnitude of the vertical deformation at the surface of the embankments. Although construction projects lead to compression of soil since the entire structure is sitting on the ground, post-settlement is expected to occur once the construction is completed. Nevertheless, for soil that is susceptible to loadings and stresses, small significant settlements can affect the stability of structure and hence lead to different structure failures.

Table 2.10 Geotechnical properties of PET plastic blends

| Blend | PET |
|----------------------|------|
| Gravel content (%) | 68.1 |
| Sand content (%) | 31.9 |
| D max (mm) | 5 |
| D ₁₀ (mm) | 1.3 |
| D ₃₀ (mm) | 2.2 |
| D ₆₀ (mm) | 3.1 |
| C _u | 2.4 |
| C _c | 1.2 |
| Classification | GP |
| Specific gravity | 1.37 |

Note: N/A – Data is not available

Source: Arulrajah et al. (2020)

The composition of gravel content makes up 68.1% which is more than 50% as stated in Table 2.10 and is classified as coarse-grain material. The PET blends tend to deform faster in a shorter period when compression occurs on it, while the classification of GP shows that PET blends are generally poorly graded gravel which is predominantly one size or can also be classified as uniform graded. During compression, the compressibility level increases and causes the particles to crush where different shapes of particles will respond differently. Generally, the cut PET plastics with sharp edges will crush first compared to well-rounded particles due to their exposure area. The sharp edges particles are to be stressed more when the shear stress and confining stress increase and hence they tend to break faster.

2.5.4 Mechanical Properties of Polyethylene Terephthalate (PET)

2.5.4.1 Compaction

Compaction is a mechanical and artificial process that rapidly reduces the volume of soil by the expulsion of air voids in the soil at the same time increasing the soil density. During the compaction process, densification of soil happens naturally due to the consolidation process of the soil foundation that is caused by the expulsion of pore water as a result of the exerted loadings. Theoretically, soil compaction happens when the space between soil particles is reduced. To measure how the soil is being compacted, the concept of degree of soil compaction is applied to measure soil under compaction while for non-cohesive soil, it is sometimes known as density index. It is measured by dry unit weight which depends on the water content with the compact effort. The maximum dry unit weight of the sample is obtained at optimum moisture content. Compaction of soil is mainly important as it can increase the strength of the compacted soil, decrease the permeability of soil as the particles get closer, and decrease the compressibility of soil due to the expulsion of air voids within the soil particles. In the application of mechanical energy, the term compaction is defined as the densification of soil and soil aggregate mixture. The soil particles are redistributed within its soil mass, while the mechanical energy that converts it into stress may come from the dynamic load, static methods, or kneading. As reported by Alamanis et al. (2020), there are several effects upon doing soil compaction including the stabilization of soil foundation for technical work, promotion of the homogenization of foundation soil, improvement of the passive soil resistance towards the lateral loads, and improvement of carrying capacity of the soil.

Al-Obaidi et al. (2020) studied that many variables can affect the compaction of cohesive soil, the first of which is the type of soil including the distribution of grain sizes, the shape of the soil grains, the specific gravity of the soil solids, and the presence and type of clay minerals. The second variable is the compact effort. Haque (2021) reported that higher strength of concrete is achieved in the addition of smaller particle sizes of PET plastic fibres for making plastic coarse aggregate (PCA) concrete. In other words,

the well-graded and smaller size of PET plastic fibres can then increase the content of the mixture as the particles are closely packed as compared to large-size particles. Moreover, plastic granules may offer a high resistance to compaction, thus lowering density by their presence (Jaber et al., 2021). This can relate to the properties of PET as it tends to be cohesionless and thus, it shows less significance when exposed to water content, especially during compaction where cohesionless property allows fluid to pass through it. Apart from that, other engineering properties to evaluate in the geotechnical field include soil compressibility, permeability condition, and shear strength. Upon compaction, the shear strength will decrease, decreasing its permeability and compressibility from the effect of soil particles getting closer. Beyond the maximum dry density and optimum moisture content, both values will drop simultaneously. Generally, the increase of shear strength in the compaction of soil will decrease its compressibility and permeability. Table 2.11 shows the result from the compaction test for the mixture of PET plastic in percentage in producing modified subbase.

Table 2.11 Optimum moisture content and maximum dry density of mixture of PET plastic with subbase soil from compaction test

| No. | Polyethylene Terephthalate (PET) waste (%) | Optimum Moisture Content (OMC) (%) | Maximum Dry Density (MDD) (%) (g/cm ³) |
|-----|--|------------------------------------|--|
| 1 | 0.0 | 7.3 | 2.196 |
| 2 | 2.5 | 7.1 | 2.169 |
| 3 | 5.0 | 6.8 | 2.093 |
| 4 | 7.5 | 6.3 | 2.088 |
| 5 | 10.0 | 5.9 | 2.083 |
| 6 | 12.5 | 7.3 | 1.978 |

Source: Jaber et al. (2021)

Kumar & H.P (2017) investigated the result of a standard compaction test where the plastic waste is found to increase the maximum dry density of cohesive soil if the content increases by 0.4% by mass due to the increase in internal friction of soil due to presence of plastic waste, but further increment of plastic content from 0.8% to 1.2% will cause reduction in maximum dry density and its optimum moisture content due to lower specific gravity of plastic waste reduces the shear strength of soil. Peddaiah et al. (2018) stated that the amount of PET plastic to be replaced as coarse aggregate is 0.4% by mass where this is the optimum value to obtain the value of maximum dry unit weight and optimum moisture content of 16.75 kN/m³ and 16.8% respectively.

To let the soil particles get compacted upon compaction, the water contents should be increased at a certain value so that the water is available to lubricate the soil particles when it is under compaction as water films around the particles will turn larger if additional water is being added. The water content should be moderate since the excessive water will cause the soil particles to be moving apart, freely, and difficult to get closer. Figure 2.11 shows the standard and modified compaction curves of clayey soil.

With constant compact effort, it can then reduce the optimum moisture content by reducing the distances between the particles, increasing the maximum dry density. The maximum dry density is inversely proportional to optimum moisture content until its peak point. Theoretically, the cause of soil compaction is classified as a natural process and a human factor. Soil compaction depends on bulk density, soil strength, soil porosity, and pores connectivity, and the optimum moisture content and maximum dry density of subbase soil with 0.0 – 12.5% plastic waste replacement ranged from 5.9 – 7.3% and 1.978 – 2.196 g/cm³ (Jaber et al., 2021)

PET shredded particles lying in the region of coarse-grained materials are mostly categorized under cohesionless soils. Referring to it, it shows little significance towards the effect of moisture content upon compaction. Hence, cohesive soils are generally show

higher values of both parameters from the compaction test as compared to non-cohesive soils. The influence of compact effort on the moisture-density relation on cohesive soils is better than on cohesionless soils. However, Meenakshi & Mohini (2020) stated that since sand particles have a higher density than PET plastic waste, this is the cause of the drop in the maximum dry density. A higher figure of the dry density value can be obtained when the soil is in the condition of a saturated and completely dried-up situation. When classifying the soil whether it is in cohesive or non-cohesive soil, and it is crucial to notify their category as it affects the soil compaction analysis.

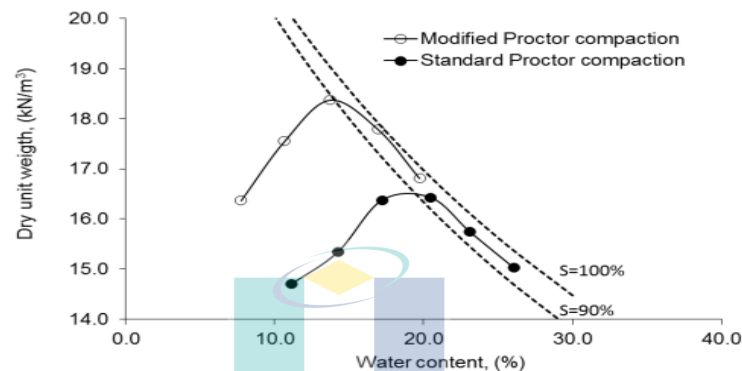


Figure 2.11 Standard and Modified Proctor compaction curves of the soil

Source: Yilmaz et al. (2016)

2.5.4.2 Permeability

Permeability of a substance is known as the ability of the fluid to pass through its filter while in soil mechanics, it is also known as hydraulic conductivity where the interconnection of soil relates to permeability is the flow of water through the void spaces of soil. According to Elhakim (2016), because interconnecting gaps in soils let the movement of fluids when there is a difference in energy head, soils are permeable materials. Referring to the previous studies, PET plastic is a low specific gravity material and is categorized as a poorly graded material thus, the permeability is expected to be relatively low. As investigated by Solanki & Bhattarai (2018), using PET material as a substitute in aggregate mixing with lower PET content or decreasing the A/P

(aggregate/PET) ratio can produce a mixture that has high permeability because of its natural properties. In other words, the usage of PET content should be in a minimum range to obtain maximum permeability, where the classification of GP for PET material can also be categorized as uniformly graded material by having almost the same size particles will have an impact on the figure of permeability. Table 2.12 shows the permeability results from the mixture of PET plastic with soil and coarse aggregate by using different ratios. The minimum content of PET material to replace other materials will then increase the tortuosity through the increment of the straight distance between the ends of the flow path.

Table 2.12 Results of permeability of PET plastic from previous research works

| Mix | PET (%) | Soil (%) | Coarse Aggregate (%) | (Aggregate +soil)/PET ratio (A/S/P) | Aggregate/PET ratio (A/P) | Average permeability in ft/day (m/day) |
|-----|---------|----------|----------------------|-------------------------------------|---------------------------|--|
| 1 | 5 | 5 | 90 | 19 | 18 | 2226 (679) |
| 2 | 75 | 5 | 87.5 | 12.3 | 11.7 | 1210 (369) |
| 3 | 10 | 5 | 85 | 9 | 8.5 | 1163 (355) |
| 4 | 10 | 0 | 90 | 9 | 9 | 1242 (379) |
| 5 | 10 | 10 | 80 | 9 | 8 | 42 (13) |

Source: Solanki & Bhattarai (2018)

Generally, soil permeability can be affected by factors including grain size distribution, void ratio, composition of soil, structural arrangement, presence of foreign particles, and degree of saturation. While producing the shredded particles of soil or substituent material, the particles with smooth texture particles can have higher permeability as compared to rough surface texture particles due to having less frictional resistance on its surface that allows more fluid to pass through. The particles that have a rough surface texture tend to give more frictional resistance to flow compared to smooth texture particles.

2.5.5 Morphological Characteristics of Polyethylene Terephthalate (PET)

Through the utilization of scanning electron microscopy (SEM), it investigates the characteristics of PET plastic to determine its particle shape and surface texture without the chemical composition. Besides, SEM photomicrographs give a detailed image regarding the behaviour of PET materials. Kusumocahyo et al. (2021) investigated that PET membrane and its resin had an asymmetric structure that consists of a microporous cross-section and a smooth surface as the active layer of the membrane. Moreover, the whole cross-section of the membrane from the PET bottle consisted of globular clusters, and the pores were not interconnected, whereas a small part of the cross-section of the membrane from PET resin had interconnected pores. Figure 2.12 and 2.13 shows the SEM photographs of the cross-section of the PET membrane and PET resin with magnification of 1000 and 5000. Ahangar et al. (2021) have found that the PET material appears as sheets with rough surfaces and by undergoing the calcination process, the PET material exhibits a nanotube structure with large irregularly shaped particles. The study above, also found that the addition of polyethylene glycol with a molecular weight of 40Da (PEG 400) will cause the PET membrane to increase its porosity and its hydrophilicity of the membrane, which will subsequently decrease its membrane pore size.

Due to its low specific gravity with an average of 1.27, the porosity of PET tends to be larger. Besides, the angularity affects the particle interlocking where the surface of contact area decides the performance while the rough surface texture restricts the movement of the particles. Both PET bottles and resin show different figures, where increasing of porosity is possible to apply in ultrafiltration membrane systems. Table 2.13 shows the porosity and the water contact angle of the PET bottle and resin.

Table 2.13 Comparison of porosity and water contact angle of the membrane from PET bottle and those from PET resin without additive

| Membrane | Polymer source | Porosity (%) | Water contact angle (°) |
|-----------------------|-----------------|----------------|-------------------------|
| Membrane – PET bottle | Used PET bottle | 69.7 ± 0.5 | 65.5 ± 1.4 |
| Membrane – PET resin | PET resin | 71.0 ± 1.2 | 65.8 ± 1.1 |

Source: Kusumocahyo et al. (2021)

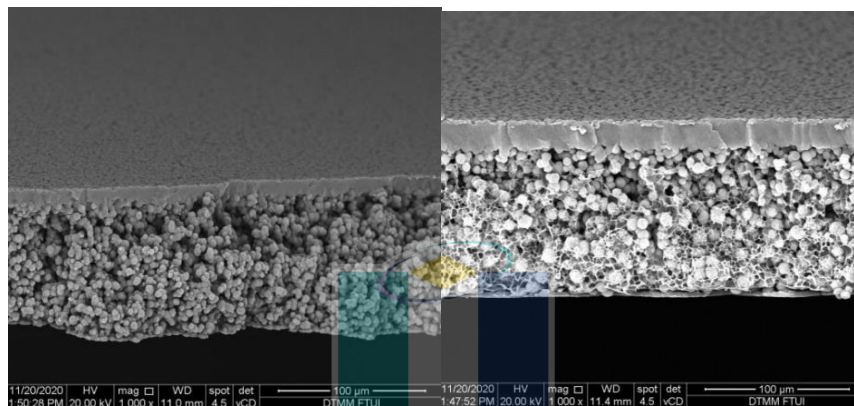


Figure 2.12 SEM photomicrograph of the cross section of the PET membranes bottle and PET resin with magnification of 1000

Source: Kusumocahyo et al. (2021)

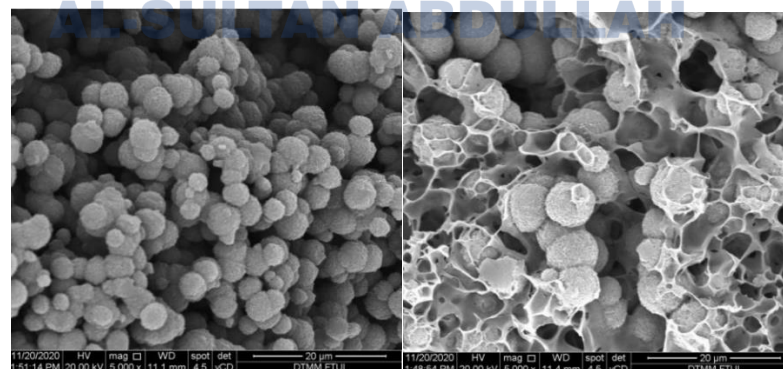


Figure 2.13 SEM photomicrograph of the cross section of the PET membranes bottle and PET resin with magnification of 5000

Source: Kusumocahyo et al. (2021)

2.6 Ground Improvement

The process of ground improvement is generally understood as the involvement of the utilization of mechanical tools to improve the poor quality of soil. The quality of the treated soil mass is improved by ground improvement techniques to meet the project performance criteria when the soil mass does not meet the design criteria. Some classic ground improvement techniques are dewatering, densification of soil, and addition of admixtures that are used to treat the problematic soil where the concept of soil and ground improvement are mostly associated together to prevent foundation failure during construction. On the other hand, ground improvement techniques are composed of different types of methods where they apply based on the type of soils, the nature of strata, and the purpose of adopting certain techniques.

According to Schaefer et al. (2012), the study classified the ground improvement technique based on the category, methods, and its functions as shown in Table 2.14. However, based on the findings by Herrmann & Bucksch (2014), the ground improvement techniques were classified according to cohesive and cohesionless soil as shown in Table 2.15. Based on the authors' classification, the types of available ground improvement techniques are generally to improve the soil's strength and accelerate the consolidation. Nonetheless, these methods consolidate the initial soil conditions, turning them into disturbed soils by offering the compaction piles or stone columns following the soil type acting as the artificial reinforcement as referred to in Table 2.15.

Table 2.14 Ground improvement techniques, functions and methods

| Category | Function | Methods |
|---------------|---|---|
| Densification | Increase density, bearing capacity, and frictional strength | Compaction in vibro, dynamic, blasting, compaction and surface. |

Table 2.14 Continued

| Category | Function | Methods |
|--------------------------------|---|---|
| Consolidation | Accelerate consolidation, reduce settlement, and increase strength | Preloading without drains, with vertical drains, and vacuum consolidation |
| Load reduction | Reduce load on foundation solids, reduce settlement, increase slope stability | Geofoam and foamed concrete |
| Reinforcement | Inclusion of reinforcing elements in soil to improve engineering characteristics; provide lateral stability | Mechanical stabilised earth, soil nailing, micro piles, geosynthetic, and reinforcement |
| Chemical treatment | Increase density, increase compressive and tensile strength, fill voids, form seepage cutoffs | Chemical and fracture grouts, bulk filling, jet and compaction grouting, and lime columns |
| Thermal stabilization | Increase shear strength, provide cutoffs | Ground freezing, heating, and vitrification |
| Biotechnological stabilization | Increase strength, reinforcement | Vegetation in slopes, and microbial methods |
| Miscellaneous | Remediate contaminated soils | Electro kinetic methods, chemical methods |

Source: Schaefer et al. (2012)

Table 2.15 Classification of ground improvement techniques based on type of soils

| Type of soil | Ground improvement technique |
|--------------|--|
| Cohesive | Vertical drains, vacuum dewatering, stone columns, and in-situ deep mixing |

Table 2.15 Continued

| Type of soil | Ground improvement technique |
|--------------|--|
| Cohesionless | Compaction piles, vibro compaction, stone columns, dynamic compaction, deep blasting, and grouting |

Source: Herrmann & Bucksch (2014)

Referring to the previous study, the usage of ground improvement techniques depends on the type of soil. Non-cohesive soil known as cohesionless soils consisting of a gravel-sandy mixture which do not clump together will have low shear strength and hence, require backfill as a supportive material to provide additional strength. Besides, cohesive soils such as soft clay have low shear strength by having high moisture content and compressibility. This type of cohesive soil typically has a shear strength of not more than 20kPa since they are easily deformed when subjected to loadings.

Defective structure not only occurs due to the concrete reinforcement structural design, but the foundation itself is causing settlement from the expansive soil characteristics that lead to the cracking of the structure. The expansive property is mostly possessed by soft clay as the high amount of moisture content makes it difficult to be completely drained out. Scharifi et al. (2019) reviewed that preloading, stone columns, soil reinforcement with geotextiles, dynamic compaction, soil enhancement with additives, and sand and wick drainage columns are the most efficient methods for enhancing the qualities of soft clay soil.

2.7 Stone Column

The stone column method is a type of vibro-displacement technique where a cylindrical vibrating probe is used to displace the weak soil (Hasan et al. 2021), creating a stone column made up of good quality aggregate and compacted appropriately. According to Jamal et al. (2020), the failure modes of stone columns are general shear

failure, load shear failure, bulging failure, and failure by sliding. McKelvey et al. (2004) carried out experimental research on a collection of five stone columns and found that while the edge columns bulged away from the neighbouring columns, the central column deformed or bulged consistently. In real-life applications, geotechnical engineers build and construct a large number of stone columns for foundation design but the on-site acceptance tests will be conducted in either single column or group columns that consist of several single columns within that particular area.

Stone column which is made up of granular material and freely drained material has been successfully applied especially in isolated footings to provide independent support from the superstructure loading as it has higher frictional strength. The previous study showed that PET plastic has the potential to be used as a substituent material for granular in-stone columns, while the nature of granular material can speed up the consolidation settlement but minimize the post-construction settlement. Figure 2.14 shows the effectiveness between Ordinary Stone Column (OSC) and Encased Stone Column (ESC) on underlying foundation soil.

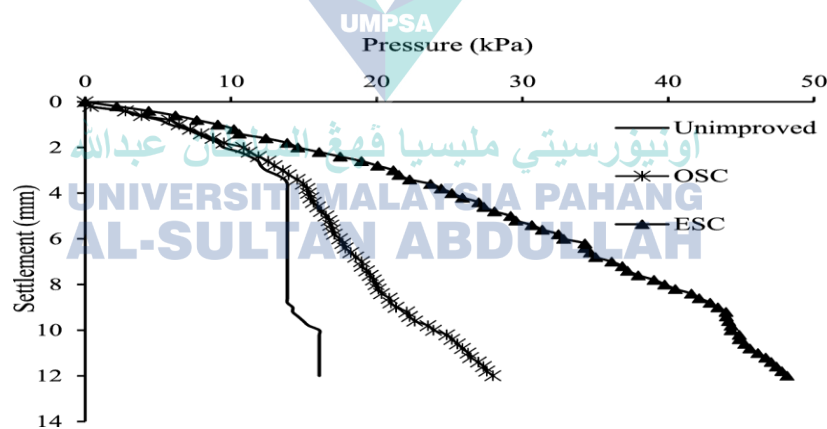


Figure 2.14 Effectiveness of Ordinary Stone Column (OSC) and Encased Stone Column (ESC) on underlying foundation soil

Source: Menon et al. (2021)

Nevertheless, it is found that the usage of stone columns in treating soft clayey soil has certain limitations that show no effects on certain parameters. A study conducted

by Mohanty & Samanta (2015) analysed that up to four times the diameter of the stone column, the top soft soil is found to influence the limiting axial stress of the entire improved soil. However, after that, the topsoil's clay content has very little of an impact on the treated soil's limiting axial stress. The clay particles will get clogged around the stone column and hence reduce the radial drainage when using the stone column (Mokhtari & Kalantar, 2012).

The installation of stone columns on the ground accelerates the rate of consolidation by providing an additional drainage path and reducing the excessive pore water pressure from the soil itself with the method of transferring the loads to the stone column. Compared with other alternatives to be used as ground improvement techniques, several reasons have made the researchers and developers investigate and apply stone columns where they include the risk relief of differential settlements, increase the stiffness of foundation system, improve the drainage condition, speed up the consolidation rate, enhance the soil bearing capacity, and economic alternatives.

Constructing a firm structure without settlement is impossible as the soil may change from time to time, especially the soft clayey soil. Inserting stone columns can reduce the differential settlement of soil but the settlement is influenced by several factors. According to Shien & Ann (2014), the settlement improvement factors for stone column groups are influenced by friction angle, bed thickness, column and soil stiffness.

Ground improvement by a stone column is affected by its design which includes column diameter, arrangement pattern, column spacing, replacement ratio, stress concentration factor, and the backfill of the stone column used. Other than the design factors mentioned that influence the stone column, Dheerendra Babu et al. (2013) found that the flexibility of the footing, the strength of the in-situ soil, the strength of the column material, and the installation process are some of the variables that affect how well this ground improvement technique performs overall. Thus, the insertion of stone columns to treat weak soil is not a replacement method. Due to its advantages in using stone columns

as compared to other techniques, the use of stone columns by vibro-replacement method has been a famous method around the world. Figure 2.15 shows the schematic diagram of installing a vibro-stone column.

Beena (2010) found that due to the installation of a stone column for a 10 mm settlement, the load-bearing ability of clay soil is raised by 74%, and its ultimate bearing capacity is further increased by 52%. Ng & Tan (2015) claimed that the stone column made up of high permeability material can have a permeability ratio of 100,000 times between the stone column and the surrounding soil but it depends on material grading with construction method.

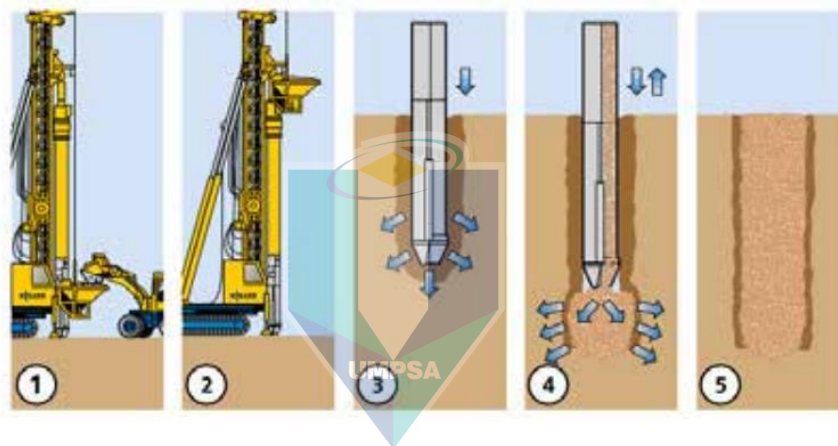


Figure 2.15 Schematic diagram of installing vibro stone column using dry bottom-feed method

Source: Sondermann et al. (2016)

Based on the arrangement of stone columns which is then classified into single and group columns, Lajevardi et al. (2019) presented the study of single and group columns arrangement and found out that placing other columns around the single stone column will lead to an increment in bearing capacity for 6.3%. In terms of formation pattern for group column arrangement, square formation of group columns is better than triangle formation as it shows an additional 5 % bearing capacity increment. Regardless of either single or group stone column installation, it can generally improve the rate of

consolidation of soil hence reducing the stress in soil. To further study the behaviour of stone columns that affects the rate of consolidation, the stress concentration ratio will be considered an important parameter to determine the relationship between them.

2.7.1 Physical Modelling of Stone Columns

The general design of a stone column consists of crushed stones, where installation in cohesive soil such as clayey soil is mostly designed as a load-bearing column by providing drainage, soil densification purpose, and acting as reinforcement for the neighbouring soil mass (Najjar, 2013). A favourable situation for using stone columns in clayey soil with an undrained shear strength of soil is from 7 – 50 kPa, associating with the sand-column clay system referring to the fundamental theory Young's Modulus (Najjar et al., 2012).

Based on the study by McKelvey et al. (2004) investigated that punching was widely known in shorter columns while bulging showed significant long columns. Although several effects may be detected using different lengths of columns, they show great improvement in the soil-bearing capacity when carrying more loads. Beyond the column length approximately six times its diameter, the stone column used beneath the ground shows no improvement in terms of the load-carrying capacity. Referring to the arrangement of stone columns, it is needed to determine the suitable length or optimum column length to achieve the highest improvement and saving cost of construction in a foundation system, especially in footing design.

Some typical stone columns installation such as the vibro-flotation method are commonly applied as it is practical for weak natural soils and fills, where silty-clayey soils are mostly known for this technique. This technique consists of mechanical vibration using a water or air jet to compact the soil particles to a more densified state. Since the stone column will be beneath the ground, it will increase the lateral deformation when it receives the loading from the superstructure. Besides, the axial capacity of stone columns

is derived from the development of passive earth pressure due to the bulging effect of the column. Moreover, it is less effective using stone columns for very sensitive clays where settlement risk is higher as this kind of clay shows an insignificant effect in providing lateral restraint.

Generally, using stone columns as an improvement method is gaining popularity worldwide including ASEAN countries as it is a distinctive method in improving the bearing capacity and reducing settlements of soft soils. Since the beginning of the idea of applying stone columns, many researchers and engineers have conducted relevant modelling of stone columns to deeply analyse the reaction and its behaviour when applied in different conditions. Mohanty & Samanta (2015) used a physical and numerical method and found that the behaviour of stone columns in the soil is largely dependent on the thickness and physical properties of the first layer of soil. carried out the laboratory physical model to determine the nature of stone columns, especially the behaviour of stone columns when installed in soft soil. Mohtasham & Khodaparast (2018) conducted a numerical analysis of a single stone column of 10 m in length and noted that an increment in stone column length at a given replacement ratio will have significant effects on the reduction of soil subsidence time but if it does not show improvement in reducing drainage spacing between clayey soil, it will not sharply improve the consolidation rate.

Regarding the design of the stone column, the diameter of the stone column is determined by the layers of soil penetrated and their characteristics such as undrained shear strength, and total amount of energy applied, and it may vary over its length, mainly depending on the resistance of different layers penetrated. Besides, the formation of the stone column through compaction is achieved through a vibrating probe or ramming, and hence, the characteristic of the vibrating probe is another consideration in the design. Mukul C. Bora (2010) conducted a modal test on footing stone columns which were reinforced with a clay bed with constant clay undrained shear strength of 5 kPa. The crushed stone aggregate with a particle size of 2 – 10 mm was used to construct a stone column with a diameter of 100 mm while the clayey soil had a liquid limit, plastic limit,

and plasticity index of 40%, 21%, and 19 respectively. The clay soil bed and its construction dimensions were built with 1000 mm x 1000 mm x 13000 mm (depth).

The installation of the stone column was drilled in the influence zone of the subsoils, the length of the stone column even approximately the same as its diameter will show a significant increment in the performance of the foundation bed. Jamal et al. (2020) reported the stone column is applicable to provide support and increase load-bearing capacity with significant settlement reduction for isolated footing, large raft foundations, and embankments. Proper design of stone columns includes the consideration of the stress concentration factor and this factor relies on the soil stiffness and the built-in stone column on that particular soil.

2.7.2 Failure Mechanism of Stone Column

Although the use of stone columns can increase the bearing capacity of soil, it might cause failure under a limit of compressive load, where it translates into a larger value of confining pressure when it is fully compacted under certain loadings. According to Najjar et al. (2010), the authors used 100kPa, 200kPa, and 400kPa of confining pressure and reported the confining pressure presented a significant effect towards the sand columns. The shear failures of stone columns relate to the geometry, soil type, and loading situation. Figure 2.16 shows the single and group stone columns under different types of situations. Najjar (2013) stated the happen of the failure of stone column is due to the increase in pressure which is generated from the load exerted on the footing.

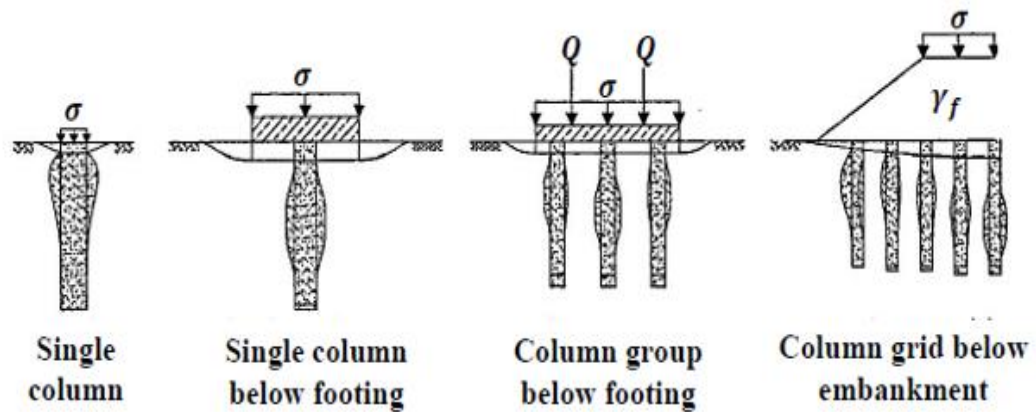


Figure 2.16 Single and group stone columns under different type of situation
Source: Kirsch & Kirsch (2016)

Referring to Figure 2.16, the interaction of load application between footing, column, and soil in the foundation system have distinct interactions, where the design of the stone column is linked to the design of the foundation system in either the footing or raft system, the foundation stress developed depends on the stiffness of the stone column and soil. The relationship between the stiffness level of soil on the ground or compacted aggregate used in stone columns and the contact stress level has shown a directly proportional relation.

2.7.2.1 Single Stone Column

Jamal et al. (2020) mentioned a single stone column can be constructed on a firm stratum under soft soil by end bearing capacity or as a floating column with the tip of the column embedded in it. The tip and skin resistance that affect the single stone column as a pile foundation relies on the lateral confinement that produces strength where it is dependent on the transmission of load from superstructure by inducing the lateral earth pressure from soil to column Kirsch & Kirsch (2016). The bulging of the stone column becomes obvious as the lateral stress increases in the soil, leading the shape to deform depending on the lateral stress exerted on the stone column. Ghanti & Kashliwal (2008)

found the failure mechanism of the single stone column in several modes by referring to Figure 2.18 and they are as follows.

- i. Long stone column with firm or floating support – Bulging failure
- ii. Short column with rigid base – Shear failure
- iii. Short floating column – Punching failure

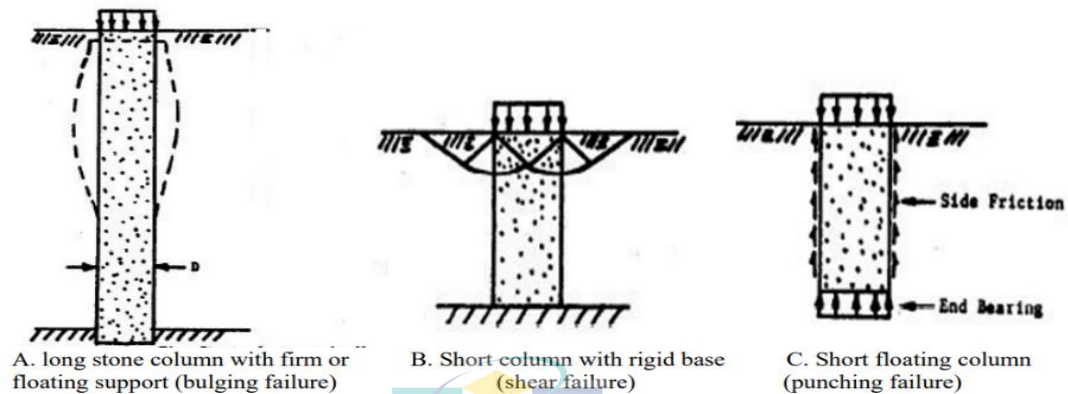


Figure 2.17 Failure mechanism of single stone column in a homogeneous soft layer
Source: Ghanti & Kashliwal (2008)

The reason behind the long column in either a floating or firm base is a failure in bulging because its length is generally greater than the critical length beneath the soil when the neighbouring soil is unable to give additional support to overcome the lateral stress. The critical length shown in Figure 2.17 (a) is approximately 2 to 3 times the diameter of the entire length. From Figure 2.17 (b), a short column is defined as having more than its critical length being built in a rigid base or end bearing will generally have shear failure. While for floating column situations, it will fail in punching failure for a short column as shown in Figure 2.17 (c). Mukul C. Bora (2010) reported that if the length of a stone column is less than 3 times its diameter, it will have no effect on bulging risk and when the loading is applied, it will simply punch through the soft clay.

2.7.2.2 Group of Stone Columns

Single and group stone columns are different as group columns will interact with each other as both give supporting effects and can prevent the expansion of the adjacent columns from experiencing failures. Wood & Mair (2010) demonstrate the modes of failure mechanism developed in the group of stone columns as shown in Figure 2.18 which are bulging, shear failure, punching, and bending or buckling. For the installation of group columns, replacement, and displacement techniques are to be used for them in the soft soil. The replacement technique involves the extraction of the original soft soil at a certain amount then only replacing it with a specifically designed stone column while the displacement technique is directly installing the stone column on the soft clay soil without removing any soft soil at first.

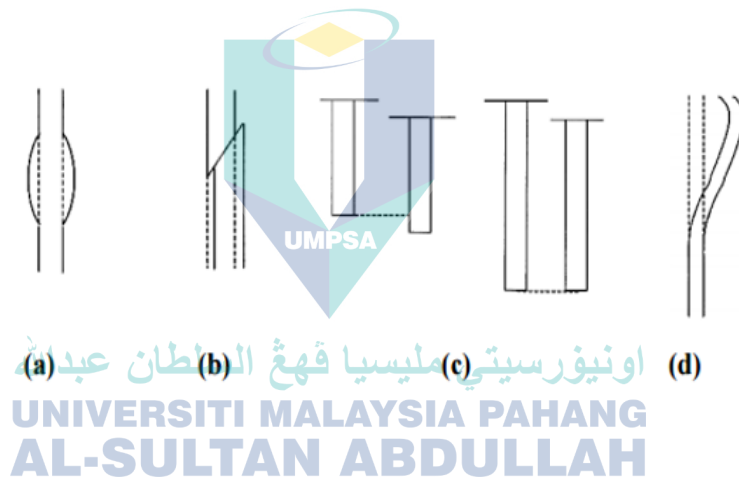


Figure 2.18 Modes of failure mechanism develop in group of stone columns

(a) Bulging (b) Shear Failure (c) Punching (d) Bending (buckling)

Source: Wood & Mair (2010)

Based on the study by Muir-Wood et al. (2001) for the analysis of the deformation behaviour of group floating stone columns were setting the length to its column diameter (L/d) between 6 to 15 by applying loading at a constant rate of displacement through a rigid circular footing on reconstituted kaolin clay. The authors classified four types of failure modes which are bulging, shearing, punching, and bending column bulging occurs

due to the lateral restraint provided by the neighbouring columns, while bulging magnitude turns larger as the bulging depth increases with the area ratio.

Beneath the footing edge approaching the ground surface, shearing failure was notified when low lateral restraint was provided to the columns. When the column's length is not long enough to transfer the load to the ground, punching failure occurs and is likely to happen for columns that have a low area ratio or closely spaced columns, while bending mode was noted when lateral loads were imposed on the columns. Figure 2.19 presents photographs of deformed floating sand columns on reconstituted soft clay. The authors concluded that the existence of critical length of columns but the footing diameter affects the strain in the column but not the column diameter itself.

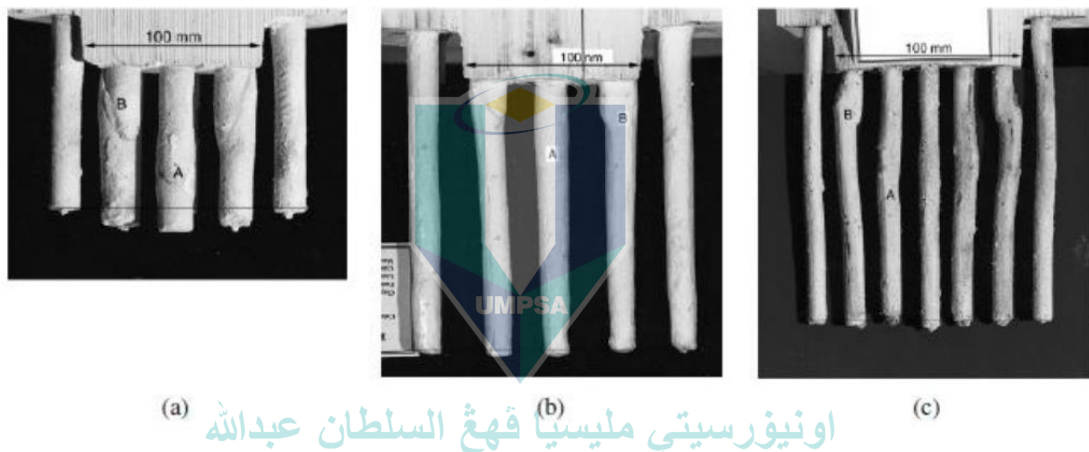


Figure 2.19 Photographs of deformed sand columns exhumed at the end of the footing penetration

(a) Bulging failure (b) Shearing failure (c) Bending failure

Source: Muir-Wood et al. (2001)

According to McKelvey et al. (2004), the authors conducted a similar experiment (see Figure 2.20) to Muir-Wood et al. (2001) but the floating stone columns were beneath circular, strip, and pad footings, setting the same columns length for $L = 6d$ and $10d$. Another significant research reported that beyond the critical column length of $6d$, it showed no increase in its bearing capacity, but the undrained stiffness of footing was

reported to have increased beyond 6d. Figure 2.21 shows the photos for the typical loading configurations for single and group columns in clay.

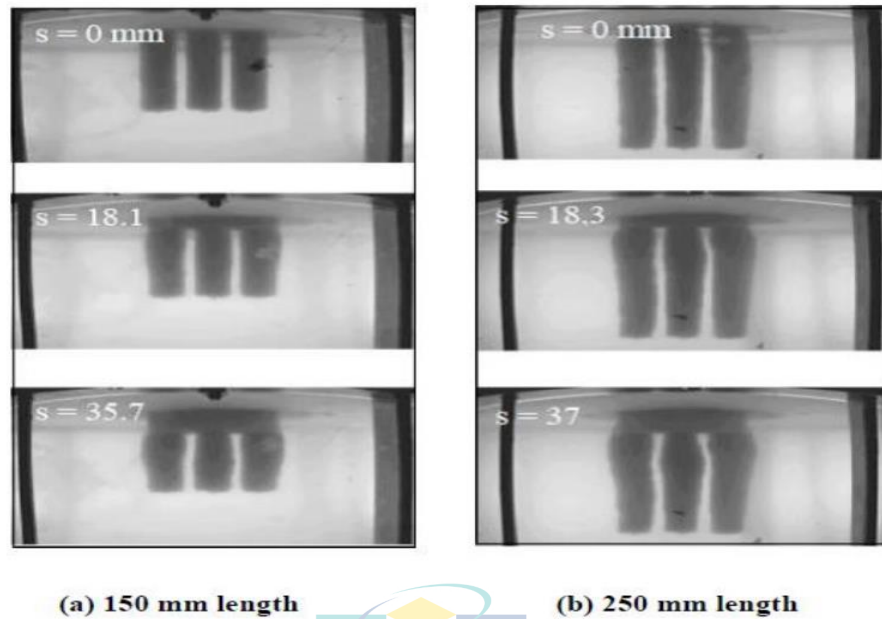


Figure 2.20 Photographs of group of sand columns beneath the strip footings
(a) $L/D = 6$ and (b) $L/D = 10$

Source: McKelvey et al. (2004)

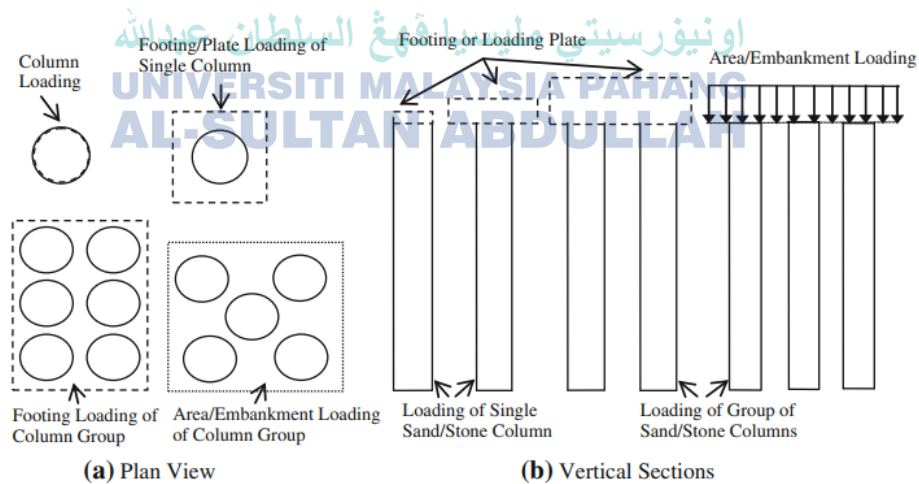


Figure 2.21 Typical loading configurations for single and group columns in clay

Source: Najjar (2013)

2.7.3 Undrained Shear Strength of Reinforced Clay

A long stone column built on soft clay for a length of 2 to 3 times its diameter when it is under an applied vertical load and the lateral passive resistance surrounding the soil mass can cause a bulging effect. Fattah & Majeed (2012) concluded a very soft clay ground condition such as peat soil is when the undrained shear strength, C_u is less than 15kN/m^2 . Karkush (2018) found that the floating stone column enhances the degree of ground improvement as it reduces settlement corresponding to the failure load by 86% for group stone columns and 57% for single stone columns. Several factors that can affect the reinforced soil are the properties of the material used for the stone column, replacement factor, loading patterns such as static and cyclic loads, and the radial drainage through the stone column. For group stone columns constructed on soft clay, the lateral confining pressure within the columns prevents them from undergoing bulging failure and then making them collapse. In the study by Najjar (2013), the authors made a design chart as shown in Figure 2.22 for determining the relationship between the ratio of column limiting stress by undrained shear strength of clay and stone column spacing by its diameter concerning soil friction angle. The authors summarized the applied loading towards the group stone columns that turned into stress will be certainly passed to the surrounding clay.

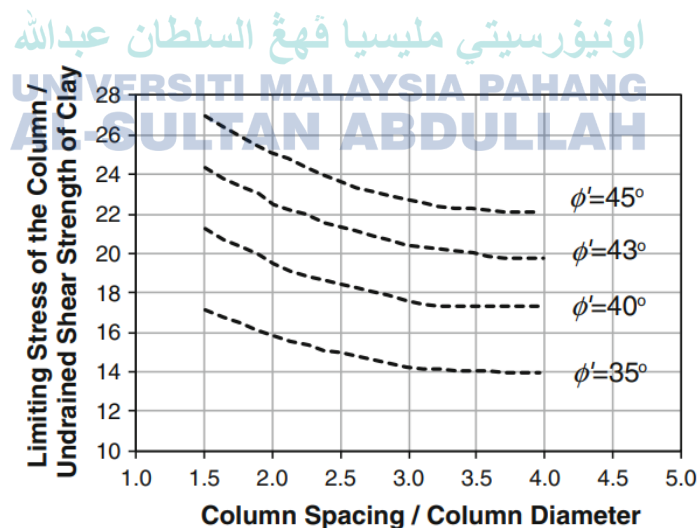


Figure 2.22 Design chart for stone columns

Source: Najjar (2013)

Lajevardi et al. (2019) conducted a small-scale laboratory test as it is important to analyse the performance of single and group columns on the clay bed with a constant undrained shear strength of 13kPa. Mukul C. Bora (2010) used a small-scale laboratory test on the characteristics of floating stone columns such as their load-carrying capacity, stone columns' deformation behaviour, and their interaction on clay bed with a constant undrained shear strength of 5kPa. Pivarč (2011) reported using laboratory tests to test the floating stone columns surrounded by clayey soil with a fraction of crushed aggregate ranging from 2 – 5 mm. However, all the authors used granular material as filling material to construct stone columns and thus, the stone column is better to refer to as floating granular columns. The design of the stone column by the soil profile should be known as the design should be varied, especially its depth to maximize its ground improvement effect so that it can be built up to the maximum strata that gives improvement to the foundation settlement.

The materials being used to fill the sand column are mostly non-cohesive soil or coarse grain material that can be sand or gravel, and because of non-cohesive properties, it is appropriate to reduce settlement and increase bearing capacity as it provides additional drainage and high permeability effect. The permeability effect makes the water to be easily drained out and prevents flowing within itself which will increase the pore water pressure internally. Dheerendra Babu et al. (2013) found that many researchers conducted laboratory tests and large-scale field load tests in determining the behaviour of stone columns as ground improvement techniques. The authors made a summary mentioning with a similar area replacement ratio, that the group stone columns will have a better reduction in the stiffness when making comparisons to single stone columns. Najjar et al. (2010) studied the characteristics of soft clay reinforced with sand columns and found out it was an improvement of undrained strength and decreased pore water pressure although at a low area replacement ratio specimen. Generally, the installation of stone columns using popular replacement material such as bottom ash and plastic provide additional strength for the soft clay. Moreover, a partial penetrating column and fully penetrating column has always an issue with their performance in improving the soil but

theoretically, partially penetrating column which has a certain length being constructed beneath the ground can balance the stress from the superstructure loading and transmit some loading to the ground thus giving better performance than fully penetrating column.

2.7.4 Critical Column Length

Critical column length is defined as the maximum measurement of a stone column mostly referred to its diameter installed in soil that provides the biggest improvement to the soil, while beyond the maximum measurement, it will not have any significant effect on the soil. Najjar (2013b) concluded the column length constructed to about 5 to 8 times its diameter, is the optimum length of a stone column for effective load transference from superstructure loading. Miranda et al. (2021) found that when the critical column length is decreased, it shows an increment in its area replacement ratio, soil strength, and soil stiffness. The authors also concluded that it is practical to apply the concept of critical column length such as footings or small groups of stone columns because larger structures like embankments where the critical length is larger than the soil thickness is no longer appropriate to apply this concept.

Aghili et al. (2021) reported the group stone columns being built on soft clay was seen as obvious on lateral deformation experiencing bulging, where columns bending were more obvious. The floating column with a length of 6m was having serious deformation compared to the full-length penetrated column with a length of 10m. The authors also mentioned that the encasement of stone columns can prevent the column from experiencing bulging extending to a more considerable depth. For encased stone columns, the highest deformation occurred at a depth beginning at twice the column diameter and continuing until 5.65 times the column diameter. The column material used such as gravel, undrained shear strength of soft clay, friction angle of soil, and material geometry can generally affect the critical column length. Dheerendra Babu et al. (2013) stated that the safety factor is significantly increased with increasing the equivalent width of the stone column and friction angle of column materials. The authors made a summary

pointing out the reduction in settlements and horizontal displacement, increment in improvement factor, and acceleration of consolidation through the increment of area replacement ratio and stiffness with a friction angle of column material since the possible column failure modes are going to occur at a deeper depth as the critical column length increases concerning the column diameter.

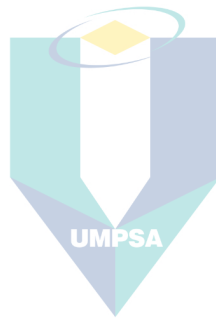
2.8 The Use of Correlation Technique in Shear Strength Parameters

The expected shear strength parameters which include shear strength value, soil cohesion, and friction angle that would be generated from the UCT and UU are correlated accordingly. As reported by Jun Shen et al. (2024), the shear strength parameters were correlated through the regression technique with the incorporation of column ratios. The regression equations are expected to be generated with the R^2 as the reference of accuracy of result. The above method was also applied by Hasan et al. (2021), in simplifying the variables. Coherent to that, the regression technique does not limit to the complexity of variables, however, it streamlines the equations to a simple formula in respect to the values.

2.9 Research Gap

The utilisation of stone columns as a ground improvement technique has been widely used in construction activities to resolve insufficient soil-bearing capacity and settlement risk issues through the practice of the sustainability concept. The current research which focused on applying the PET sands as a substituent of coarse aggregate in constructing the granular columns within a small-scale laboratory test can provide a new understanding of the PET material in treating the problematic kaolin clay soil. Many researchers had carried out studies using different materials in constructing stone columns and substituent materials to make a better improvement on it by complying the sustainable construction aspects.

Typically, installing stone columns from coarse material or non-cohesive soils such as PP plastic can reduce the pore water pressure within itself and increase overall stability. By referring to the previous research findings as the reference, this research determined the engineering properties of soft clay soil and PET sands, and the association of both materials to analyse the shear strength of the soft kaolin clay soil after being reinforced with single and groups of PET columns. This research also provided an understanding of the effect of the different effective confining pressures on the performance of single and group PET columns.



اونيفرسيتي مليسيا قهغ السلطان عبدالله
UNIVERSITI MALAYSIA PAHANG
AL-SULTAN ABDULLAH

CHAPTER 3

METHODOLOGY

3.1 Introduction

This chapter presented and introduced the entire experiment works including the detailed procedure of every required lab work, calibration work, laboratory testing, and program for data analysis. The first step was to choose a reinforcement method based on the material followed by the selection and collection of the required study material. Typical standards such as the American Society of Testing Material (ASTM) and British Standard (BS) were applied for the classification for suitability and availability of equipment tested on the selected material for research purposes such as kaolin and PET sand. Figure 3.1 presented the flow chart for the methodology process.

In this chapter, the overall model test setup with method, material testing, and typical procedures were discussed and explained in detail.

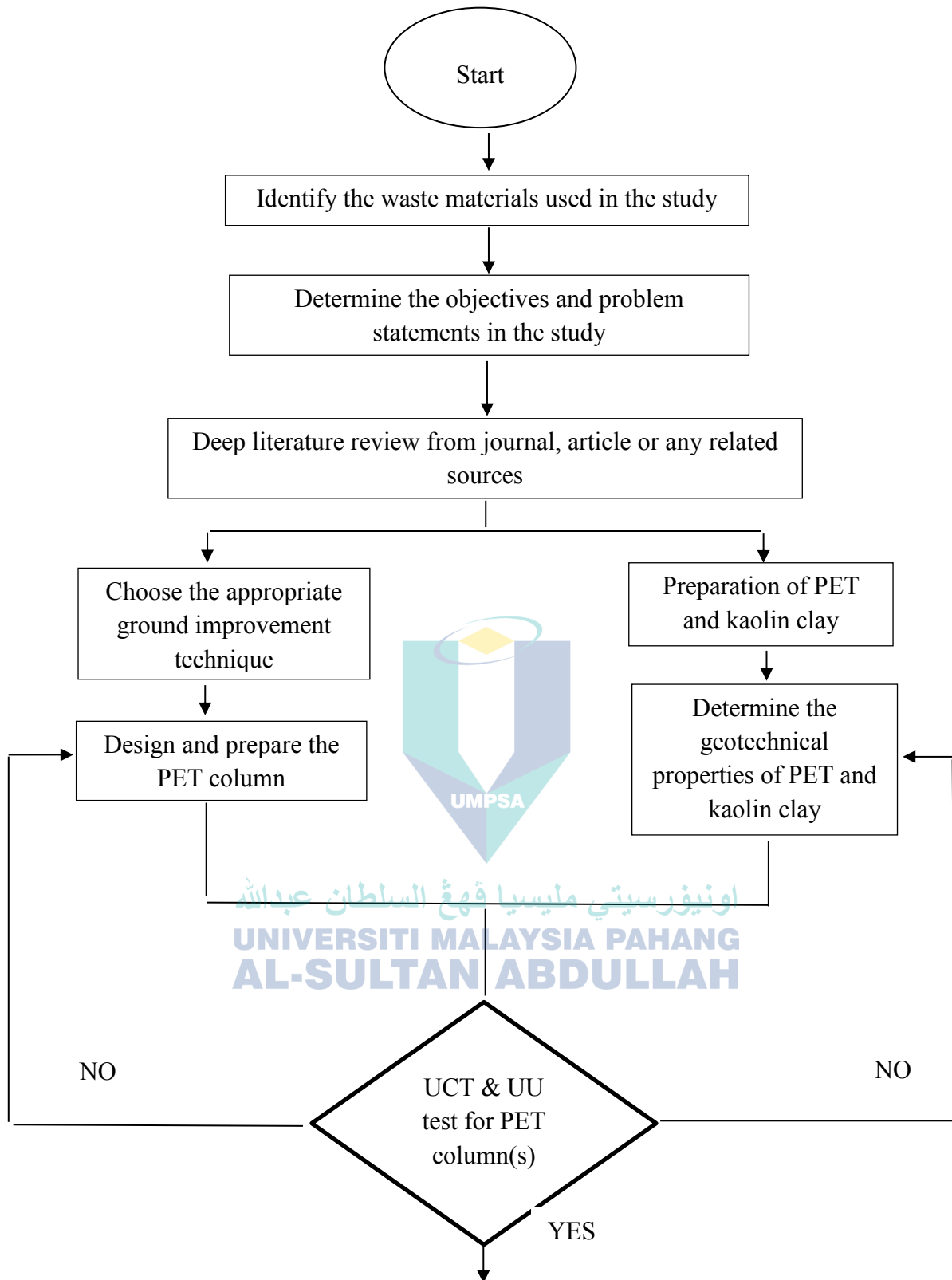


Figure 3.1 Flow chart for methodology process

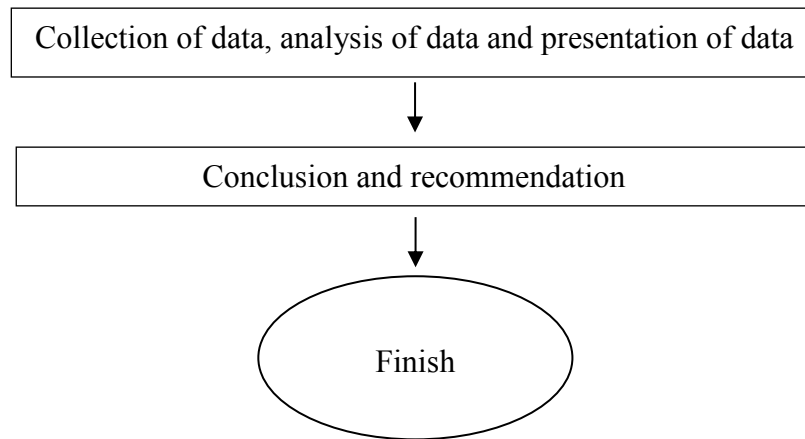


Figure 3.1 Continued

3.2 Selection of Ground Improvement Technique

Through the identification of objectives for this study and its problems, practical solutions for solving the problems and fulfilling the objectives were required through the suitable ground improvement technique. Besides, the selected improvement technique prioritized the sustainability concept as it dealt with the environmental problem with impacts, and the execution of vibro-replacement method was practical and appropriate within the laboratory scale.

By considering various factors including the soil condition of kaolin clay S300, scale size of the research, appropriateness of replacement material, and the supporting data from previous researchers, the stone column technique from all the available techniques was selected to treat the soft clay soil as it improved the shear strength parameters. After the selection of the technique, the next step was to choose a suitable material that meets the basic requirement for the substitution of coarse aggregate in the stone column.

3.3 Selection of Materials

The required material for the research was confirmed and identified by referring to the previous similar research data. The main selected material for this research was PET which was purchased from Glowmore Express Sdn. Bhd., where the PET plastic came in the sand form where they were crushed to a certain particle size as shown in Figure 3.2(a). Referring to the research objectives, PET plastic was used as a substitute material in stone columns to replace coarse aggregates such as sand and gravel. Besides, a replacement method was applied for the installation of PET in soft clay. Furthermore, the raining method was chosen as it was the best method to create homogeneous PET columns in the clay specimens.

The selection of second material in the research, kaolin clay S300 was referred to the previous study conducted by other researchers to make homogenous soft clay samples as shown in Figure 3.2(b). The kaolin powder was purchased from Kaolin (M) Sdn. Bhd, which is located in Selangor, Malaysia. The kaolin clay was prepared from kaolin powder Grade S300 as the main material for producing the repeatable homogeneous soft clay samples. Besides, in terms of price, kaolin had the advantage that it was cheap and accessible. Kaolinite was a clay mineral with a chemical composition of $\text{Al}_2\text{Si}_2\text{O}_5(\text{OH})_4$ that meant for aluminum silicate hydroxide which can be easily to form water as it had a hydrophilic platy structure, having the ability to mix with or absorb water creating a slurry to generate uniform soft clay.



(a)



(b)

Figure 3.2 The raw materials for geotechnical testing
(a)PET sand (b)Kaolin clay S300

3.4 Determination of Physical, Mechanical and Morphological Properties of the Materials

The diameter of the column and the particle size of granular material play an important role in choosing the appropriate size of the column to be used in the model tests. In this research, the stone column diameter used was ranging from 0.6 to 1m. The design of the diameter for the PET column in this study ranged between 10 to 16 mm, and for the laboratory test, the PET plastic particles were determined by sieve analysis. To analyse the properties of kaolin and PET, the required tests by its standard and method were presented in Table 3.1.

Table 3.1 Test standard with methods for the kaolin clay S300 and PET

| Material | Tests | Standard/ Method |
|----------------------------------|-------------------------------|----------------------------|
| Kaolin Clay S300 | Atterberg Limit | |
| | - Liquid Limit | BS 1377: Part 2: 1990: 4.3 |
| | - Plastic Limit | BS 1377: Part 2: 1990: 5.3 |
| | Particle Size Distribution | |
| | - Hydrometer | BS 1377: Part 2: 1990: 9.6 |
| | Compaction | |
| | - Standard Compaction | BS 1377: Part 4: 1990: 3.3 |
| | Specific Gravity | BS 1377: Part 2: 1990: 8 |
| | Permeability | |
| Polyethylene Terephthalate (PET) | - Falling Head | BS 1377: Part 5: 1990 |
| | One-Dimensional Consolidation | ASTM D 2435 |
| | Particle Size Distribution | |
| | - Sieve | BS 1377: Part 2: 1990: 9 |
| | Specific Gravity | BS 1377: Part 2: 1990: 8 |
| | Compaction | |
| | - Standard Compaction | BS 1377: Part 4: 1990: 3.3 |
| | Direct Shear | BS 1377: Part 7: 1990: 4 |
| | Permeability | |
| | - Constant Head | BS 1377: Part 5: 1990 |
| | Relative Density | BS 1377: Part 4: 1990: 4 |

Since it was to replace a certain portion of coarse aggregate such as sand or gravel, the particle size distribution of PET was decided to follow the range of sand particles so that it can construct vertical stone columns that are reinforced with soft kaolin clay.

3.4.1 Atterberg Limit

The moisture contents at which fine-grained clay and silt soils change between the solid, semi-solid, plastic, and liquid states were determined through Atterberg limits. Besides, the moisture content of clayey soil was also referred to as plastic consistency, using numerical expression can be the best way to measure its range. The particle size distribution of the test was according to the classification of fine-grained soil which was finer than 63 μm for the kaolin clay as it was important to classify and differentiate the type of soil used. While in Atterberg limits tests, it had a total of three different tests included which are liquid limit (w_L), plastic limit (w_P), and shrinkage limit (w_s) tests. However, for this research, only the liquid limit and plastic limit were carried out. The behaviour of the clay happened in the mentioned four (4) states, but it varied according to the moisture content. Through the utilization of a semi-automated cone penetrometer, as shown in Figure 3.3, the liquid limit test was carried out referring to the standards BS 1377: Part 2: 1990: clause 4.3. Another important test, the plastic limit was carried out referring to the standards BS 1377: Part 2: 1990: clause 5.3. The final value obtained from both tests produces the parameter, plasticity index which was according to BS 1377: Part 2: 1990: clause 5.4, a figure derived from the numerical difference between the liquid limit and plastic limit.



Figure 3.3 Cone penetrometer test

3.4.2 Particle Size Distribution

It was important to classify the particle size based on BS 1377: Part 2: 1990: 9 and ASTM D 422 for sieve analysis and hydrometer test while the finest particle size for coarse-grained soil was usually at $63\ \mu\text{m}$ while fine-grained soil was finer than $63\ \mu\text{m}$. Separation of particle size was conducted through two available tests which are sieve analysis and hydrometer test. Sieve analysis was practical for particle sizes larger than $0.063\ \text{mm}$ in diameter while fine analysis or hydrometer test was for particle sizes smaller than $0.063\ \text{mm}$. Knowing the particle size distribution from the applied materials in the study was crucial to give detailed information and further analysis of the engineering behaviour of the soil.

3.4.2.1 Sieve Analysis

The sieve analysis test was carried out to categorize the particles of soil by the sieve size opening where they were being retained through the mechanical shaker. Both main materials were analysed for their particle size using this test based on BS 1377: Part 2: 1990: 9, and further classify them following the standard soil classification. The test sieves used in this experiment were 6.30 , 5.00 , 3.35 , 1.18 , 0.60 , 0.30 , 0.15 , and $0.063\ \text{mm}$

for classification. The structure of the sieve sizes was arranged from the biggest sieve size opening at the top, then only followed the size in descending order. A pan was located at the bottom to collect the smallest particle size from the specimen used, while the retained soil was referred to as each sieve mesh aperture size. During the mechanical shaking process, a lid or cover was covered at the top of the sieves to prevent losing the specimen, and this process was run for 10 minutes. Afterward, the soil retained on each sieve was carefully transferred to the weighing process.

Separation and classification of soil particles were done based on the dry weight obtained in a certain size range, and then processing of data was done by plotting a semilogarithmic graph with a passing percentage of soil against particle size. All the data obtained from the results of PET were utilized for the analysis of the similarity of the material with the group of soil in the classification system.

3.4.2.2 Hydrometer Analysis

Fine grained soil which had the particle size passing the 63 μm or 0.063 mm sieve was determined using the hydrometer test based on the ASTM D 422: 1998. This test was designed based on Stoke's law stating that denser particles will sink faster than lighter particles when they were suspended in liquid, and assuming soil particles had the same specific gravity. It was analysed using kaolin only since it had 50% of particles that were finer than 63 μm . Figure 3.4 showed the hydrometer apparatus.



Figure 3.4 Hydrometer Apparatus

3.4.3 Compaction Test

The main purpose of conducting a compaction test was to determine the relationship between the optimum moisture content and the maximum dry density for kaolin and PET. For the compaction test, the Standard Proctor compaction test was used for the study as shown in Figure 3.5 following the BS 1377: Part 4: 1990: 3.3. The required equipment for this test were a 2.5 kg hammer and 1-liter capacity mould, applying a free fall method when compacting the three layers of soil and material. The layer was compacted layer by layer by dropping the 2.5 kg hammer from a distance of about 30 cm from the tip of the hammer to the soil with 25 blows per layer. In this test, the new materials were replaced for different moisture content, and from the results obtained at every different moisture content, a proctor curve was produced by plotting the graph of dry unit weight against the moisture content. From the graph plotted, maximum dry density and optimum moisture content were determined.



Figure 3.5 Standard Proctor compaction test

3.4.4 Specific Gravity

The determination of particle density was conducted on polyethylene terephthalate through the small pycnometer test based on BS 1377: Part 2: 1990:8. The mass of the specimen was transferred to the pycnometer bottle and added half or three-quarters of distilled water to then placed in the vacuum desiccators, processing the mixture until no further loss in air for 24 hours. The distilled water was then added to full and left for 1 hour before weighing it. To calculate the specific gravity of the materials, Equation 3.1 was used.

$$G_s = \frac{m_2 - m_1}{(m_4 - m_1) - (m_3 - m_2)} \quad 3.1$$

Where:

m_1 : mass of empty pycnometer (g)

m_2 : mass of the pycnometer + dry soil (g)

m_3 : mass of the pycnometer + soil + water (g)

m_4 : mass of the pycnometer + water (g)

G_s : specific gravity of soils

3.4.5 Permeability

Permeability or hydraulic conductivity of materials used was determined through its coefficient of permeability, where the constant head test based on ASTM D 2434 was for PET since it behaved similarly to coarse grain materials like sand. The equipment used was permeameter and three layers were formed from the material used. Each layer was tamped with 27 blows. Determination of the coefficient of permeability of the specimen was obtained through the collection of the data at certain intervals of time from the permeability test.

Similarly, for fine grain material for this case kaolin clay material, the coefficient of permeability was then determined by conducting a falling head test following ASTM D 2434. The equipment needed for this test was similar to the constant head test where this test used the lower half of the permeability cell with a burette while the constant head was using the constant head tank.

3.4.6 One Dimensional Consolidation Test

The objective of the one-dimensional consolidation test was used to determine the amount of settlement referring to the time taken for the soil sample to undergo consolidation and its volume changes when a laterally confined soil specimen was undergoing different vertical pressures. This test was conducted based on ASTM D 2435 where at the end of the test several parameters such as compression index recompression index, and the pre-consolidation pressure (maximum past pressure) of the specific soil can be obtained. Through running the program, data figures for the coefficient of volume compressibility and consolidation were obtained. The test was carried out by placing the specimen in the provided consolidation ring which was supported by a glass plate at the bottom, and the specimen was placed following the geometry of the consolidation ring where 75 mm in diameter and 20 mm in height as shown in Figure 3.6(a) and Figure 3.6(b). The density for PET and kaolin clay were obtained from a relative density test. The density from two main materials which are kaolin clay and PET played an important

role as they were needed for the following tests, Unconfined Compression Test (UCT) and Unconsolidated Undrained Test (UU) for their uniformity.

A micrometer dial gauge was used to measure the compression when the load was applied through the lever arm and while conducting the test, water was placed inside the specimen for constant moisture, each applied load was conducted for 24 hours. The subsequent test was re-started by increasing the load compared to the previous loading where the weight on the lever was 500g, 1000g, 2000g, 4000g, 8000g, and 16000g, and the unloading stage was carried through unloading the weight on the lever to $\frac{1}{4}$ of the last stage. After completing the above stages, the wet specimen was weighed and dried in an oven for 24 hours at 105°. The weight of the dried specimen was then weighted.

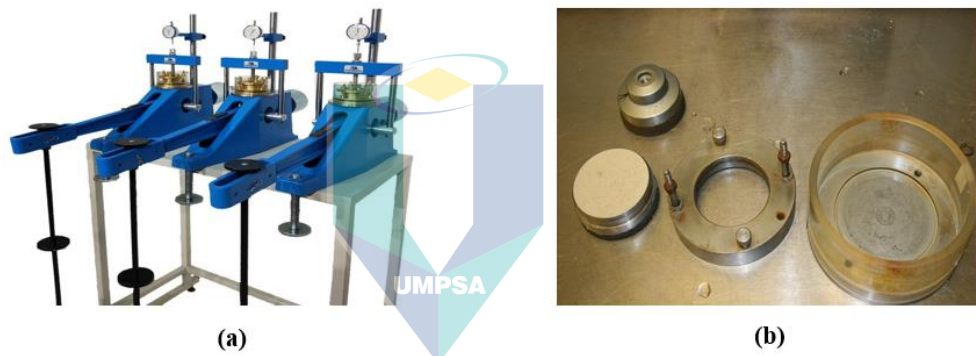


Figure 3.6 One dimensional consolidation test equipment
(a) Consolidation machine (b) Consolidation apparatus

3.4.7 Direct Shear Test

Direct Shear Test focused on the relationship between measured shear stress and limiting shear stress, where the failure occurs when shear stress was greater than limiting shear stress. This test was carried out based on BS 1377: Part 4: 1990: 4, while from conducting this test, certain parameters were obtained such as cohesion, c , and angle of shearing resistance, ϕ . The specimen used for this experiment was compacted up to its maximum dry density of 95%. This test primarily used a shear box by filling up the PET. The equipment used for the direct shear test was shown in Figure 3.7.



Figure 3.7 Direct shear test equipment

3.4.8 Relative Density

This test measures the denseness of the soil following BS 1377: Part 4: 1990: 4 when a load is applied to it. It was conducted by determining its relative density which was defined as the difference between the maximum void ratio at the loosest state and its natural in-situ density to the difference between the maximum void ratio at the loosest and densest condition of the soil used. In this research, the vibrating table was used and the sand replacement method was chosen for coarse grain material like sand but in this case was PET. By conducting this test, several parameters were obtained such as the unit weight of the specimen, and the maximum and minimum unit weight of the specimen. Therefore, the relative density of the PET used for forming the vertical column was computed by knowing the unit weight of the PET using Equation 3.2.

$$D_r = \frac{\gamma_{max}(\gamma - \gamma_{min})}{\gamma(\gamma_{max} - \gamma_{min})} \times 100\% \quad 3.2$$

In which:

D_r : Relative density

γ : Unit weight of current sample

γ_{min} : Minimum unit weight

γ_{max} : Maximum unit weight

3.4.9 Scanning Electron Microscope (SEM)



Figure 3.8 Scanning Electron Microscope model ZEISS EVO 50

This test was a microscopic examination to analyse the behaviour of PET in terms of its angularity, particle shape, and surface texture of the materials without the determination of chemical composition. This test was carried out by using the SEM model ZEISS EVO 50. The machine provided the detailed images with high resolution through scanning it. The machine scanning method operated in such a way that the focused beam of electrons will pass across the surface and detect secondary or backscattered electron signals. The images of the specimen were taken on photomicrographs (micrographs) and these images were captured by a microscope. For creating the vertical column, the range of PET particles used in the physical model study was not more than 2.36 mm. Figure 3.8 displayed the SEM model ZEISS EVO 50.

3.5 Determination of Shear Strength Parameters of the Material

The PET column from single and group category installed beneath the kaolin clay were examined through the UCT based on the ASTM D 2166, and the UU test were conducted following BS 1377: Part 7: 1990

3.5.1 Unconfined Compression Test (UCT)

The test was carried out following ASTM D 2166 where its main objective was to analyse the shear strength of cohesive soil such as clay by shearing it at a fixed rate of axial deformation without lateral confining pressure. An unconfined Compression Test was carried out on kaolin clay specimens that were reinforced with PET column since it was the appropriate method to determine the shear strength of soft clay samples reinforced with single and group PET columns. For this test, numerical data of axial load at failure and the corresponding axial strain were noticed.

By categorizing these specimens, it was then prepared the specimens with different area replacement ratios of 4.00%, 10.24%, 12.00%, and 30.72%. This section comprises different height penetration ratios that were being installed in kaolin clay where they were 0, 0.6, 0.8, and 1.0. There was a specimen labelled as a “controlled sample” since there was no reinforcement of the PET column installed in the kaolin clay specimen. Excluding the controlled sample, 52 samples of kaolin clay specimen reinforcement together were undergone unconfined compression tests. Referring to this number, it was further classified into 13 batches and each batch had 4 specimens with different penetrating heights. Theoretically, the value of undrained shear strength (S_u) of the cohesive soil obtained from conducting the test will be equivalent to the cohesion value but it's half of the value of unconfined compressive strength (q_u). Figure 3.9 showed the ongoing process of the UCT test for the kaolin specimen, followed by the Equation 3.3 as shown.



Figure 3.9 Unconfined compression test (UCT) on kaolin specimen

$$S_u = c = q_u/2$$

3.3

In which:

S_u : Undrained shear strength

c : Cohesion

q_u : Unconfined compressive strength



3.5.2 Unconsolidated Undrained (UU) Triaxial Test

The Unconsolidated Undrained Triaxial Test (UU) was conducted following BS 1377: 1990: Part 7 to determine the shear strength with its total stress of soft clay reinforced with single and group PET columns. For this test, it had 4 different types of samples with different area replacement ratios of 4.00%, 10.24%, 12.00%, and 30.72% used respectively, and thus, 39 samples were used in this test for analysis purposes.

It was a common type of triaxial test that determined the shear strength of soil for cohesive soil, especially clayey soil, and it was sheared at a fixed axial deformation rate until failure occurs then the test will only stop. Figure 3.10 demonstrated a prepared specimen was placed in the triaxial cell chamber on the platform of the compression

machine. After placing it, the piston was adjusted on the top part of the specimen as shown in Figure 3.11 followed by opening the valves to let the water flow into the triaxial cell chamber. When it was full of water and all the air had displaced through the air vent, the valves were closed afterward. The applied cell pressure, σ_3 was 100, 200, and 400 kPa respectively to the specimens tested through the chamber fluid where this step was followed by opening certain valves and setting the gauge to the required pressure. To prevent drainage from the specimen from occurring, all drainage to and from the specimen was closed after setting the required pressure. When reaching the strain of 20%, it was now releasing the chamber pressure together draining out the input water from the triaxial setup, reversing the compression machine, then lowering the triaxial cell, and lastly only shutting off the machine operation. After doing all the steps, the tested specimen was then carefully removed from the cell followed by disassembling all the setup.



Figure 3.10 Specimen was placed on the platform carefully

From Table 3.2, it showed the testing programme of UU triaxial tests with required parameters for unreinforced clay and clay reinforced with PET columns. After conducting the test, the shear strength of the kaolin reinforced with PET columns was calculated using Equation 3.4.

$$\tau_f = c + \sigma \tan \phi$$

3.4

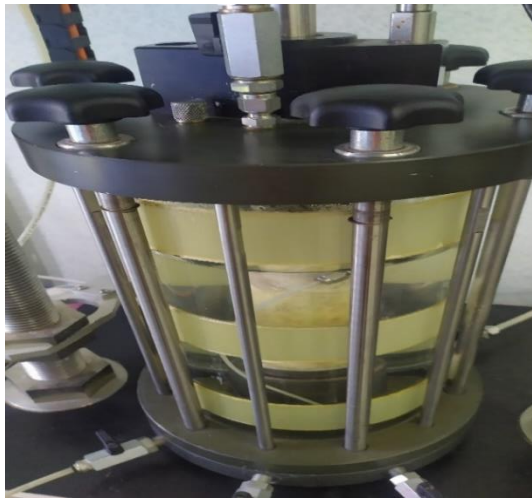


Figure 3.11 Soil specimens inside the triaxial chamber

Table 3.2 Sample of coding and testing programme of UU triaxial tests for unreinforced clay and clay reinforced with PET column

| Sample | Column Number | Column Diameter (mm) | Area Ratio, A_c/A_s (%) | Column Height (mm) | Column Height Penetrating Ratio, H_c/H_s (%) | Column Volume, (mm ³) | Volume Penetrating Ratio, V_c/V_s (%) |
|---------------|---------------|----------------------|---------------------------|--------------------|--|-----------------------------------|---|
| C | - | - | - | - | - | - | - |
| S1060 | 1 | 10 | 4 | 60 | 0.6 | 4712.39 | 2.40 |
| S1080 | 1 | 10 | 4 | 80 | 0.8 | 6283.19 | 3.20 |
| S10100 | 1 | 10 | 4 | 100 | 1 | 7853.98 | 4.00 |
| S1660 | 1 | 16 | 10.24 | 60 | 0.6 | 12063.72 | 6.14 |
| S1680 | 1 | 16 | 10.24 | 80 | 0.8 | 16084.95 | 8.19 |
| S16100 | 1 | 16 | 10.24 | 100 | 1 | 20106.19 | 10.24 |
| G1060 | 3 | 10 | 12 | 60 | 0.6 | 14137.17 | 7.20 |
| G1080 | 3 | 10 | 12 | 80 | 0.8 | 18849.56 | 9.60 |
| G10100 | 3 | 10 | 12 | 100 | 1 | 23561.94 | 12.00 |
| G1660 | 3 | 16 | 30.72 | 60 | 0.6 | 36191.15 | 18.43 |

Table 3.2 Continued

| Sample | Column Number | Column Diameter (mm) | Area Ratio, A_c/A_s (%) | Column Height (mm) | Column Height Penetrating Ratio, H_c/H_s (%) | Column Volume, (mm ³) | Volume Penetrating Ratio, V_c/V_s (%) |
|---------------|---------------|----------------------|---------------------------|--------------------|--|-----------------------------------|---|
| G1680 | 3 | 16 | 30.72 | 80 | 0.8 | 48254.86 | 24.58 |
| G16100 | 3 | 16 | 30.72 | 100 | 1 | 60318.58 | 30.72 |

C* Control Sample

3.6 Design of Polyethylene Terephthalate Column Model

3.6.1 Sample Preparation

3.6.1.1 Polyethylene Terephthalate Sample

Obtaining from the UU test, the prepared PET samples had the same characteristics such as density were also used for the installation of PET columns on the soft clay specimen. The PET sand was poured into the split form mould where they were lined with double-layer rubber membranes. After that, it was then positioned at the triaxial test apparatus. To prevent wastage and leakage during the pouring process of PET, double-layer rubber membranes can avoid this problem since PET behaved as a granular material, double layer rubber membranes were used to avoid any leakage occurred.

3.6.1.2 Kaolin Clay Sample

Figure 3.12 presented the soft kaolin clay specimen preparation process. The design of the moisture content was set to be 20% following the result obtained from the standard proctor compaction test of the air-dried kaolin powder as shown in Figure 3.12(a). Before pouring to the prepared kaolin specimen into the customized steel mould with 180 mm height and 50 mm internal diameter as shown in Figure 3.12(b), the mass

of kaolin for each specimen was set constant to ensure the uniformity of result. The prepared kaolin sample was mixed evenly with the determined moisture content as shown in Figure 3.12(c). The process was followed by compacting it with a 3.10 kg customized steel hammer up to 5 free fall blows, this process was repeated for 3 layers. To ensure minimum air trap inside the kaolin clay, it was then pressed at both ends of the customized mould as shown in Figure 3.12(d).

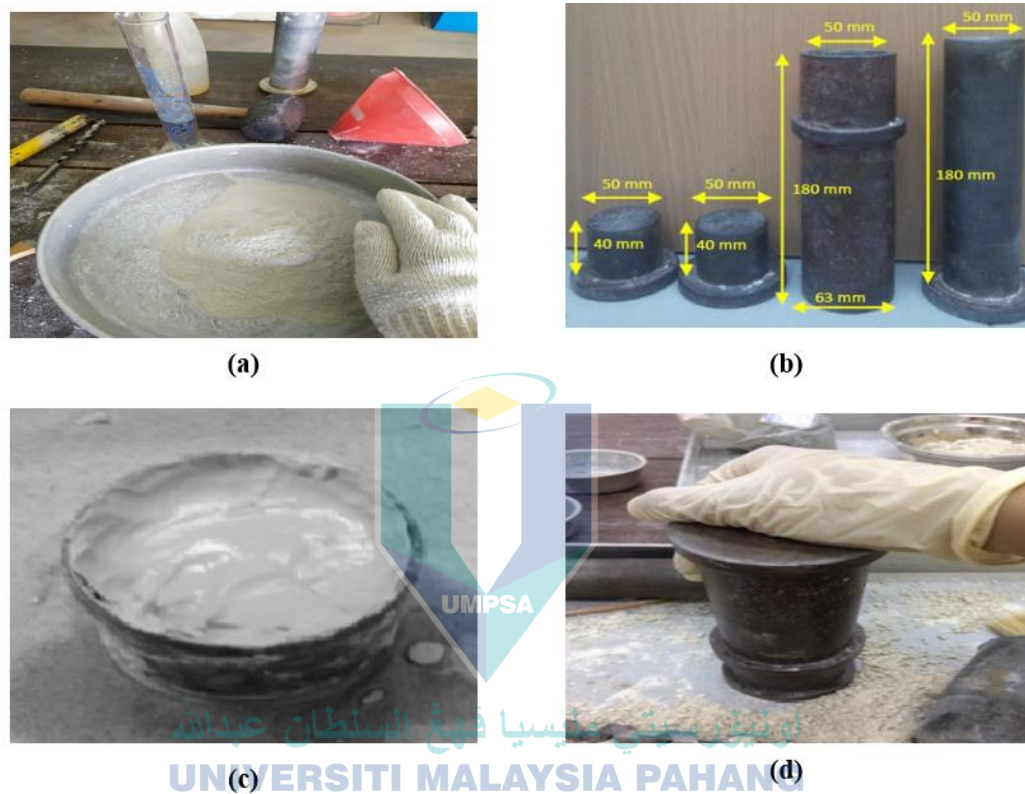


Figure 3.12 Soft kaolin clay preparation process
 (a) Prepare the kaolin clay powder (b) Prepare the customized steel mould (c) Compacted specimen in customized steel mould (d) Pressing of both ends of customized steel mould

3.6.2 Polyethylene Terephthalate Column Installation

It was a challenging process when drilling the kaolin sample for the installation of PET into the soft clay soil as shown in Figure 3.13(a). It was done based on the design in Table 3.3 as it should meet the drilled borehole diameter and then was placed carefully into the borehole. Besides, to perform the work accurately and easily, the raining method

was chosen as the best means to produce homogeneous PET columns in kaolin clay specimens.

During the pouring of PET, it was densified as being poured into the predrilled borehole of the soft clay specimen from 10 mm height as the fixed falling height through free fall from the tube to the clay specimen. The backside of the drilling bits was also used for compaction purposes as it compacted the PET sand to ensure minimum air trap or air voids between the particles. The compaction purpose can also make sure that the soft clay has the minimum disturbance during the preparation process. The volume of the predrilled hole was important as it was used as a reference for the mass of PET because required to maintain the uniform density for each PET column. By following all the mentioned steps above, the PET column produced that was reinforced with kaolin clay had the same density. The specimen was then extruded out and stored inside the special case as shown in Figure 3.13(b), and the last process was to let the pore water pressure inside the specimen be stable and hence, leaving it for 24 hours.



Figure 3.13 Preparation of PET column
(a) The hole diameter was drilled for 10 mm and 16 mm diameter (b) Extrusion of specimen and being stored in special case

Table 3.3 Density of various dimensions of PET columns installed in kaolin specimens

| Column diameter (mm) | Column length (mm) | Volume (mm ³) |
|----------------------|--------------------|---------------------------|
| 10 | 60 | 4712.39 |
| | 80 | 6283.19 |
| | 100 | 7853.98 |
| 16 | 60 | 12063.72 |
| | 80 | 16084.95 |
| | 100 | 20106.19 |

3.6.3 Detailed Arrangement for PET Column

In this research, two types of groups of columns were studied including single and group PET columns. The single PET column was installed at the centre of the clay specimen while triangular pattern installation was carried out for the group PET column in Figure 3.14(a) Figure 3.14(b). This method was chosen due to it was easier to maintain the position and location and the group columns being installed on the soft clay where it is referring to the column spacing between each other. The spacing between the columns was chosen by evaluating the area ratio and the column area ratio for the overall clay area. Furthermore, the measurement and arrangement of columns were taken into account for several parameters that needed to evaluate the performance and arrangement of the column which are area replacement ratio (A_c/A_s), height penetrating ratio (H_c/H_s), and volume penetrating ratio (V_c/V_s). This method was carried out by locating the column in the middle, using fundamental mathematics to evaluate the location of the column according to the boundary so the applied load can transfer evenly to either a single or group column. The detailed arrangement of single and group PET columns installed in clay specimens were shown in Figure 3.15, where Figure 3.15(a) and Figure 3.15(b) were

for the single 10 mm and 16 mm diameter PET column, while Figure 3.15 (c) and Figure 3.15(d) were for the group 10mm and 16 mm diameter PET column.

Apart from that, some important parameters were considered including the column diameter and particle size distribution of the granular material used as substituent material in deciding the column size for the modal test, while according to Fattah & Majeed (2012), the most effective length to diameter ratio of stone column, L/d is found to be 7 – 8 for undrained shear strength of clay having 20 – 40 kPa, and 10 -11 for clay having 10 kPa. Generally, the stone column design had a diameter of 0.6 – 1.0 m and the particle size of crushed aggregate mostly sand or gravel varies between 20 – 75 mm. In this study, the design for the column diameters were between 10 and 16 mm whereas the particle sizes of PET were classified as coarse aggregate. The small-scale laboratory test designed the PET columns by considering its diameter within the limited area so that it can achieve the best performance.

Furthermore, the PET column diameter ranged between 10 to 16 mm, the area ratio which was the ratio between the area of the column to the area of the specimen (A_c/A_s) was 4% and 10.24% respectively. For group columns, the area ratio was 12% and 30.72% respectively. The height penetration ratio which was the ratio of the height of the column to the height of the specimen (H_c/H_s) were between 0.6 to 0.8 for partially penetrating columns and 1.0 for fully penetrating column.



Figure 3.14 Reinforced kaolin sample with PET
(a) Single PET column (b) Group PET columns

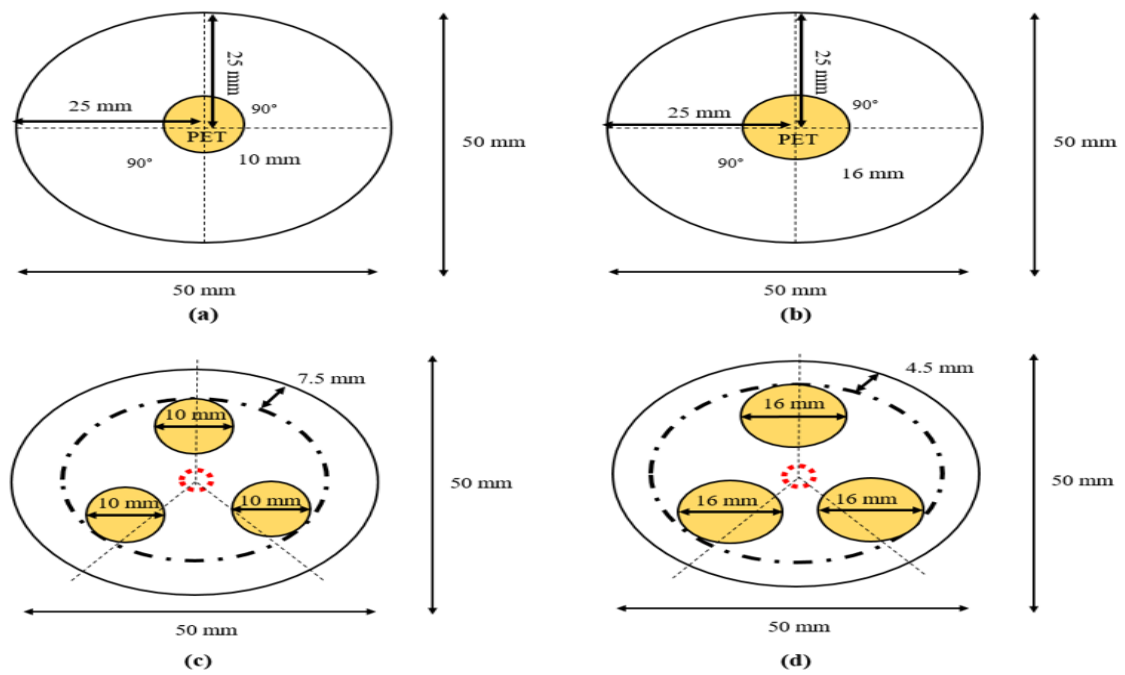


Figure 3.15 Detailed column arrangement for single and group PET column installed in clay specimens

(a) Single 10 mm diameter PET column (b) Single 16 mm diameter PET column (c) Group 10 mm diameter PET column (d) Group 16 mm diameter PET column

3.7 Summary of Methodology

The methodology focused on the determination of the physical, and mechanical properties of kaolin clay as well as PET plastic, where morphological study was only applicable for PET plastic to comply with the first objectives of the study. The required materials, kaolin clay S300 and PET plastic were used from the same manufacturer throughout the study. The installation of the PET column was carried out after preparing kaolin clay S300 with specific moisture content and then followed by the pouring of PET plastic to the specified diameter. The shear strength parameters were determined from the UCT test and UU test from the design of the PET column referred to in table 3.3 following the detailed arrangement from Figure 3.20. The values obtained was further analysed and correlated to comply with the second and third objectives of this study.

CHAPTER 4

RESULTS AND DISCUSSION

4.1 Introduction

This chapter focused on the discussion of the engineering properties of kaolin clay S300, PET plastic for the achievement of objective 1, while the shear strength parameters were obtained to achieve the objective 2 and 3 after the installation of single and group PET columns to kaolin clay S300. The parameters included were the particle size, specific gravity, moisture content, dry density, coefficient of permeability, shear strength, cohesion and soil friction angle. The tests involved for the determination of the materials engineering properties were Atterberg Limit, Sieve Analysis, Hydrometer, Specific Gravity, Standard Compaction, Falling Head, Constant Head, Direct Shear, and One-Dimensional Consolidation.

A total of 52 specimens were constructed specifically for these two tests. In comparison, UCT utilized 13 specimens and the UU test utilized 39 specimens as the UU test required 3 specimens for each trial where the shear strength, shear strength improvement, soil cohesion, and friction angle were determined.

4.2 Engineering Properties of Materials

The materials involved in this study were kaolin clay S300 and PET plastic, whose material properties were presented and summarized in Table 4.1 based on the relevant laboratory conducted, which met the objective 1. The details discussion and analysis began with the physical properties of materials which included the soil classification, Atterberg limit, relative density and the specific gravity. The next topic

focused on the interpretation of the mechanical properties of materials, comprised of compaction parameters, permeability and the one-dimensional consolidation result.

Table 4.1 Engineering properties of PET and kaolin clay S300

| Material | Test | Parameter | Value |
|-------------|----------------------------|-----------------------------|----------------------------|
| PET | Soil Classification | AASHTO | A-1-a |
| | Relative Density | Maximum Dry Density | 0.530 |
| | | Minimum Dry Density | 0.430 |
| | | Relative Density | 56.59% |
| | Small Pycnometer | Specific Gravity | 1.40 |
| | Constant Head Permeability | Coefficient of Permeability | 2.503×10^{-4} m/s |
| Kaolin S300 | Soil Classification | AASHTO | A-4 |
| | | USCS (Plasticity Chart) | ML |
| | Atterberg Limit | Liquid Limit | 35.39% |
| | | Plastic Limit | 29.51% |
| | | Plasticity Index | 5.88% |

Table 4.1 Continued

| Material | Test | Parameter | Value |
|----------|------------------------------|--------------------------------|------------------------------|
| | Standard Compaction | Maximum Dry Density | 1.54 Mg/m ³ |
| | | Optimum Moisture Content | 20% |
| | Specific Gravity | Specific Gravity | 2.62 |
| | Falling Head Permeability | Coefficient of Permeability | 4.197 x 10 ⁻⁸ m/s |

4.2.1 Particle Size Distribution

Based on the ASSTHO, the particle size distribution of PET plastic was under the group of A-1 and classified as A-1-a. From the result obtained from the sieve analysis, the PET plastic behaved like the coarse type material. The result was referred to **Appendix A** and Figure 4.1. For the kaolin clay S300, it was showing the behaviour of clay to silt based on the Hydrometer test. According to ASSTHO, it fell under the category of A-4, signifying that it was a low plasticity silt soil. The particle size of clay was ranging from 0.001 – 0.0625 mm and the value was supported by M. Hasan et al. (2021a) mentioned that the kaolin clay was an inorganic clay with medium plasticity which was similar to the study. The detail of the result was referred to **Appendix B** and Figure 4.2.

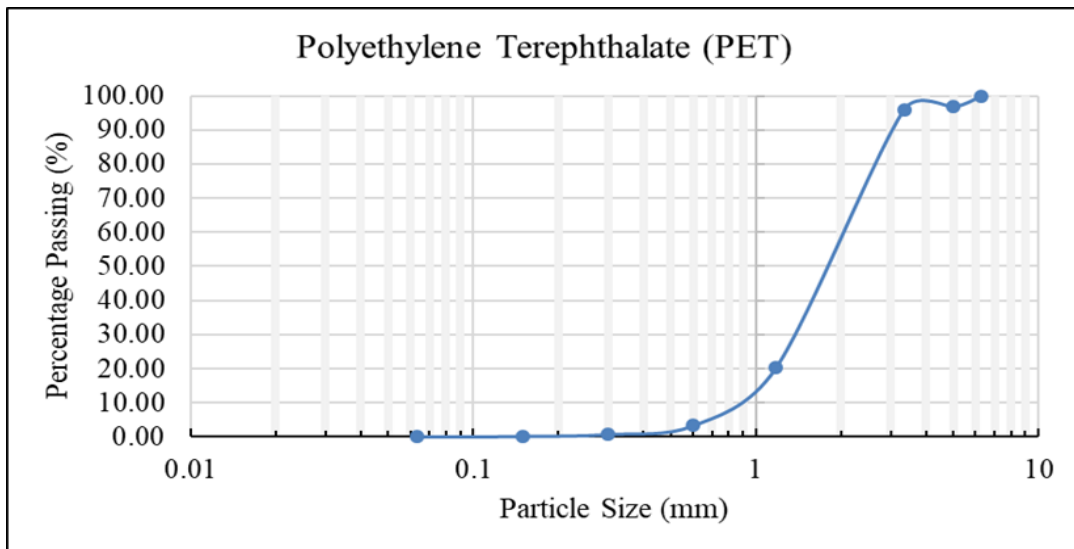


Figure 4.1 Particle distribution of PET plastic

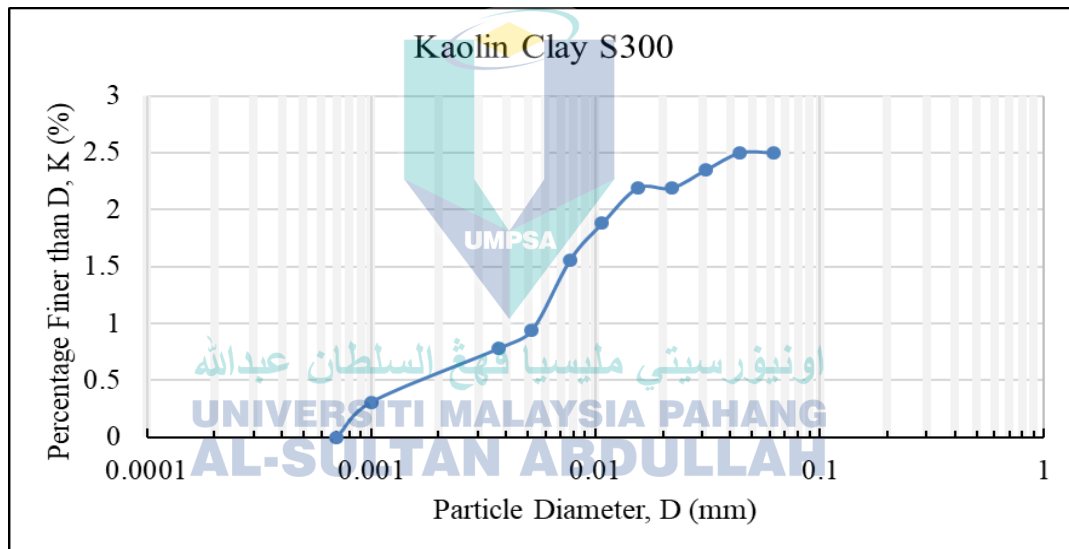


Figure 4.2 Particle distribution of kaolin clay 300

From Figure 4.1, it was noticed that the majority of the grinded PET plastic lied within 1 – 6 mm, and it was well graded coarse gravel type material with the C_c and C_u value of 1.25 and 2.22 respectively. According to Table 2.15, the PET plastic was also proven that this type of material behaved like gravel material from researchers Arulrajah et al. (2020). From their research study, the values of C_c and C_u obtained were 1.2 and

2.4, which were similar to the current study of 1.25 and 2.22 respectively. Based on all the values, it had been verified that the kaolin clay was fine grained soil with the similar trend, PET plastic was proven with the average coefficient of curvature, C_c as well as average coefficient of uniformity, C_u .

4.2.2 Atterberg Limit

The Atterberg limit test indicates that the behaviour of the kaolin clay behaves and transits within the states with the amount of water needed. It refers to the liquid limit and the plastic limit which will further obtain the plasticity index after calculation. From this study, the liquid limit and plastic limit obtained were 35.39% and 29.51% respectively based on the cone penetration test and hence, producing the plasticity index value 5.88% according to the ASTM standard. While based on another standard, USCS showed that the kaolin clay S300 was under the category of ML (red star as depicted in Figure 4.4), further proving that it was silty soil behaved slightly plasticity, which was similar like ASSTHO standard. According to Hasan et al. (2021), the researchers proved that the kaolin clay S300 fell under the category of ML, which was also supported by Hasan et al. (2016) which obtained the same result, showing that the kaolin clay S300 was low plasticity silt type of soil. The result of Atterberg Limit was presented in **Appendix C** and the graph between penetration and moisture content was shown in Figure 4.3.

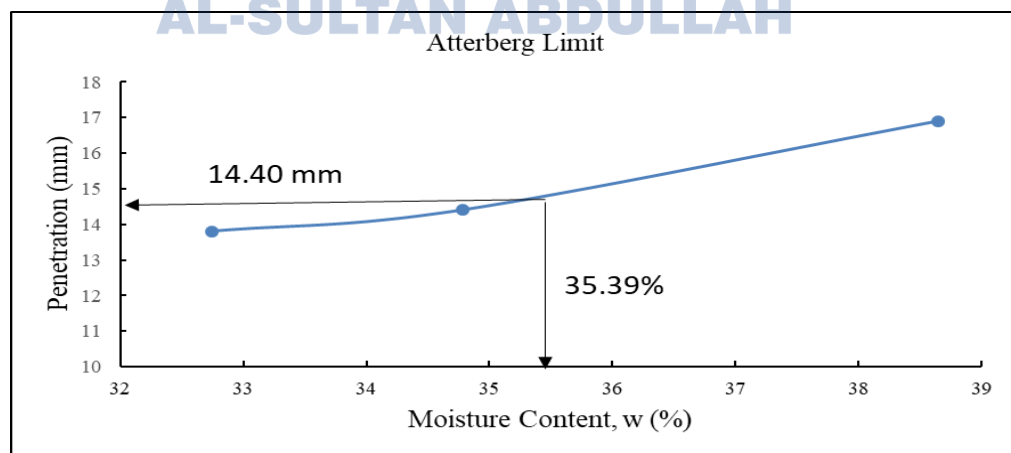


Figure 4.3 Penetration against moisture content

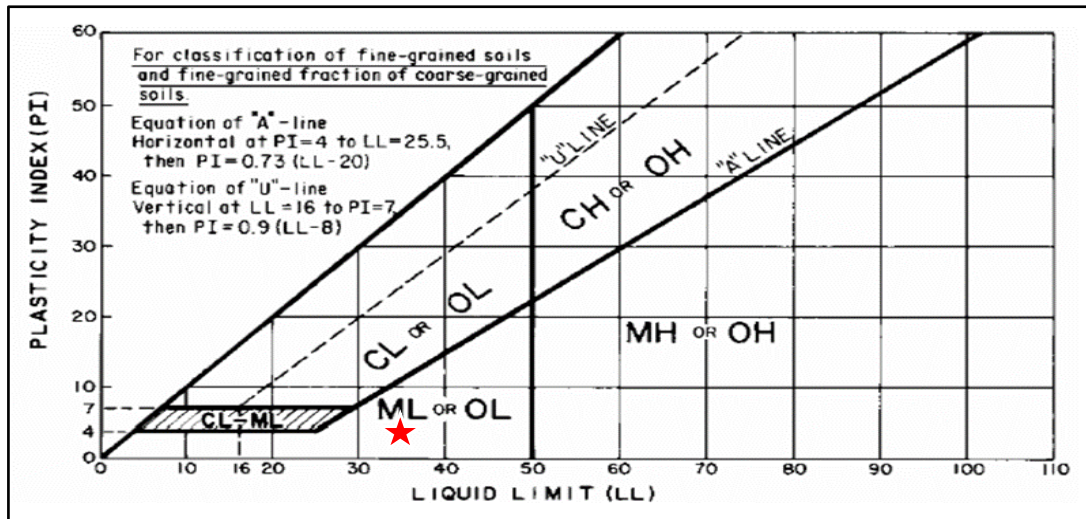


Figure 4.4 Location of kaolin clay based on the USCS chart

4.2.3 Relative Density

By using the relative density vibrating table, the minimum and maximum density obtained for the PET plastic were approximately 0.430 and 0.527 Mg/m^3 respectively. From the previous study by M. Hasan et al. (2021a), the PP plastic used as a granular material in acting as a column reinforcement has obtained minimum and maximum density, 0.56 and 0.76 Mg/m^3 respectively. Hence, the relative density of PET plastic was a less dense material as compared to PP plastic. The relative density of the PET column installed in the kaolin clay was referring to these values. During the PET column installation through the raining method, the average density of PET column was obtained as 0.480 Mg/m^3 and hence, the relative density of PET was analysed as 56.59 %. The addition of PET plastic associated with kaolin clay gives reinforcement effect as well as providing better vertical drain behaviour, it was estimated to accelerate the reduction of pore water pressure in the soil. The result of relative density was shown in **Appendix D**.

4.2.4 Specific Gravity

After using the formula of dividing the density of the materials used to the density of the water through the small pycnometer method, it was found that the specific gravity of PET plastic and kaolin clay was 1.40 and 2.62 respectively. In comparing with other researchers' values, the PET specific gravity value is 1.38 (Bozyigit et al. 2021; Deraman et al., 2021). However, researchers like Arulrajah et al. (2020) obtained 1.37, and Choudhary et al. (2018) found 1.30, and the average value of the researchers' values is 1.35. For kaolin clay S300, Hasan et al. (2011) reported the specific gravity value of kaolin clay was 2.65, which was close to the current study value. Other than PET plastic, Pham (2021) reported the LDPE plastic had 0.945 for the specific gravity value while Kassa et al. (2020) found that specific gravity for HDPE plastic was 1.33. Either it is a low-density PET or high-density PET, they have lower value than PET plastic. Hence, PET plastic is denser than LDPE and HDPE plastic as well as water. PET plastic specific gravity varies can be due to the grinding process of the PET plastic to different particle size from different sources of PET like PET plastic bottle as well as PET plastic container. Thus, the result obtained may not be accurately precise as the preparation process may be altered by different manufactures. The detail of the materials was being shown in **Appendix E**.

Table 4.2 Comparison between the PET specific gravity by different researchers

| Researchers | Specific gravity |
|-------------------------|------------------|
| Bozyigit et al. (2021) | 1.38 |
| Deraman et al. (2021) | 1.38 |
| Arulrajah et al. (2020) | 1.37 |
| Choudhary et al. (2018) | 1.30 |

As mentioned by researchers Kim et al. (2005), the low value of specific gravity of a material shows that it has a higher percentage of porous and popcorn-like texture of the particles within the specimen. It indicates that the higher the amounts of porous particles causes the reduction in specific gravity, proving it is an inversely proportional trend for this factor. PET plastic is likely to have a higher amount of porous particles while kaolin clay being a cohesive soil is less porous than PET plastic and hence the value difference between is more than 1. Jaafar et al. (2018) reported that the increment of carbon volume percentage in the tested material can cause decrement in specific gravity as the higher carbon volume makes the specimen to be lighter. Table 4.2 demonstrated the specific gravity of PET plastic analysed from the previous researchers.

4.3 Mechanical Properties

4.3.1 Compaction

Referring to the result from the compaction test, the maximum dry density and optimum moisture content of kaolin clay obtained were 1.54 Mg/m^3 and 20%. According to the results reported by Hasan et al. (2021), Aghili et al. (2021), and Zaini et al. (2022), the value of maximum dry density was 1.60 Mg/m^3 , 1.63 Mg/m^3 , and 1.61 Mg/m^3 respectively. However, Hasan et al. (2015) reported that the value was 1.53 Mg/m^3 , which was slightly smaller than the current study value and previous researchers' results. For the optimum moisture content value, there were three (3) reported values including 19.0% from (Hasan et al. 2021; Zaini et al., 2022), 19.5% from Hasan et al. (2014), and 20.0% by Aghili et al. (2021), where the current study reported the value was 20.0%. A summary table of the values was displayed in Table 4.3. The detail of the result was referred to **Appendix F**.

Table 4.3 Comparison between maximum dry density and optimum moisture content by different researchers

| Researchers | Maximum dry density (Mg/m ³) | Optimum moisture content (%) |
|----------------------|---|---------------------------------|
| Hasan et al. (2021) | 1.60 | 19.0 |
| Aghili et al. (2021) | 1.63 | 20.0 |
| Zaini et al. (2022) | 1.61 | 19.0 |
| Hasan et al. (2014) | 1.53 | 19.50 |

The dry density and moisture content are generally affected during the compaction test, where the compaction effort will alter the air void content inside the material. Besides, the size distribution of soil, shape of the soil and the foreign material content presence in the soil can also affect the result of compaction. Peddaiah et al. (2018) emphasized on the presence of foreign material like PET plastic with the amount of 0.4% will decrease the optimum moisture content to 16.8%. Furthermore, by comparison with other types of plastics, an increase of HDPE content will obtain high optimum moisture content but low maximum dry density, and the authors concluded that the 0.4% is the optimum amount of HDPE to obtain the best improvement M. Kumar et al. (2022) Similarly, the addition of a larger amount of PP fibre up to 2.0% into black cotton soil resulted in obtaining the largest value for maximum dry density and optimum moisture content Murthi et al. (2020)

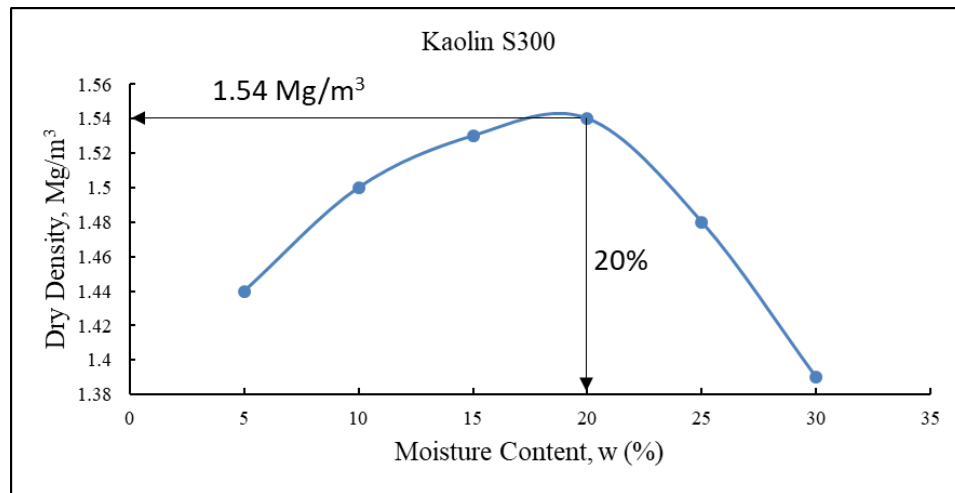


Figure 4.5 Relationship between dry density and moisture content of kaolin S300

4.3.2 Permeability

The permeability or hydraulic conductivity refers to the flow rate of water to pass a soil or substance, taking place in the air voids of soil. The value of permeability of PET plastic and kaolin clay S300 were 2.503×10^{-4} m/s and 5.197×10^{-8} m/s respectively as tabulated in Table 4.4 and Table 4.5. They were obtained from the falling head and constant head test. From the value of falling head test, it had the similar result with researchers Hasan et al. (2017) with the value of 1.124×10^{-9} m/s, the low permeability value of kaolin clay indicates the impermeable behaviour further proving that it has a poor drainage system to discharge the excessive water and thus facing difficulty to relieve the pore water pressure.

Table 4.4 The permeability result of PET by constant head test

| Test No. | Discharge volume, Q (cm ³) | Time, t (s) | Head difference, h | Permeability, k (m/s) |
|----------|---|-------------|-----------------------|--------------------------|
| 1 | 768.47 | 30 | 230 | 2.5206×10^{-4} |
| 2 | 759.31 | 30 | 230 | 2.4906×10^{-4} |

Table 4.4 Continued

| Test No. | Discharge volume, Q (cm ³) | Time, t (s) | Head difference, h | Permeability, k (m/s) |
|---|---|-------------|-----------------------|---------------------------|
| 3 | 763.49 | 30 | 230 | 2.5043 x 10 ⁻⁴ |
| 4 | 762.88 | 30 | 230 | 2.5023 x 10 ⁻⁴ |
| 5 | 761.73 | 30 | 230 | 2.4985 x 10 ⁻⁴ |
| Average permeability, $k_{avg} = 2.5033 \times 10^{-4}$ m/s | | | | |

Table 4.5 The permeability result of kaolin clay S300 by falling head test

| Test No. | Time, s | Head, h ₁ (cm) | Head, h ₂ (cm) | Permeability, k (m/s) |
|---|---------|------------------------------|------------------------------|---------------------------|
| 1 | 14400 | 50 | 48 | 5.1972 x 10 ⁻⁸ |
| 2 | 14400 | 50 | 48 | 5.1972 x 10 ⁻⁸ |
| 3 | 14400 | 50 | 48 | 5.1972 x 10 ⁻⁸ |
| 4 | 14400 | 50 | 48 | 5.1972 x 10 ⁻⁸ |
| 5 | 14400 | 50 | 48 | 5.1972 x 10 ⁻⁸ |
| Average permeability, $k_{avg} = 5.1972 \times 10^{-8}$ m/s | | | | |

While the coefficient of permeability result of PET plastic indicated that the 1.18 mm size was suitable to substitute inside the kaolin clay to provide a better drainage system with medium to high permeability degree. According to Arulrajah et al. (2020), the PET blends were categorized as poorly graded gravel or GP based on the USCS,

which had less than 5% of fines. The results were based on the **Appendix G** and **Appendix H**.

4.3.3 One Dimensional Consolidation Test

One Dimensional Consolidation Test or Oedometer Test was conducted using different applied load to the kaolin clay in a water submerging condition, turning the soft kaolin clay into saturated condition indicating that no excess water can be further absorbed by the clay. The test result includes 3 stages being conducted during the test which are initial compression, primary consolidation and secondary consolidation stage. Figure 4.6 showed the relationship between the void ratio and the applied pressure of kaolin clay S300 by using the square root time method. Based on the study by Ali et al. (2010) the authors studied square root time and logarithm of time method and showed the compression curve of the soil specimen best fit the square root of time theoretical curve. By referring to the graph, it was calculated that the Pre-compression Index, P_c was 88kPa using the Casagrande method, Compression Index, C_c was 0.0296 and the settlement of kaolin, S_c is 0.10 mm. Besides, the parameter of coefficient of volume compressibility, m_v as well as coefficient of consolidation, c_v are shown in **APPENDIX I**.

اونيفرسيتي مليسيا قهغ السلطان عبدالله
UNIVERSITI MALAYSIA PAHANG
AL-SULTAN ABDULLAH

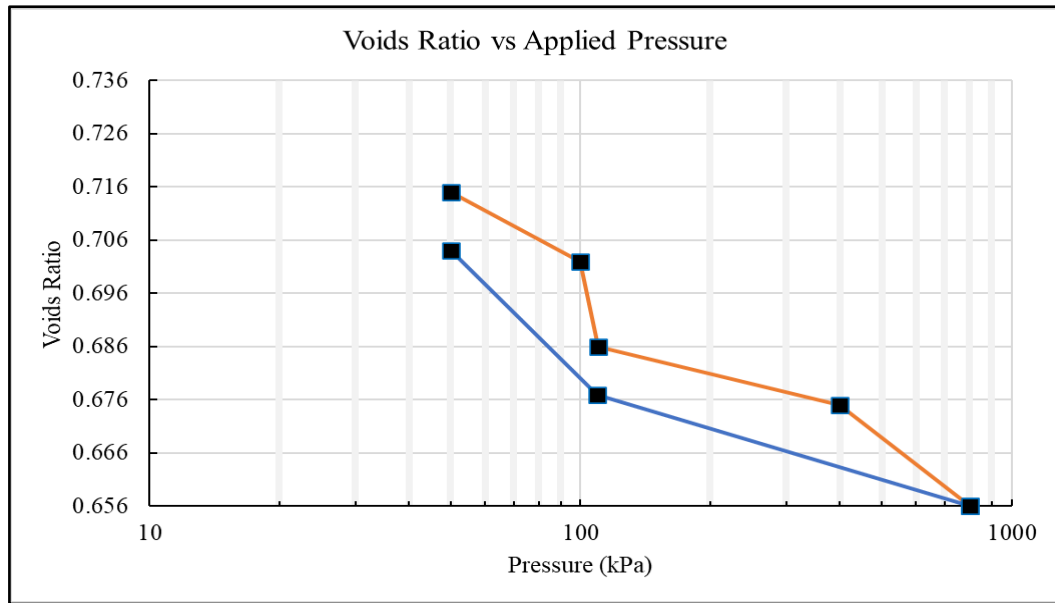


Figure 4.6 Void ratio against the applied pressure of kaolin S300

4.4 Undrained Shear Strength

4.4.1 Direct Shear Test

Throughout the test, the PET plastic used had the same density with the PET being used for the column installation. From the data sheet, a graph of maximum shear stress against applied normal stress was plotted and shown in Figure 4.7. According to the direct shear result, it was found that the cohesion and friction angle value of PET plastic are 23.25kPa and 10.66°. The data was obtained with the incremental load of 5kg to maximum 15kg. Previous researcher like Mohammed Ali (2021) had conducted similar tests where the author had proven that the 43.5% increment in direct shear was recorded with 1.25% of PET fibre volume used in concrete beam. The author also showed that the increment of 0.5% of PET plastic can withstand approximately 11% extra shear stress compared with no addition of PET plastic to the soil. Perera et al. (2020) used 5% of PET plastic into the recycled concrete aggregate (RCA) as well as crushed brick (CB) where it showed the increment of shear stress compared to material with no PET plastic addition. As mentioned by Ferreira et al. (2021), the addition of optimum amount of PET fibres in the sand matrix increased the soil bearing capacity and reduced the vertical and horizontal

deformation directions. The raw sample data sheet of grinded PET plastic was presented in **Appendix J**.

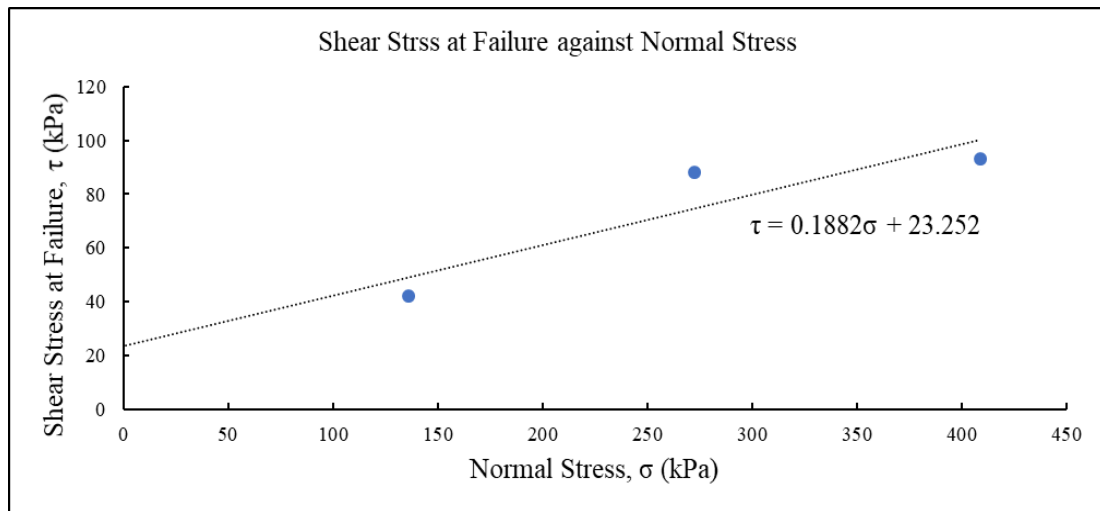


Figure 4.7 Maximum shear stress against the normal stress

4.5 Morphological Characteristics

It has been recognized that the morphological characteristic of the PET type for instance PET sand can affect the engineering properties and its performance if used as a substituent material. There are different type of PET available such as the PET bottle and PET resin, where Kusumocahyo et al. (2021) reported that there were no difference in terms of its chemical structures of the membrane. According to the result from SEM, Figure 4.8, Figure 4.9 and Figure 4.10 showed different magnificent levels of the PET plastic for 35 X, 1.00 KX and 2.00 KX. Referring to Figure 4.8, it was noticed the PET plastics had a smooth surface, asymmetric and spherical shape. The asymmetric shape was described as the structures were not interconnected between each other, but certain parts of it were interconnected between the pores. The previous data supported the above statement where the authors mentioned the asymmetric shape of PET plastic has an smooth surface, and acts as the active layer (Kusumocahyo et al., 2021). When enlargement was applied, the PET plastic was seen to have a porous cross section in Figure 4.9. From these figures, it was noticed that the PET plastic had an asymmetric

and spherical shape. Besides, at 2000 X magnification, a clear image was shown in Figure 4.10 where the PET plastic was in irregular shape, some pores were clearly seen on the surface.

As reported by Kusumocahyo et al. (2021) the PET resin used in the study had only a small part of pores interconnected which was similar to the current study. The authors also stated that the types of PET plastic such as PET resin and PET bottle had no significant difference in terms of its morphological characteristics. The pore formation on top of the PET surface may be due to the presence of water that created the interconnectivity. This statement was supported by previous research stating that the PET plastic can absorb moisture from surrounding at approximately 50 ppm (Stoughton, 2014). The samples were prepared with no additives during the test. From the research, the author deduced the membrane of PET plastic had the hydrophilic characteristic, by measuring it through the water contact angle method. Coherent to that, this characteristic is significant as the utilization of the PET plastic is favourable since it is not only cost-effective, but also promote the efforts of plastic recycling that towards a sustainable development. Thus, the substitution of the PET sand has a great potential to resolve the heap of water.

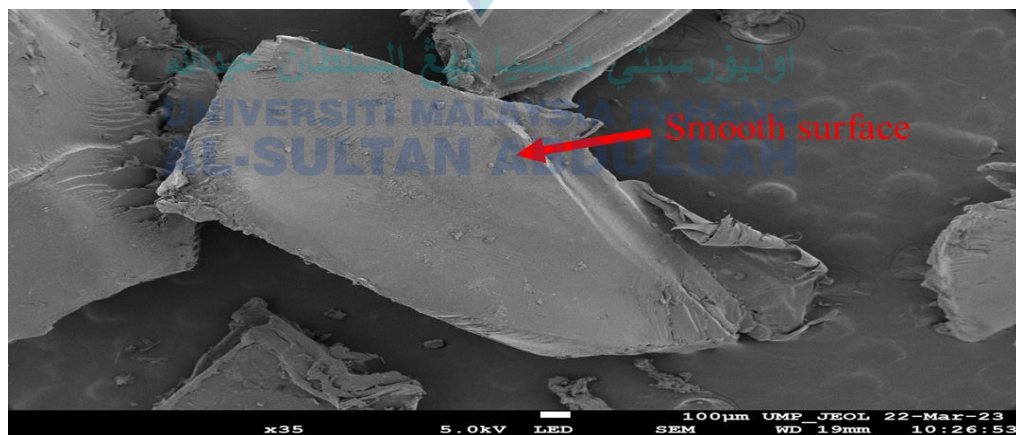


Figure 4.8 PET plastic at 35 X magnification

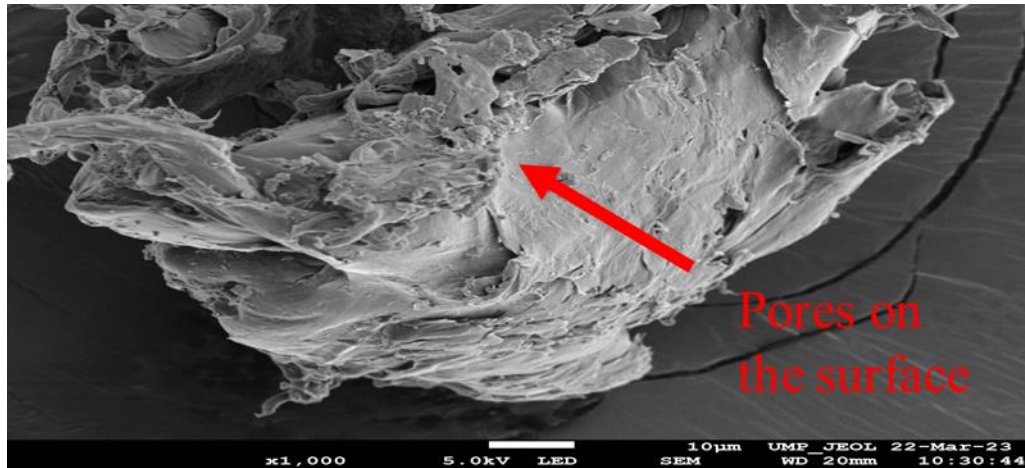


Figure 4.9 PET plastic at 1000 X magnification

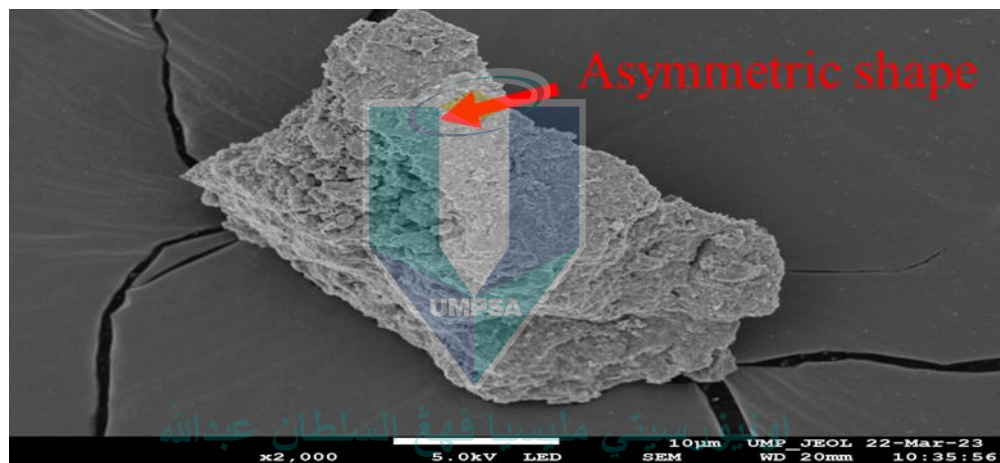


Figure 4.10 PET plastic at 2000 X magnification

4.6 Soft Kaolin Clay Reinforced with Single and Group PET Column

4.6.1 Unconfined Compression Test (UCT)

According to the result from the UCT, the average shear strength of the controlled sample from three samples was 11.08kPa and was used for shear strength comparison. For this test, the single PET column with 10 mm diameter with 0.6 height penetration ratio showed 15.87kPa, indicating 35.52% of shear strength improvement. The

percentage of shear strength improvement declines to 29.37% followed by 27.49% when the ratio was 0.8 and 1.0 respectively. Figure 11 presented the data obtained from UCT.

| PET Column Category | Column Diameter (mm) | Column Height (mm) | Unconfined Compression Stress, q_u (kPa) | Shear Strength, S_u (kPa) | Shear Strength Improvement, ΔS_u (kPa) |
|--------------------------|----------------------|--------------------|--|-----------------------------|--|
| Control | 0 | 0 | 24.43 | 11.71 | 0 |
| Single (1 PET column) | 10 | 60 | 31.75 | 15.87 | 35.52 |
| | | 80 | 30.24 | 15.12 | 29.37 |
| | | 100 | 29.86 | 14.93 | 27.49 |
| | 16 | 60 | 28.35 | 14.17 | 21.00 |
| | | 80 | 36.28 | 18.14 | 54.91 |
| | | 100 | 36.66 | 18.33 | 56.53 |
| | 10 | 60 | 34.39 | 17.19 | 46.79 |
| | | 80 | 32.50 | 16.25 | 38.77 |
| | | 100 | 34.77 | 17.38 | 48.42 |
| Group (3 PET columns) | 16 | 60 | 28.35 | 14.17 | 21.00 |
| | | 80 | 28.72 | 14.36 | 22.63 |
| | | 100 | 26.08 | 13.04 | 11.35 |

Figure 4.11 Result of Unconfined Compression Test

However, for 16 mm single PET column showed a reverse trend as compared to 10 mm single PET column as 16 mm single PET column showed increasing trend when the height penetration ratio increased. For 60% and 80% height penetrating ratio, the average shear strengths were 14.17kPa and 18.14kPa or 21.00% and 54.91% of shear strength improvement. While for fully penetrating columns with 1.0 ratio, the highest shear strength improvement was obtained throughout the sample of single column for 10 and 16 mm which had 18.33kPa or 56.53%. As compared from both cases, the 10 mm PET column had the highest shear strength improvement at 0.6 height penetrating ratio while the 16 mm PET column was at 1.0, indicating that 0.8 did not show the best performance.

For the group PET column, they were all arranged and constructed in triangular pattern shape. For the 10 mm PET column, the highest shear strength improvement was recorded when the height penetrating ratio was 100% or fully penetrated beneath the

kaolin, recorded 17.38kPa or 48.42%. The shear strength improvement value was followed by 60% and 80% height penetrating ratio which showed 17.19kPa and 16.25kPa or 46.79% and 38.77%.

Discussing the 16 mm group PET column, the highest shear strength improvement was recorded when the height penetrating ratio was 0.8, showing 14.36kPa or 22.63%. The value drops to 14.17kPa then 13.04kPa when the ratio was 0.6 and 1.0 respectively while the shear strength improvement dropping percentage from 21.00% to 11.35%. Considering the performance for both group PET column performance, the fully penetrating column for 10 mm group PET column produced the highest shear strength improvement but 16 mm group PET column has the best improvement when the ratio is 0.8.

| PET Column Category | A_c / A_s | H_c / H_s | H_c / D_c | Average Max Deviator Stress, q_u (kPa) | Average Axial Strain (%) |
|--------------------------|-------------|-------------|-------------|--|--------------------------|
| Control | 0 | 0 | 0 | 23.43 | 2.35 |
| Single (1 PET column) | 4 | 60 | 6 | 31.75 | 3.66 |
| | | 80 | 8 | 30.24 | 3.29 |
| | | 100 | 10 | 29.86 | 3.48 |
| | 10.24 | 60 | 3.75 | 28.35 | 2.95 |
| | | 80 | 5 | 36.28 | 3.97 |
| | | 100 | 6.25 | 36.66 | 3.95 |
| Group (3 PET columns) | 12.00 | 60 | 6 | 34.39 | 3.70 |
| | | 80 | 8 | 32.50 | 3.59 |
| | | 100 | 10 | 34.77 | 2.93 |
| | 30.72 | 60 | 3.75 | 28.35 | 3.96 |
| | | 80 | 5 | 28.72 | 3.91 |
| | | 100 | 3.25 | 26.08 | 3.64 |

Figure 4.12 Maximum deviator stress and the axial strain values obtained from UCT

Figure 4.12 showed the maximum deviator stress and the axial strain values for the control sample, single PET column and group triangular arrangement PET column for 10 mm and 16 mm diameter. After conducting the UCT, the undrained shear strength of the kaolin was increased after reinforcing with PET for both single and group columns,

showing that the PET was able to act as reinforcement in kaolin clay in providing additional shear strength.

4.6.2 Effect of Area Replacement Ratio

Based on Figure 4.13, it showed the shear strength improvement against the area replacement ratio in accordance with height penetrating ratio, H_c/H_s . From Figure 4.13, the trend of the graph is showing a decrease of shear strength improvement as the value of column diameter increased. The highest shear strength improvement with area replacement ratio of 10.24% except the height penetrating ratio of 0.6 compared to area replacement ratio of 30.72% which showed the least shear strength improvement among all the samples.

The decrease in shear strength for fully penetrating column, or 100 mm height of PET column built in the kaolin clay had caused the larger amount of soil has been taken out and hence, it affected and disturbed the kaolin natural state where it led to the reduction of shear strength for group triangular PET column. As reported by Najjar (2013) where the author reviewed the stone or sand column reinforcing in the clay can reduce soil settlement then increasing the soil bearing capacity when changing the area replacement ratio.

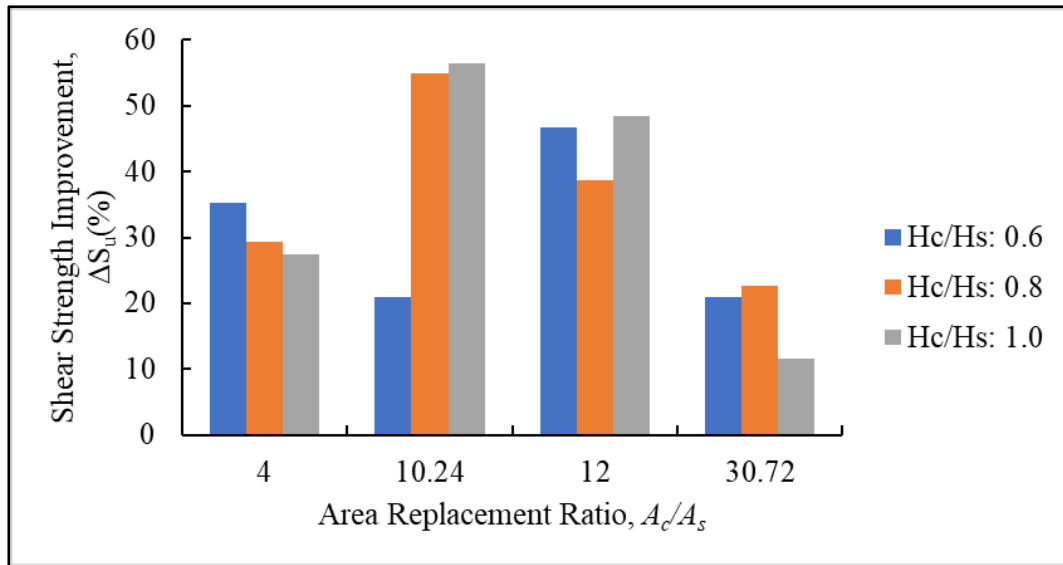


Figure 4.13 Shear strength improvement versus area replacement ratio

From Table 4.6, it presented the previous study from different researchers of fully penetrating columns beneath the clay and its shear strength improvement. For the current study, the shear strength improvement showed an increment trend when the area replacement ratio was from 4% to 10.24%, showing decrement trend from 12% to 30.72% due to its lower confining stress in the column and thus lowering the column stiffness when a larger diameter was drilled. This was supported by the previous researchers, Tandel et al. (2013) concluded that smaller diameter of reinforced column causes the higher confining stress in the column producing higher stiffness of column.

The current study results also showed that the least shear strength improvement happens when the area replacement ratio was 30.72% with 11.53% improvement when 16 mm of triangular group PET column were installed in the kaolin. As compared to the group triangular 10 mm PET column, it showed 48.42% of improvement with area replacement ratio of 12%. For a single PET column, the largest shear strength improvement was obtained when a 16 mm PET column was installed in the kaolin clay or 10.24% of area replacement ratio with 56.53% improvement as compared to 10 mm PET column or 4% of area replacement ratio with only 27.49% improvement. Beyond a certain value of area replacement ratio, the shear strength improvement can show

decrement. As the vertical load imposed on the reinforced column, the reinforced column under loading will show bulging and the kaolin clay is not enough to hold the reinforced column due to the larger amount of kaolin being replaced with foreign material. Referring to this situation, the shear strength of kaolin can decrease after drilling process before the PET column installation due to the disturbance of the kaolin natural state.

Table 4.6 Effect of fully penetrating column towards the clay undrained shear strength

| Researcher | Area replacement ratio, A_c/A_s (%) | Shear strength improvement (%) |
|-------------------------|--|-----------------------------------|
| Black et al. (2007) | 10 12 | 33 55 |
| Najjar et al. (2010) | 7.9 17.8 | 19.5 75 |
| Hasan et al. (2014) | 1.44 4 | 12.84 13.39 |
| Hasan et al. (2021) | 7.84 16 4 | 49.88 37.59 27.49 |
| Current study | 10.24 12 30.72 | 56.53 48.42 11.53 |

4.6.3 Effect of Column Penetration Ratio

From Figure 4.14, it showed the effect of height over diameter of column towards shear strength improvement. This figure showed how the difference in height over diameter of column can influence its undrained shear strength after single and group PET columns being installed. Based on the graph plotted in Figure 4.9, it was noticeable that among the 10 mm and 16 mm single with group PET column where the highest shear strength improvement is recorded when the height penetration ratio was 1.0 with single 16 mm PET column. Thus, the critical height penetration ratio for this study was 1.0.

The result suggests that it may vary depending on the substitute coarse material used as it can show different critical height penetration ratio where researchers like Hasan et al. (2021) obtained critical height penetration ratio at 1.0 when PP material was used. While for height over column diameter ratio, H_c/D_c , researchers Najjar et al. (2010) and

Hasan et al. (2014) stated that the value should be around 4 – 8 times in order to get the optimum value of shear strength improvement where a purple colour triangular shape was drawn in Figure 4.14. Based on the result obtained, the shear strength improvement which was more than 50% is found within the purple triangular shape region, 4 – 8 times and the height penetrating ratio is within 0.8 – 1.0. Hence, it was suggested that these two ratios were potentially affecting the overall shear strength improvement.

The use of coarse material made column or granular column was also regarded as granular piles where fill material, coarse aggregate material was filled within it Johnson & Sandeep (2016). These piles will be penetrating beneath the weak soil such as clay or silty sand for the transmission of load from the exerted vertical load until the column base. Variation in the piles length to its diameter ratio will certainly affect the load transmission as the exerted vertical loading is spreading across the surface of the soil and thus, the load transmission may not fully transmit to the column base when the granular column height increases or decreases.

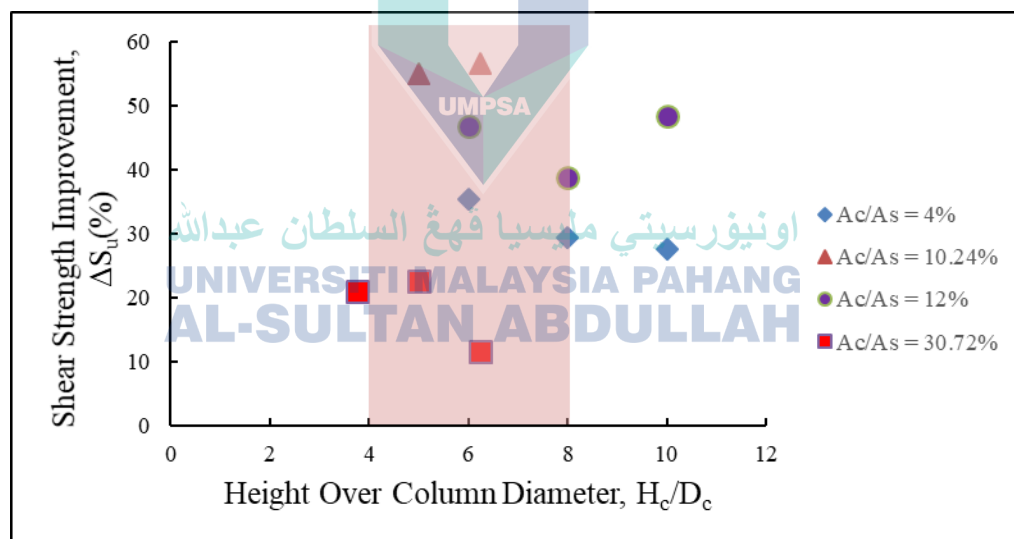


Figure 4.14 Effect of height over column diameter towards the shear strength improvement

According to the graph plotted in Figure 4.15, the shear strength improvement for both 10mm and 16mm single and group PET columns were showing inconsistent trend.

For the 60mm height of PET column, all the samples tested had shown increasing shear strength improvement trend. For further increment of height to 80mm, both 10mm of single and group PET column had recorded decrease in shear strength improvement while 16 mm of single and group PET columns had recorded increment. This can be due to group PET columns which had larger amounts of PET content inside the kaolin clay have provided a better drainage system to reduce the excess pore water pressure. Besides, the further increment of PET column to 100mm for single and group had either recorded increment or decrement, and hence the column height penetration ratio was considered substantial for the shear strength improvement.

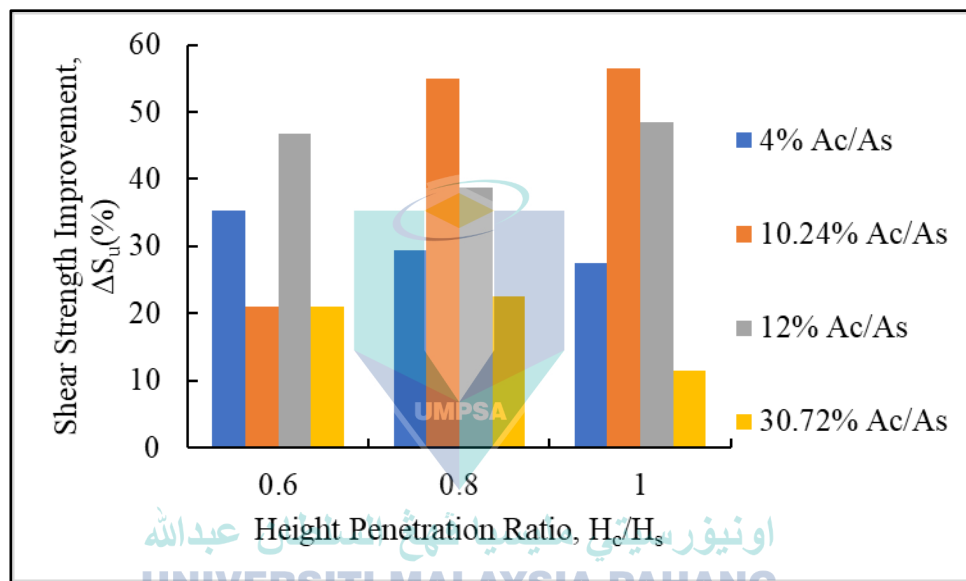


Figure 4.15 Shear strength improvement against height penetration ratio for single and group PET column

4.6.4 Effect of Volume Replacement Ratio

Referring to Figure 4.16, it showed the effect of volume replacement ratio of column in accordance to its shear strength improvement. From this Figure it was noticed that the shear strength had been increased and this statement was further proven by Najjar et al. (2012) who concluded that installation of granular columns can increase the bearing

capacity, stiffness and its overall reinforced clay system. The shear strength improvement was seen to drop drastically when it dealt with the group 16mm PET columns and this may be due to the large portion of the clay soil being drilled out replacing with PET plastic, and the data sample sheet was referred to **Appendix K**. Hence, it affected the natural state of clay and cause the shear strength to reduce. It was also supported by Hasan et al. (2021) where a 20mm diameter of single PP column was installed in kaolin clay showed less improvement as compared to a 14mm of single PP column for same height penetrating ratio.

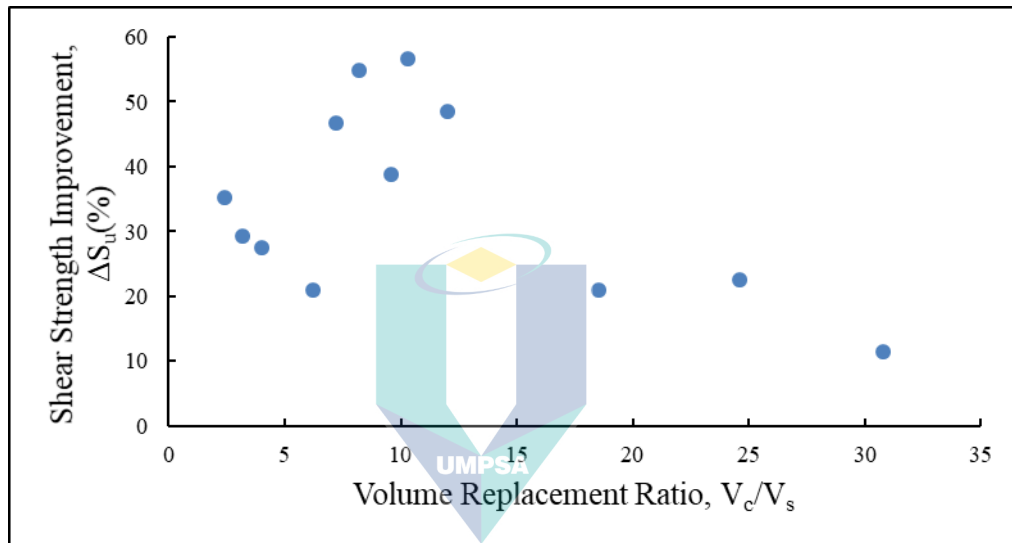


Figure 4.16 Shear strength improvement against volume replacement ratio for single and group PET column

4.6.5 Unconsolidated Undrained (UU) Triaxial Test

UU test was carried out to assess the shear strength of soft kaolin clay after the installation of single and group PET columns at different penetrating height by applying different confining pressure on it. The complete data with respective parameters, column penetrating ratio (H_c/H_s), area replacement ratio (A_c/A_s), and column height over column diameter ratio (H_c/D_c) together with the shear strength parameters, cohesion and friction angle were displayed in **Appendix L**. This test made it different from other related

geotechnical testing in the confining pressure, where 100kPa, 200kPa and 400kPa were applied.

4.6.5.1 Effect of Cohesion and Friction Angle

This sub-topic discussed the improvement in cohesion and friction angle by using the control sample as a reference. A set of complete data for the cohesion and friction angle improvement was tabulated in Table 4.7, and the cohesion improvement was recorded higher as compared to friction angle. Typically, the insertion of PET plastic inside the kaolin enabled the column to withstand higher stress.

Table 4.7 The cohesion and friction angle value with their improvement rate

| Sample | Cohesion, c (kPa) | Cohesion Improvement, Δc (%) | Friction Angle, ϕ | Friction Angle Improvement, $\Delta \phi$ (%) |
|---------|----------------------|--|---------------------------|---|
| Control | 42.2 | - | 30.0 | - |
| S1060 | 47.5 | 12.56 | 34.0 | 13.33 |
| S1080 | 51.4 | 21.80 | 31.0 | 3.33 |
| S10100 | 47.8 | 13.27 | 31.5 | 5.00 |
| S1660 | 47.0 | 11.37 | 31.8 | 6.00 |
| S1680 | 46.0 | 9.00 | 32.8 | 9.33 |
| S16100 | 49.6 | 17.54 | 33.0 | 10.00 |
| G1060 | 49.1 | 16.35 | 31.4 | 4.67 |
| G1080 | 54.5 | 29.15 | 31.8 | 6.00 |

Table 4.7 Continued

| Sample | Cohesion, c (kPa) | Cohesion Improvement, Δc (%) | Friction Angle, ϕ | Friction Angle Improvement, $\Delta\phi$ (%) |
|--------|----------------------|--|---------------------------|--|
| G10100 | 46.3 | 9.72 | 31.2 | 4.00 |
| G1660 | 47.1 | 11.61 | 31.5 | 5.00 |
| G1680 | 57.3 | 35.78 | 32.9 | 9.67 |
| G16100 | 44.4 | 5.21 | 33.2 | 10.67 |

The cohesion of a control sample or with no PET reinforcement had 42.2kPa while specimens with 10 mm diameter with H_c/H_s 0.6, 0.8 and 1.0 had the value of 47.5kPa, 51.4kPa and 47.8kPa. For 16 mm diameter, the values were 47.0kPa, 46.0kPa and 49.6kPa where the highest cohesion improvement value recorded when specimen S1080 was used with 21.80% or 1.03% of PET fibre used. As reported by Hernández & Botero (2020) the cohesion of soil was recorded 47.5% improvement under UU triaxial test when 0.7% of PET fibre was used. While for group columns with 10 mm diameter for 0.6, 0.8 and 1.0 of H_c/H_s , recorded 16.35%, 29.15% and 9.72%. The 16 mm diameter group columns had the same inconsistent trend similar to 10 mm diameter group columns, showing 11.61%, 35.78% and 5.21%. The largest cohesion improvement among all the tested specimens occurred on G1680 design with approximately 7.93% of PET fibre used to its total weight.

For the friction angle, the control sample had 30.0 and it recorded slight difference improvement as compared to cohesion. For a single column with 10 mm diameter, the largest friction angle improvement, 13.33% was recorded when the H_c/H_s is 0.6, followed

by 5.00% and 3.33% with 1.0 and 0.8 respectively. For the same category but 16 mm diameter, it showed an increasing trend with respect to H_c/H_s where the improvement values are 6.00%, 9.33% and 10.00% for 0.6, 0.8 and 1.0 respectively. Hernández & Botero (2020) reported that the increment of friction angle increased up to 0.5% PET fibre and showed decrement trend, and the current study obtained the similar result where the group columns had the PET fibre more than 0.5%. The group column with 10 mm diameter recorded 4.67%, 6.00% and 4.00% when the PET columns were built 60 mm, 80 mm and 100 mm inside the kaolin. For 16 mm diameter group columns, the friction angle improvement values were 5.00%, 9.67% and 10.67% respectively. As mentioned by Frikha et al. (2015) the use of granular columns for the clayey soil must consider the particle size of the column materials as it will significantly affect the entire structure in terms of its shear strength characteristics and rigidity.

4.6.5.2 Stress-Strain Behaviour

The UU test was conducted to determine the relationship between the axial strain and the maximum deviator stress occurring for the reinforcement of single and group PET columns. By preparing 3 specimens per design for 3 different confining pressures, the 13 designs comprising of 39 specimens were categorized into 4 groups based on its area replacement ratio which were 4.00%, 10.24%, 12.00% and 30.72%.

For all the tested specimens, the values obtained for the maximum deviator stress and the axial strain value from the UU test was referred to **Appendix L**. By following the previous method used in this study, control sample or no PET column reinforcement is used as a reference for the comparison between single and group PET columns. From the results, it presented an improvement after the soft kaolin clay being reinforced with either single or group PET columns.

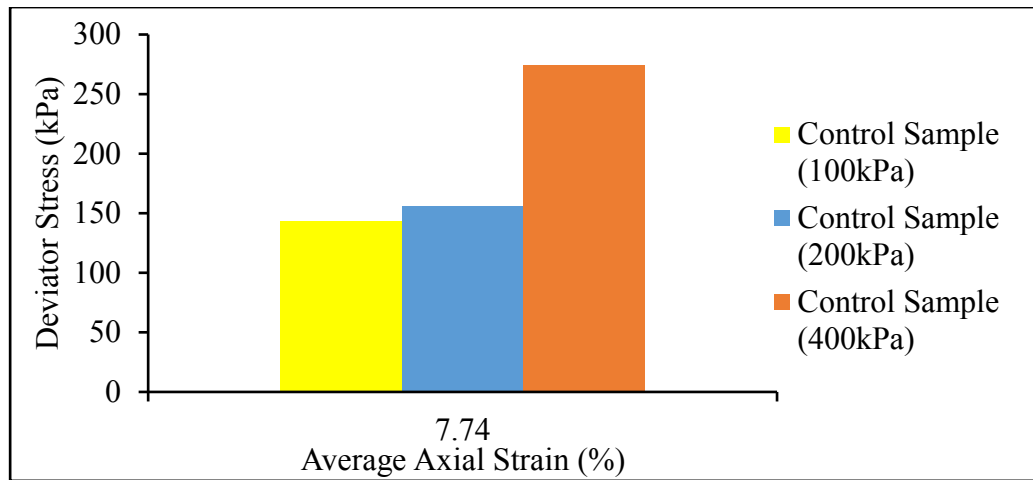


Figure 4.17 Maximum deviator stress and axial strain recorded at failure mode

Figure 4.17 showed the control sample for its maximum deviator stress and axial strain. For single PET columns with 10 mm and 16 mm diameter for 0.6, 0.8 and 1.0 height penetrating ratio at 100kPa, 200kPa and 400kPa, the graphs were plotted in Figure 4.18, 4.19 and 4.20 respectively. According to Figure 4.18, the largest deviator stress improvement for 100kPa confining pressure was recorded at 1.0 H_c/H_s , 22.32% for 16 mm diameter column but also the least improvement recorded for the same value of H_c/H_s for 10 mm diameter, only 1.18%. For Figure 4.19, the same trend occurred similar to Figure 4.18 as the maximum and minimum improvement occurred at the same category of H_c/H_s at 0.6, showing 94.48% and 36.87% for 10 mm and 16 mm respectively. The highest confining pressure in this study, 400kPa had also been applied to single PET columns for 10 mm and 16mm diameter and was shown in Figure 4.20. For the 400kPa category, the highest improvement was shown at 0.8 and 1.0 height penetrating ratio for 10mm and 16 mm diameter, recorded 48.62% and 50.31%.

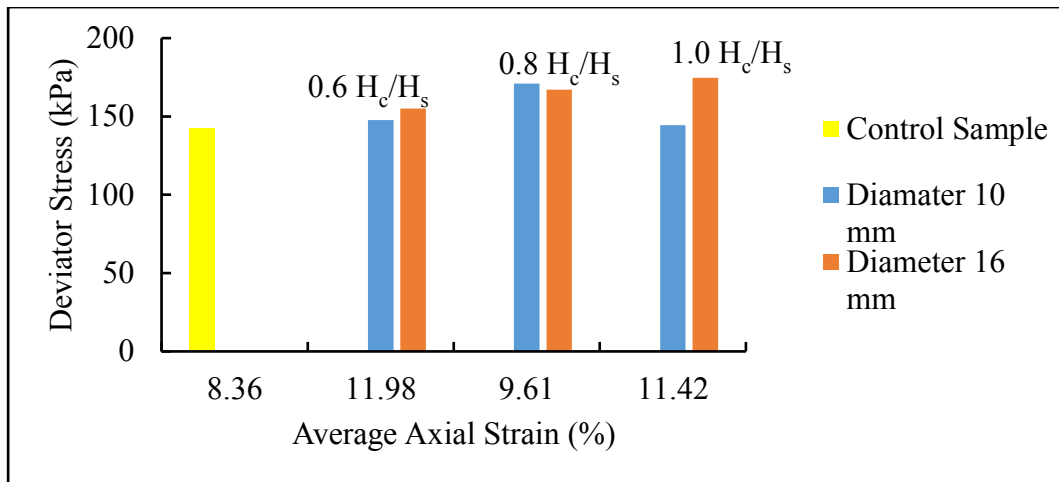


Figure 4.18 Maximum deviator stress versus average axial strain for single PET column with 10 mm and 16 mm diameter at 100kPa confining pressure

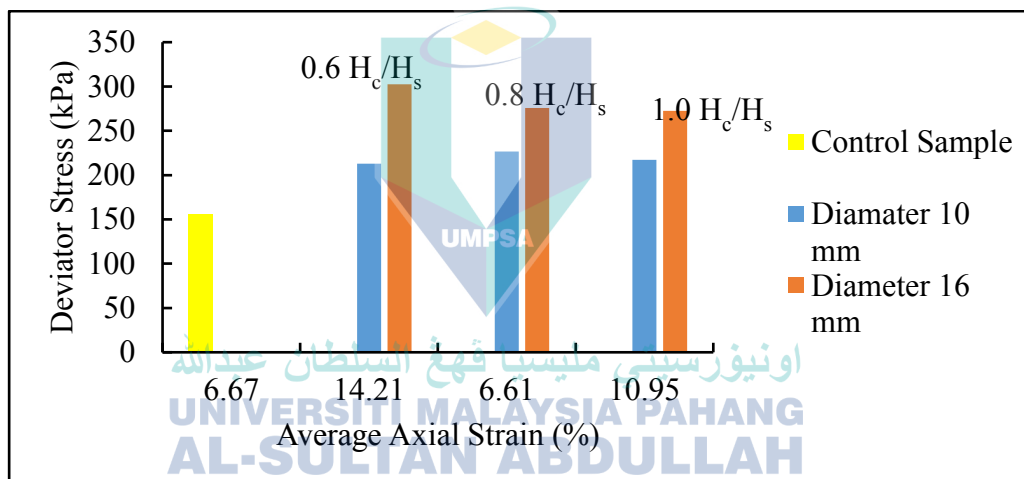


Figure 4.19 Maximum deviator stress versus average axial strain for single PET column with 10 mm and 16 mm diameter at 200kPa confining pressure

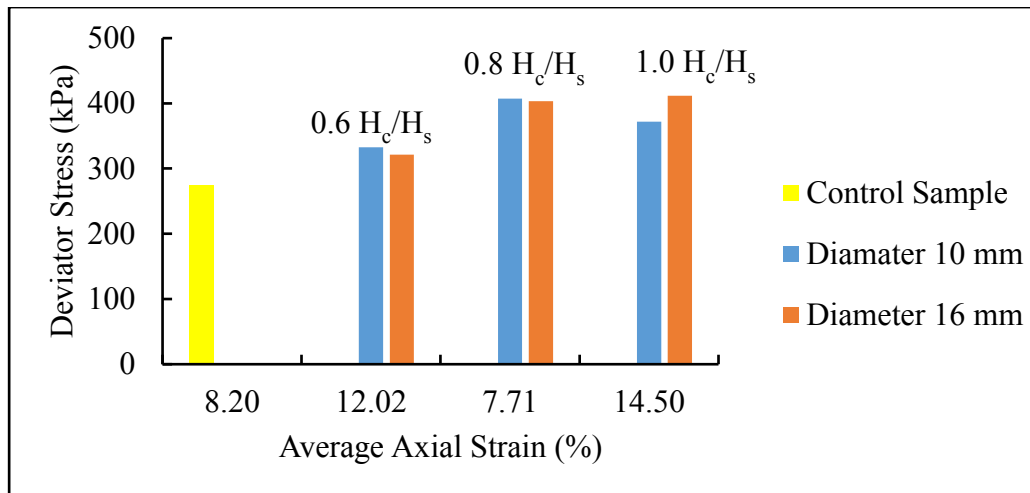


Figure 4.20 Maximum deviator stress versus average axial strain for single PET column with 10 mm and 16 mm diameter at 400kPa confining pressure

While for group PET columns at the same applied confining pressures, the plotted graphs were shown in Figure 4.21, 4.22 and 4.23. From Figure 4.21, it was noticed that the average axial strain values were not more than 10%, the specimens was not able to withstand a higher maximum deviator stress as compared to a single PET column at the same confining pressure. Referring to Figure 4.22, it showed the highest improvement among the samples recorded more than 50% of improvement for all tested specimens. At 400kPa confining pressure, the highest average axial strain value was recorded for 1.0 H_c/H_s as it may due to the largest amount of foreign material, PET being inserted into it caused the stiffness of the columns to increase and hence, increasing the axial strain value. Najjar et al. (2010) proposed the concept of critical column length where an installed granular column can only achieve certain improvement until certain length

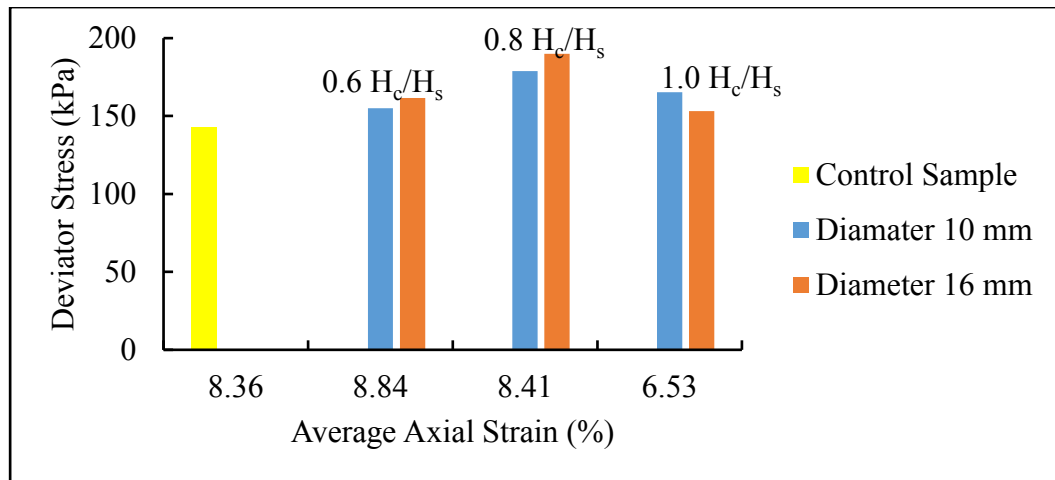


Figure 4.21 Maximum deviator stress versus average axial strain for group PET columns with 10 mm and 16 mm diameter at 100kPa confining pressure

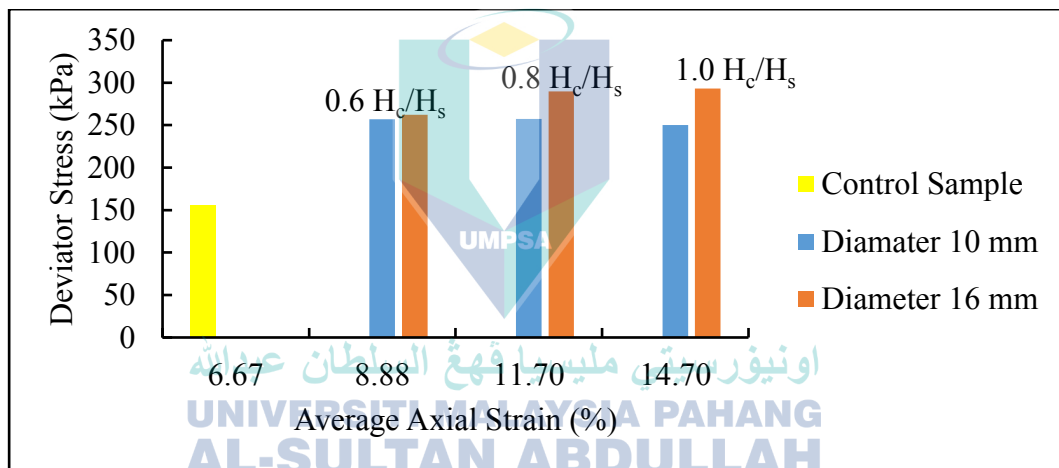


Figure 4.22 Maximum deviator stress versus average axial strain for group PET columns with 10 mm and 16 mm diameter at 200kPa confining pressure

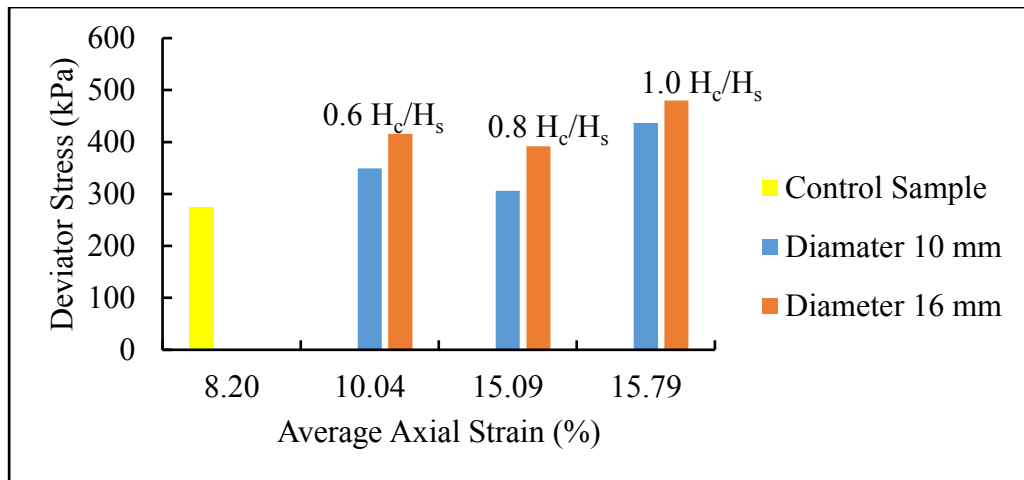


Figure 4.23 Maximum deviator stress versus average axial strain for group PET columns with 10 mm and 16 mm diameter at 400kPa confining pressure

4.6.6 Correlation of Cohesion and Friction Angle with Column Parameters

The improvement in cohesion and friction angle can be attributed to the foreign material which can provide additional forces (cohesion) and better bonding with interlocking between soil particles by the PET plastic. Moreover, when deep analysis was conducted through the cyclic triaxial system for UU test, the cohesion and friction angle did show improvement. However, the percentage of cohesion and friction angle were highly dependent on the PET column design itself and hence, this sub-topic will discuss clearly about their relationship with detailed explanation. For column parameters, it was focused to the previous sub-topic regarding to the column penetrating ratio, height over column diameter ratio and volume replacement ratio.

4.6.6.1 Correlation of Column Penetrating Ratio to the Cohesion and Friction Angle Improvement

Referring to column penetrating ratio, H_c/H_s was defined as how long a granular column was built with respect to the original height of the specimen. In this study, a

floating column or partially penetrating column with 60 mm and 80 mm height and an end-bearing column or fully penetrating column with 100 mm height was built inside the soft kaolin clay. The cohesion improvement with different values of H_c/H_s for single and group PET was interpreted by correlation as shown in Figure 4.24 and 4.25. As shown in Figure 4.24, the largest cohesion improvement was recorded 21.80% when a S1080 PET column was built or 0.8 H_c/H_s . When the same height of column was used with 16 mm diameter although same value of H_c/H_s , it had recorded the least cohesion improvement, only 9.00%. The difference between these two designs were the column diameter and hence, it was explained by the stiffness of the column or the optimum replacement value of foreign was achieved. Referring to S1080 design, the PET plastic replacement amount was 1.03% to the total mass of kaolin clay where S1680 design had 2.64%. This result was supported by the previous researchers, Hasan et al. (2014) stated that the critical column length fell within 4 – 8 times to its diameter value, where S1080 design fell within this category. Thus, in this study for a single column, the suggested replacement amount for PET plastic was 1.03% to its total mass.

Equation 4.1 and 4.2 were the equations generated from single columns with 10 mm and 16 mm diameter for 0.6, 0.8 and 1.0 H_c/H_s . They were interpreted in polynomial form, showing quadratic function. The equations for 4.1 and 4.2 were having $R^2 = 0.8307$ and $R^2 = 0.8773$

$$\Delta c = -28.69(H_c/H_s)^2 + 44.315(H_c/H_s) - 0.3364 \quad 4.1$$

$$\Delta c = 3.0449(H_c/H_s)^2 + 12.872(H_c/H_s) + 0.2319 \quad 4.2$$

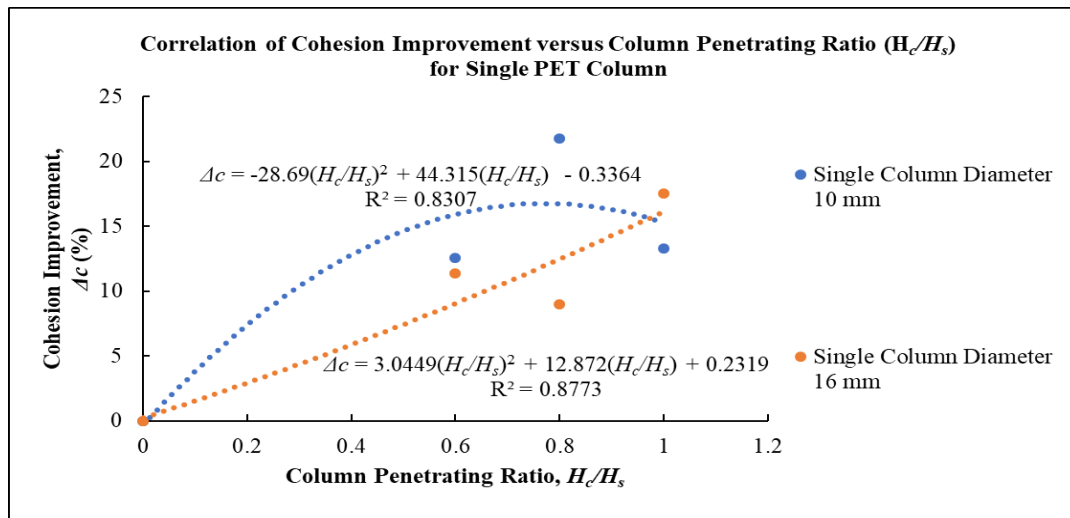


Figure 4.24 Correlation of cohesion improvement versus column penetrating ratio for single PET column

For group PET columns, the correlation as shown in Figure 4.25 had proven that 0.8 H_c/H_s produced the largest value of cohesion improvement. From the result, design G1680 with 3 columns installed inside the soft kaolin clay had 35.78% improvement followed by G1080, 29.15%. Besides, the study also proved that the value of 1.0 H_c/H_s was not recommended as both 10 mm and 16 mm showed cohesion improvement less than 10%, 9.72% and 5.21% respectively. The scenario was explained by the disturbance of the kaolin original state, which affected the degree of improvement and subsequently reduces the cohesion value or the ability to hold the soil particles together within a soil since PET plastic had larger void ratios as compared to kaolin itself. Therefore, replacement of PET plastic in group category (3 columns) for 100 mm height or 1.0 H_c/H_s had not resulted in the significant cohesion improvement although the stiffness of columns would be increased significantly.

From Figure 4.25, it showed the equations 4.3 and 4.4 which were the equations generated from the correlation of cohesion improvement against the column penetrating

ratio for group PET columns with 10 mm and 16 mm diameter. The equations for 4.3 and 4.4 were having $R^2 = 0.7146$ and $R^2 = 1$ respectively.

$$\Delta c = -60.686(H_c/H_s)^2 + 74.572(H_c/H_s) - 0.5951 \quad 4.3$$

$$\Delta c = -811.12(H_c/H_s)^3 + 1262.4(H_c/H_s)^2 - 446.11(H_c/H_s) \quad 4.4$$

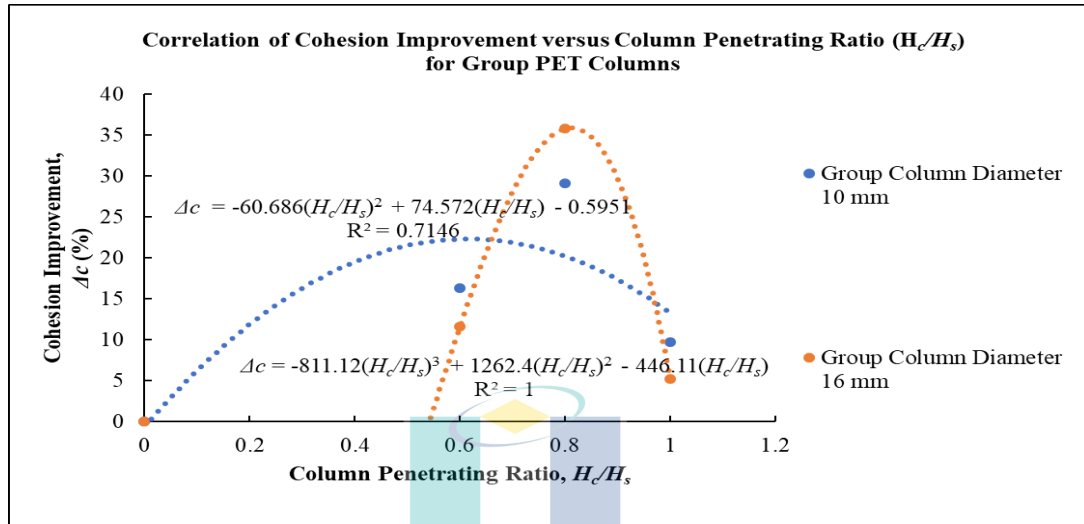


Figure 4.25 Correlation of cohesion improvement versus column penetrating ratio for group PET columns

In regards with the relationship between the single PET and group columns friction angle improvement and column penetrating ratio, it showed inconsistent trend. As compared to the previous results demonstrated in Figure 4.26 and 4.27, it had proven that the increment in cohesion will lead to the decrease of friction angle and was supported by Soltani-Jigheh (2016). From Figure 4.26, the data presented the S1080 design had the least friction angle improvement, only 3.33% although it showed the largest cohesion improvement within the single PET column category. The significant improvement was observed in S1060 design up to 13.33% but it did not show the highest improvement rate in cohesion. For the current study, the highest improvement result in respect to H_c/H_s for diameter 10 mm and 16 mm were 0.6 and 1.0 respectively. Typically, the addition of PET plastic with the diameter size, $d = 1.18$ mm had led to the soil strength

improvement through Mohr-Circles due to the significant increment in the soil friction angle.

The graph plotted for the correlation of these values was shown in Figure 4.26 and having the equations 4.5 and 4.6 with $R^2 = 0.6322$ and $R^2 = 0.9824$.

$$\Delta\phi = -34.17(H_c/H_s)^2 + 36.978(H_c/H_s) + 0.3131 \quad 4.5$$

$$\Delta\phi = -1.5615(H_c/H_s)^2 + 11.947(H_c/H_s) - 0.0551 \quad 4.6$$

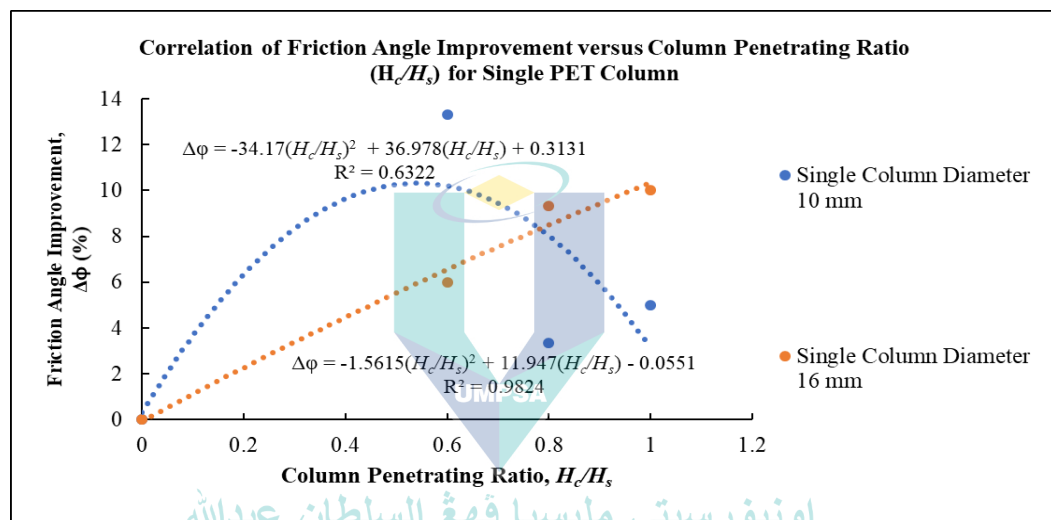


Figure 4.26 Correlation of friction angle improvement versus column penetrating ratio for single PET column

For group PET columns, it showed the same trend to single PET columns which was an inconsistent trend. The G16100 design had the highest friction angle improvement, 10.67% recorded while the least was G10100 design. This result further proved that Soltani-Jigheh (2016) statement which stated that the cohesion and friction angle was inversely proportional to each other as G16100 design had the least cohesion improvement. Both designs had the equal of H_c/H_s value, 1.0 but the results obtained showed differently. Alvarez et al. (2020) reported that an optimum friction angle

improvement value is achieved beyond a certain amount of added PET plastic into the clayey soil. Hence, the H_c/H_s value is considered as one of the factors that affects the friction angle improvement, but the diameter design is considered to achieve optimum friction angle improvement.

Figure 4.27 showed the correlation of friction angle improvement versus the column penetrating ratio for group PET columns, having the equations 4.7 and 4.8 with $R^2 = 0.963$ and $R^2 = 0.9486$.

$$\Delta\phi = 3.413(H_c/H_s)^2 + 7.857(H_c/H_s) - 0.0857 \quad 4.7$$

$$\Delta\phi = -10.969(H_c/H_s)^2 + 15.342(H_c/H_s) - 0.0533 \quad 4.8$$

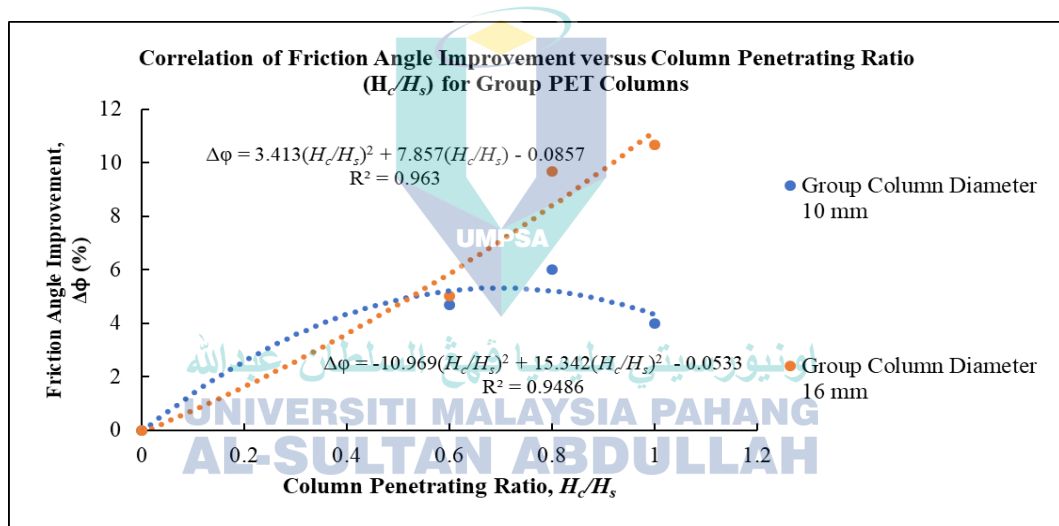


Figure 4.27 Correlation of friction angle improvement versus column penetrating ratio for group PET columns

4.6.6.2 Correlation of Height over Column Diameter Ratio to the Cohesion and Friction Angle Improvement

This sub-topic specifically focused on the relationship between the height of the PET column to its diameter and how it affected the performance in terms of the cohesion

and friction angle. Previous study by Najjar (2013) had stated the axial stress will be reduced if there is increment in stiffness of geosynthetic which is dependent on the column height will subsequently increase the column stability. The column stiffness was by the addition of PET plastic and it achieved the maximum improvement and began to decrease after the optimum value. For a 10 mm diameter single PET column with 60 mm, 80 mm and 100 mm height, the H_c/D_c value was 6, 8 and 10 respectively. For a 16 mm diameter single PET column, the H_c/D_c value was 3.75, 5 and 6.25.

Based on the graph plotted in Figure 4.28, the highest cohesion improvement occurs when H_c/D_c was equal to 8, followed by 6.25. Thus, the range of optimum improvement value for this category was within 6.25 – 8, which was similar to previous study by Hasan et al. (2014), stating the critical column length was within 4 – 8 times to its diameter. The correlation equations for both 10 mm and 16 mm single PET columns were shown in equation 4.9 and 4.10 with $R^2=0.8307$ and $R^2=0.8773$ respectively.

$$\Delta c = -0.2869(H_c/D_c)^2 + 4.4315(H_c/D_c) - 0.3364 \quad 4.9$$

$$\Delta c = 0.0779(H_c/D_c)^2 + 2.0595(H_c/D_c) + 0.2319 \quad 4.10$$

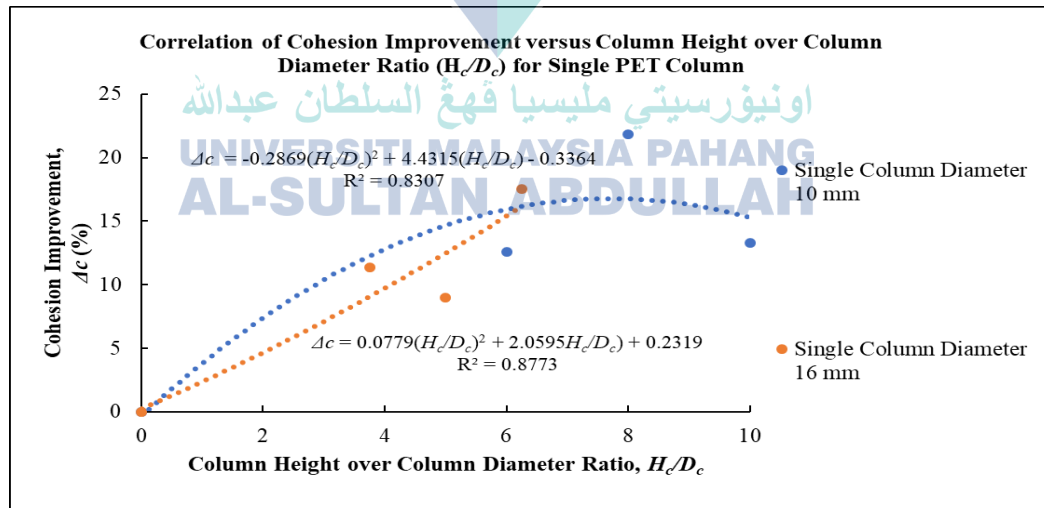


Figure 4.28 Correlation of cohesion improvement versus column height over column diameter ratio for single PET column

For group PET columns, the maximum cohesion improvement recorded was 35.78% followed by 29.15% which had the H_c/D_c equal to 5 and 8 respectively. From this study, it was proven that regardless of either single or group PET columns, the range of the H_c/D_c was around 5 – 8 times to its diameter, which had a smaller scale as compared to previous study. Beyond the stated values, although the columns did not show the least cohesion improvement value and it did not produce the best improvement result. Figure 4.29 presented the correlation of these values with a quadratic function. The correlation equations were shown in equation 4.11 and 4.12 with $R^2=0.7146$ and $R^2=1$ respectively.

$$\Delta c = -0.6069(H_c/D_c)^2 + 7.4572(H_c/D_c) - 0.5951 \quad 4.11$$

$$\Delta c = -3.3224(H_c/D_c)^3 + 32.319(H_c/D_c)^2 - 71.378(H_c/D_c) \quad 4.12$$

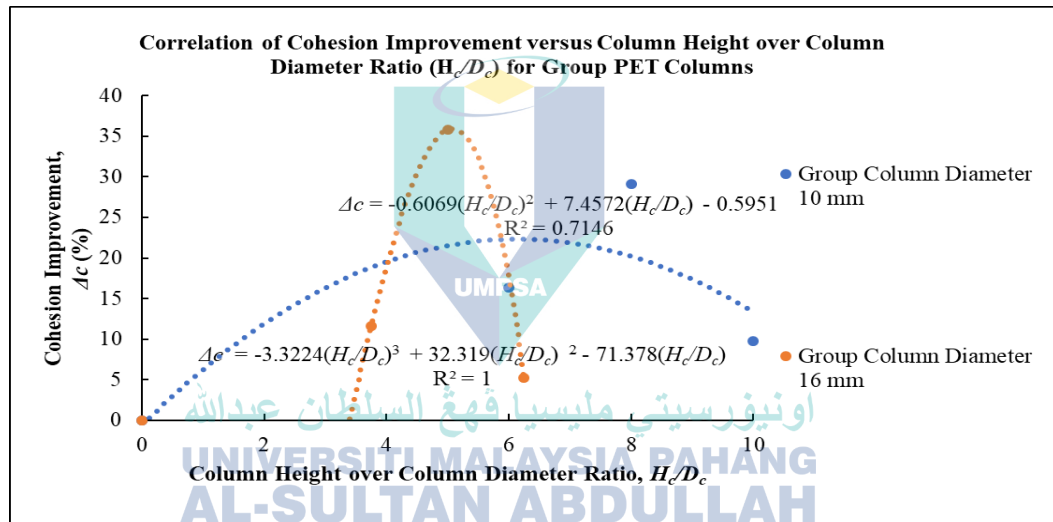


Figure 4.29 Correlation of cohesion improvement versus column height over column diameter ratio for group PET columns

Similar to the previous sub-topic about column penetrating ratio, the friction angle was related to the cohesion value but related to H_c/D_c . For a single 10 mm and 16 mm PET column which was depicted in Figure 4.30, the highest friction angle improvement occurs when H_c/D_c was 6 and 6.25 while the least values were 8 and 3.75 respectively. In order to achieve highest friction angle improvement, the range lied within 6 to 6.25

but out of this range, the least improvement value showed inconsistent trend. According to Alvarez et al. (2020), the optimum value of PET plastic reinforcement was about 1.0% as it produced the best performance which had less vertical variation. For S1060 design which had the value of H_c/D_c equal to 6 has approximately 0.77% of PET plastic reinforcement. Equations 4.13 and 4.14 were the correlation equations which had $R^2 = 0.6322$ and $R^2 = 0.9824$ respectively.

$$\Delta\phi = -0.3417(H_c/D_c)^2 + 3.6978(H_c/D_c) + 0.3131 \quad 4.13$$

$$\Delta\phi = -0.04(H_c/D_c)^2 + 1.9116(H_c/D_c) - 0.0551 \quad 4.14$$

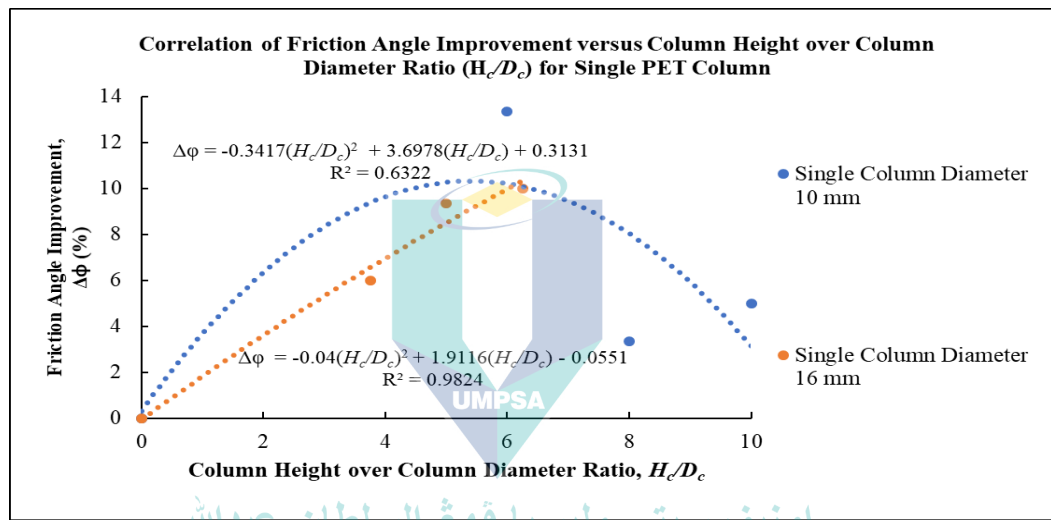


Figure 4.30 Correlation of friction angle improvement versus column height over column diameter ratio for single PET column

Referring to Figure 4.31 about the correlation of group PET columns, the highest friction angle improvement design had the value of H_c/D_c equal to 6.25 which was the same as a single 10 mm PET column. However, the G1060 design only showed 4.67% of improvement and it had the value of H_c/D_c equal to 6. Thus, the study on height over column diameter ratio proved that there was a higher probability to obtain the best friction angle improvement where the optimum value of H_c/D_c should be around 6 to 6.25. Figure

4.31 provides equations 4.15 and 4.16 which had the values of $R^2 = 0.9630$ and $R^2 = 0.9486$ respectively.

$$\Delta\phi = 0.0874(H_c/D_c)^2 + 1.2571(H_c/D_c) - 0.0857 \quad 4.13$$

$$\Delta\phi = -0.1097(H_c/D_c)^2 + 1.5342(H_c/D_c) - 0.0533 \quad 4.14$$

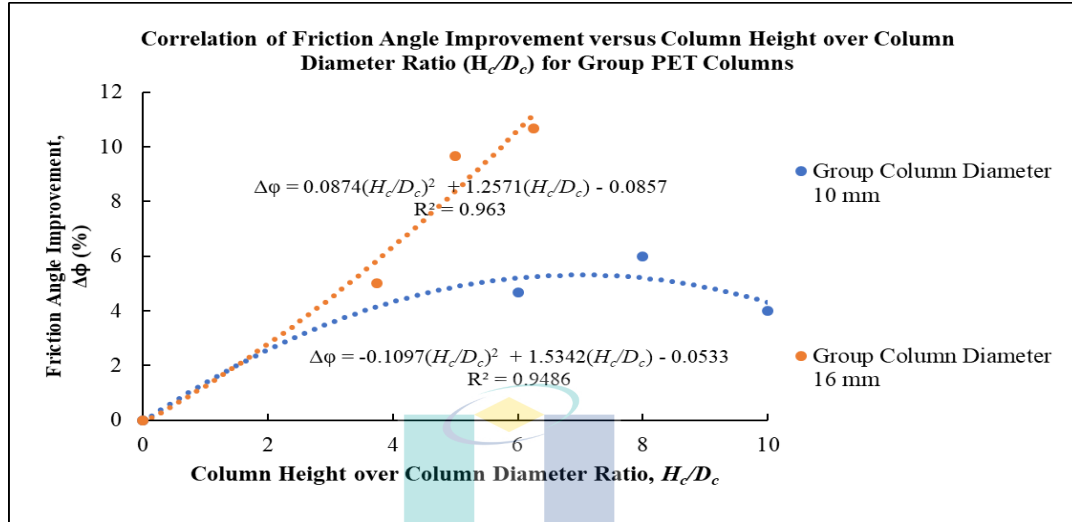


Figure 4.31 Correlation of friction angle improvement versus column height over column diameter ratio for group PET columns

4.6.6.3 Correlation of Volume Replacement Ratio to the Cohesion and Friction Angle Improvement

The researcher also analysed how the volume of the PET plastic had affected the performance of cohesion and friction angle improvement. Theoretically, the use of a larger volume of PET plastic can increase the shear strength value and thus leads to the increment of cohesion by increasing the column stiffness since it is a coarse-type material rather than soft kaolin clay. However, previous researchers like Najjar (2013) stated that the disturbance of the soil's original state may lead to further decrement of the shear strength. The previous analysis of shear strength with respect to volume replacement ratio was discussed and reviewed in sub-topic 4.5.4 with Figure 4.16.

As tabulated in table 4.9 and shown in Figure 4.32, for single PET columns the largest and least cohesion improvement when S1080 and S1680 was used with V_c/V_s equals 3.2 and 8.19 respectively. Referring to a single PET column with 10 mm diameter, all the samples were showing cohesion improvement more than 10% with the V_c/V_s ranging from 2.4 – 4. For a single PET column with 16 diameter, the V_c/V_s was ranging 6.14 – 10.24 but showing inconsistent trend of improvement. Hence, for this specific parameter, V_c/V_s the study suggested that the value from 2.4 – 4 was preferable. The equations 4.15 and 4.16 which had $R^2 = 0.8307$ and $R^2 = 0.8773$ were the correlation equation for a single PET column.

$$\Delta c = -1.7931(V_c/V_s)^2 + 11.079(V_c/V_s) - 0.3364 \quad 4.15$$

$$\Delta c = 0.0288(V_c/V_s)^2 + 1.259(V_c/V_s) + 0.2325 \quad 4.16$$

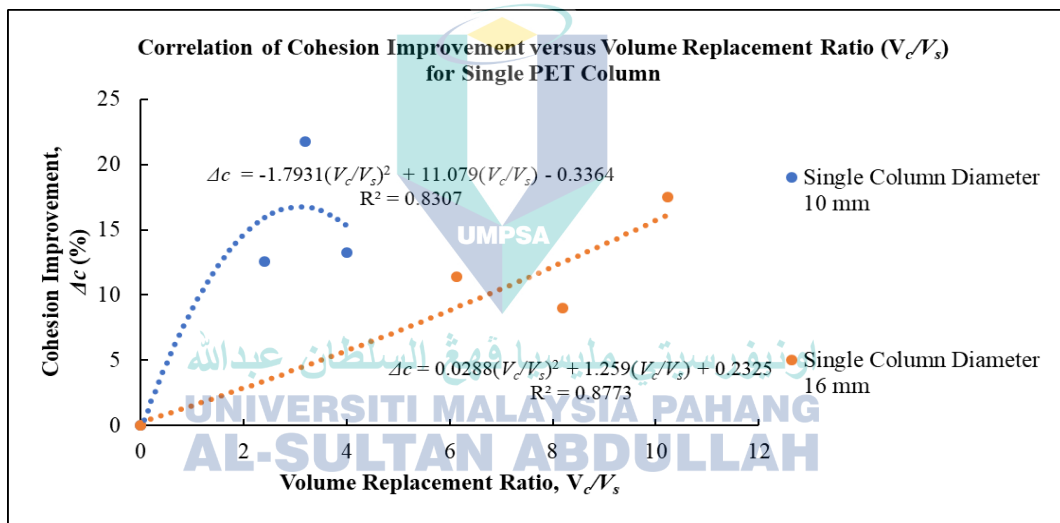


Figure 4.32 Correlation of cohesion improvement versus volume replacement ratio for single PET column

As referred to in Figure 4.33 for group PET columns, the V_c/V_s had a bigger value as compared to single PET columns. Since 3 columns were installed on it, the G1680 design had 24.58 of V_c/V_s produced the largest cohesion improvement, 35.78% for 16 mm diameter followed by 9.6 of V_c/V_s from G1080 produced 29.51% for 10 mm

diameter. From this trend, it was noticed that the middle value of V_c/V_s or columns which had 80 mm showed the highest improvement value within a 50 mm diameter soft kaolin clay specimen. The correlation equations for 4.17 and 4.18 with $R^2 = 0.7146$ and $R^2 = 1$ were shown below.

$$\Delta c = -0.4214(V_c/V_s)^2 + 6.2144(V_c/V_s) - 0.5951 \quad 4.17$$

$$\Delta c = -0.028(V_c/V_s)^3 + 1.3371(V_c/V_s)^2 - 14.514(V_c/V_s) \quad 4.18$$

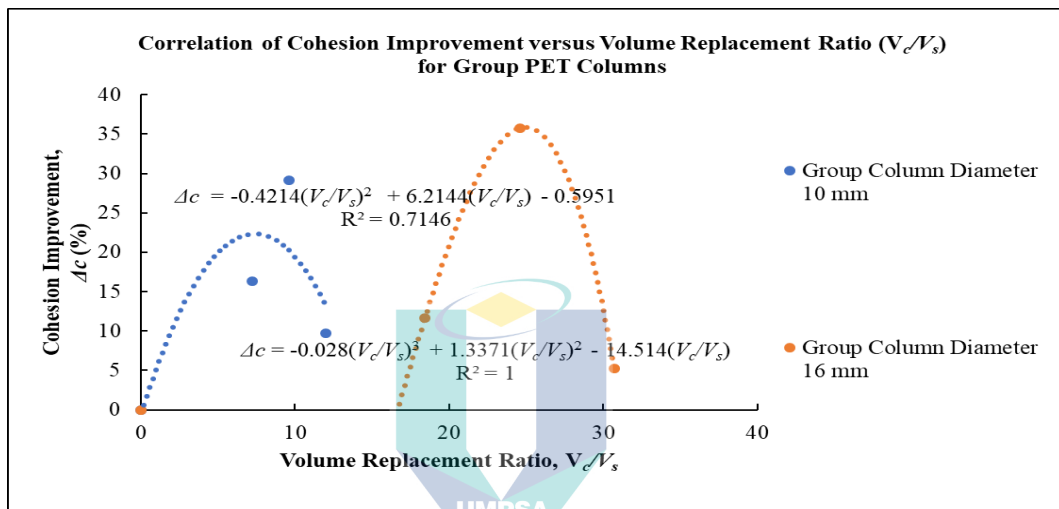


Figure 4.33 Correlation of cohesion improvement versus volume replacement ratio for group PET columns

The following discussion focused on the friction angle improvement by evaluating the volume replacement ratio. For a single PET column with 10 mm diameter plotted in Figure 4.34, the V_c/V_s which had 2.4 and 3.2 shows the largest and least improvement, 13.33% and 3.33% respectively. Category for 16 mm showed the largest improvement when a S16100 column was used, recorded 10.00% improvement or 10.24 V_c/V_s . Beyond these two values, the recorded values were only showing moderate friction angle improvement. This situation linked to the porosity of the PET plastic, workmanship and particle size of PET plastic. The correlation equations 4.19 and 4.20 which had $R^2 = 0.6322$ and $R^2 = 0.9825$ were shown below.

$$\Delta\phi = -2.1356(V_c/V_s)^2 + 9.2445(V_c/V_s) + 0.3131 \quad 4.19$$

$$\Delta\phi = -0.0151(V_c/V_s)^2 + 1.1683(V_c/V_s) - 0.0552 \quad 4.20$$

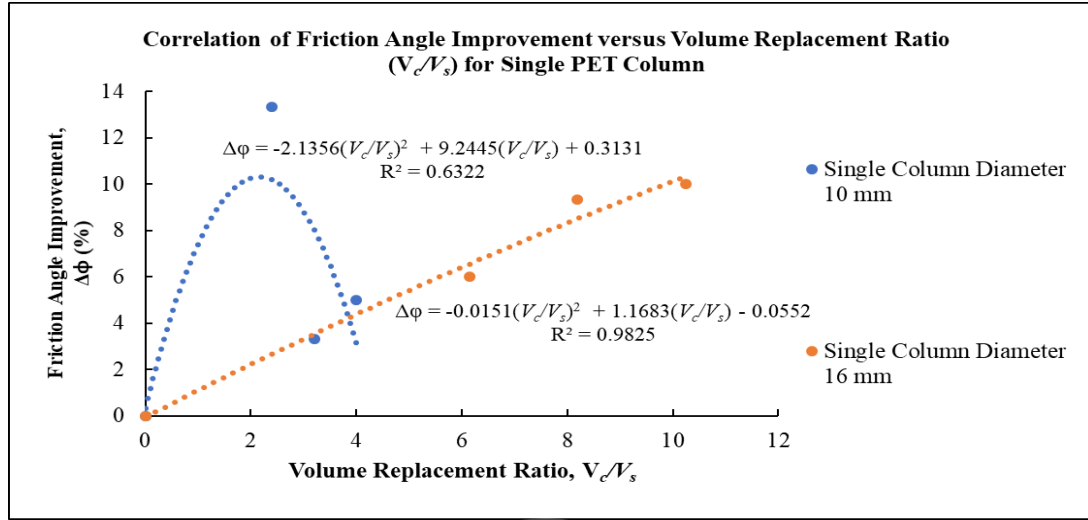


Figure 4.34 Correlation of friction angle improvement versus volume replacement ratio for single PET column

For group PET columns, the trend was showing increased friction angle improvement with respect to volume replacement ratio. The highest friction angle improvement was recorded when a G16100 column or 50.72 V_c/V_s was used, proving that the stiffness of the column increased when the PET plastic increased as demonstrated in Figure 4.35. Although it showed the largest friction angle, it showed the least cohesion value. In short, the volume replacement ratio proved that the range to obtain maximum friction angle improvement was extreme where 2.4 and 50.72 V_c/V_s showed the largest values for single and group PET columns respectively. Equations 4.21 and 4.22 with $R^2 = 0.9486$ and $R^2 = 0.9631$ were shown below.

$$\Delta\phi = -0.0762(V_c/V_s)^2 + 1.2785(V_c/V_s) - 0.0533 \quad 4.21$$

$$\Delta\phi = 0.0036(V_c/V_s)^2 + 0.2557(V_c/V_s) - 0.0857 \quad 4.22$$

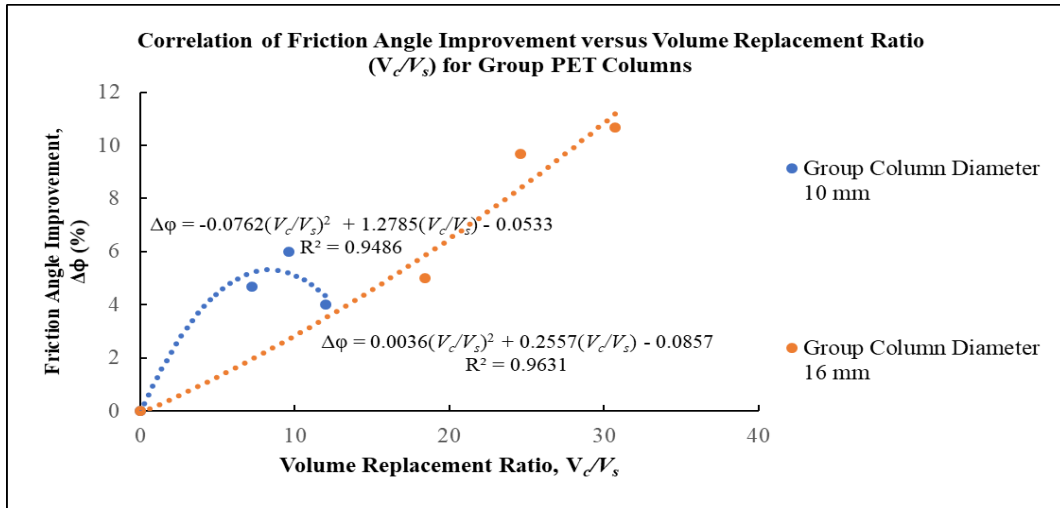


Figure 4.35 Correlation of friction angle improvement versus volume replacement ratio for group PET columns

4.7 Summary of Results and Discussion

Based on all the figures and tables demonstrated above, the engineering properties of the kaolin clay S300 and PET plastic were examined through the proposed tests. Besides, the shear strength parameters were determined by constructing the single and PET columns beneath the kaolin clay S300 within the small-scale laboratory test. From the information, the objectives 1 was achieved by gathering and analysing the information of the kaolin clay S300 and PET plastic engineering properties thoroughly. Furthermore, the shear strength and its improvement of kaolin clay S300 were successfully obtained, the column parameters that affected the entire performance of specimen were interpreted accordingly. Therefore, the UCT execution had attained the objective 2.

After gathering the data from the UCT for objective 2, the subsequent target, objective 3 was reached through the execution of UU test and the cohesion and soil friction angle were obtained. The utilization of correlation technique had successfully correlated the shear strength variables and simplified the complex engineering system to a quadratic equation.

CHAPTER 5

CONCLUSIONS

5.1 Introduction

This chapter focused on the summary of the discussion and analysis from the overall study. It was split into the conclusion of objective 1, 2 and 3 as all the stated objectives were successfully achieved, and they were discussed in the following subsection. Furthermore, the recommendation and suggestion were proposed to improve, enhance, and provide the detail ideas for the future analysis.

5.2 Conclusion

In conclusion, there were several conclusions had been made and they are as follows.

- i. Based on the soil classification standard, AASTHO the kaolin S300 was classified as A-4 or low plasticity silt soil. From the Atterberg limit test, the liquid limit was 35.39% and 5.88% of the plasticity index. Thus, it fell under the ML category based on the USCS plasticity chart. A-4 meant that the kaolin S300 was a silty soil while ML proved that it was an inorganic silt and very fine sand material. From the particle size distribution plotted graph, the well graded particle size of kaolin clay was ranging 0.001 – 0.0625 mm. The optimum moisture content obtained was 20% and the coefficient of hydraulic conductivity proved that it was low permeability soil, 4.197×10^{-8} m/s. For PET plastic, it was a well graded plastic with A-1-a from AASTHO soil classification. From this standard, it was

treated as granular type material behaving like gravel or sand soil. A significant amount of PET plastic had been retained on 1.18 mm sieve size from sieve analysis test. Besides, the relative density test proved the PET plastic had a maximum and minimum dry density of 0.530 and 0.430 respectively but the in-situ dry density only 56.59%, meaning that PET plastic was a porous material. Based on constant head test, the permeability value was 2.503×10^{-4} m/s and hence, it can be associated with kaolin S300 to provide a good drainage to delay soil settlement. From the direct shear test, the value of cohesion and angle of shearing resistance were 23.25kPa and 10.66° respectively. The rough surface texture developed a high interlocking degree and prevented the particles from further sliding.

- ii. From the UCT test, the effect of shear strength parameters such as H_c/H_s , H_c/D_c and V_c/V_s had played an important role in affecting the shear strength value. The UCT results showed that a S1680 column or with 0.8 H_c/H_s produced the maximum shear strength improvement rate for single PET column with 16 mm category while G10100 column or with 1.0 H_c/H_s showed the largest improvement rate for group PET columns with 10 mm category. The remaining categories showed maximum improvement rate when a S1060 was used and a G1680 column as well. Hence, the study concluded that the 10 mm and 16 mm diameters of PET columns are suitable to obtain the largest shear strength improvement for group category and single category respectively.
- iii. Through UU test, the maximum deviator stress with axial strain, cohesion and friction angle improvement were determined. The maximum deviator stress improvement did not occur when the PET specimens were tested under 400kPa confining pressure, but 200kPa when a S1660 specimen was tested with 94.48% of improvement. For the group PET columns category, it also had the same trend where a 86.21% improvement was recorded when a G1680 specimen was tested under 200kPa confining pressure. Typically, most of the specimens which had 0.6 and 0.8 H_c/H_s performed better than H_c/H_s for single and group PET columns regardless of its proposed diameter. This statement was supported by previous

studies where the researchers stated that the larger extrusion of soil will disturb the original soil's state which may lead to the decrease of shear strength. This study proposed that $0.8 H_c/H_s$ was the general optimum value for all parameters other than maximum deviator stress. The study showed that the addition of PET plastic inside the kaolin clay increased the force to hold all the particles within a soil through the increase of cohesion value, but it also proved that change of cohesion improvement is inversely proportional to the change of friction angle improvement. Furthermore, the cohesion and soil friction angle were expressed through the correlation technique, with the regression equations for each parameter. From these equations, the R^2 values were all showing greater than 0.5 and hence, the objective 3 was accurately achieved.

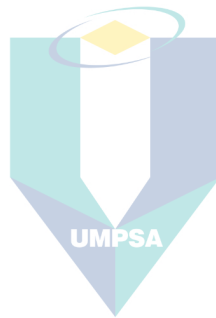
5.3 Recommendation for Future Study

Although the results obtained from laboratory had achieved the stated objectives, but several recommendations can be given to improve the results for future study and it can be done in several ways;

- i. The results obtained from this study can compare with the actual fieldworks on site since one is small-scale laboratory testing while the other is large-scale. Thus, the performance of PET columns on site can observe how the behaviours of these materials react.
- ii. Further analysis can be carried out towards the chemical properties of PET as it is expected to have prolonged the lifespan of the modified materials due to its non-biodegradable properties.
- iii. The similar study can be repeated however alteration can be made to the PET column designs for instance the column diameter and height.
- iv. Different factors that may influence the improvement result must be analysed like the drilling process since it is hand-drilled, so it might induce angle during this process. Drilling machine that is suitable for small-scale laboratory testing must

also be considered so that the poor workmanship during the column construction process can be addressed.

- v. Critical analysis can also be implemented through other cyclic triaxial tests like Consolidated Undrained (CU) test to especially determine the compressibility of the kaolin clay using the same design in this study in future work.



اونيفرسيتي مليسيا قهغ السلطان عبدالله
UNIVERSITI MALAYSIA PAHANG
AL-SULTAN ABDULLAH

REFERENCES

- Acidri Samuel. (2019). A Comparative Analysis of Foundations using Prescriptive Design and Static Loading Test Methods. *International Journal of Engineering Research And*, V8(11), 671–680. <https://doi.org/10.17577/ijertv8is110244>
- Aghili, E., Hosseinpour, I., Jamshidi Chenari, R., & Ahmadi, H. (2021). Behavior of granular column-improved clay under cyclic shear loading. *Transportation Geotechnics*, 31(May), 100654. <https://doi.org/10.1016/j.trgeo.2021.100654>
- Ahangar, F. A., Rashid, U., Ahmad, J., Tsubota, T., & Alsalmeh, A. (2021). Conversion of waste polyethylene terephthalate (Pet) polymer into activated carbon and its feasibility to produce green fuel. *Polymers*, 13(22). <https://doi.org/10.3390/polym13223952>
- Ahmed, A., Ugai, K., & Kamei, T. (2011). Investigation of recycled gypsum in conjunction with waste plastic trays for ground improvement. *Construction and Building Materials*, 25(1), 208–217. <https://doi.org/10.1016/j.conbuildmat.2010.06.036>
- Alamanis, N., Papageorgiou, G., Xafoulis, N., & Chouliaras, I. (2020). Effects of Landslides and Soil Settlements on the Built Environment : A Meta- analysis Effects of Landslides and Soil Settlements on the Built Environment : A Meta-analysis. *European Journal of Advances in Engineering and Technology*, 7(May), 6–15.
- Ali, F. H., Sing, W. L., & Hashim, R. (2010). Engineering properties of improved fibrous peat. *Scientific Research and Essays*, 5(2), 154–169.
- Aljanabi, Q. A., Chik, Z., & Kasa, A. (2013). Construction of a new highway embankment on the soft clay soil treatment by stone columns in Malaysia. *Journal of Engineering Science and Technology*, 8(4), 448–456.
- Al-Obaidi, A. L., Yousif, M. A., & Hamid, A. I. (2020). Effect of Relative Compaction on the Bearing Capacity of Cohesive Soils. *IOP Conference Series: Materials Science and Engineering*, 737(1). <https://doi.org/10.1088/1757-899X/737/1/012108>

- Al-Salem, S. M., Lettieri, P., & Baeyens, J. (2009). Recycling and recovery routes of plastic solid waste (PSW): A review. *Waste Management*, 29(10), 2625–2643. <https://doi.org/10.1016/j.wasman.2009.06.004>
- Alvarez, A., Sosa, J., Duran, G., & Pacheco, L. (2020). Improved mechanical properties of a high plasticity clay soil by adding recycled PET. *IOP Conference Series: Materials Science and Engineering*, 758(1). <https://doi.org/10.1088/1757-899X/758/1/012075>
- Archna, Moses, V., Sagar, S., Shivraj, V., & Chetan, S. (2015). A Review on Processing of Waste PET (Polyethylene Terephthalate) Plastics. *International Journal of Polymer Science Engineering*, 1(2), 1–13. www.journalspub.com
- Arulrajah, A., Perera, S., Wong, Y. C., Horpibulsuk, S., & Maghool, F. (2020). Stiffness and flexural strength evaluation of cement stabilized PET blends with demolition wastes. *Construction and Building Materials*, 239, 117819. <https://doi.org/10.1016/j.conbuildmat.2019.117819>
- Azad Sahib, A., & Robinson, R. G. (2020). A review of isotache modeling and secondary consolidation behavior of soft clays. *IOP Conference Series: Earth and Environmental Science*, 491(1). <https://doi.org/10.1088/1755-1315/491/1/012050>
- Baierl, T.-M., & Bogner, F. X. (2021). Plastic Pollution. *The American Biology Teacher*, 83(5), 320–324. <https://doi.org/10.1525/abt.2021.83.5.320>
- Bayat, H., Ebrahimi, E., & Fallah, M. (2018). Estimation of soil moisture using confined compression curve parameters. *Geoderma*, 318(November 2016), 64–77. <https://doi.org/10.1016/j.geoderma.2017.12.034>
- Beena, K. S. (2010). *Scholars ' Mine*. 0–6.
- bin Hasan, M., binti Yusuf, N., binti Noor Shahrudeen, N. A., & Kassim, A. M. H. (2015). Strength of soft clay reinforced with group crushed polypropylene (PP) columns. *Electronic Journal of Geotechnical Engineering*, 20(22), 12291–12308.
- Birmpilis, G., Mohammadi, A. S., Villanova, J., Boller, E., Ando, E., & Dijkstra, J. (2022). Fabric Investigation of Natural Sensitive Clay from 3D Nano- and

Microtomography Data. *Journal of Engineering Mechanics*, 148(2), 1–12.
[https://doi.org/10.1061/\(asce\)em.1943-7889.0002044](https://doi.org/10.1061/(asce)em.1943-7889.0002044)

Black, J. A., Sivakumar, V., Madhav, M. R., & Hamill, G. A. (2007). Reinforced Stone Columns in Weak Deposits: Laboratory Model Study. *Journal of Geotechnical and Geoenvironmental Engineering*, 133(9), 1154–1161.
[https://doi.org/10.1061/\(asce\)1090-0241\(2007\)133:9\(1154\)](https://doi.org/10.1061/(asce)1090-0241(2007)133:9(1154))

Bozyigit, I., Bulbul, F., Alp, C., & Altun, S. (2021). Effect of randomly distributed pet bottle strips on mechanical properties of cement stabilized kaolin clay. *Engineering Science and Technology, an International Journal*, 24(5), 1090–1101.
<https://doi.org/10.1016/j.jestch.2021.02.012>

Cai, G., & Waldmann, D. (2019). A material and component bank to facilitate material recycling and component reuse for a sustainable construction: concept and preliminary study. *Clean Technologies and Environmental Policy*, 21(10), 2015–2032. <https://doi.org/10.1007/s10098-019-01758-1>

Cheng, Y.-L., Lee, C.-Y., Huang, Y.-L., Buckner, C. A., Lafrenie, R. M., Dénomée, J. A., Caswell, J. M., Want, D. A., Gan, G. G., Leong, Y. C., Bee, P. C., Chin, E., Teh, A. K. H., Picco, S., Villegas, L., Tonelli, F., Merlo, M., Rigau, J., Diaz, D., ... Mathijssen, R. H. J. (2016). We are IntechOpen, the world's leading publisher of Open Access books Built by scientists, for scientists TOP 1 %. *Intech, 11*(tourism), 13. <https://www.intechopen.com/books/advanced-biometric-technologies/liveness-detection-in-biometrics>

Choi, Y. W., Moon, D. J., Chung, J. S., & Cho, S. K. (2005). Effects of waste PET bottles aggregate on the properties of concrete. *Cement and Concrete Research*, 35(4), 776–781. <https://doi.org/10.1016/j.cemconres.2004.05.014>

Choudhary, R., Kumar, A., & Murkute, K. (2018). Properties of waste polyethylene terephthalate (PET) modified asphalt mixes: Dependence on PET size, PET content, and mixing process. *Periodica Polytechnica Civil Engineering*, 62(3), 1–9.
<https://doi.org/10.3311/PPci.10797>

Commissioner, T., Generation, W., Inquiry, R. E., Commission, P., Weickhardt, D., Efficiency, R., Paper, I., & Generation, W. (2006). *Plastics and Chemicals Industries Association*.

- Cui, T., Song, K., & Zhang, S. (2010). Research on utilizing recycled plastic to make environment-friendly plywood. *Forestry Studies in China*, 12(4), 218–222. <https://doi.org/10.1007/s11632-010-0401-y>
- Deraman, R., Nawi, M. N. M., Yasin, M. N., Ismail, M. H., & Ahmed, R. S. M. O. M. (2021). Polyethylene Terephthalate Waste Utilisation for Production of Low Thermal Conductivity Cement Sand Bricks. *Journal of Advanced Research in Fluid Mechanics and Thermal Sciences*, 88(3), 117–136. <https://doi.org/10.37934/arfmts.88.3.117136>
- Dheerendra Babu, M. R., Nayak, S., & Shivashankar, R. (2013). A Critical Review of Construction, Analysis and Behaviour of Stone Columns. *Geotechnical and Geological Engineering*, 31(1), 1–22. <https://doi.org/10.1007/s10706-012-9555-9>
- Dhianty, E., & Mochtar, I. B. (2018). Method of removing secondary compression on clay using preloading. *MATEC Web of Conferences*, 195, 1–10. <https://doi.org/10.1051/mateconf/201819503006>
- El Gendy, M., Mohamady, A., Nabil, T., & Shams, M. (2019). Effect of the Presence of Soft Clay on the Structural Design of Highway Sections. *Port-Said Engineering Research Journal*, 23(2), 26–33. <https://doi.org/10.21608/pserj.2019.49559>
- Elhakim, A. F. (2016). Estimation of soil permeability. *Alexandria Engineering Journal*, 55(3), 2631–2638. <https://doi.org/10.1016/j.aej.2016.07.034>
- Esfandiari, A., Kaghazchi, T., & Soleimani, M. (2012). Preparation and evaluation of activated carbons obtained by physical activation of polyethyleneterephthalate (PET) wastes. *Journal of the Taiwan Institute of Chemical Engineers*, 43(4), 631–637. <https://doi.org/10.1016/j.jtice.2012.02.002>
- Fattah, M. Y., & Majeed, Q. G. (2012). Finite Element Analysis of Geogrid Encased Stone Columns. *Geotechnical and Geological Engineering*, 30(4), 713–726. <https://doi.org/10.1007/s10706-011-9488-8>
- Ferreira, J. W. dos S., Senez, P. C., & Casagrande, M. D. T. (2021). Pet fiber reinforced sand performance under triaxial and plate load tests. *Case Studies in Construction Materials*, 15(October). <https://doi.org/10.1016/j.cscm.2021.e00741>

- Frikha, W., Bouassida, M., & Canou, J. (2015). Parametric Study of a Clayey Specimen Reinforced by a Granular Column. *International Journal of Geomechanics*, 15(5), 1–12. [https://doi.org/10.1061/\(asce\)gm.1943-5622.0000419](https://doi.org/10.1061/(asce)gm.1943-5622.0000419)
- Ghanti, Rudrabir., & Kashliwal, Abhijeet. (2008). Ground Improvement Techniques – with a Focused Study on Stone Columns. *Dura Build Care PVT LTD*, 30(Retrieved on January), 1–11.
- Haque, R. (2021). Performance Of Partially Replaced Plastic Bottles (Pet) As Coarse Aggregate In Producing Green Concrete. *Brilliant Engineering*, 2(4), 15–19. <https://doi.org/10.36937/ben.2021.004.004>
- Hasan, M. Bin, Marto, A. B., & Hyodo, M. (2014). Strength of Soft Clay Reinforced with Single and Group Bottom Ash Columns. *The 2014 World Congress on Civil, Environmental & Materials Research (ACEM 2014)*.
- Hasan, M. Bin, Marto, A. B., Hyodo, M., & Makhtar, A. M. Bin. (2011). The strength of soft clay reinforced with singular and group bottom ash columns. *Electronic Journal of Geotechnical Engineering*, 16 N(January), 1215–1227.
- Hasan, D., Juhari, N., Rofi, M. H., & Albar, A. (2019). The effect of polyethylene terephthalate (road barrier waste) in concrete for rigid pavement. *Journal of Physics: Conference Series*, 1349(1). <https://doi.org/10.1088/1742-6596/1349/1/012009>
- Hasan, M., Husaini, N. A., & Pangee, N. (2017). Shear strength of clay reinforced with square and triangular arrangement of group encapsulated bottom ash columns. *International Journal of GEOMATE*, 12(33), 127–133. <https://doi.org/10.21660/2017.33.2608>
- Hasan, M., Pangee, N., & Husaini, N. A. (2016). Strength of Soft Clay Reinforced with Square and Triangular Pattern Encapsulated Bottom Ash Columns. *Second International Conference on Science, Engineering & Environment, November*, 21–23. [internal-pdf://214.47.198.8/Strength Of Soft Clay Reinforced With square a.pdf](https://doi.org/10.21447.198.8/Strength%20Of%20Soft%20Clay%20Reinforced%20With%20square%20a.pdf)
- Hasan, M., Zaini, M. S. I., Hong, N. A. W., Wahab, A., Masri, K. A., Jaya, R. P., Hyodo, M., Winter, M. J., Sholichin, M., & Haribowo, R. (2021a). Sustainable ground improvement method using encapsulated polypropylene (PP) column reinforcement.

IOP Conference Series: Earth and Environmental Science, 930(1).
<https://doi.org/10.1088/1755-1315/930/1/012016>

Hasan, M., Zaini, M. S. I., Hong, N. A. W., Wahab, A., Masri, K. A., Jaya, R. P., Hyodo, M., Winter, M. J., Sholichin, M., & Haribowo, R. (2021b). Sustainable ground improvement method using encapsulated polypropylene (PP) column reinforcement. *IOP Conference Series: Earth and Environmental Science*, 930(1).
<https://doi.org/10.1088/1755-1315/930/1/012016>

Hernández, C., & Botero, E. (2020). Characterization of the dynamics of a clay soil reinforced with polyethylene terephthalate fiber (PET). *17th World Conference on Earthquake Engineering, 17WCEE*, 1–10.

Herrmann, H., & Bucksch, H. (2014). Ground Improvement Technique. *Dictionary Geotechnical Engineering/Wörterbuch GeoTechnik*, 2, 638–638.
https://doi.org/10.1007/978-3-642-41714-6_72392

Hoornweg, D., & Bhada-Tata, P. (2015). *Publication: What a Waste : A Global Review of Solid Waste Management*.

Jaafar, T. R., Zaharudin, A. M., Pahmi, A., Kasiran, R., & Alam, S. (2018). *Effect of Carbon in Brake Friction Materials on Friction Characteristics*. 14, 47–59.

Jaber, N. H., Radhi, M. S., & Alsaad, A. J. (2021). Ecological Applications of Polyethylene Terephthalate Plastic in Producing Modified Subbase Soil. *IOP Conference Series: Materials Science and Engineering*, 1067(1), 012006.
<https://doi.org/10.1088/1757-899x/1067/1/012006>

Jamal, M., Patel, H. V., & Senapati, A. (2020). *Construction, Analysis and Behaviour of Stone Column: A Review*. May.

Johnson, N., & Sandeep, M. N. (2016). Ground Improvement Using Granular Pile Anchor Foundation. *Procedia Technology*, 24, 263–270.
<https://doi.org/10.1016/j.protcy.2016.05.035>

- Jun Shen, N., Hasan, M., & Yong Ler, L. (2024). INFLUENCE OF CRUSHED BRICK COLUMNS ON GEOTECHNICAL PROPERTIES OF EXPANSIVE SOIL. *Jurnal Teknologi*, 86(4). <https://doi.org/10.11113/jurnalteknologi.v86.21191>
- Kaiser, K., Schmid, M., & Schlummer, M. (2018). Recycling of polymer-based multilayer packaging: A review. *Recycling*, 3(1). <https://doi.org/10.3390/recycling3010001>
- Karkush, M. (2018). *Lectures of Soil Mechanics*. April.
- Kassa, R. B., Workie, T., Abdela, A., Fekade, M., Saleh, M., & Dejene, Y. (2020). Soil Stabilization Using Waste Plastic Materials. *Open Journal of Civil Engineering*, 10(01), 55–68. <https://doi.org/10.4236/ojce.2020.101006>
- KeTTTHA. (2017). Green Technology Master Plan Malaysia (2017-2030). In *Ministry of Energy Green Technology and Water Malaysia*. <https://www.malaysia.gov.my/portal/content/30920>
- Kim, B., Prezzi, M., & Salgado, R. (2005). *Geotechnical Properties of Fly and Bottom Ash Mixtures for Use in Highway Embankments*. July, 914–924.
- Kirsch, K., & Kirsch, F. (2016). Ground Improvement by Deep Vibratory Methods: Second Edition. In *Ground Improvement by Deep Vibratory Methods: Second Edition*. <https://doi.org/10.1201/9781315372341>
- Kumar, A., & H.P, V. (2017). Effect of Discarded Plastic Waste as Stabilizer on Engineering Properties of Effect of Discarded Plastic Waste as Stabilizer on Engineering Properties of Cohesive Soil. *International Journal of Engineering Technology Science and Research*, 4(12), 779–786.
- Kumar, M., Azhar, M., Mondal, S., & Singh, R. P. (2022). Stabilization of expansive soil subgrade by waste plastic. *Arabian Journal of Geosciences*, 15(10). <https://doi.org/10.1007/s12517-022-10112-7>
- Kusumocahyo, S. P., Ambani, S. K., & Marceline, S. (2021). Improved permeate flux and rejection of ultrafiltration membranes prepared from polyethylene terephthalate (PET) bottle waste. *Sustainable Environment Research*, 31(1). <https://doi.org/10.1186/s42834-021-00091-x>

- Lajevardi, S. H., Enami, S., Shamsi, H. R., & Hamidi, M. (2019). Amirkabir Journal of Civil Engineering Experimental Study of Single and Groups of Stone Columns Encased by Geotextile. *Civil Eng*, 50(6), 337–340. <https://doi.org/10.22060/ceej.2018.12789.5269>
- Later, T., Figure, P. E. T., & Pet, A. (2015). *The Facts about PET What is PET ? PET as a packaging material*. 1–7.
- Lebreton, L., & Andrady, A. (2019). Future scenarios of global plastic waste generation and disposal. *Palgrave Communications*, 5(1), 1–11. <https://doi.org/10.1057/s41599-018-0212-7>
- Letcher, T. M., & Vallero, D. A. (2019). Waste: A Handbook for Management, Second Edition. In *Journal of Chemical Information and Modeling* (Vol. 53, Issue 9).
- Li, T. T., Wang, K., Sueyoshi, T., & Wang, D. D. (2021). Esg: Research progress and future prospects. *Sustainability (Switzerland)*, 13(21). <https://doi.org/10.3390/su132111663>
- Maharaj, C., Maharaj, R., & Maynard, J. (2015). The Effect of Polyethylene Terephthalate Particle Size and Concentration on the Properties of Asphalt and Bitumen as an Additive. *Progress in Rubber, Plastics and Recycling Technology*, 31(1), 1–23. <https://doi.org/10.1177/147776061503100101>
- Manuel, M., & Joseph, shyla A. (2014). *Stability Analysis of Kuttanad Clay Reinforced with PET Bottle Strips*. 3(11), 361–363.
- McKelvey, D., Sivakumar, V., Bell, A., & Graham, J. (2004). Modelling vibrated stone columns in soft clay. *Proceedings of the Institution of Civil Engineers: Geotechnical Engineering*, 157(3), 137–149. <https://doi.org/10.1680/geng.2004.157.3.137>
- Meenakshi, M., & Mb, M. (2020). *Analyzing the Behavior of Soil Reinforced with Polyethylene Terephthalate (PET) Wastes*. 1527–1530.
- Menon, A. R., Konnur, S., & Bhasi, A. (2021). Model Tests on Coir Geotextile-Encased Stone Columns with Tyre Crumb-Infilled Basal Coir Geocell. *International Journal*

of Geosynthetics and Ground Engineering, 7(2). <https://doi.org/10.1007/s40891-021-00274-x>

- Miranda, M., Fernández-Ruiz, J., & Castro, J. (2021). Critical length of encased stone columns. *Geotextiles and Geomembranes*, 49(5), 1312–1323. <https://doi.org/10.1016/j.geotexmem.2021.05.003>
- Mohammed Ali, T. K. (2021). Shear strength of a reinforced concrete beam by PET fiber. *Environment, Development and Sustainability*, 23(6), 8433–8450. <https://doi.org/10.1007/s10668-020-00974-w>
- Mohanty, P., & Samanta, M. (2015). Experimental and Numerical Studies on Response of the Stone Column in Layered Soil. *International Journal of Geosynthetics and Ground Engineering*, 1(3), 1–14. <https://doi.org/10.1007/s40891-015-0029-z>
- Mohtasham, M. R., & Khodaparast, M. (2018). Investigation of the Effect of Dimensional Characteristics of Stone Column on Load-Bearing Capacity and Consolidation Time. *Civil Engineering Journal*, 4(6), 1437. <https://doi.org/10.28991/cej-0309184>
- Mokhtari, M., & Kalantar, B. (2012). Soft soil stabilization using stone columns-a review. *Electronic Journal of Geotechnical Engineering*, 17 J(September), 1659–1666.
- MPMA, & MPRA. (2019). *An Advanced Plastics Recycling Industry for Malaysia*. 1–29. <https://www.اوتفورسيني مليسيا فمع السلطان عبدالله>
- Muir-Wood, D., Hu, W., & Nash, D. F. T. (2001). Group effects in stone column foundations: model tests. *Géotechnique*, 51(7), 649–649. <https://doi.org/10.1680/geot.51.7.649.51392>
- Mukul C. Bora, S. K. D. (2010). Load Deformation Behaviour of Floating Stone Columns in Soft Clay. *Indian Geotechnical Conference-GEOTrendz, December*, 251–254. <https://doi.org/10.13140/2.1.2965.4407>
- Murthi, P., Saravanan, R., & Poongodi, K. (2020). Studies on the impact of polypropylene and silica fume blended combination on the material behaviour of black cotton soil. *Materials Today: Proceedings*, 39(xxxx), 621–626. <https://doi.org/10.1016/j.matpr.2020.09.004>

- Mwanza, B. G., & Mbohwa, C. (2017). Major Obstacles to Sustainability in the Plastic Industry. *Procedia Manufacturing*, 8(October 2016), 121–128.
<https://doi.org/10.1016/j.promfg.2017.02.021>
- Najjar, S. S. (2013). A State-of-the-Art Review of Stone/Sand-Column Reinforced Clay Systems. *Geotechnical and Geological Engineering*, 31(2), 355–386.
<https://doi.org/10.1007/s10706-012-9603-5>
- Najjar, S. S., Sadek, S., & Maakaroun, T. (2010). Effect of Sand Columns on the Undrained Load Response of Soft Clays. *Journal of Geotechnical and Geoenvironmental Engineering*, 136(9), 1263–1277.
[https://doi.org/10.1061/\(asce\)gt.1943-5606.0000328](https://doi.org/10.1061/(asce)gt.1943-5606.0000328)
- Najjar, S. S., Sadek, S., Zakharia, M., & Khalaf, S. (2012). *Effect of Sand Column Inclusions on the Drained Response of Soft Clays. September*, 4079–4088.
<https://doi.org/10.1061/9780784412121.419>
- National Solid Waste Management Department. (2011). *A Study on Plastic Management In Peninsular Malaysia. December*, 282.
- Nazirah Zainul Abidin. (2010). Sustainable Construction in Malaysia – Developers ' Awareness. *Proceedings of World Academy of Science, Engineering and Technology*, 5(2), 122–129.
- Ng, K. S., & Tan, S. A. (2015). Simplified homogenization method in stone column designs. *Soils and Foundations*, 55(1), 154–165.
<https://doi.org/10.1016/j.sandf.2014.12.012>
- Nkwachukwu, O., Chima, C., Ikenna, A., & Albert, L. (2013). Focus on potential environmental issues on plastic world towards a sustainable plastic recycling in developing countries. *International Journal of Industrial Chemistry*, 4(1), 34.
<https://doi.org/10.1186/2228-5547-4-34>
- Nováková, K., Kurilla, L., & Achten, H. (2013). 150 000 – Parametric Control of PET Bottle Structure. *Proceedings of the International Conference on Education and Research in Computer Aided Architectural Design in Europe*, 2, 555–562.

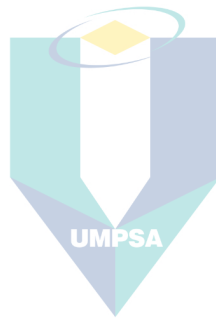
- Ogundipe, O. M. (2019). The Use of Polyethylene Terephthalate Waste for Modifying Asphalt Concrete Using the Marshall Test. *Slovak Journal of Civil Engineering*, 27(2), 9–15. <https://doi.org/10.2478/sjce-2019-0010>
- Peddaiah, S., Burman, A., & Sreedeeep, S. (2018). Experimental Study on Effect of Waste Plastic Bottle Strips in Soil Improvement. *Geotechnical and Geological Engineering*, 36(5), 2907–2920. <https://doi.org/10.1007/s10706-018-0512-0>
- Perera, S., Arulrajah, A., Wong, Y., Maghool, F., & Horpibulsuk, S. (2020). Evaluation of shear strength properties of unbound PET plastic in blends with demolition wastes. *Construction and Building Materials*, 262, 120545. <https://doi.org/10.1016/j.conbuildmat.2020.120545>
- Pham, N. T. H. (2021). Characterization of low-density polyethylene and ldp-based/ethylene-vinyl acetate with medium content of vinyl acetate. *Polymers*, 13(14). <https://doi.org/10.3390/polym13142352>
- Pivarč, J. (2011). Stone Columns - Determination of the soil improvement factor. *Slovak Journal of Civil Engineering*, 19(3), 17–21. <https://doi.org/10.2478/v10189-011-0014-z>
- Rabbee, T., Rafizul, I. M., Assaduzzaman, Md., & Alamgir, M. (2012). Investigate the effect of pre-consolidation pressure and organic content on the shear strength and compressibility parameter of reconstituted soil. *International Journal of Applied Science and Engineering Research*, 1(6), 725–738. <https://doi.org/10.6088/ijaser.0020101073>
- Rehman, A., Ma, H., Ahmad, M., Irfan, M., Traore, O., & Chandio, A. A. (2021). Towards environmental Sustainability: Devolving the influence of carbon dioxide emission to population growth, climate change, Forestry, livestock and crops production in Pakistan. *Ecological Indicators*, 125, 107460. <https://doi.org/10.1016/j.ecolind.2021.107460>
- Saikia, N., & De Brito, J. (2013). Waste polyethylene terephthalate as an aggregate in concrete. *Materials Research*, 16(2), 341–350. <https://doi.org/10.1590/S1516-14392013005000017>

- Saxena, R., Siddique, S., Gupta, T., Sharma, R. K., & Chaudhary, S. (2018). Impact resistance and energy absorption capacity of concrete containing plastic waste. *Construction and Building Materials*, 176, 415–421. <https://doi.org/10.1016/j.conbuildmat.2018.05.019>
- Schaefer, V. R., Mitchell, J. K., Berg, R. R., Filz, G. M., & Douglas, S. C. (2012). *Ground Improvement in the 21st Century: A Comprehensive Web-Based Information System*. February, 272–293. <https://doi.org/10.1061/9780784412138.0011>
- Scharifi, E., Danilenko, A., Weidig, U., & Steinhoff, K. (2019). Influence of plastic deformation gradients at room temperature on precipitation kinetics and mechanical properties of high-strength aluminum alloys. *Journal of Engineering Research and Application*, 9(1), 24–29. <https://doi.org/10.9790/9622>
- Shien, N. K., & Ann, T. S. (2014). Parametric study on the settlement improvement factor of stone column groups. *ESTEEM Academic Journal*, 10(1), 55–65. <https://doi.org/10.13140/2.1.5092.8328>
- Singh, A., & Noor, S. (2012). Soil Compression Index Prediction Model for Fine Grained Soils. *International Journal of Innovations in Engineering and Technology*, 1(4), 4.
- Sinha, V., Patel, M. R., & Patel, J. V. (2010). Pet waste management by chemical recycling: A review. *Journal of Polymers and the Environment*, 18(1), 8–25. <https://doi.org/10.1007/s10924-008-0106-7>
- Smith's Elements of Soil Mechanics. (n.d.).
- Sojobi, A. O., Nwobodo, S. E., & Aladegboye, O. J. (2016). Recycling of polyethylene terephthalate (PET) plastic bottle wastes in bituminous asphaltic concrete. *Cogent Engineering*, 3(1). <https://doi.org/10.1080/23311916.2015.1133480>
- Solanki, P., & Bhattarai, S. (2018). Strength and permeability of pervious composite prepared by using post-consumer plastic waste bottles. *MATEC Web of Conferences*, 174. <https://doi.org/10.1051/matecconf/201817402001>

- Soltani-Jigheh, H. (2016). Compressibility and shearing behavior of clayey soil reinforced by plastic waste. *International Journal of Civil Engineering*, 14(7), 479–489.
<https://doi.org/10.1007/s40999-016-0068-4>
- Sondermann, W., Raju, V. R., Daramalinggam, J., Yohannes Keller, M., & Bhd, S. (2016). *Practical Design of Vibro Stone Columns*. August.
<https://www.researchgate.net/publication/335274285>
- Stoughton, P. (2014). How to Dry PET for Container Applications. *Plastics Technology Online*, 1–12.
- Sudakov, A., Chudyk, I., Sudakova, D., & Dziubyk, L. (2019). Innovative technology for insulating the borehole absorbing horizons with thermoplastic materials. *E3S Web of Conferences*, 123, 1–13. <https://doi.org/10.1051/e3sconf/201912301033>
- Sulyman, M., Haponiuk, J., & Formela, K. (2016). Utilization of Recycled Polyethylene Terephthalate (PET) in Engineering Materials: A Review. *International Journal of Environmental Science and Development*, 7(2), 100–108.
<https://doi.org/10.7763/ijesd.2016.v7.749>
- Suriya, P., Naveenkumar, K., Raj, E. S. M., Prabakaran, M., & Kumar, R. V. (2020). Analyzing the shear strength of clay soil by stone column aided with geosynthetics and waste plastics. *AIP Conference Proceedings*, 2271(September).
<https://doi.org/10.1063/5.0024748>
- Syamsul, M., Zaini, I., Hasan, M., Nursyafiqah, W., & Wan, B. (2023). Utilization of bottom ash waste as a granular column to enhance the lateral load capacity of soft kaolin clay soil. *Environmental Science and Pollution Research*, February.
<https://doi.org/10.1007/s11356-023-25966-x>
- Tandel, Y. K., Solanki, C. H., & Desai, A. K. (2013). Laboratory experimental analysis on encapsulated stone column. *Archives of Civil Engineering*, 59(3), 359–379.
<https://doi.org/10.2478/ace-2013-0020>
- Thorneycroft, J., Orr, J., Savoikar, P., & Ball, R. J. (2018). Performance of structural concrete with recycled plastic waste as a partial replacement for sand. *Construction and Building Materials*, 161, 63–69.
<https://doi.org/10.1016/j.conbuildmat.2017.11.127>

- Turan, C., Javadi, A., Consoli, N. C., Turan, C., Cuisinier, O., Russo, G., Turan, C., Javadi, A., Consoli, N. C., Turan, C., & Vinai, R. (2020). *Mechanical Properties Of Calcareous Fly Ash Stabilized Soil To cite this version : HAL Id : hal-02439634*.
- Umasabor, R. I., & Daniel, S. C. (2020). The effect of using polyethylene terephthalate as an additive on the flexural and compressive strength of concrete. *Heliyon*, 6(8), e04700. <https://doi.org/10.1016/j.heliyon.2020.e04700>
- Welle, F. (2011). Twenty years of PET bottle to bottle recycling - An overview. *Resources, Conservation and Recycling*, 55(11), 865–875. <https://doi.org/10.1016/j.resconrec.2011.04.009>
- Wood, D. M., & Mair, R. (2010). Sir Alan Muir Wood. *Géotechnique*, 60(2), 153–156. <https://doi.org/10.1680/geot.ob.8.0008>
- Yilmaz, Y., Kheirjouy, A. B., & Akgungor, A. P. (2016). Investigation of the effect of different saturation methods on the undrained shear strength of a clayey soil compacted with standard and modified proctor energies. *Periodica Polytechnica Civil Engineering*, 60(3), 323–329. <https://doi.org/10.3311/PPci.8891>
- Yoobanpot, N., Jamsawang, P., & Horpibulsuk, S. (2017). Strength behavior and microstructural characteristics of soft clay stabilized with cement kiln dust and fly ash residue. *Applied Clay Science*, 141, 146–156. <https://doi.org/10.1016/j.clay.2017.02.028>
- Zaini, M. S. I., & Hasan, M. (2023). Effectiveness of Silica Fume Eggshell Ash and Lime Use on the Properties of Kaolinitic Clay. *International Journal of Engineering and Technology Innovation*, 13(4), 337–352. <https://doi.org/10.46604/ijeti.2023.11936>
- Zaini, M. S. I., Hasan, M., Yie, L. S., Masri, K. A., Jaya, R. P., Hyodo, M., & Winter, M. J. (2022). the Effect of Utilizing Silica Fume and Eggshell Ash on the Geotechnical Properties of Soft Kaolin Clay. *Jurnal Teknologi*, 84(1), 159–170. <https://doi.org/10.11113/jurnalteknologi.v84.17115>
- Zeng, L. L., & Hong, Z. S. (2015). Experimental study of primary consolidation time for structured and destructured clays. *Applied Clay Science*, 116–117, 141–149. <https://doi.org/10.1016/j.clay.2015.08.027>

- Zhang, J., Li, C., Ding, L., & Li, J. (2021). Performance evaluation of cement stabilized recycled mixture with recycled concrete aggregate and crushed brick. *Construction and Building Materials*, 296, 123596.
<https://doi.org/10.1016/j.conbuildmat.2021.123596>
- Zhang, Z., Wang, X., Zhang, Y., Gao, Y., Liu, Y., Sun, X., Zhi, J., & Yin, S. (2023). Simulating land use change for sustainable land management in rapid urbanization regions: a case study of the Yangtze River Delta region. *Landscape Ecology*, 38(7), 1807–1830. <https://doi.org/10.1007/s10980-023-01657-3>
- Zhao, J. J., Lee, M. L., Lim, S. K., & Tanaka, Y. (2015). Unconfined compressive strength of PET waste-mixed residual soils. *Geomechanics and Engineering*, 8(1), 53–66.
<https://doi.org/10.12989/gae.2015.8.1.053>



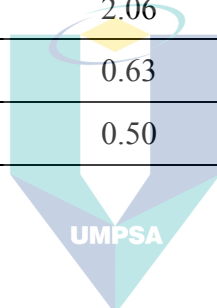
اونيفرسيتي مليسيا قهغ السلطان عبدالله
UNIVERSITI MALAYSIA PAHANG
AL-SULTAN ABDULLAH



اونيفرسيتي مليسيا قهغ السلطان عبدالله
UNIVERSITI MALAYSIA PAHANG
AL-SULTAN ABDULLAH

APPENDIX A
SIEVE ANALYSIS RESULT

| Sieve Size (mm) | Mass of Sieve (g) | Mass Retained on Sieve (g) | Percent Retained (%) | Percent Passing (%) |
|-----------------|-------------------|----------------------------|----------------------|---------------------|
| 6.30 | 515.36 | 0.42 | 0.11 | 99.89 |
| 5.00 | 497.18 | 12.43 | 3.18 | 96.71 |
| 3.35 | 542.90 | 2.85 | 0.73 | 95.98 |
| 1.18 | 514.39 | 295.33 | 75.60 | 20.38 |
| 0.600 | 461.37 | 66.33 | 16.98 | 3.40 |
| 0.300 | 431.59 | 10.11 | 2.58 | 0.82 |
| 0.15 | 417.11 | 2.06 | 0.53 | 0.29 |
| 0.063 | 300.92 | 0.63 | 0.16 | 0.13 |
| Pan | 299.36 | 0.50 | 0.13 | 0.00 |



اونيفرسيتي مليسيا قهغ السلطان عبدالله
UNIVERSITI MALAYSIA PAHANG
AL-SULTAN ABDULLAH

APPENDIX B

HYDROMETER TEST RESULT

Sample: Kaolin S300

Reference: BS 1377: Part 2: 1990: 9.6

Meniscus Correction, $C_m = 0$

Reading in Dispersant, $R_o' = 1.000$

Dry Mass of Soil, $m = 51.72\text{g}$

Particle Density = 2.62

| Date | Time | Elapsed Time, t (min) | Temperature, T (°C) | Hydrometer Reading, R_h' | True Reading, R_h | Effective Depth, H_R (mm) | Modified Reading, R_d | Particle Diameter, D (mm) | Percentage Finer, K (%) |
|-----------|----------|-----------------------|---------------------|----------------------------|---------------------|-----------------------------|-------------------------|---------------------------|-------------------------|
| 8/3/2023 | 1.35p.m. | 0 | 27.4 | - | - | - | - | - | - |
| 8/3/2023 | 1.35p.m. | 0.5 | 27.4 | 1.0080 | 1.0080 | 122.04 | 0.0080 | 0.0625 | 2.50 |
| 8/3/2023 | 1.35p.m. | 1 | 27.4 | 1.0080 | 1.0080 | 122.04 | 0.0080 | 0.0442 | 2.50 |
| 8/3/2023 | 1.36p.m. | 2 | 27.2 | 1.0075 | 1.0075 | 120.19 | 0.0075 | 0.0311 | 2.35 |
| 8/3/2023 | 1.38p.m. | 4 | 27.2 | 1.0070 | 1.0070 | 118.34 | 0.0070 | 0.0218 | 2.19 |
| 8/3/2023 | 1.42p.m. | 8 | 27.2 | 1.0070 | 1.0070 | 118.34 | 0.0070 | 0.0154 | 2.19 |
| 8/3/2023 | 1.50p.m. | 16 | 27.0 | 1.0060 | 1.0060 | 114.64 | 0.0060 | 0.0107 | 1.88 |
| 8/3/2023 | 2.06p.m. | 30 | 27.3 | 1.0050 | 1.0050 | 110.94 | 0.0050 | 0.0077 | 1.56 |
| 8/3/2023 | 2.36p.m. | 60 | 28.2 | 1.0030 | 1.0030 | 103.54 | 0.0030 | 0.0052 | 0.94 |
| 8/3/2023 | 4.36p.m. | 120 | 28.0 | 1.0025 | 1.0025 | 101.69 | 0.0025 | 0.0037 | 0.78 |
| 9/3/2023 | 2.35p.m. | 1440 | 27.5 | 1.0010 | 1.0010 | 96.14 | 0.0010 | 0.0010 | 0.31 |
| 10/3/2023 | 2.35p.m. | 2880 | 27.1 | 1.0000 | 1.0000 | 92.44 | 0.0000 | 0.0007 | 0.00 |

APPENDIX C

ATTEBERG LIMIT TEST RESULT

Atterberg Limit Test

Reference: BS 1377: Part 2: 1990: Clause 4.3, 5.3

Sample Description: Kaolin S300

PLASTIC LIMIT (PL)

| Container Number | D1 | D2 |
|--------------------------------|-------|-------|
| Container Weight | 10.65 | 10.38 |
| Wet Soil + Container (g) | 26.25 | 21.20 |
| Wet Soil, W_w (g) | 15.60 | 10.82 |
| Dry Soil + Container (g) | 22.63 | 18.78 |
| Dry Soil, W_d (g) | 11.98 | 8.40 |
| Moisture Loss, $W_w - W_d$ (g) | 3.62 | 2.42 |
| Moisture Content (%) | 30.22 | 28.80 |
| Plastic Limit % | 29.51 | |

LIQUID LIMIT (LL)

| Test Number | 1 | | 2 | | 3 | |
|--------------------------------|-------|-------|-------|-------|-------|-------|
| Cone penetration (mm) | 13.90 | 13.70 | 14.60 | 14.20 | 16.50 | 17.30 |
| Average Penetration (mm) | 13.80 | | 14.40 | | 16.90 | |
| Container No. | 1 | 2 | 1 | 2 | 1 | 2 |
| Container Weight (g) | 10.29 | 9.63 | 10.87 | 10.69 | 10.37 | 10.01 |
| Wet Soil + Container (g) | 32.27 | 29.12 | 32.68 | 23.24 | 27.35 | 24.04 |
| Wet Soil, W_w (g) | 21.98 | 19.49 | 22.29 | 12.55 | 16.98 | 14.03 |
| Dry Soil + Container (g) | 26.83 | 24.33 | 27.50 | 19.95 | 22.70 | 20.06 |
| Dry Soil, W_d (g) | 16.54 | 14.70 | 16.63 | 9.26 | 12.33 | 10.05 |
| Moisture Loss, $W_w - W_d$ (g) | 5.44 | 4.79 | 5.66 | 3.29 | 4.65 | 3.98 |
| Moisture Content (%) | 32.89 | 32.59 | 34.03 | 35.53 | 37.71 | 39.60 |
| Liquid Limit % | 35.39 | | | | | |

Plasticity Index (PI) = 35.39 – 29.51

$$= 5.88$$

APPENDIX D

RELATIVE DENSITY TEST RESULT

Sample: PET

Test Method: BS1377: Part 2: 1990: 9.3

Reference: BS 1377: Part 4: 1990: 4

Mould Diameter = 15.2 cm

Mould Height = 15.5 cm

Volume of the Mould = 28.12.61 cm³

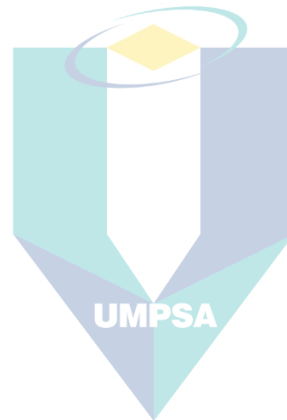
Minimum Density Determination (0% Relative Density)

| Test Sample No. | 1 | 2 |
|--|-------|-------|
| Mass of Mould, m_1 (g) | 9300 | 9300 |
| Mass of Mould + Soil, m_2 (g) | 10520 | 10520 |
| Mass of Soil, $m_a = m_2 - m_1$ (g) | 1220 | 1220 |
| Minimum Density of soil, $\rho_a = m_a/V$ (g/cm ³) | 0.43 | 0.43 |
| Average Minimum Density (g/cm ³) | 0.43 | |

Maximum Density Determination (100% Relative Density)

| Test Sample No. | 1 | | | | | 2 | | | | |
|--------------------------------------|------|-----|-----|-----|-----|------|-----|-----|-----|-----|
| Gauge Reading (cm) | 1.7 | 1.6 | 1.7 | 1.7 | 1.6 | 1.5 | 1.7 | 1.8 | 1.6 | 1.7 |
| (Initial Reading Set to 0mm) | 1.66 | | | | | 1.66 | | | | |
| Gauge Reading + Plate Thickness (cm) | 2.76 | | | | | 2.76 | | | | |
| Mass of Mould, m_3 (g) | 9300 | | | | | 9300 | | | | |

| | | |
|--|---------|---------|
| Mass of Mould + Soil, m_4 (g) | 10520 | 10520 |
| Mass of Soil, $m_b = m_4 - m_3$ (g) | 1220 | 1220 |
| Volume of Soil, V_s (cm ³) | 2311.78 | 2311.78 |
| Maximum density of Soil, $\rho_b = m_b/V_s$ (g/cm ³) | 0.53 | 0.53 |
| Average Maximum Density (g/cm ³) | 0.53 | |



اونيفرسيتي مليسيا قهغ السلطان عبدالله
UNIVERSITI MALAYSIA PAHANG
AL-SULTAN ABDULLAH

APPENDIX E

SPECIFIC GRAVITY TEST RESULT

Specific Gravity Test

Sample: Kaolin

Test Method: BS 1377: Part 2: 1990:8.3

| TEST NO | 1 | 2 | 3 | 4 |
|--|--------|--------|--------|--------|
| Density Bottle No. | | | | |
| Weight of Density Bottle, g | 43.42 | 43.08 | 42.56 | 40.35 |
| Weight of Bottle + Stopper (W_1), g | 47.51 | 47.52 | 47.01 | 44.88 |
| Weight of Bottle + Stopper + Dry Soil (W_2), g | 53.12 | 55.08 | 48.89 | 51.39 |
| Weight of Bottle + Stopper + Soil + Water (W_3), g | 151.53 | 151.96 | 147.18 | 149.09 |
| Weight of Bottle + Stopper + Water (W_4), g | 148.03 | 147.30 | 146.02 | 145.05 |
| Weight of Dry Soil ($W_2 - W_1$), g | 5.61 | 7.56 | 1.88 | 6.51 |
| Weight of Water ($W_4 - W_1$), g | 100.52 | 99.78 | 99.01 | 100.17 |
| Weight of Soil ($W_3 - W_2$), g | 98.41 | 96.88 | 98.29 | 97.70 |
| Specific Gravity, Gs | 2.65 | 2.61 | 2.61 | 2.64 |
| Average Specific Gravity, Gs | 2.62 | | | |

Sample: PET

| TEST NO | 1 | 2 | 3 |
|--|-------|-------|-------|
| Density Bottle No. | | | |
| Weight of Density Bottle, g | 24.61 | 25.53 | 23.16 |
| Weight of Bottle + Stopper (W_1), g | 28.31 | 29.63 | 27.04 |
| Weight of Bottle + Stopper + Dry Soil (W_2), g | 32.22 | 32.04 | 30.81 |
| Weight of Bottle + Stopper + Soil + Water (W_3), g | 79.45 | 81.28 | 77.98 |
| Weight of Bottle + Stopper + Water (W_4), g | 78.31 | 80.51 | 77.04 |
| Weight of Dry Soil ($W_2 - W_1$), g | 3.91 | 2.41 | 3.77 |
| Weight of Water ($W_4 - W_1$), g | 50 | 50.88 | 50 |
| Weight of Soil ($W_3 - W_2$), g | 47.23 | 49.24 | 47.17 |
| Specific Gravity, Gs | 1.41 | 1.47 | 1.33 |
| Average Specific Gravity, Gs | 1.40 | | |

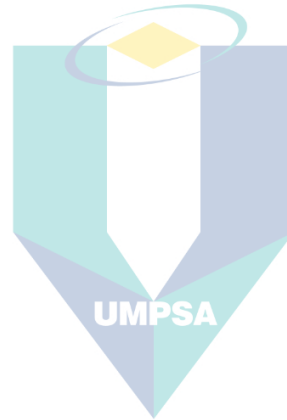
APPENDIX F
STANDARD COMPACTION TEST RESULT

Sample: Kaolin S300

Test Method: BS 1377: Part 4: 1990: 3.3

| Water Content | 5% | | 10% | | 15% | | 20% | | 25% | | 30% | |
|---|-------|-------|-------|-------|-------|-------|-------|-------|-------|-------|-------|-------|
| Mass of Mould + Base, m_1 (g) | 5540 | | 5540 | | 5540 | | 5540 | | 5540 | | 5540 | |
| Mass of Mould + Base + Compacted Specimen, m_2 (g) | 7030 | | 7160 | | 7290 | | 7370 | | 7360 | | 7330 | |
| Mass of Compacted Specimen, $m_2 - m_1$ (g) | 1490 | | 1620 | | 1750 | | 1830 | | 1820 | | 1790 | |
| Bulk Density, ρ (g/cm ³) | 1.50 | | 1.63 | | 1.76 | | 1.84 | | 1.83 | | 1.80 | |
| Moisture Content Container No. | A | B | C | D | E | F | G | H | I | J | K | L |
| Container Weight (g) | 10.28 | 10.79 | 9.28 | 10.49 | 9.91 | 10.46 | 9.42 | 15.15 | 10.30 | 9.73 | 9.58 | 10.28 |
| Wet Soil + Contain (g) | 27.13 | 21.92 | 26.73 | 31.11 | 25.12 | 27.92 | 22.32 | 29.12 | 25.13 | 21.28 | 29.78 | 30.93 |
| Wet Soil, W_w (g) | 16.85 | 11.13 | 17.45 | 20.62 | 15.21 | 17.46 | 12.90 | 13.97 | 14.83 | 11.55 | 20.20 | 20.65 |
| Dry Soil + Contain (g) | 26.40 | 21.46 | 25.30 | 29.41 | 23.17 | 25.65 | 20.20 | 26.84 | 22.30 | 19.06 | 25.23 | 26.27 |
| Dry Soil, W_d (g) | 16.12 | 10.67 | 16.02 | 18.92 | 13.26 | 15.19 | 10.78 | 11.69 | 12.00 | 9.33 | 15.65 | 15.99 |
| Moisture Loss, $W_w - W_d$ (g) | 0.73 | 0.46 | 1.43 | 1.70 | 1.95 | 2.27 | 2.12 | 2.28 | 2.83 | 2.22 | 4.55 | 4.66 |

| | | | | | | | | | | | | |
|--|------|------|------|------|-------|-------|-------|-------|-------|-------|-------|-------|
| Moisture Content, ($W_w - W_d$)/ W_d (%) | 4.53 | 4.31 | 8.93 | 8.99 | 14.71 | 14.94 | 19.67 | 19.50 | 23.58 | 23.79 | 29.07 | 29.14 |
| Average Moisture Content, W_{avg} (%) | 4.42 | | 8.96 | | 14.83 | | 19.56 | | 23.69 | | 29.11 | |
| Dry Density, γ_d (kN/m ³) | 1.44 | | 1.50 | | 1.53 | | 1.54 | | 1.48 | | 1.39 | |



اونيفرسيتي مليسيا قهغ السلطان عبدالله
UNIVERSITI MALAYSIA PAHANG
AL-SULTAN ABDULLAH

APPENDIX G

FALLING HEAD TEST RESULT

Sample: Kaolin S300

Reference: ASTM D 2434

Diameter of the specimen, D: 9.99 cm

Length of the specimen, L: 12.47 cm

Area of the specimen, A: 78.39 cm²

Diameter of the burette, d: 0.50 cm

Area of the burette, a: 0.20 cm²

| Test No. | Time, s | Head, h ₁ (cm) | Head, h ₂ (cm) | Permeability, k (cm/s) |
|----------|---------|---------------------------|---------------------------|---------------------------|
| 1 | 14400 | 50 | 48 | 5.1972 x 10 ⁻⁶ |
| 2 | 14400 | 50 | 48 | 5.1972 x 10 ⁻⁶ |
| 3 | 14400 | 50 | 48 | 5.1972 x 10 ⁻⁶ |
| 4 | 14400 | 50 | 48 | 5.1972 x 10 ⁻⁶ |
| 5 | 14400 | 50 | 48 | 5.1972 x 10 ⁻⁶ |

$$k = a/A \times 1/t \times 2.3 \log h_1/h_2$$

Average permeability, k = 5.1972 x 10⁻⁶ cm/s

اونیورسیتی ملیسیا قهغ السلطان عبدالله
 UNIVERSITI MALAYSIA PAHANG
 AL-SULTAN ABDULLAH

APPENDIX H

CONSTANT HEAD TEST RESULT

Sample: PET plastic (1.18 mm)

Reference: ASTM D 2434

Diameter of the specimen, D: 7.50 cm

Length of the specimen, L: 10.00 cm

Area of the specimen, A: 44.18 cm²

| Test No. | Discharge volume, Q (cm ³) | Time of collection, t (s) | Head difference, h | k = QL/Aht (cm/s) |
|----------|--|---------------------------|--------------------|---------------------------|
| 1 | 768.47 | 30 | 230 | 2.5206 x 10 ⁻² |
| 2 | 759.31 | 30 | 230 | 2.4906 x 10 ⁻² |
| 3 | 763.49 | 30 | 230 | 2.5043 x 10 ⁻² |
| 4 | 762.88 | 30 | 230 | 2.5023 x 10 ⁻² |
| 5 | 761.73 | 30 | 230 | 2.4985 x 10 ⁻² |

Average permeability, k = 2.5033 x 10⁻² cm/s


 اونیورسیتی ملیسیا قوۃ الساطن عبدالله
 = 2.5033 x 10⁻⁴ m/s
 UNIVERSITI MALAYSIA PAHANG
 AL-SULTAN ABDULLAH

APPENDIX I

ONE CONSOLIDATION DIMENSIONAL TEST RESULT

One Dimensional Consolidation Test

Reference: ASTM D 2435

Type of sample: Kaolin Clay S300

Mass of ring: 67.94g

Inside diameter ring: 50 mm/ 5.0 cm

Height of ring, H: 19 mm/ 1.9 cm

Area of ring, A: 19.635 cm/ 1.963x10³ mm²

Mass of wet specimen: 71.01 g

Mass of dry specimen: 56.06 g

Specific gravity, G_s: 2.62 Mg/m³

| | | | |
|-----------------|------------------|----------------|-------------|
| Client | KAOLIN CLAY S300 | Lab Ref | |
| Project | | Job | 12042023-JS |
| Borehole | | Sample | 12042023-JS |

| Test Details | | | |
|----------------------------------|--|-------------------------|------------------------|
| Standard | BS 1377: Part 5 : 1990 : Clause 3 | Particle Density | 2.62 Mg/m ³ |
| Sample Type | Core sample | Lab Temperature | 0.0 deg.C |
| Sample Depth | 0.00 m | | |
| Sample Description | اونيفورسيٲى مليسيا فھغ السلطان عبداللہ | | |
| Variations from Procedure | None | | |

| Specimen Details | | | |
|----------------------------|----------|----------------------------------|------------------|
| Specimen Reference | A | Description | |
| Depth within Sample | 0.00mm | Orientation within Sample | |
| Specimen Mass | 71.68 g | Condition | Natural Moisture |
| Specimen Height | 19.00 mm | Preparation | |
| Comments | | | |

| Test Apparatus | | | |
|--------------------|---|----------------------|----------|
| Ring Number | 1 | Ring Diameter | 50.00 mm |

| | | | |
|--------------------|-----------|--------------------|---------|
| Ring Height | 19.00 mm | Ring Weight | 67.94 g |
| Lever Ratio | 10.00 : 1 | | |

| | | | |
|-------------------------------------|------------------------|-----------------------------------|------------------------|
| Height of Solid Particles | 1090 mm | Swelling Pressure | 0.0 kPa |
| Initial Moisture Content* | 27.9 % | Final Moisture Content | 26.7 % |
| Initial Bulk Density | 1.92 Mg/m ³ | Final Bulk Density | 1.95 Mg/m ³ |
| Initial Dry Density | 1.50 Mg/m ³ | Final Dry Density | 1.54 Mg/m ³ |
| Initial Void Ratio | 0.7435 | Final Void Ratio | 0.7028 |
| Initial Degree of Saturation | 98.18 % | Final Degree of Saturation | 99.42 % |

- Calculated from initial and dry weights of whole specimen

| Pressure (Loading Stages) | Coefficient of Volume Compressibility (m_v) | Coefficient of Consolidation (c_v) |
|--------------------------------------|--|---|
| 0.00 | | |
| 50.0 kPa | 0.34 m ² /MN | 44.21 m ² /yr |
| 99.9 kPa | 0.15 m ² /MN | 43.12 m ² /yr |
| 199.8 kPa | 0.08 m ² /MN | 42.44 m ² /yr |
| 399.7 kPa | 0.04 m ² /MN | 47.56 m ² /yr |
| 799.4 kPa | 0.03 m ² /MN | 42.68 m ² /yr |
| 199.8 kPa | 0.02 m ² /MN | ----- |
| 50.0 kPa | 0.10 m ² /MN | ----- |
| | | |
| | | |
| | | |
| | | |
| | | |
| | | |
| | | |

| | |
|------------------------------------|------------------|
| Method of Time Fitting Used | Square Root Time |
|------------------------------------|------------------|

$$\begin{aligned}\text{Given, } G_s &= 2.62 \text{ Mg/m}^3 \\ &= 2.62 \times 10^6 \text{ g/m}^3\end{aligned}$$

$$\begin{aligned}P_w &= 1000 \text{ kg/m}^3 \\ &= 1 \text{ Mg/m}^3\end{aligned}$$

1) The equivalent height of the solid particles, H_s

$$H_s = \frac{M_s \times 1000}{G_s P_w \times A}$$

$$= \frac{56.06 \text{ g} \times 1000}{(2.62 \times 1) \text{ g/mm}^3 (1.963 \times 10^3) \text{ mm}^2}$$

$$= 10.9 \text{ mm}$$

2) The void ratio at the end of each loading or unloading stage for 500g loading.

$$e_{0.5} = \frac{H - H_s}{H_s}$$

$$= \frac{19 - (10.9)}{(10.9)}$$

$$= 0.743$$

3) Amount of Settlement

$$S_c = C_c [H / (1 + e_0)] \text{Log} [P/P_0]$$

$$C_c = \frac{e_0 - e}{\text{Log} (P/P_0)}$$

From the graph, we obtained below:

$$e_0 = 0.6050, \quad P_0 = 399.7 \text{ kpa}$$

$$e = 0.6561, \quad P = 799.4 \text{ kpa}$$

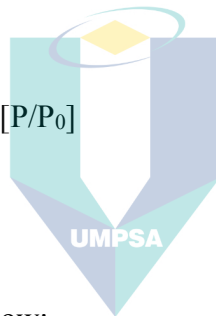
Hence,

$$C_c = \frac{e_0 - e}{\text{Log} (P/P_0)}$$

$$= \frac{(0.665 - 0.6561)}{\text{Log} (799.4/399.7)}$$

$$= 0.0296$$

$$S_c = C_c [H / (1 + e_0)] \text{Log} [P/P_0]$$

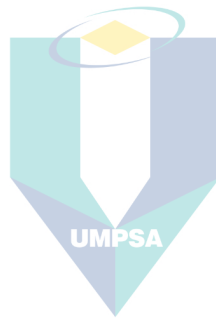


اونيفرسيتي مليسيا قهغ السلطان عبدالله
UNIVERSITI MALAYSIA PAHANG
AL-SULTAN ABDULLAH

$$= 0.0296 [19 / (1+0.665)] \text{ Log } (799.4/399.7)$$

$$= 0.10 \text{ mm}$$

Pre-compressions stress, $P_c = 88 \text{ kPa}$



اونيفرسيتي مليسيا قهغ السلطان عبدالله
UNIVERSITI MALAYSIA PAHANG
AL-SULTAN ABDULLAH

APPENDIX J DIRECT SHEAR TEST

Direct Shear Test

Reference: BS 1377: Part 1990: Clause 4.0

Sample Description: PET plastic

Sample A

| Test Detail | | | |
|------------------------------|------------------------------------|-----------------------|------------------------|
| Standard | BS 1377: Part 7: 1990: Clause 4 | Particle Density | 1.40 Mg/m ³ |
| Sample Type | Small disturbed sample | Single or Multi Stage | Single Stage |
| Lab. Temperature | 0.0 deg.C | Location | |
| Sample Description | | | |
| Variations from procedure | None | | |

| Specimen Details | | | |
|----------------------|------------------------|------------------------------|-------------------------|
| Specimen Reference | A | Description | |
| Depth within Sample | 0.00 mm | Orientation within Sample | |
| Initial Height | 28.000 mm | Area | 3600.00 mm ² |
| Preparation | | Initial Moisture Content* | 705.5% |
| Bulk Density | 0.49 Mg/m ³ | Dry Density | 0.06 Mg/m ³ |
| Initial Voids Ration | 21.7981 | Degree of Saturation | 45.31% |
| Dry or Submerged | Dry | | |
| Comments | | | |

| Conditions at Failure | |
|------------------------------------|-----------|
| Applied Normal Stress | 136.2 kPa |
| Maximum Shear Stress | 42.0 kPa |
| Horizontal Deformation | 4.404 mm |
| Residual Shear Stress | 0.0 kPa |
| Vertical Deformation | -0.701 mm |
| Cumulative Horizontal Displacement | 4.505 mm |

Sample B

| Test Detail | | | |
|---------------------------|---------------------------------|-----------------------|------------------------|
| Standard | BS 1377: Part 7: 1990: Clause 4 | Particle Density | 1.40 Mg/m ³ |
| Sample Type | Small disturbed sample | Single or Multi Stage | Single Stage |
| Lab. Temperature | 0.0 deg.C | Location | |
| Sample Description | | | |
| Variations from procedure | None | | |

| Specimen Details | | | |
|----------------------|------------------------|---------------------------|-------------------------|
| Specimen Reference | B | Description | |
| Depth within Sample | 0.00 mm | Orientation within Sample | |
| Initial Height | 28.000 mm | Area | 3600.00 mm ² |
| Preparation | | Initial Moisture Content* | 467.5% |
| Bulk Density | 0.52 Mg/m ³ | Dry Density | 0.09 Mg/m ³ |
| Initial Voids Ration | 14.4230 | Degree of Saturation | 45.38 % |
| Dry or Submerged | Dry | | |
| Comments | | | |

| Conditions at Failure | |
|------------------------------------|-----------|
| Applied Normal Stress | 272.5 kPa |
| Maximum Shear Stress | 88.3 kPa |
| Horizontal Deformation | 4.170 mm |
| Residual Shear Stress | 0.0 kPa |
| Vertical Deformation | -0.008 mm |
| Cumulative Horizontal Displacement | 4.372 mm |

Sample C

| Test Detail | | | |
|---------------------------|---------------------------------|-----------------------|------------------------|
| Standard | BS 1377: Part 7: 1990: Clause 4 | Particle Density | 1.40 Mg/m ³ |
| Sample Type | Small disturbed sample | Single or Multi Stage | Single Stage |
| Lab. Temperature | 0.0 deg.C | Location | |
| Sample Description | | | |
| Variations from procedure | None | | |

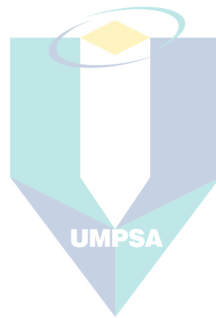
| Specimen Details | | | |
|----------------------|------------------------|---------------------------|-------------------------|
| Specimen Reference | C | Description | |
| Depth within Sample | 0.00 mm | Orientation within Sample | |
| Initial Height | 28.000 mm | Area | 3600.00 mm ² |
| Preparation | | Initial Moisture Content* | 307.8% |
| Bulk Density | 0.46 Mg/m ³ | Dry Density | 0.11 Mg/m ³ |
| Initial Voids Ration | 11.5329 | Degree of Saturation | 37.37 % |
| Dry or Submerged | Dry | | |
| Comments | | | |

| Conditions at Failure | |
|------------------------------------|-----------|
| Applied Normal Stress | 408.8 kPa |
| Maximum Shear Stress | 93.3 kPa |
| Horizontal Deformation | 3.968 mm |
| Residual Shear Stress | 0.0 kPa |
| Vertical Deformation | -0.011 mm |
| Cumulative Horizontal Displacement | 4.170 mm |

APPENDIX K
UNCONFINED COMPRESSION TEST

| Sample | Volume of Sample, V_s (mm ³) | Volume of Column, V_c (mm ³) | Volume replacement ratio, V_c/V_s (%) | Shear Strength Improvement, ΔS_u (%) |
|---------------------------|--|--|---|--|
| Control Sample | | | | |
| Control | 1.95×10^5 | 0 | 0 | 0 |
| Single PET Column (10 mm) | | | | |
| S1060 | 1.95×10^5 | 4712.39 | 2.40 | 35.52 |
| S1080 | | 6283.19 | 3.20 | 29.37 |
| S10100 | | 7853.98 | 4.00 | 27.49 |
| Single PET Column (16 mm) | | | | |
| S1660 | 1.95×10^5 | 12063.72 | 6.14 | 21.00 |
| S1680 | | 16084.95 | 8.19 | 54.91 |
| S16100 | | 20106.19 | 10.24 | 56.53 |
| Group PET Columns (10 mm) | | | | |
| G1060 | 1.95×10^5 | 14137.17 | 7.20 | 46.79 |
| G1080 | | 18849.57 | 9.60 | 38.77 |

| | | | | |
|----------------------------------|------------------------|----------|-------|-------|
| G10100 | | 23561.94 | 12.00 | 48.42 |
| Group PET Columns (16 mm) | | | | |
| G1660 | 1.95 x 10 ⁵ | 36191.16 | 18.43 | 21.00 |
| G1680 | | 48254.85 | 24.58 | 22.63 |
| G16100 | | 60318.57 | 30.72 | 11.35 |



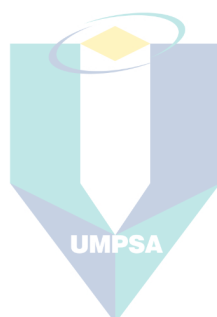
اونيفرسيتي مليسيا قهغ السلطان عبدالله
UNIVERSITI MALAYSIA PAHANG
AL-SULTAN ABDULLAH

APPENDIX L
UNCONSOLIDATED UNDRAINED TRIAXIAL TEST

| Sample | Cell Pressure (kPa) | A_c/A_s (%) | H_c/D_c (%) | H_c/H_s (%) | c (kPa) | ϕ (°) |
|---------|---------------------|---------------|---------------|---------------|---------|------------|
| Control | 100 | 0 | 0 | 0 | 42.2 | 30.0 |
| | 200 | | | | | |
| | 400 | | | | | |
| S1060 | 100 | 6 | 0.6 | 0.6 | 47.5 | 34.0 |
| | 200 | | | | | |
| | 400 | | | | | |
| S1080 | 100 | 4 | 8 | 0.8 | 51.4 | 31.0 |
| | 200 | | | | | |
| | 400 | | | | | |
| S10100 | 100 | 10 | 1.0 | 1.0 | 47.8 | 31.5 |
| | 200 | | | | | |
| | 400 | | | | | |
| S1660 | 100 | 10.24 | 3.75 | 0.6 | 47.0 | 31.8 |
| | 200 | | | | | |

| | | | | | | |
|--------|-----|-------|------|-----|------|------|
| | 400 | | | | | |
| S1680 | 100 | | | | | |
| | 200 | | 5.00 | 0.8 | 46.0 | 32.8 |
| | 400 | | | | | |
| S16100 | 100 | | | | | |
| | 200 | | 6.25 | 1.0 | 49.6 | 33.0 |
| | 400 | | | | | |
| G1060 | 100 | | | | | |
| | 200 | | | 0.6 | 49.1 | 31.4 |
| | 400 | | | | | |
| G1080 | 100 | | | | | |
| | 200 | 12.00 | 8 | 0.8 | 54.5 | 31.8 |
| | 400 | | | | | |
| G10100 | 100 | | | | | |
| | 200 | | 10 | 1.0 | 46.3 | 31.2 |
| | 400 | | | | | |
| G1660 | 100 | 30.72 | 3.75 | 0.6 | 47.1 | 31.5 |
| | 200 | | | | | |

| | | | | | | |
|--------|-----|--|------|-----|------|------|
| | 400 | | | | | |
| G1680 | 100 | | 5.00 | 0.8 | 57.3 | 32.9 |
| | 200 | | | | | |
| | 400 | | | | | |
| G16100 | 100 | | 6.25 | 1.0 | 44.4 | 33.2 |
| | 200 | | | | | |
| | 400 | | | | | |

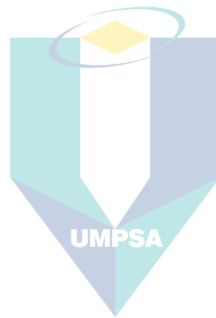


اونيفرسيتي مليسيا قهغ السلطان عبدالله
UNIVERSITI MALAYSIA PAHANG
AL-SULTAN ABDULLAH

| Sample | Cell Pressure (kPa) | H _c /H _s (%) | Max. Deviator Stress (kPa) | Max. Deviator Stress Improvement (%) | Axial Strain (%) | Average Axial Strain (%) |
|---------|---------------------|------------------------------------|----------------------------|--------------------------------------|------------------|--------------------------|
| Control | 100 | - | 142.82 | - | 8.36 | 7.74 |
| | 200 | | 155.59 | | 6.67 | |
| | 400 | | 273.86 | | 8.20 | |
| S1060 | 100 | 0.6 | 147.66 | 3.39 | 15.33 | 14.62 |
| | 200 | | 212.95 | 36.87 | 14.01 | |
| | 400 | | 332.73 | 21.50 | 14.52 | |
| S1080 | 100 | 0.8 | 171.03 | 19.75 | 9.57 | 8.07 |
| | 200 | | 226.67 | 45.68 | 6.88 | |
| | 400 | | 407.01 | 48.62 | 7.77 | |
| S10100 | 100 | 1.0 | 144.51 | 1.18 | 19.73 | 17.90 |
| | 200 | | 217.31 | 39.67 | 13.95 | |
| | 400 | | 371.92 | 35.81 | 20.01 | |
| S1660 | 100 | 0.6 | 155.06 | 8.57 | 8.62 | 10.84 |
| | 200 | | 302.59 | 94.48 | 14.40 | |

| | | | | | | |
|--------|-----|-----|--------|-------|-------|-------|
| | 400 | | 321.15 | 17.27 | 9.51 | |
| S1680 | 100 | 0.8 | 167.03 | 16.95 | 9.65 | 7.88 |
| | 200 | | 275.73 | 77.22 | 6.33 | |
| | 400 | | 403.55 | 47.36 | 7.65 | |
| S16100 | 100 | 1.0 | 174.70 | 22.32 | 3.10 | 6.68 |
| | 200 | | 272.38 | 75.06 | 7.95 | |
| | 400 | | 411.3 | 50.31 | 8.98 | |
| G1060 | 100 | 0.6 | 155.06 | 8.57 | 8.62 | 8.43 |
| | 200 | | 256.78 | 65.04 | 6.63 | |
| | 400 | | 349.04 | 27.45 | 10.05 | |
| G1080 | 100 | 0.8 | 178.77 | 25.17 | 3.30 | 9.47 |
| | 200 | | 257.27 | 65.35 | 10.12 | |
| | 400 | | 305.86 | 11.68 | 14.99 | |
| G1010 | 100 | 1.0 | 165.33 | 14.36 | 3.38 | 8.16 |
| | 200 | | 249.95 | 60.65 | 9.42 | |
| | 400 | | 436.83 | 59.51 | 11.67 | |
| G1660 | 100 | 0.6 | 161.66 | 13.19 | 9.05 | 10.07 |
| | 200 | | 262.10 | 68.46 | 11.12 | |

| | | | | | | |
|--------|-----|-----|--------|-------|-------|-------|
| | 400 | | 415.59 | 51.75 | 10.03 | |
| G1680 | 100 | 0.8 | 189.94 | 32.99 | 13.52 | 13.99 |
| | 200 | | 289.72 | 86.21 | 13.28 | |
| | 400 | | 391.80 | 43.07 | 15.18 | |
| G16100 | 100 | 1.0 | 153.20 | 7.27 | 9.67 | 16.52 |
| | 200 | | 293.01 | 53.62 | 19.98 | |
| | 400 | | 479.74 | 75.18 | 19.90 | |



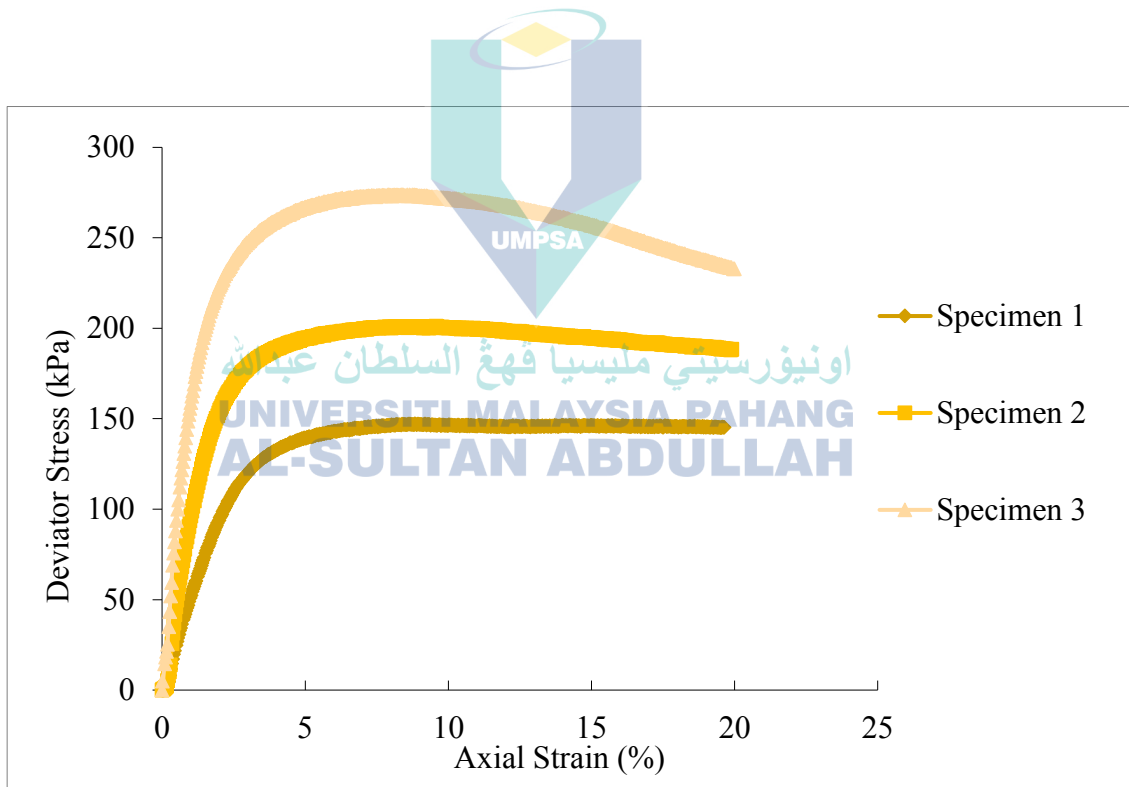
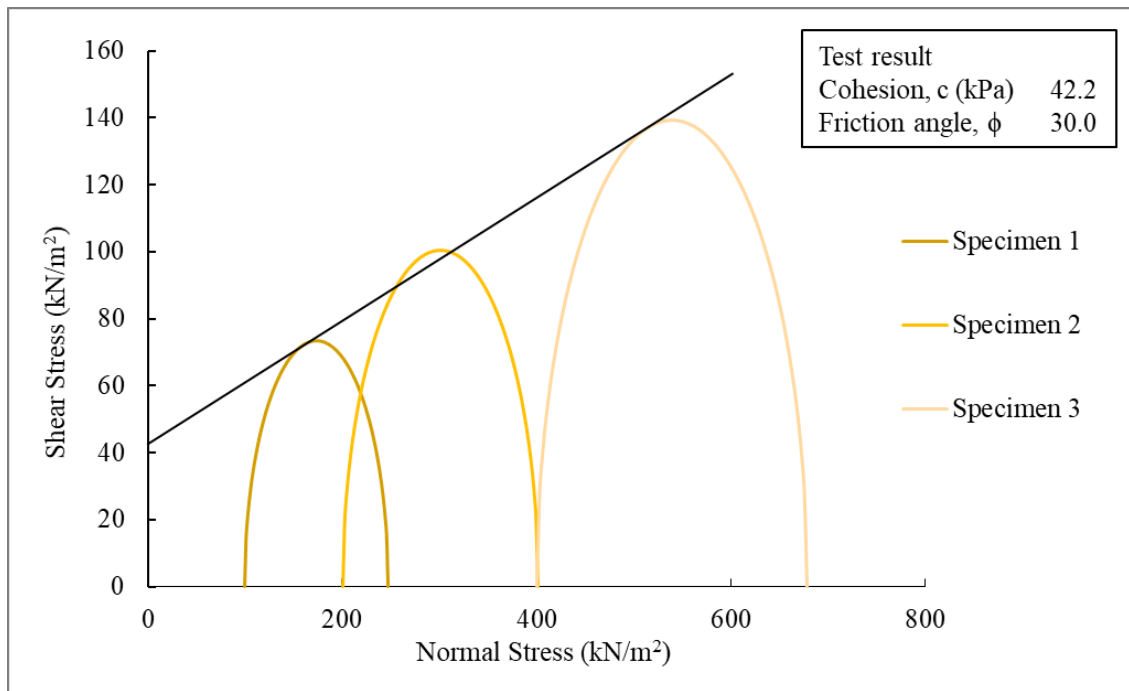
اونيفرسيتي مليسيا قهغ السلطان عبدالله
UNIVERSITI MALAYSIA PAHANG
AL-SULTAN ABDULLAH

| | Specimen 1 | Specimen 2 | Specimen 3 |
|--|-------------------|-------------------|-------------------|
| Height (mm) | 100.00 | 100.00 | 100.00 |
| Diameter (mm) | 50.00 | 50.00 | 50.00 |
| Weight (g) | 350 | 350 | 350 |
| Particle Density, p_s | 2.62 | 2.62 | 2.62 |
| | | | |
| Specimen | Specimen 1 | Specimen 2 | Specimen 3 |
| Cell Pressure, σ_3 (kPa) | 100 | 200 | 400 |
| Moisture Content (%) | 20 | 20 | 20 |
| Bulk Density, (Mg/m ³) | 1.78 | 1.88 | 2.04 |
| Dry Density, (Mg/m ³) | 1.49 | 1.57 | 1.58 |
| Void Ratio | 0.76 | 0.67 | 0.66 |
| Deg of Saturation (%) | 68.95 | 78.21 | 79.39 |
| Strain at failure, ϵ_f (%) | 8.36 | 6.67 | 8.20 |
| Shear Strength, C_u (kPa) | 73.59 | 100.57 | 186.86 |
| Max Deviator Stress, (kPa) | 142.82 | 155.59 | 273.86 |
| Total Normal Stress ($\sigma_1 - \sigma_3$), (kPa) | 142.82 | 155.59 | 273.86 |

Test method: BS1377: Part 7: 1990

Borehole: Control Sample

(delete as appropriate)



TOTAL STRESS TRIAXIAL COMPRESSION

| | Strain (mm) | Strain, ϵ (%) | Load (N) | Deviator Stress (1-3) (kPa) |
|----|-------------|------------------------|----------|-----------------------------|
| 1 | 0.01 | 0 | 0 | 0 |
| 2 | 0.35 | 0.16 | 37 | 19.03 |
| 3 | 0.7 | 0.51 | 68 | 34.93 |
| 4 | 1.05 | 0.86 | 102 | 52.23 |
| 5 | 1.42 | 1.23 | 131 | 67.13 |
| 6 | 1.77 | 1.58 | 157 | 80.19 |
| 7 | 2.12 | 1.94 | 181 | 92.38 |
| 8 | 2.48 | 2.29 | 202 | 102.99 |
| 9 | 2.83 | 2.64 | 218 | 111.30 |
| 10 | 3.18 | 3.00 | 232 | 118.31 |
| 11 | 3.53 | 3.35 | 242 | 123.54 |
| 12 | 3.88 | 3.70 | 251 | 128.00 |
| 13 | 4.25 | 4.06 | 258 | 131.67 |
| 14 | 4.60 | 4.41 | 263 | 134.11 |
| 15 | 4.95 | 4.76 | 267 | 136.28 |
| 16 | 5.30 | 5.12 | 271 | 138.43 |
| 17 | 5.66 | 5.48 | 274 | 139.83 |
| 18 | 6.01 | 5.83 | 276 | 140.75 |
| 19 | 6.36 | 6.19 | 278 | 141.65 |
| 20 | 6.71 | 6.54 | 278 | 142.07 |
| 21 | 7.08 | 6.90 | 279 | 142.48 |
| 22 | 7.43 | 7.26 | 280 | 142.64 |
| 23 | 7.78 | 7.61 | 279 | 142.57 |
| 24 | 8.15 | 7.97 | 279 | 142.48 |
| 25 | 8.53 | 8.36 | 280 | 142.82 |
| 26 | 8.85 | 8.67 | 279 | 142.56 |
| 27 | 9.20 | 9.03 | 279 | 142.23 |
| 28 | 9.56 | 9.39 | 278 | 141.90 |
| 29 | 9.91 | 9.74 | 278 | 141.81 |

| | | | | |
|----|-------|-------|-----|--------|
| 30 | 10.26 | 10.10 | 277 | 141.48 |
| 31 | 10.61 | 10.45 | 277 | 141.15 |
| 32 | 10.98 | 10.81 | 276 | 140.82 |
| 33 | 11.33 | 11.16 | 276 | 140.70 |
| 34 | 11.68 | 11.51 | 275 | 140.38 |
| 35 | 12.03 | 11.86 | 274 | 140.04 |
| 36 | 12.40 | 12.23 | 273 | 139.46 |
| 37 | 12.75 | 12.58 | 273 | 139.35 |
| 38 | 12.78 | 12.61 | 273 | 139.30 |
| 39 | 12.81 | 12.65 | 273 | 139.25 |
| 40 | 13.81 | 13.65 | 272 | 138.53 |
| 41 | 14.16 | 14.01 | 271 | 138.40 |
| 42 | 14.51 | 14.36 | 271 | 138.27 |
| 43 | 14.88 | 14.71 | 270 | 137.91 |
| 44 | 15.23 | 15.07 | 270 | 137.76 |
| 45 | 15.58 | 15.42 | 270 | 137.63 |
| 46 | 15.93 | 15.78 | 269 | 137.47 |
| 47 | 16.30 | 16.14 | 269 | 137.31 |
| 48 | 16.65 | 16.49 | 269 | 137.17 |
| 49 | 17.00 | 16.85 | 269 | 137.00 |
| 50 | 17.36 | 17.21 | 268 | 136.83 |
| 51 | 17.71 | 17.56 | 269 | 137.09 |
| 52 | 18.06 | 17.91 | 268 | 136.92 |
| 53 | 18.41 | 18.26 | 268 | 136.96 |
| 54 | 18.78 | 18.63 | 268 | 136.96 |
| 55 | 19.13 | 18.98 | 268 | 136.79 |
| 56 | 19.48 | 19.33 | 268 | 136.81 |
| 57 | 19.85 | 19.75 | 268 | 136.52 |
| 58 | 20.01 | 19.81 | 267 | 136.41 |

Test name: Specimen 1

Borehole: Control

TOTAL STRESS TRIAXIAL COMPRESSION

| | Strain (mm) | Strain, ϵ (%) | Load (N) | Deviator Stress (1-3) (kPa) |
|----|-------------|------------------------|----------|-----------------------------|
| 1 | 0.008 | 0 | 0 | 0.00 |
| 2 | 0.35 | 0.28 | 50 | 25.96 |
| 3 | 0.7 | 0.64 | 119 | 61.08 |
| 4 | 1.06 | 0.99 | 165 | 84.07 |
| 5 | 1.41 | 1.34 | 200 | 102.03 |
| 6 | 1.76 | 1.70 | 228 | 116.36 |
| 7 | 2.13 | 2.06 | 250 | 127.42 |
| 8 | 2.48 | 2.41 | 264 | 134.68 |
| 9 | 2.83 | 2.77 | 276 | 140.80 |
| 10 | 3.18 | 3.12 | 285 | 145.06 |
| 11 | 3.55 | 3.48 | 291 | 148.22 |
| 12 | 3.90 | 3.83 | 296 | 150.57 |
| 13 | 4.25 | 4.19 | 300 | 152.89 |
| 14 | 4.60 | 4.54 | 302 | 153.88 |
| 15 | 4.96 | 4.89 | 305 | 155.12 |
| 16 | 5.31 | 5.25 | 305 | 155.55 |
| 17 | 5.66 | 5.60 | 306 | 155.73 |
| 18 | 6.01 | 5.95 | 306 | 155.64 |
| 19 | 6.41 | 6.36 | 306 | 155.79 |
| 20 | 6.73 | 6.67 | 306 | 155.99 |
| 21 | 7.08 | 7.02 | 306 | 155.60 |
| 22 | 7.43 | 7.38 | 305 | 155.48 |
| 23 | 7.80 | 7.74 | 305 | 155.12 |
| 24 | 8.15 | 8.09 | 304 | 154.77 |
| 25 | 8.50 | 8.44 | 303 | 154.40 |
| 26 | 8.85 | 8.79 | 302 | 154.04 |
| 27 | 9.21 | 9.16 | 300 | 152.91 |
| 28 | 9.56 | 9.51 | 300 | 152.54 |
| 29 | 9.91 | 9.86 | 298 | 151.93 |

| | | | | |
|----|-------|-------|-----|--------|
| 30 | 10.26 | 10.22 | 297 | 151.06 |
| 31 | 10.63 | 10.58 | 295 | 150.45 |
| 32 | 10.98 | 10.93 | 295 | 150.09 |
| 33 | 11.33 | 11.29 | 293 | 149.23 |
| 34 | 11.70 | 11.64 | 291 | 148.37 |
| 35 | 12.05 | 11.99 | 290 | 147.77 |
| 36 | 12.40 | 12.35 | 289 | 147.15 |
| 37 | 12.75 | 12.70 | 288 | 146.56 |
| 38 | 13.10 | 13.06 | 286 | 145.71 |
| 39 | 13.46 | 13.42 | 285 | 145.11 |
| 40 | 13.81 | 13.77 | 284 | 144.74 |
| 41 | 14.16 | 14.13 | 283 | 143.89 |
| 42 | 14.53 | 14.49 | 282 | 143.53 |
| 43 | 14.88 | 14.84 | 281 | 142.93 |
| 44 | 15.23 | 15.19 | 280 | 142.55 |
| 45 | 15.58 | 15.54 | 279 | 141.95 |
| 46 | 15.95 | 15.91 | 278 | 141.33 |
| 47 | 16.30 | 16.26 | 276 | 140.73 |
| 48 | 16.65 | 16.61 | 275 | 140.14 |
| 49 | 17.01 | 16.98 | 274 | 139.75 |
| 50 | 17.36 | 17.33 | 274 | 139.61 |
| 51 | 17.71 | 17.69 | 272 | 138.76 |
| 52 | 18.06 | 18.04 | 272 | 138.39 |
| 53 | 18.43 | 18.39 | 270 | 137.55 |
| 54 | 18.78 | 18.75 | 268 | 136.71 |
| 55 | 19.13 | 19.10 | 268 | 136.33 |
| 56 | 19.48 | 19.46 | 266 | 135.71 |
| 57 | 19.85 | 19.85 | 265 | 134.85 |
| 58 | 20.01 | 19.95 | 264 | 134.67 |

Test name: Specimen 2

Borehole: Control

TOTAL STRESS TRIAXIAL COMPRESSION

| | Strain (mm) | Strain, ϵ (%) | Load (N) | Deviator Stress (1-3) (kPa) |
|----|-------------|------------------------|----------|-----------------------------|
| 1 | 0.008 | 0 | 0 | 0 |
| 2 | 0.35 | 0.33 | 117 | 59.41 |
| 3 | 0.70 | 0.69 | 239 | 121.75 |
| 4 | 1.05 | 1.04 | 319 | 162.38 |
| 5 | 1.42 | 1.39 | 377 | 192.03 |
| 6 | 1.77 | 1.75 | 417 | 212.48 |
| 7 | 2.12 | 2.10 | 445 | 226.48 |
| 8 | 2.47 | 2.45 | 464 | 236.36 |
| 9 | 2.83 | 2.82 | 480 | 244.70 |
| 10 | 3.18 | 3.17 | 492 | 250.42 |
| 11 | 3.53 | 3.52 | 501 | 254.96 |
| 12 | 3.88 | 3.88 | 508 | 258.56 |
| 13 | 4.25 | 4.24 | 515 | 262.16 |
| 14 | 4.60 | 4.59 | 520 | 264.59 |
| 15 | 4.95 | 4.94 | 523 | 266.40 |
| 16 | 5.30 | 5.29 | 526 | 267.94 |
| 17 | 5.67 | 5.65 | 530 | 270.00 |
| 18 | 6.02 | 6.01 | 532 | 270.90 |
| 19 | 6.37 | 6.36 | 533 | 271.26 |
| 20 | 6.72 | 6.71 | 535 | 272.45 |
| 21 | 7.08 | 7.07 | 536 | 272.76 |
| 22 | 7.43 | 7.43 | 536 | 273.06 |
| 23 | 7.78 | 7.78 | 537 | 273.37 |
| 24 | 8.13 | 8.14 | 537 | 273.64 |
| 25 | 8.42 | 8.20 | 537 | 273.86 |
| 26 | 8.85 | 8.84 | 537 | 273.64 |
| 27 | 9.20 | 9.20 | 536 | 272.79 |
| 28 | 9.55 | 9.55 | 535 | 272.50 |
| 29 | 9.90 | 9.90 | 534 | 271.95 |

| | | | | |
|----|-------|-------|-----|--------|
| 30 | 10.27 | 10.27 | 533 | 271.61 |
| 31 | 10.62 | 10.62 | 531 | 270.51 |
| 32 | 10.97 | 10.98 | 531 | 270.18 |
| 33 | 11.32 | 11.33 | 529 | 269.34 |
| 34 | 11.68 | 11.69 | 527 | 268.49 |
| 35 | 12.03 | 12.04 | 526 | 267.88 |
| 36 | 12.38 | 12.39 | 524 | 266.76 |
| 37 | 12.73 | 12.74 | 522 | 265.65 |
| 38 | 13.10 | 13.11 | 519 | 264.25 |
| 39 | 13.45 | 13.46 | 517 | 263.13 |
| 40 | 13.80 | 13.81 | 513 | 261.51 |
| 41 | 14.17 | 14.18 | 512 | 260.61 |
| 42 | 14.52 | 14.53 | 509 | 259.25 |
| 43 | 14.87 | 14.88 | 506 | 257.64 |
| 44 | 15.22 | 15.24 | 503 | 256.01 |
| 45 | 15.58 | 15.59 | 499 | 254.38 |
| 46 | 15.93 | 15.94 | 496 | 252.53 |
| 47 | 16.28 | 16.30 | 492 | 250.65 |
| 48 | 16.65 | 16.66 | 488 | 248.55 |
| 49 | 17.00 | 17.02 | 485 | 246.93 |
| 50 | 17.35 | 17.37 | 481 | 245.11 |
| 51 | 17.70 | 17.72 | 478 | 243.54 |
| 52 | 18.07 | 18.08 | 475 | 241.71 |
| 53 | 18.42 | 18.44 | 471 | 239.88 |
| 54 | 18.77 | 18.79 | 468 | 238.58 |
| 55 | 19.13 | 19.14 | 464 | 236.54 |
| 56 | 19.48 | 19.49 | 461 | 235.01 |
| 57 | 19.83 | 19.85 | 459 | 233.68 |
| 58 | 20.02 | 19.99 | 457 | 232.85 |

Test name: Specimen 3

Borehole: Control

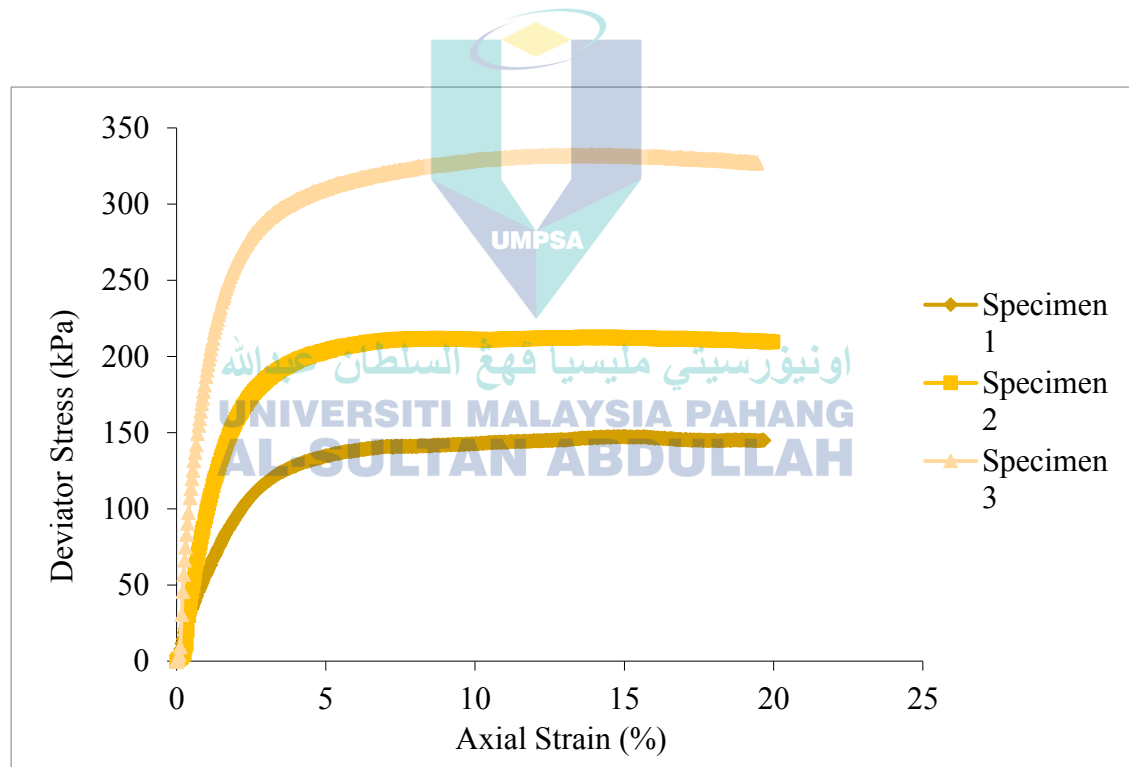
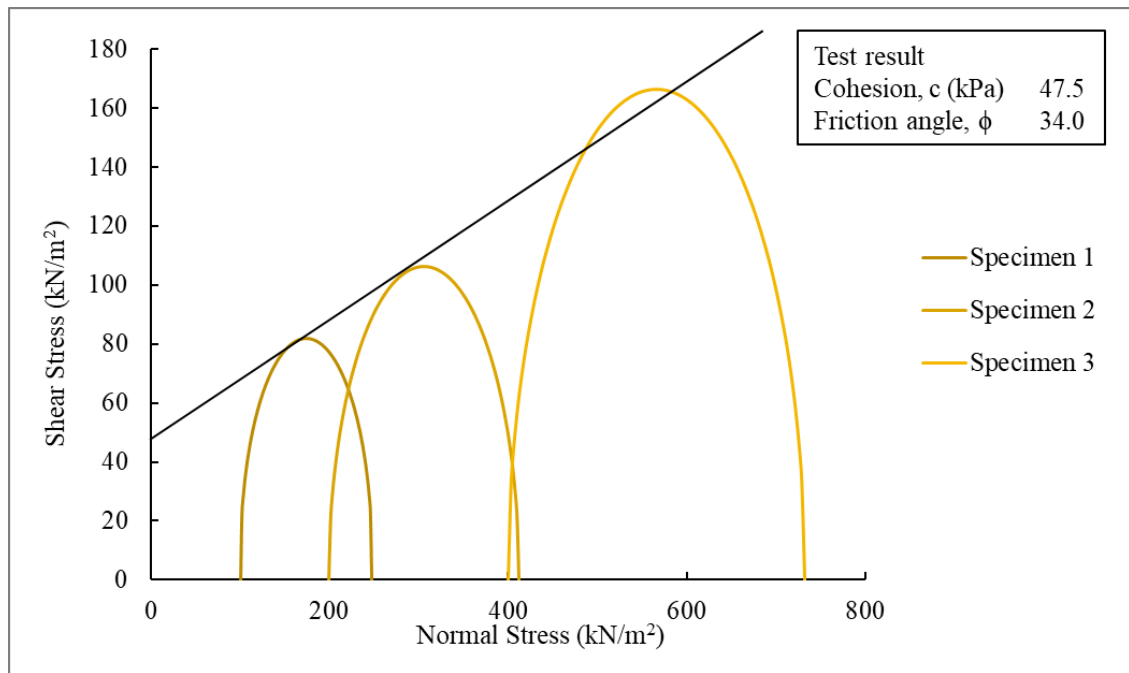
UNCONSOLIDATED UNDRAINED (UU) TRIAXIAL TEST

| | Specimen 1 | Specimen 2 | Specimen 3 |
|--|------------|------------|------------|
| Height (mm) | 100.00 | 100.00 | 100.00 |
| Diameter (mm) | 50.00 | 50.00 | 50.00 |
| Weight (g) | 350 | 350 | 350 |
| Particle Density, p_s | 2.62 | 2.62 | 2.62 |
| | | | |
| Specimen | Specimen 1 | Specimen 2 | Specimen 3 |
| Cell Pressure, σ_3 (kPa) | 100 | 200 | 400 |
| Moisture Content (%) | 20 | 20 | 20 |
| Bulk Density, (Mg/m ³) | 1.78 | 1.79 | 1.85 |
| Dry Density, (Mg/m ³) | 1.48 | 1.50 | 1.54 |
| Void Ratio | 0.77 | 0.74 | 0.70 |
| Deg of Saturation (%) | 68.05 | 70.81 | 74.86 |
| Strain at failure, ϵ_f (%) | 15.33 | 14.01 | 14.52 |
| Shear Strength, C_u (kPa) | 81.83 | 106.47 | 166.37 |
| Max Deviator Stress, (kPa) | 147.66 | 212.95 | 332.73 |
| Total Normal Stress ($\sigma_1 - \sigma_3$), (kPa) | 147.66 | 212.95 | 332.73 |

Test method: BS1377: Part 7: 1990

Borehole: S1060

(delete as appropriate)



TOTAL STRESS TRIAXIAL COMPRESSION

| No. | Strain (mm) | Strain, ϵ (%) | Load (N) | Deviator Stress (1-3) (kPa) |
|-----|-------------|------------------------|----------|-----------------------------|
| 1 | 0.36 | 0.00 | 0 | 0.00 |
| 2 | 0.37 | 0.01 | 1 | 0.51 |
| 3 | 0.72 | 0.36 | 51 | 25.88 |
| 4 | 1.08 | 0.73 | 89 | 45.50 |
| 5 | 1.43 | 1.08 | 120 | 60.96 |
| 6 | 1.80 | 1.45 | 149 | 75.79 |
| 7 | 2.15 | 1.80 | 174 | 88.53 |
| 8 | 2.50 | 2.15 | 195 | 99.18 |
| 9 | 2.87 | 2.51 | 213 | 108.24 |
| 10 | 3.22 | 2.86 | 226 | 115.27 |
| 11 | 3.58 | 3.23 | 237 | 120.75 |
| 12 | 3.93 | 3.58 | 245 | 124.73 |
| 13 | 4.30 | 3.95 | 252 | 128.17 |
| 14 | 4.65 | 4.30 | 257 | 131.12 |
| 15 | 5.02 | 4.66 | 261 | 133.04 |
| 16 | 5.37 | 5.01 | 265 | 134.97 |
| 17 | 5.73 | 5.38 | 268 | 136.38 |
| 18 | 6.08 | 5.73 | 271 | 137.80 |
| 19 | 6.45 | 6.10 | 272 | 138.69 |
| 20 | 6.80 | 6.45 | 274 | 139.61 |
| 21 | 7.17 | 6.81 | 276 | 140.48 |
| 22 | 7.52 | 7.16 | 277 | 140.90 |
| 23 | 7.88 | 7.53 | 276 | 140.82 |
| 24 | 8.23 | 7.88 | 276 | 140.75 |
| 25 | 8.60 | 8.25 | 277 | 141.13 |
| 26 | 8.95 | 8.60 | 278 | 141.52 |
| 27 | 9.32 | 8.96 | 279 | 141.88 |
| 28 | 9.67 | 9.31 | 279 | 142.26 |
| 29 | 10.03 | 9.68 | 280 | 142.60 |

| | | | | |
|----|-------|-------|-----|--------|
| 30 | 10.38 | 10.03 | 281 | 142.97 |
| 31 | 10.75 | 10.40 | 281 | 143.30 |
| 32 | 11.10 | 10.75 | 282 | 143.64 |
| 33 | 11.47 | 11.11 | 283 | 143.96 |
| 34 | 11.82 | 11.46 | 283 | 144.29 |
| 35 | 12.18 | 11.83 | 284 | 144.60 |
| 36 | 12.53 | 12.18 | 284 | 144.47 |
| 37 | 12.90 | 12.55 | 285 | 145.20 |
| 38 | 13.25 | 12.90 | 285 | 145.06 |
| 39 | 13.62 | 13.26 | 286 | 145.78 |
| 40 | 13.97 | 13.61 | 288 | 146.51 |
| 41 | 14.33 | 13.98 | 288 | 146.77 |
| 42 | 14.68 | 14.33 | 289 | 147.04 |
| 43 | 15.05 | 14.70 | 289 | 147.28 |
| 44 | 15.33 | 14.98 | 290 | 147.66 |
| 45 | 15.77 | 15.41 | 289 | 147.33 |
| 46 | 16.12 | 15.76 | 289 | 147.15 |
| 47 | 16.48 | 16.13 | 288 | 146.51 |
| 48 | 16.85 | 16.50 | 286 | 145.87 |
| 49 | 17.20 | 16.85 | 286 | 145.69 |
| 50 | 17.57 | 17.21 | 286 | 145.46 |
| 51 | 17.92 | 17.56 | 285 | 145.27 |
| 52 | 18.28 | 17.93 | 285 | 145.04 |
| 53 | 18.63 | 18.28 | 284 | 144.84 |
| 54 | 19.00 | 18.65 | 285 | 145.02 |
| 55 | 19.35 | 19.00 | 285 | 145.22 |
| 56 | 19.72 | 19.36 | 285 | 144.97 |
| 57 | 20.03 | 19.68 | 284 | 144.81 |

Test name: Specimen 1

Borehole: S1060

TOTAL STRESS TRIAXIAL COMPRESSION

| No. | Strain (mm) | Strain, ϵ (%) | Load (N) | Deviator Stress (1-3) (kPa) |
|-----|-------------|------------------------|----------|-----------------------------|
| 1 | 0.057 | 0 | 0 | 0 |
| 2 | 0.35 | 0.29 | 18 | 9.29 |
| 3 | 0.72 | 0.66 | 125 | 63.68 |
| 4 | 1.07 | 1.01 | 193 | 98.16 |
| 5 | 1.42 | 1.36 | 245 | 124.84 |
| 6 | 1.78 | 1.73 | 286 | 145.91 |
| 7 | 2.13 | 2.08 | 316 | 160.95 |
| 8 | 2.48 | 2.43 | 339 | 172.67 |
| 9 | 2.83 | 2.78 | 355 | 180.57 |
| 10 | 3.20 | 3.14 | 367 | 186.79 |
| 11 | 3.55 | 3.49 | 377 | 191.93 |
| 12 | 3.90 | 3.84 | 384 | 195.45 |
| 13 | 4.27 | 4.21 | 391 | 198.91 |
| 14 | 4.62 | 4.56 | 395 | 201.31 |
| 15 | 4.98 | 4.93 | 399 | 203.15 |
| 16 | 5.33 | 5.28 | 404 | 205.51 |
| 17 | 5.68 | 5.63 | 406 | 206.82 |
| 18 | 6.03 | 5.98 | 408 | 207.60 |
| 19 | 6.40 | 6.34 | 411 | 209.35 |
| 20 | 6.75 | 6.69 | 413 | 210.11 |
| 21 | 7.10 | 7.04 | 414 | 210.85 |
| 22 | 7.47 | 7.41 | 415 | 211.54 |
| 23 | 7.82 | 7.76 | 415 | 211.24 |
| 24 | 8.17 | 8.11 | 416 | 211.95 |
| 25 | 8.52 | 8.46 | 416 | 211.64 |
| 26 | 8.87 | 8.81 | 416 | 211.83 |
| 27 | 9.22 | 9.16 | 415 | 211.52 |
| 28 | 9.58 | 9.53 | 415 | 211.16 |
| 29 | 9.93 | 9.88 | 415 | 211.33 |

| | | | | |
|----|-------|-------|-----|--------|
| 30 | 10.28 | 10.23 | 414 | 211.00 |
| 31 | 10.65 | 10.59 | 415 | 211.12 |
| 32 | 11.00 | 10.94 | 415 | 211.27 |
| 33 | 11.35 | 11.29 | 415 | 211.41 |
| 34 | 11.72 | 11.66 | 415 | 211.51 |
| 35 | 12.07 | 12.01 | 416 | 211.63 |
| 36 | 12.42 | 12.36 | 416 | 211.75 |
| 37 | 12.78 | 12.73 | 417 | 212.30 |
| 38 | 13.13 | 13.08 | 416 | 211.93 |
| 39 | 13.50 | 13.44 | 417 | 212.45 |
| 40 | 13.85 | 13.79 | 417 | 212.54 |
| 41 | 14.07 | 14.01 | 418 | 212.95 |
| 42 | 14.57 | 14.51 | 417 | 212.18 |
| 43 | 14.92 | 14.86 | 418 | 212.71 |
| 44 | 15.28 | 15.23 | 417 | 212.26 |
| 45 | 15.63 | 15.58 | 417 | 212.31 |
| 46 | 16.00 | 15.94 | 416 | 211.84 |
| 47 | 16.35 | 16.29 | 415 | 211.42 |
| 48 | 16.67 | 16.61 | 415 | 211.53 |
| 49 | 17.07 | 17.01 | 415 | 211.43 |
| 50 | 17.42 | 17.36 | 415 | 211.44 |
| 51 | 17.78 | 17.73 | 414 | 210.96 |
| 52 | 18.13 | 18.08 | 414 | 210.96 |
| 53 | 18.85 | 18.79 | 413 | 210.44 |
| 54 | 19.20 | 19.14 | 413 | 210.42 |
| 55 | 19.57 | 19.51 | 412 | 209.91 |
| 56 | 19.92 | 19.86 | 412 | 209.87 |
| 57 | 20.03 | 19.98 | 411 | 209.57 |

Test name: Specimen 2

Borehole: S1060

TOTAL STRESS TRIAXIAL COMPRESSION

| No. | Strain (mm) | Strain, ϵ (%) | Load (N) | Deviator Stress (1-3) (kPa) |
|-----|-------------|------------------------|----------|-----------------------------|
| 1 | 0.58 | 0.00 | 0 | 0.00 |
| 2 | 0.35 | -0.23 | -6 | -3.14 |
| 3 | 0.70 | 0.12 | 18 | 9.39 |
| 4 | 1.07 | 0.49 | 223 | 113.49 |
| 5 | 1.42 | 0.84 | 332 | 169.01 |
| 6 | 1.77 | 1.19 | 410 | 208.66 |
| 7 | 2.13 | 1.55 | 468 | 238.11 |
| 8 | 2.48 | 1.90 | 506 | 257.55 |
| 9 | 2.83 | 2.25 | 533 | 271.33 |
| 10 | 3.20 | 2.62 | 552 | 281.29 |
| 11 | 3.55 | 2.97 | 567 | 288.80 |
| 12 | 3.90 | 3.32 | 579 | 295.02 |
| 13 | 4.27 | 3.69 | 588 | 299.34 |
| 14 | 4.62 | 4.04 | 595 | 303.06 |
| 15 | 4.97 | 4.39 | 601 | 306.15 |
| 16 | 5.33 | 4.75 | 606 | 308.56 |
| 17 | 5.68 | 5.10 | 612 | 311.58 |
| 18 | 6.03 | 5.45 | 614 | 312.80 |
| 19 | 6.40 | 5.82 | 619 | 315.13 |
| 20 | 6.75 | 6.17 | 623 | 317.49 |
| 21 | 7.10 | 6.52 | 626 | 318.65 |
| 22 | 7.47 | 6.89 | 628 | 319.73 |
| 23 | 7.82 | 7.24 | 630 | 320.85 |
| 24 | 8.17 | 7.59 | 633 | 322.54 |
| 25 | 8.53 | 7.95 | 636 | 324.14 |
| 26 | 8.88 | 8.30 | 637 | 324.63 |
| 27 | 9.25 | 8.67 | 639 | 325.62 |
| 28 | 9.60 | 9.02 | 641 | 326.66 |
| 29 | 9.95 | 9.37 | 643 | 327.67 |

| | | | | |
|----|-------|-------|-----|--------|
| 30 | 10.32 | 9.74 | 644 | 328.04 |
| 31 | 10.67 | 10.09 | 646 | 329.02 |
| 32 | 11.02 | 10.44 | 647 | 329.43 |
| 33 | 11.38 | 10.80 | 649 | 330.32 |
| 34 | 11.73 | 11.15 | 649 | 330.69 |
| 35 | 12.10 | 11.52 | 650 | 330.99 |
| 36 | 12.45 | 11.87 | 651 | 331.33 |
| 37 | 12.80 | 12.22 | 651 | 331.67 |
| 38 | 13.17 | 12.59 | 653 | 332.47 |
| 39 | 13.52 | 12.94 | 652 | 332.23 |
| 40 | 13.88 | 13.30 | 653 | 332.47 |
| 41 | 14.10 | 13.52 | 652 | 332.18 |
| 42 | 14.23 | 13.65 | 652 | 332.21 |
| 43 | 14.52 | 13.94 | 653 | 332.73 |
| 44 | 14.95 | 14.37 | 652 | 332.13 |
| 45 | 15.32 | 14.74 | 651 | 331.78 |
| 46 | 15.67 | 15.09 | 651 | 331.48 |
| 47 | 16.02 | 15.44 | 651 | 331.70 |
| 48 | 16.38 | 15.80 | 651 | 331.32 |
| 49 | 16.70 | 16.12 | 650 | 331.12 |
| 50 | 17.10 | 16.52 | 649 | 330.59 |
| 51 | 17.47 | 16.89 | 649 | 330.70 |
| 52 | 17.82 | 17.24 | 649 | 330.34 |
| 53 | 18.17 | 17.59 | 647 | 329.47 |
| 54 | 18.53 | 17.95 | 646 | 329.03 |
| 55 | 18.88 | 18.30 | 645 | 328.65 |
| 56 | 19.25 | 18.67 | 644 | 328.19 |
| 57 | 19.97 | 19.39 | 642 | 326.81 |
| 58 | 20.03 | 19.45 | 642 | 327.05 |

Test name: Specimen 3

Borehole: S1060

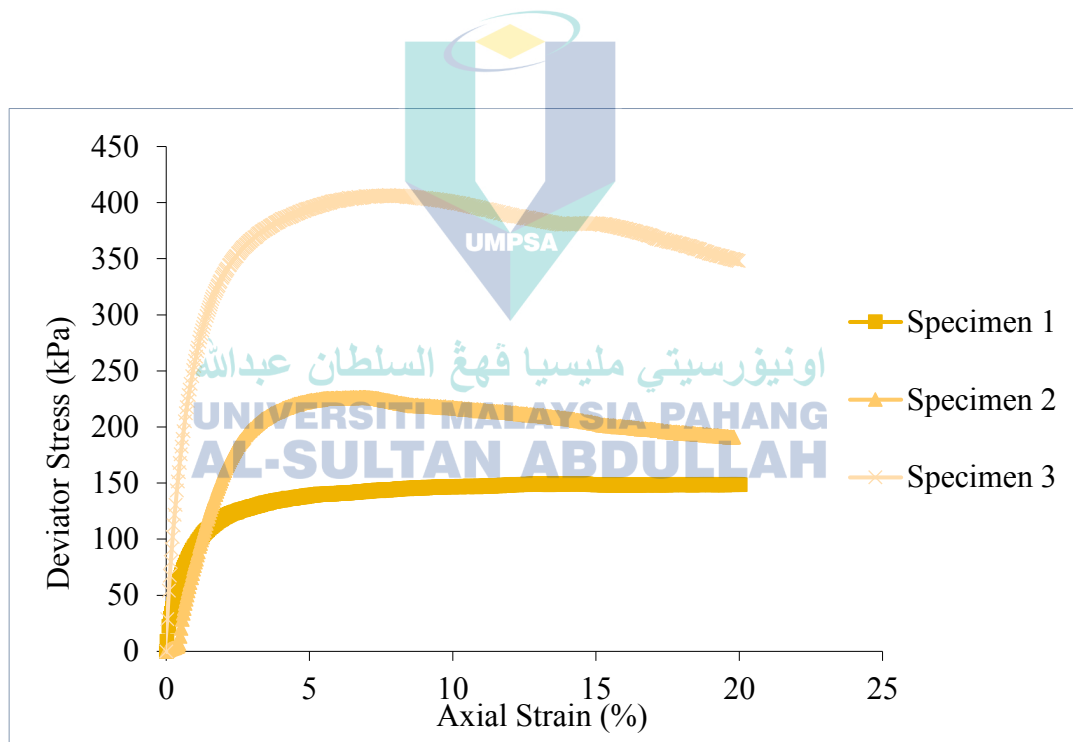
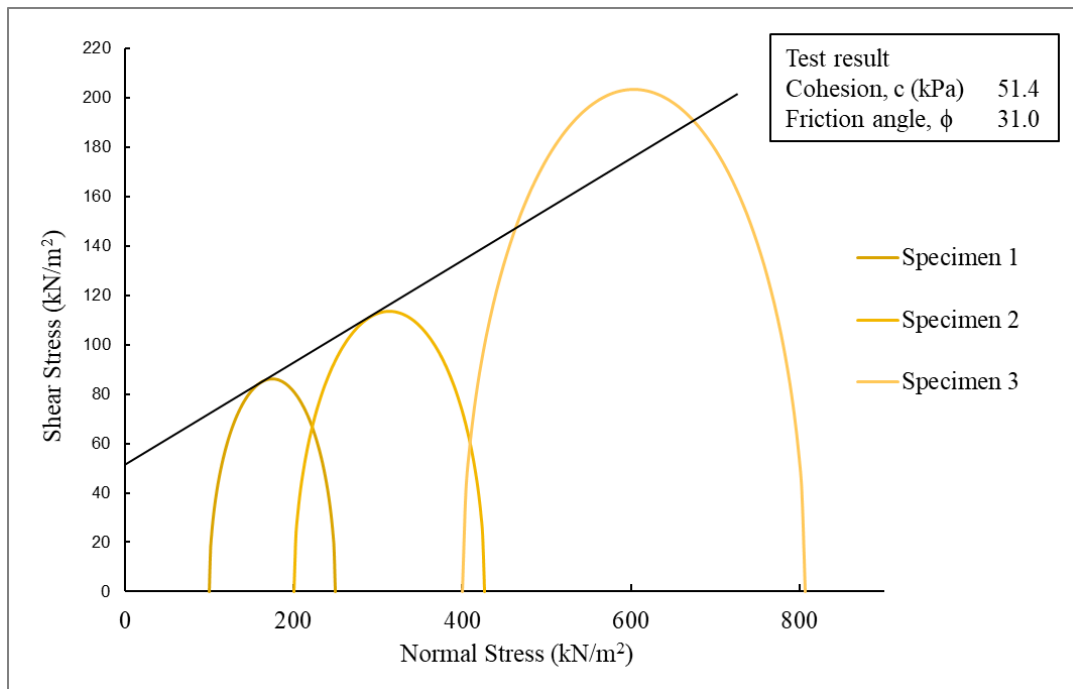
UNCONSOLIDATED UNDRAINED (UU) TRIAXIAL TEST

| | Specimen 1 | Specimen 2 | Specimen 3 |
|--|------------|------------|------------|
| Height (mm) | 100.00 | 100.00 | 100.00 |
| Diameter (mm) | 50.00 | 50.00 | 50.00 |
| Weight (g) | 350 | 350 | 350 |
| Particle Density, p_s | 2.62 | 2.62 | 2.62 |
| Specimen | Specimen 1 | Specimen 2 | Specimen 3 |
| Cell Pressure, σ_3 (kPa) | 100 | 200 | 400 |
| Moisture Content (%) | 20 | 20 | 20 |
| Bulk Density, (Mg/m ³) | 1.78 | 1.82 | 1.85 |
| Dry Density, (Mg/m ³) | 1.49 | 1.52 | 1.55 |
| Void Ratio | 0.76 | 0.72 | 0.69 |
| Deg of Saturation (%) | 68.95 | 72.78 | 75.94 |
| Strain at failure, ϵ_f (%) | 9.57 | 6.88 | 7.77 |
| Shear Strength, C_u (kPa) | 74.81 | 113.34 | 203.50 |
| Max Deviator Stress, (kPa) | 171.03 | 226.67 | 407.01 |
| Total Normal Stress ($\sigma_1 - \sigma_3$), (kPa) | 171.03 | 226.67 | 407.01 |

Test method: BS1377: Part 7: 1990

Borehole: S1080

(delete as appropriate)



TOTAL STRESS TRIAXIAL COMPRESSION

| No. | Strain (mm) | Strain, ϵ (%) | Load (N) | Deviator Stress (1-3) (kPa) |
|-----|-------------|------------------------|----------|-----------------------------|
| 1 | 0.004 | 0 | 0 | 0 |
| 2 | 0.35 | 0.30 | 84 | 42.75 |
| 3 | 0.72 | 0.66 | 150 | 76.49 |
| 4 | 1.07 | 1.02 | 196 | 99.97 |
| 5 | 1.42 | 1.37 | 230 | 117.39 |
| 6 | 1.78 | 1.72 | 254 | 129.54 |
| 7 | 2.13 | 2.08 | 272 | 138.28 |
| 8 | 2.48 | 2.43 | 283 | 144.16 |
| 9 | 2.85 | 2.79 | 292 | 148.71 |
| 10 | 3.20 | 3.15 | 299 | 152.46 |
| 11 | 3.55 | 3.50 | 305 | 155.42 |
| 12 | 3.90 | 3.85 | 310 | 157.87 |
| 13 | 4.27 | 4.21 | 314 | 160.02 |
| 14 | 4.62 | 4.57 | 317 | 161.41 |
| 15 | 4.97 | 4.92 | 320 | 163.04 |
| 16 | 5.33 | 5.28 | 322 | 164.14 |
| 17 | 5.68 | 5.63 | 324 | 165.01 |
| 18 | 6.03 | 5.98 | 326 | 165.88 |
| 19 | 6.38 | 6.34 | 327 | 166.70 |
| 20 | 6.75 | 6.70 | 329 | 167.76 |
| 21 | 7.10 | 7.05 | 331 | 168.59 |
| 22 | 7.45 | 7.41 | 332 | 169.14 |
| 23 | 7.82 | 7.77 | 333 | 169.68 |
| 24 | 8.17 | 8.12 | 334 | 169.99 |
| 25 | 8.52 | 8.47 | 335 | 170.51 |
| 26 | 8.87 | 8.82 | 335 | 170.57 |
| 27 | 9.23 | 9.19 | 335 | 170.58 |
| 28 | 9.62 | 9.57 | 336 | 171.03 |
| 29 | 9.95 | 9.90 | 335 | 170.65 |

| | | | | |
|----|-------|-------|-----|--------|
| 30 | 10.30 | 10.25 | 335 | 170.68 |
| 31 | 10.65 | 10.61 | 334 | 170.22 |
| 32 | 11.00 | 10.96 | 334 | 170.02 |
| 33 | 11.37 | 11.32 | 333 | 169.78 |
| 34 | 11.72 | 11.67 | 333 | 169.78 |
| 35 | 12.07 | 12.02 | 333 | 169.55 |
| 36 | 12.43 | 12.38 | 333 | 169.53 |
| 37 | 12.78 | 12.74 | 332 | 169.05 |
| 38 | 13.13 | 13.09 | 331 | 168.81 |
| 39 | 13.50 | 13.46 | 329 | 167.64 |
| 40 | 13.85 | 13.81 | 329 | 167.41 |
| 41 | 14.20 | 14.16 | 328 | 166.93 |
| 42 | 14.57 | 14.52 | 327 | 166.44 |
| 43 | 14.92 | 14.87 | 325 | 165.53 |
| 44 | 15.27 | 15.23 | 324 | 164.83 |
| 45 | 15.62 | 15.58 | 323 | 164.36 |
| 46 | 15.98 | 15.95 | 321 | 163.63 |
| 47 | 16.33 | 16.30 | 320 | 163.15 |
| 48 | 16.68 | 16.65 | 319 | 162.68 |
| 49 | 17.05 | 17.02 | 318 | 162.17 |
| 50 | 17.40 | 17.37 | 317 | 161.69 |
| 51 | 17.75 | 17.72 | 316 | 160.76 |
| 52 | 18.12 | 18.08 | 315 | 160.27 |
| 53 | 18.47 | 18.43 | 313 | 159.57 |
| 54 | 18.82 | 18.79 | 312 | 159.07 |
| 55 | 19.17 | 19.14 | 311 | 158.16 |
| 56 | 19.53 | 19.51 | 309 | 157.43 |
| 57 | 19.88 | 19.86 | 308 | 156.94 |

Test name: Specimen 1

Borehole: S1080

TOTAL STRESS TRIAXIAL COMPRESSION

| No. | Strain (mm) | Strain, ϵ (%) | Load (N) | Deviator Stress (1-3) (kPa) |
|-----|-------------|------------------------|----------|-----------------------------|
| 1 | 0.22 | 0.00 | 0 | 0.00 |
| 2 | 0.35 | 0.13 | 4 | 2.17 |
| 3 | 0.70 | 0.48 | 27 | 13.52 |
| 4 | 1.05 | 0.83 | 121 | 61.43 |
| 5 | 1.42 | 1.20 | 189 | 96.10 |
| 6 | 1.77 | 1.55 | 248 | 126.25 |
| 7 | 2.12 | 1.90 | 298 | 151.92 |
| 8 | 2.48 | 2.27 | 339 | 172.59 |
| 9 | 2.83 | 2.62 | 369 | 187.85 |
| 10 | 3.18 | 2.97 | 389 | 198.25 |
| 11 | 3.55 | 3.33 | 405 | 206.43 |
| 12 | 3.90 | 3.68 | 416 | 211.96 |
| 13 | 4.27 | 4.05 | 424 | 215.85 |
| 14 | 4.62 | 4.40 | 431 | 219.73 |
| 15 | 4.97 | 4.75 | 436 | 222.03 |
| 16 | 5.33 | 5.12 | 439 | 223.76 |
| 17 | 5.68 | 5.47 | 442 | 224.99 |
| 18 | 6.03 | 5.82 | 443 | 225.69 |
| 19 | 6.40 | 6.18 | 443 | 225.83 |
| 20 | 6.75 | 6.53 | 445 | 226.51 |
| 21 | 7.10 | 6.88 | 445 | 226.67 |
| 22 | 7.45 | 7.23 | 443 | 225.82 |
| 23 | 7.82 | 7.60 | 440 | 223.92 |
| 24 | 8.17 | 7.95 | 437 | 222.58 |
| 25 | 8.52 | 8.30 | 433 | 220.73 |
| 26 | 8.87 | 8.65 | 430 | 218.90 |
| 27 | 9.23 | 9.02 | 430 | 219.01 |
| 28 | 9.58 | 9.37 | 429 | 218.66 |
| 29 | 9.93 | 9.72 | 428 | 217.81 |

| | | | | |
|----|-------|-------|-----|--------|
| 30 | 10.30 | 10.08 | 426 | 216.93 |
| 31 | 10.65 | 10.43 | 424 | 216.09 |
| 32 | 11.00 | 10.78 | 423 | 215.24 |
| 33 | 11.35 | 11.13 | 422 | 214.88 |
| 34 | 11.72 | 11.50 | 419 | 213.51 |
| 35 | 12.07 | 11.85 | 419 | 213.15 |
| 36 | 12.42 | 12.20 | 418 | 212.78 |
| 37 | 12.77 | 12.55 | 415 | 211.45 |
| 38 | 13.13 | 12.92 | 413 | 210.09 |
| 39 | 13.48 | 13.27 | 412 | 209.72 |
| 40 | 13.83 | 13.62 | 409 | 208.41 |
| 41 | 14.18 | 13.97 | 408 | 207.56 |
| 42 | 14.55 | 14.33 | 405 | 206.21 |
| 43 | 14.90 | 14.68 | 401 | 204.44 |
| 44 | 15.25 | 15.03 | 399 | 203.14 |
| 45 | 15.60 | 15.38 | 395 | 201.38 |
| 46 | 15.97 | 15.75 | 393 | 200.05 |
| 47 | 16.32 | 16.10 | 393 | 200.13 |
| 48 | 16.67 | 16.45 | 390 | 198.84 |
| 49 | 17.02 | 16.80 | 389 | 198.01 |
| 50 | 17.38 | 17.17 | 387 | 197.14 |
| 51 | 17.73 | 17.52 | 385 | 195.86 |
| 52 | 18.08 | 17.87 | 383 | 195.03 |
| 53 | 18.45 | 18.23 | 381 | 194.16 |
| 54 | 18.80 | 18.58 | 380 | 193.33 |
| 55 | 19.15 | 18.93 | 379 | 192.94 |
| 56 | 19.50 | 19.28 | 377 | 192.10 |
| 57 | 19.87 | 19.65 | 375 | 190.79 |
| 58 | 20.03 | 19.82 | 376 | 191.27 |

Test name: Specimen 2

Borehole: S1080

TOTAL STRESS TRIAXIAL COMPRESSION

| No. | Strain (mm) | Strain, ϵ (%) | Load (N) | Deviator Stress (1-3) (kPa) |
|-----|-------------|------------------------|----------|-----------------------------|
| 1 | 0.06 | 0.00 | 0 | 0.00 |
| 2 | 0.35 | 0.29 | 239 | 121.81 |
| 3 | 0.72 | 0.66 | 403 | 205.23 |
| 4 | 1.07 | 1.01 | 508 | 258.95 |
| 5 | 1.42 | 1.36 | 580 | 295.27 |
| 6 | 1.78 | 1.72 | 631 | 321.19 |
| 7 | 2.13 | 2.07 | 665 | 338.84 |
| 8 | 2.48 | 2.42 | 691 | 351.98 |
| 9 | 2.85 | 2.79 | 712 | 362.47 |
| 10 | 3.20 | 3.14 | 726 | 369.84 |
| 11 | 3.55 | 3.49 | 739 | 376.53 |
| 12 | 3.92 | 3.86 | 751 | 382.48 |
| 13 | 4.27 | 4.21 | 759 | 386.60 |
| 14 | 4.63 | 4.57 | 767 | 390.61 |
| 15 | 4.98 | 4.92 | 774 | 394.05 |
| 16 | 5.33 | 5.27 | 779 | 396.84 |
| 17 | 5.70 | 5.64 | 786 | 400.13 |
| 18 | 6.05 | 5.99 | 789 | 401.65 |
| 19 | 6.40 | 6.34 | 792 | 403.15 |
| 20 | 6.77 | 6.71 | 796 | 405.15 |
| 21 | 7.12 | 7.06 | 796 | 405.41 |
| 22 | 7.47 | 7.41 | 798 | 406.25 |
| 23 | 7.83 | 7.77 | 799 | 407.01 |
| 24 | 8.18 | 8.12 | 797 | 406.05 |
| 25 | 8.53 | 8.47 | 795 | 405.09 |
| 26 | 8.88 | 8.82 | 795 | 404.71 |
| 27 | 9.25 | 9.19 | 793 | 403.66 |
| 28 | 9.60 | 9.54 | 790 | 402.10 |
| 29 | 9.95 | 9.89 | 786 | 400.55 |

| | | | | |
|----|-------|-------|-----|--------|
| 30 | 10.30 | 10.24 | 785 | 399.57 |
| 31 | 10.67 | 10.61 | 779 | 396.79 |
| 32 | 11.03 | 10.97 | 776 | 395.16 |
| 33 | 11.38 | 11.32 | 773 | 393.61 |
| 34 | 11.75 | 11.69 | 767 | 390.85 |
| 35 | 12.10 | 12.04 | 763 | 388.74 |
| 36 | 12.45 | 12.39 | 760 | 387.19 |
| 37 | 12.82 | 12.76 | 757 | 385.57 |
| 38 | 13.17 | 13.11 | 754 | 384.02 |
| 39 | 13.52 | 13.46 | 750 | 381.92 |
| 40 | 13.88 | 13.82 | 749 | 381.41 |
| 41 | 14.23 | 14.17 | 748 | 380.96 |
| 42 | 14.58 | 14.52 | 749 | 381.59 |
| 43 | 14.95 | 14.89 | 749 | 381.59 |
| 44 | 15.30 | 15.24 | 747 | 380.56 |
| 45 | 15.65 | 15.59 | 745 | 379.53 |
| 46 | 16.02 | 15.96 | 740 | 376.80 |
| 47 | 16.37 | 16.31 | 737 | 375.23 |
| 48 | 16.72 | 16.66 | 732 | 372.60 |
| 49 | 17.08 | 17.02 | 725 | 369.37 |
| 50 | 17.43 | 17.37 | 720 | 366.76 |
| 51 | 17.78 | 17.72 | 716 | 364.68 |
| 52 | 18.15 | 18.09 | 711 | 362.00 |
| 53 | 18.50 | 18.44 | 705 | 358.89 |
| 54 | 18.85 | 18.79 | 701 | 356.83 |
| 55 | 19.20 | 19.14 | 695 | 353.74 |
| 56 | 19.57 | 19.51 | 689 | 351.11 |
| 57 | 19.92 | 19.86 | 684 | 348.55 |
| 58 | 20.03 | 19.97 | 683 | 348.05 |

Test name: Specimen 3

Borehole: S1080

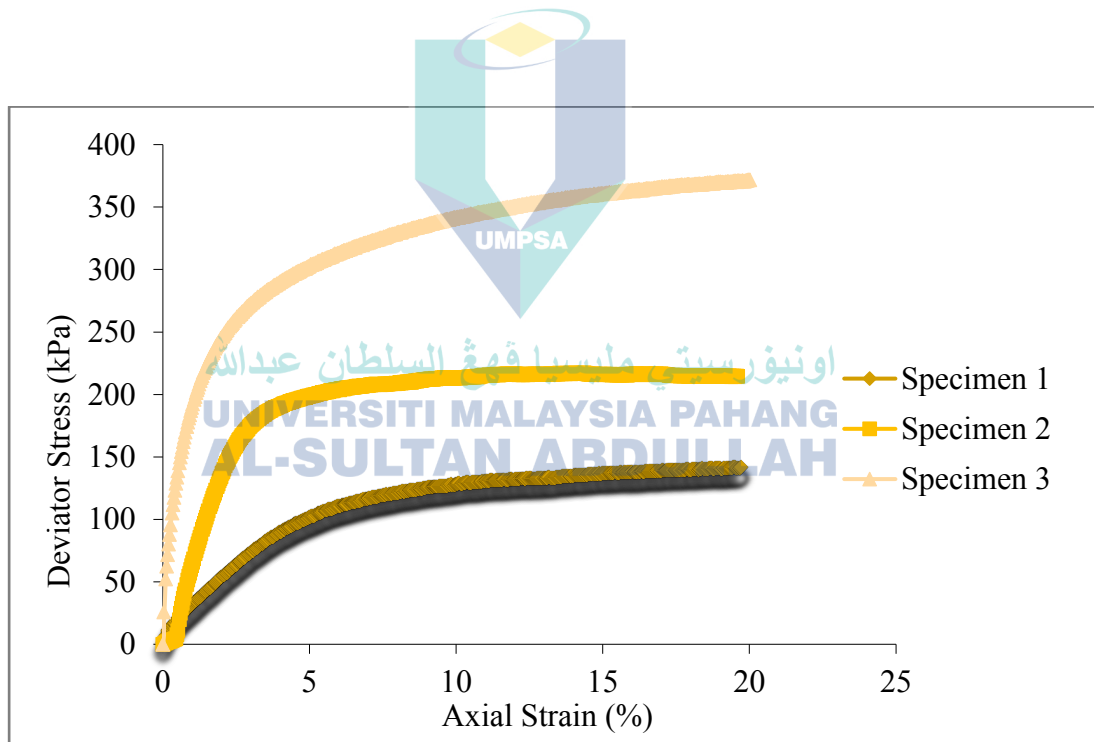
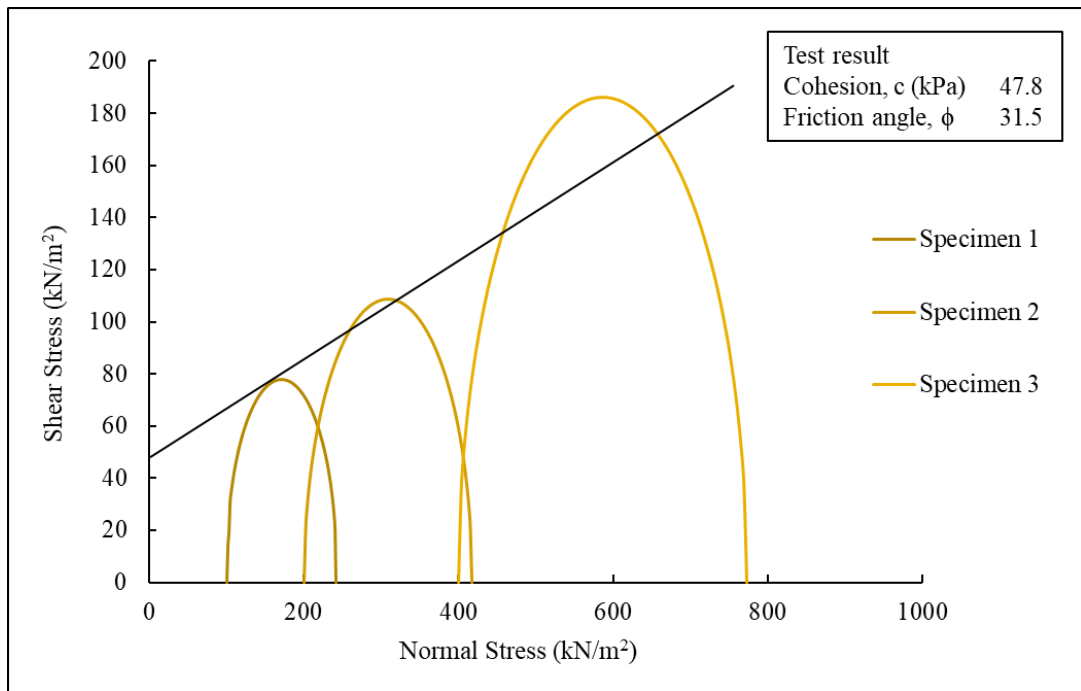
UNCONSOLIDATED UNDRAINED (UU) TRIAXIAL TEST

| | Specimen 1 | Specimen 2 | Specimen 3 |
|--|------------|------------|------------|
| Height (mm) | 100.00 | 100.00 | 100.00 |
| Diameter (mm) | 50.00 | 50.00 | 50.00 |
| Weight (g) | 350 | 350 | 350 |
| Particle Density, p_s | 2.62 | 2.62 | 2.62 |
| | | | |
| Specimen | Specimen 1 | Specimen 2 | Specimen 3 |
| Cell Pressure, σ_3 (kPa) | 100 | 200 | 400 |
| Moisture Content (%) | 20 | 20 | 20 |
| Bulk Density, (Mg/m ³) | 1.78 | 1.78 | 1.78 |
| Dry Density, (Mg/m ³) | 1.49 | 1.49 | 1.49 |
| Void Ratio | 0.76 | 0.76 | 0.76 |
| Deg of Saturation (%) | 68.95 | 68.95 | 68.95 |
| Strain at failure, ϵ_f (%) | 19.73 | 13.95 | 20.01 |
| Shear Strength, C_u (kPa) | 77.76 | 108.69 | 185.96 |
| Max Deviator Stress, (kPa) | 144.51 | 217.31 | 371.92 |
| Total Normal Stress ($\sigma_1 - \sigma_3$), (kPa) | 144.51 | 217.31 | 371.92 |

Test method: BS1377: Part 7: 1990

Borehole: S10100

(delete as appropriate)



TOTAL STRESS TRIAXIAL COMPRESSION

| No. | Strain (mm) | Strain, ϵ (%) | Load (N) | Deviator Stress (1-3) (kPa) |
|-----|-------------|------------------------|----------|-----------------------------|
| 1 | 0.267 | 0 | 0 | 0 |
| 2 | 0.35 | 0.08 | 12 | 5.98 |
| 3 | 0.72 | 0.45 | 36 | 18.54 |
| 4 | 1.07 | 0.80 | 53 | 27.06 |
| 5 | 1.42 | 1.15 | 68 | 34.85 |
| 6 | 1.78 | 1.52 | 85 | 43.24 |
| 7 | 2.13 | 1.87 | 99 | 50.27 |
| 8 | 2.48 | 2.22 | 114 | 57.90 |
| 9 | 2.85 | 2.58 | 129 | 65.46 |
| 10 | 3.20 | 2.93 | 142 | 72.33 |
| 11 | 3.55 | 3.28 | 154 | 78.50 |
| 12 | 3.92 | 3.65 | 166 | 84.61 |
| 13 | 4.27 | 4.00 | 176 | 89.41 |
| 14 | 4.62 | 4.35 | 185 | 94.18 |
| 15 | 4.98 | 4.72 | 193 | 98.26 |
| 16 | 5.33 | 5.07 | 201 | 102.32 |
| 17 | 5.68 | 5.42 | 208 | 105.72 |
| 18 | 6.03 | 5.77 | 213 | 108.46 |
| 19 | 6.40 | 6.13 | 218 | 111.16 |
| 20 | 6.75 | 6.48 | 222 | 113.23 |
| 21 | 7.10 | 6.83 | 228 | 115.91 |
| 22 | 7.47 | 7.20 | 230 | 117.30 |
| 23 | 7.82 | 7.55 | 234 | 119.32 |
| 24 | 8.18 | 7.92 | 237 | 120.69 |
| 25 | 8.53 | 8.27 | 241 | 122.67 |
| 26 | 8.90 | 8.63 | 242 | 123.39 |
| 27 | 9.25 | 8.98 | 246 | 125.34 |
| 28 | 9.60 | 9.33 | 248 | 126.07 |
| 29 | 9.97 | 9.70 | 249 | 126.76 |

| | | | | |
|----|-------|-------|-----|--------|
| 30 | 10.32 | 10.05 | 251 | 128.06 |
| 31 | 10.68 | 10.42 | 254 | 129.33 |
| 32 | 11.03 | 10.77 | 255 | 130.01 |
| 33 | 11.38 | 11.12 | 257 | 130.69 |
| 34 | 11.75 | 11.48 | 258 | 131.32 |
| 35 | 12.10 | 11.83 | 259 | 131.98 |
| 36 | 12.45 | 12.18 | 260 | 132.62 |
| 37 | 12.82 | 12.55 | 260 | 132.65 |
| 38 | 13.17 | 12.90 | 261 | 132.70 |
| 39 | 13.53 | 13.27 | 262 | 133.29 |
| 40 | 13.88 | 13.62 | 264 | 134.48 |
| 41 | 14.25 | 13.98 | 264 | 134.48 |
| 42 | 14.60 | 14.33 | 265 | 135.07 |
| 43 | 14.97 | 14.70 | 267 | 136.20 |
| 44 | 15.32 | 15.05 | 269 | 136.77 |
| 45 | 15.67 | 15.40 | 270 | 137.33 |
| 46 | 16.03 | 15.77 | 271 | 137.86 |
| 47 | 16.38 | 16.12 | 271 | 137.84 |
| 48 | 16.75 | 16.48 | 272 | 138.35 |
| 49 | 17.10 | 16.83 | 272 | 138.33 |
| 50 | 17.45 | 17.18 | 274 | 139.40 |
| 51 | 17.82 | 17.55 | 274 | 139.33 |
| 52 | 18.17 | 17.90 | 275 | 139.83 |
| 53 | 18.53 | 18.27 | 274 | 139.75 |
| 54 | 18.88 | 18.62 | 278 | 141.77 |
| 55 | 19.25 | 18.98 | 279 | 142.14 |
| 56 | 19.60 | 19.33 | 280 | 142.68 |
| 57 | 19.97 | 19.70 | 281 | 143.04 |
| 58 | 20.00 | 19.73 | 284 | 144.51 |

Test name: Specimen 1

Borehole: S10100

TOTAL STRESS TRIAXIAL COMPRESSION

| No. | Strain (mm) | Strain, ϵ (%) | Load (N) | Deviator Stress (1-3) (kPa) |
|-----|-------------|------------------------|----------|-----------------------------|
| 1 | 0.433 | 0 | 0 | 0 |
| 2 | 0.35 | -0.08 | -5 | -2.55 |
| 3 | 0.70 | 0.27 | 5 | 2.54 |
| 4 | 1.07 | 0.63 | 57 | 28.85 |
| 5 | 1.42 | 0.98 | 124 | 63.04 |
| 6 | 1.78 | 1.35 | 181 | 91.94 |
| 7 | 2.13 | 1.70 | 230 | 117.15 |
| 8 | 2.48 | 2.05 | 271 | 138.18 |
| 9 | 2.85 | 2.42 | 306 | 156.05 |
| 10 | 3.20 | 2.77 | 332 | 168.86 |
| 11 | 3.55 | 3.12 | 350 | 178.13 |
| 12 | 3.92 | 3.48 | 362 | 184.33 |
| 13 | 4.27 | 3.83 | 372 | 189.54 |
| 14 | 4.62 | 4.18 | 378 | 192.75 |
| 15 | 4.98 | 4.55 | 385 | 195.91 |
| 16 | 5.33 | 4.90 | 389 | 198.10 |
| 17 | 5.68 | 5.25 | 393 | 200.26 |
| 18 | 6.05 | 5.62 | 397 | 202.37 |
| 19 | 6.40 | 5.97 | 401 | 204.01 |
| 20 | 6.75 | 6.32 | 403 | 205.16 |
| 21 | 7.12 | 6.68 | 406 | 206.74 |
| 22 | 7.47 | 7.03 | 407 | 207.38 |
| 23 | 7.82 | 7.38 | 408 | 208.02 |
| 24 | 8.18 | 7.75 | 410 | 208.60 |
| 25 | 8.53 | 8.10 | 412 | 209.68 |
| 26 | 8.88 | 8.45 | 413 | 210.28 |
| 27 | 9.25 | 8.82 | 415 | 211.30 |
| 28 | 9.60 | 9.17 | 417 | 212.34 |
| 29 | 9.95 | 9.52 | 419 | 213.36 |

| | | | | |
|----|-------|-------|-----|--------|
| 30 | 10.32 | 9.88 | 418 | 212.96 |
| 31 | 10.67 | 10.23 | 419 | 213.50 |
| 32 | 11.03 | 10.60 | 420 | 214.00 |
| 33 | 11.38 | 10.95 | 423 | 215.43 |
| 34 | 11.73 | 11.30 | 424 | 215.93 |
| 35 | 12.10 | 11.67 | 425 | 216.39 |
| 36 | 12.45 | 12.02 | 425 | 216.43 |
| 37 | 12.82 | 12.38 | 424 | 215.97 |
| 38 | 13.17 | 12.73 | 424 | 216.00 |
| 39 | 13.53 | 13.10 | 424 | 215.98 |
| 40 | 13.88 | 13.45 | 425 | 216.43 |
| 41 | 14.38 | 13.95 | 427 | 217.37 |
| 42 | 14.60 | 14.17 | 426 | 216.82 |
| 43 | 14.95 | 14.52 | 425 | 216.37 |
| 44 | 15.32 | 14.88 | 424 | 215.88 |
| 45 | 15.67 | 15.23 | 424 | 215.85 |
| 46 | 16.03 | 15.60 | 424 | 215.78 |
| 47 | 16.38 | 15.95 | 424 | 216.17 |
| 48 | 16.75 | 16.32 | 424 | 216.08 |
| 49 | 17.10 | 16.67 | 425 | 216.45 |
| 50 | 17.45 | 17.02 | 425 | 216.39 |
| 51 | 17.82 | 17.38 | 423 | 215.43 |
| 52 | 18.17 | 17.73 | 422 | 214.94 |
| 53 | 18.53 | 18.10 | 422 | 214.81 |
| 54 | 18.88 | 18.45 | 422 | 214.73 |
| 55 | 19.23 | 18.80 | 422 | 215.05 |
| 56 | 19.60 | 19.17 | 421 | 214.48 |
| 57 | 19.95 | 19.52 | 421 | 214.38 |
| 58 | 20.03 | 19.60 | 421 | 214.56 |

Test name: Specimen 2

Borehole: S10100

TOTAL STRESS TRIAXIAL COMPRESSION

| No. | Strain (mm) | Strain, ϵ (%) | Load (N) | Deviator Stress (1-3) (kPa) |
|-----|-------------|------------------------|----------|-----------------------------|
| 1 | 0.003 | 0 | 0 | 0 |
| 2 | 0.35 | 0.35 | 219 | 111.66 |
| 3 | 0.70 | 0.70 | 319 | 162.34 |
| 4 | 1.07 | 1.06 | 385 | 196.01 |
| 5 | 1.42 | 1.41 | 430 | 218.92 |
| 6 | 1.78 | 1.78 | 466 | 237.11 |
| 7 | 2.13 | 2.13 | 490 | 249.72 |
| 8 | 2.48 | 2.48 | 511 | 260.25 |
| 9 | 2.85 | 2.85 | 529 | 269.66 |
| 10 | 3.20 | 3.20 | 543 | 276.58 |
| 11 | 3.55 | 3.55 | 557 | 283.44 |
| 12 | 3.90 | 3.90 | 567 | 288.77 |
| 13 | 4.27 | 4.26 | 576 | 293.53 |
| 14 | 4.62 | 4.61 | 587 | 298.77 |
| 15 | 4.97 | 4.96 | 594 | 302.51 |
| 16 | 5.33 | 5.33 | 602 | 306.65 |
| 17 | 5.68 | 5.68 | 608 | 309.84 |
| 18 | 6.03 | 6.03 | 616 | 313.47 |
| 19 | 6.40 | 6.40 | 622 | 316.54 |
| 20 | 6.75 | 6.75 | 629 | 320.11 |
| 21 | 7.10 | 7.10 | 634 | 322.69 |
| 22 | 7.45 | 7.45 | 639 | 325.24 |
| 23 | 7.82 | 7.81 | 644 | 328.18 |
| 24 | 8.17 | 8.16 | 649 | 330.68 |
| 25 | 8.52 | 8.51 | 654 | 333.14 |
| 26 | 8.88 | 8.88 | 658 | 335.06 |
| 27 | 9.23 | 9.23 | 663 | 337.47 |
| 28 | 9.58 | 9.58 | 666 | 339.39 |
| 29 | 9.93 | 9.93 | 671 | 341.75 |

| | | | | |
|----|-------|-------|-----|--------|
| 30 | 10.30 | 10.30 | 675 | 343.55 |
| 31 | 10.65 | 10.65 | 677 | 344.94 |
| 32 | 11.00 | 11.00 | 679 | 345.86 |
| 33 | 11.35 | 11.35 | 684 | 348.11 |
| 34 | 11.72 | 11.71 | 686 | 349.37 |
| 35 | 12.07 | 12.06 | 689 | 350.67 |
| 36 | 12.42 | 12.41 | 693 | 352.84 |
| 37 | 12.78 | 12.78 | 695 | 354.03 |
| 38 | 13.13 | 13.13 | 697 | 354.83 |
| 39 | 13.48 | 13.48 | 700 | 356.48 |
| 40 | 13.85 | 13.85 | 702 | 357.60 |
| 41 | 14.20 | 14.20 | 704 | 358.77 |
| 42 | 14.55 | 14.55 | 707 | 359.92 |
| 43 | 14.90 | 14.90 | 708 | 360.61 |
| 44 | 15.27 | 15.26 | 709 | 361.21 |
| 45 | 15.62 | 15.61 | 712 | 362.73 |
| 46 | 15.97 | 15.96 | 713 | 363.37 |
| 47 | 16.33 | 16.33 | 715 | 363.91 |
| 48 | 16.68 | 16.68 | 717 | 364.94 |
| 49 | 17.05 | 17.05 | 719 | 366.29 |
| 50 | 17.40 | 17.40 | 720 | 366.84 |
| 51 | 17.77 | 17.76 | 721 | 367.31 |
| 52 | 18.12 | 18.11 | 723 | 368.25 |
| 53 | 18.48 | 18.48 | 725 | 369.09 |
| 54 | 18.83 | 18.83 | 726 | 369.58 |
| 55 | 19.20 | 19.20 | 727 | 370.37 |
| 56 | 19.55 | 19.55 | 728 | 370.82 |
| 57 | 19.90 | 19.90 | 729 | 371.24 |
| 58 | 20.02 | 20.01 | 730 | 371.92 |

Test name: Specimen 3

Borehole: S10100

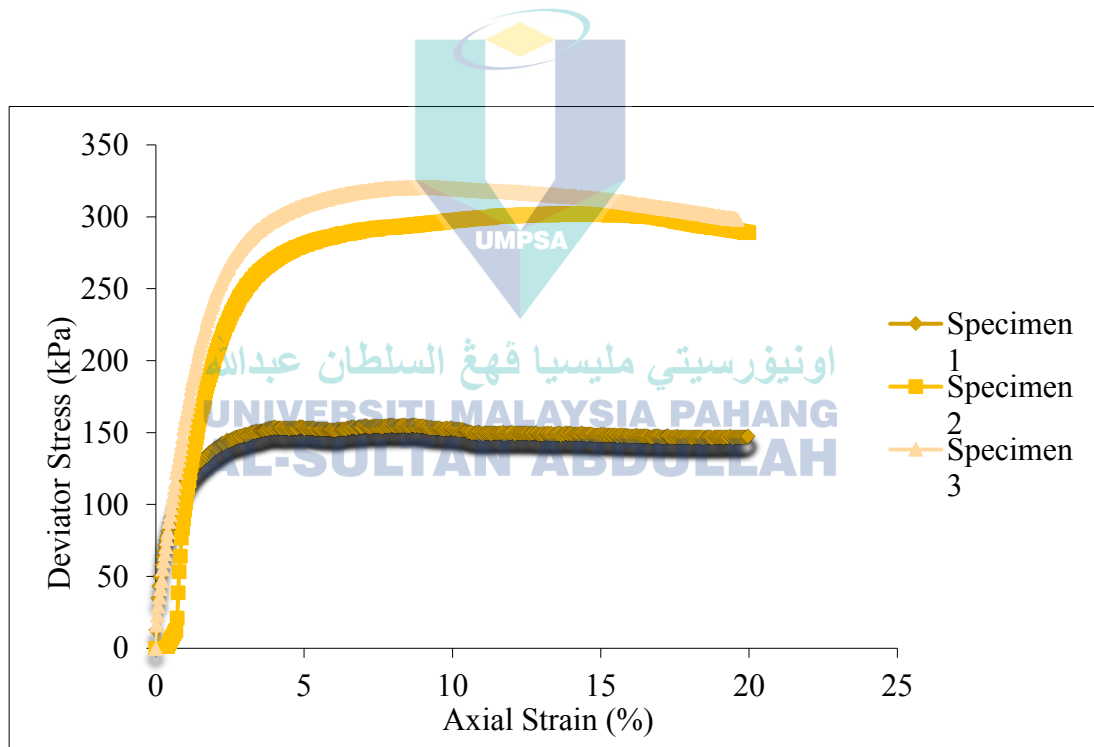
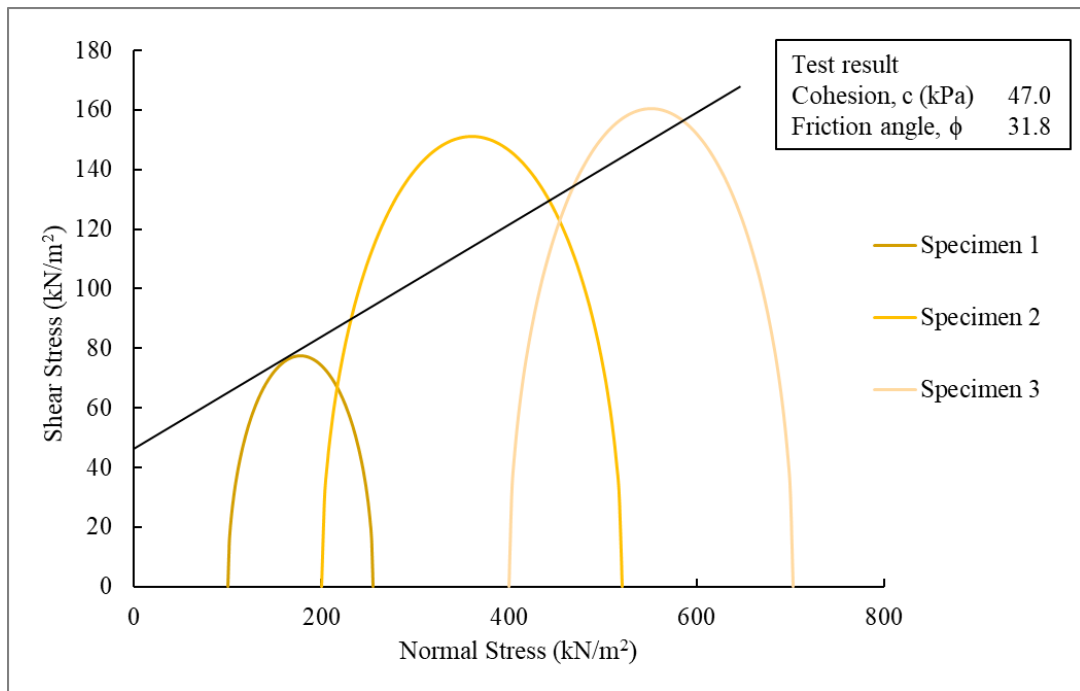
UNCONSOLIDATED UNDRAINED (UU) TRIAXIAL TEST

| | Specimen 1 | Specimen 2 | Specimen 3 |
|--|------------|------------|------------|
| Height (mm) | 100.00 | 100.00 | 100.00 |
| Diameter (mm) | 50.00 | 50.00 | 50.00 |
| Weight (g) | 350 | 350 | 350 |
| Particle Density, p_s | 2.62 | 2.62 | 2.62 |
| Specimen | Specimen 1 | Specimen 2 | Specimen 3 |
| Cell Pressure, σ_3 (kPa) | 100 | 200 | 400 |
| Moisture Content (%) | 20 | 20 | 20 |
| Bulk Density, (Mg/m ³) | 1.82 | 1.78 | 1.78 |
| Dry Density, (Mg/m ³) | 1.52 | 1.49 | 1.49 |
| Void Ratio | 0.72 | 0.76 | 0.76 |
| Deg of Saturation (%) | 72.78 | 68.95 | 68.95 |
| Strain at failure, ϵ_f (%) | 8.62 | 14.40 | 9.51 |
| Shear Strength, C_u (kPa) | 77.53 | 151.30 | 160.58 |
| Max Deviator Stress, (kPa) | 155.06 | 302.59 | 321.15 |
| Total Normal Stress ($\sigma_1 - \sigma_3$), (kPa) | 155.06 | 302.59 | 321.15 |

Test method: BS1377: Part 7: 1990

Borehole: S1660

(delete as appropriate)



TOTAL STRESS TRIAXIAL COMPRESSION

| No. | Strain (mm) | Strain, ϵ (%) | Load (N) | Deviator Stress (1-3) (kPa) |
|-----|-------------|------------------------|----------|-----------------------------|
| 1 | 0.012 | 0.000 | 0 | 0.000 |
| 2 | 0.35 | 0.34 | 148 | 75.16 |
| 3 | 0.70 | 0.69 | 199 | 101.11 |
| 4 | 1.07 | 1.06 | 231 | 117.90 |
| 5 | 1.42 | 1.41 | 251 | 127.89 |
| 6 | 1.77 | 1.76 | 265 | 134.85 |
| 7 | 2.13 | 2.12 | 275 | 140.25 |
| 8 | 2.48 | 2.47 | 283 | 144.16 |
| 9 | 2.83 | 2.82 | 289 | 147.31 |
| 10 | 3.20 | 3.19 | 294 | 149.67 |
| 11 | 3.55 | 3.54 | 297 | 151.31 |
| 12 | 3.90 | 3.89 | 300 | 152.94 |
| 13 | 4.25 | 4.24 | 301 | 153.11 |
| 14 | 4.62 | 4.61 | 301 | 153.24 |
| 15 | 4.97 | 4.96 | 301 | 153.39 |
| 16 | 5.32 | 5.31 | 300 | 152.83 |
| 17 | 5.68 | 5.67 | 299 | 152.24 |
| 18 | 6.03 | 6.02 | 298 | 151.67 |
| 19 | 6.38 | 6.37 | 299 | 152.52 |
| 20 | 6.75 | 6.74 | 301 | 153.33 |
| 21 | 7.10 | 7.09 | 303 | 154.15 |
| 22 | 7.45 | 7.44 | 303 | 154.27 |
| 23 | 7.82 | 7.81 | 303 | 154.36 |
| 24 | 8.17 | 8.16 | 303 | 154.46 |
| 25 | 8.63 | 8.62 | 304 | 155.06 |
| 26 | 8.88 | 8.87 | 304 | 154.63 |
| 27 | 9.23 | 9.22 | 301 | 153.35 |
| 28 | 9.58 | 9.57 | 300 | 152.76 |
| 29 | 9.95 | 9.94 | 300 | 152.82 |

| | | | | |
|----|-------|-------|-----|--------|
| 30 | 10.30 | 10.29 | 299 | 152.23 |
| 31 | 10.65 | 10.64 | 295 | 150.29 |
| 32 | 11.02 | 11.01 | 293 | 149.00 |
| 33 | 11.37 | 11.36 | 294 | 149.75 |
| 34 | 11.72 | 11.71 | 294 | 149.82 |
| 35 | 12.08 | 12.07 | 293 | 149.20 |
| 36 | 12.43 | 12.42 | 293 | 149.27 |
| 37 | 12.78 | 12.77 | 293 | 149.33 |
| 38 | 13.15 | 13.14 | 292 | 148.70 |
| 39 | 13.50 | 13.49 | 292 | 148.75 |
| 40 | 13.85 | 13.84 | 293 | 149.45 |
| 41 | 14.20 | 14.19 | 292 | 148.85 |
| 42 | 14.57 | 14.56 | 291 | 148.21 |
| 43 | 14.92 | 14.91 | 291 | 148.24 |
| 44 | 15.27 | 15.26 | 291 | 148.27 |
| 45 | 15.63 | 15.62 | 291 | 148.27 |
| 46 | 15.98 | 15.97 | 290 | 147.65 |
| 47 | 16.33 | 16.32 | 290 | 147.67 |
| 48 | 16.70 | 16.69 | 289 | 147.02 |
| 49 | 17.05 | 17.04 | 289 | 147.03 |
| 50 | 17.40 | 17.39 | 289 | 147.03 |
| 51 | 17.77 | 17.76 | 289 | 147.00 |
| 52 | 18.12 | 18.11 | 289 | 146.99 |
| 53 | 18.47 | 18.46 | 287 | 146.36 |
| 54 | 18.83 | 18.82 | 288 | 146.93 |
| 55 | 19.18 | 19.17 | 288 | 146.91 |
| 56 | 19.53 | 19.52 | 288 | 146.88 |
| 57 | 19.90 | 19.89 | 288 | 146.81 |
| 58 | 20.00 | 19.99 | 289 | 147.23 |

Test name: Specimen 1

Borehole: S1660

TOTAL STRESS TRIAXIAL COMPRESSION

| No. | Strain (mm) | Strain, ϵ (%) | Load (N) | Deviator Stress (1-3) (kPa) |
|-----|-------------|------------------------|----------|-----------------------------|
| 1 | 0.32 | 0.32 | -8 | -3.83 |
| 2 | 0.68 | 0.68 | 25 | 12.71 |
| 3 | 1.03 | 1.03 | 209 | 106.37 |
| 4 | 1.40 | 1.40 | 295 | 150.16 |
| 5 | 1.75 | 1.75 | 362 | 184.18 |
| 6 | 2.12 | 2.12 | 412 | 209.83 |
| 7 | 2.47 | 2.47 | 450 | 229.06 |
| 8 | 2.82 | 2.82 | 479 | 243.74 |
| 9 | 3.18 | 3.18 | 499 | 254.02 |
| 10 | 3.53 | 3.53 | 515 | 262.37 |
| 11 | 3.88 | 3.88 | 526 | 268.14 |
| 12 | 4.25 | 4.25 | 537 | 273.29 |
| 13 | 4.60 | 4.60 | 544 | 277.18 |
| 14 | 4.97 | 4.97 | 551 | 280.38 |
| 15 | 5.32 | 5.32 | 554 | 282.38 |
| 16 | 5.67 | 5.67 | 560 | 284.96 |
| 17 | 6.03 | 6.03 | 562 | 286.32 |
| 18 | 6.38 | 6.38 | 566 | 288.20 |
| 19 | 6.73 | 6.73 | 570 | 290.11 |
| 20 | 7.10 | 7.10 | 572 | 291.35 |
| 21 | 7.45 | 7.45 | 573 | 292.04 |
| 22 | 7.80 | 7.80 | 575 | 292.71 |
| 23 | 8.17 | 8.17 | 576 | 293.37 |
| 24 | 8.52 | 8.52 | 577 | 293.96 |
| 25 | 8.88 | 8.88 | 578 | 294.59 |
| 26 | 9.23 | 9.23 | 581 | 295.78 |
| 27 | 9.58 | 9.58 | 582 | 296.33 |
| 28 | 9.95 | 9.95 | 584 | 297.49 |
| 29 | 10.30 | 10.30 | 585 | 298.07 |

| | | | | |
|----|-------|-------|-----|--------|
| 30 | 10.65 | 10.65 | 586 | 298.57 |
| 31 | 11.02 | 11.02 | 587 | 299.11 |
| 32 | 11.37 | 11.37 | 588 | 299.64 |
| 33 | 11.73 | 11.73 | 590 | 300.67 |
| 34 | 12.08 | 12.08 | 590 | 300.61 |
| 35 | 12.43 | 12.43 | 591 | 301.10 |
| 36 | 12.80 | 12.80 | 592 | 301.52 |
| 37 | 13.15 | 13.15 | 593 | 301.99 |
| 38 | 13.50 | 13.50 | 593 | 301.88 |
| 39 | 13.87 | 13.87 | 594 | 302.32 |
| 40 | 14.22 | 14.22 | 593 | 302.14 |
| 41 | 14.40 | 14.40 | 594 | 302.59 |
| 42 | 14.93 | 14.93 | 593 | 301.81 |
| 43 | 15.28 | 15.28 | 591 | 301.12 |
| 44 | 15.65 | 15.65 | 592 | 301.50 |
| 45 | 16.00 | 16.00 | 591 | 300.79 |
| 46 | 16.37 | 16.37 | 590 | 300.56 |
| 47 | 16.72 | 16.72 | 589 | 299.84 |
| 48 | 17.07 | 17.07 | 587 | 299.12 |
| 49 | 17.43 | 17.43 | 584 | 297.27 |
| 50 | 17.78 | 17.78 | 581 | 296.02 |
| 51 | 18.13 | 18.13 | 580 | 295.23 |
| 52 | 18.50 | 18.50 | 577 | 293.97 |
| 53 | 18.85 | 18.85 | 575 | 292.72 |
| 54 | 19.22 | 19.22 | 572 | 291.40 |
| 55 | 19.57 | 19.57 | 571 | 290.66 |
| 56 | 19.92 | 19.92 | 568 | 289.40 |
| 57 | 20.00 | 20.00 | 568 | 289.10 |

Test name: Specimen 2

Borehole: S1660

TOTAL STRESS TRIAXIAL COMPRESSION

| No. | Strain (mm) | Strain, ϵ (%) | Load (N) | Deviator Stress (1-3) (kPa) |
|-----|-------------|------------------------|----------|-----------------------------|
| 1 | 0.37 | -0.04 | 1 | 0.00 |
| 2 | 0.72 | 0.31 | 1 | 65.76 |
| 3 | 1.07 | 0.66 | 2 | 115.93 |
| 4 | 1.42 | 1.01 | 3 | 160.69 |
| 5 | 1.78 | 1.37 | 3 | 197.65 |
| 6 | 2.13 | 1.72 | 4 | 227.82 |
| 7 | 2.48 | 2.07 | 5 | 249.36 |
| 8 | 2.85 | 2.44 | 6 | 264.30 |
| 9 | 3.20 | 2.79 | 6 | 276.62 |
| 10 | 3.55 | 3.14 | 7 | 284.96 |
| 11 | 3.92 | 3.51 | 8 | 291.26 |
| 12 | 4.27 | 3.86 | 8 | 296.98 |
| 13 | 4.62 | 4.21 | 9 | 300.75 |
| 14 | 4.98 | 4.57 | 10 | 304.92 |
| 15 | 5.33 | 4.92 | 10 | 307.66 |
| 16 | 5.68 | 5.27 | 11 | 309.88 |
| 17 | 6.03 | 5.62 | 12 | 312.03 |
| 18 | 6.40 | 5.99 | 13 | 314.20 |
| 19 | 6.75 | 6.34 | 13 | 315.40 |
| 20 | 7.12 | 6.71 | 14 | 317.00 |
| 21 | 7.47 | 7.06 | 15 | 317.69 |
| 22 | 7.82 | 7.41 | 15 | 319.31 |
| 23 | 8.17 | 7.76 | 16 | 319.91 |
| 24 | 8.53 | 8.12 | 17 | 320.09 |
| 25 | 8.88 | 8.47 | 17 | 320.66 |
| 26 | 9.23 | 8.82 | 18 | 320.35 |
| 27 | 9.60 | 9.19 | 19 | 320.96 |
| 28 | 9.92 | 9.51 | 20 | 321.15 |
| 29 | 10.30 | 9.89 | 20 | 319.79 |

| | | | | |
|----|-------|-------|----|--------|
| 30 | 10.67 | 10.26 | 21 | 319.45 |
| 31 | 11.02 | 10.61 | 22 | 318.59 |
| 32 | 11.37 | 10.96 | 22 | 318.69 |
| 33 | 11.73 | 11.32 | 23 | 318.27 |
| 34 | 12.08 | 11.67 | 24 | 317.91 |
| 35 | 12.43 | 12.02 | 24 | 317.53 |
| 36 | 12.80 | 12.39 | 25 | 317.09 |
| 37 | 13.15 | 12.74 | 26 | 316.26 |
| 38 | 13.50 | 13.09 | 27 | 315.43 |
| 39 | 13.85 | 13.44 | 27 | 314.97 |
| 40 | 14.22 | 13.81 | 28 | 314.56 |
| 41 | 14.57 | 14.16 | 29 | 314.09 |
| 42 | 14.93 | 14.52 | 29 | 313.23 |
| 43 | 15.28 | 14.87 | 30 | 312.81 |
| 44 | 15.63 | 15.22 | 31 | 311.88 |
| 45 | 15.98 | 15.57 | 31 | 310.59 |
| 46 | 16.35 | 15.94 | 32 | 310.08 |
| 47 | 16.70 | 16.29 | 33 | 308.36 |
| 48 | 17.05 | 16.64 | 34 | 307.49 |
| 49 | 17.42 | 17.01 | 34 | 306.55 |
| 50 | 17.77 | 17.36 | 35 | 305.67 |
| 51 | 18.13 | 17.72 | 36 | 304.37 |
| 52 | 18.48 | 18.07 | 36 | 303.42 |
| 53 | 18.83 | 18.42 | 37 | 302.12 |
| 54 | 19.20 | 18.79 | 38 | 300.75 |
| 55 | 19.55 | 19.14 | 38 | 299.86 |
| 56 | 19.90 | 19.49 | 39 | 298.96 |
| 57 | 20.02 | 19.61 | 39 | 298.24 |

Test name: Specimen 3

Borehole: S1660

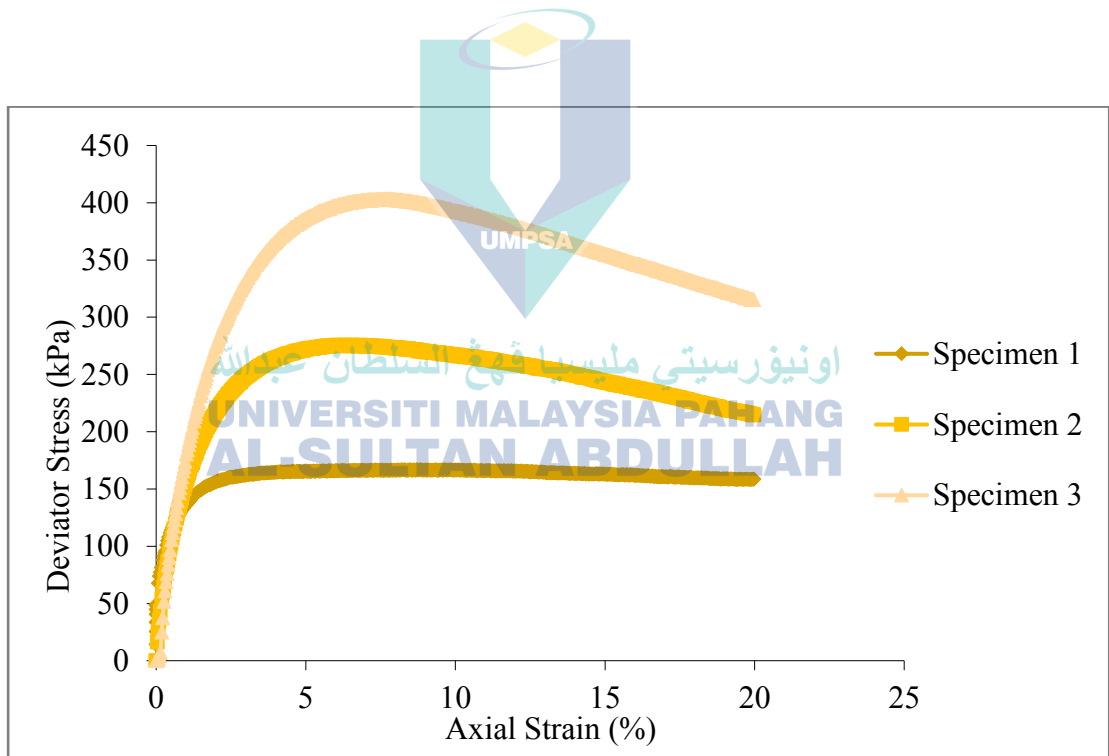
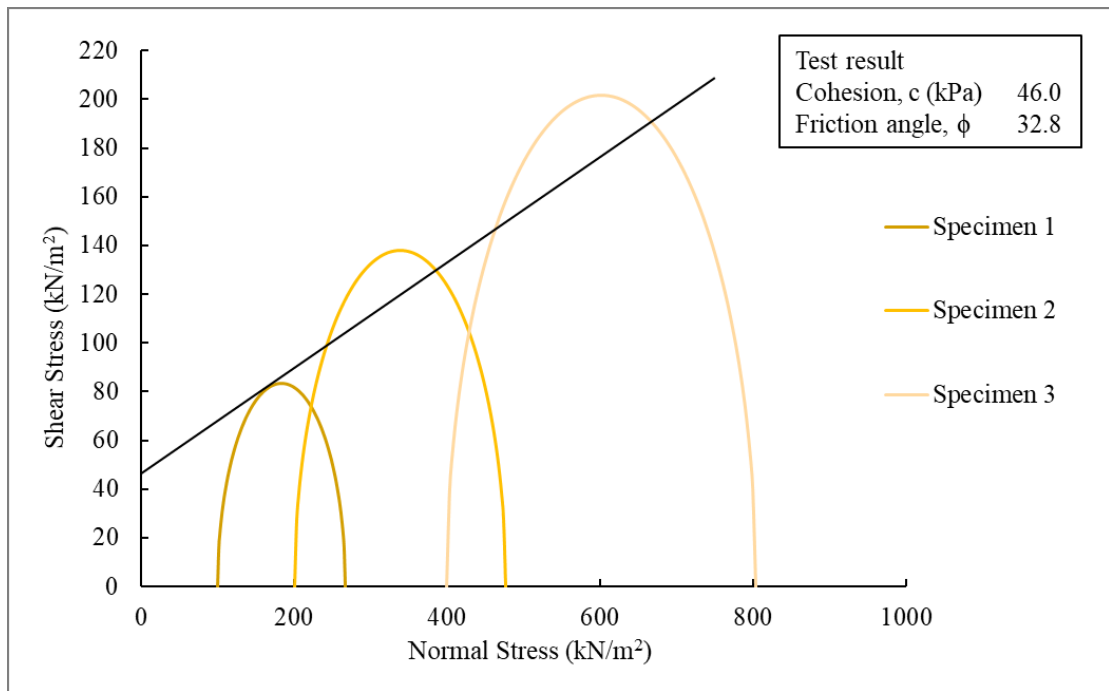
UNCONSOLIDATED UNDRAINED (UU) TRIAXIAL TEST

| | Specimen 1 | Specimen 2 | Specimen 3 |
|--|------------|------------|------------|
| Height (mm) | 100.00 | 100.00 | 100.00 |
| Diameter (mm) | 50.00 | 50.00 | 50.00 |
| Weight (g) | 350 | 350 | 350 |
| Particle Density, p_s | 2.62 | 2.62 | 2.62 |
| Specimen | Specimen 1 | Specimen 2 | Specimen 3 |
| Cell Pressure, σ_3 (kPa) | 100 | 200 | 400 |
| Moisture Content (%) | 20 | 20 | 20 |
| Bulk Density, (Mg/m ³) | 1.78 | 1.78 | 1.78 |
| Dry Density, (Mg/m ³) | 1.49 | 1.49 | 1.49 |
| Void Ratio | 0.76 | 0.76 | 0.76 |
| Deg of Saturation (%) | 68.95 | 68.95 | 68.95 |
| Strain at failure, ϵ_f (%) | 9.65 | 6.33 | 7.65 |
| Shear Strength, C_u (kPa) | 83.52 | 137.87 | 201.77 |
| Max Deviator Stress, (kPa) | 167.03 | 275.73 | 403.55 |
| Total Normal Stress ($\sigma_1 - \sigma_3$), (kPa) | 167.03 | 275.73 | 403.55 |

Test method: BS1377: Part 7: 1990

Borehole: S1680

(delete as appropriate)



TOTAL STRESS TRIAXIAL COMPRESSION

| No. | Strain (mm) | Strain, ϵ (%) | Load (N) | Deviator Stress (1-3) (kPa) |
|-----|-------------|------------------------|----------|-----------------------------|
| 1 | 0.13 | 0.13 | 152 | 77.31 |
| 2 | 0.50 | 0.50 | 224 | 114.02 |
| 3 | 0.85 | 0.85 | 258 | 131.29 |
| 4 | 1.22 | 1.22 | 281 | 142.88 |
| 5 | 1.57 | 1.57 | 296 | 150.90 |
| 6 | 1.92 | 1.92 | 305 | 155.35 |
| 7 | 2.28 | 2.28 | 312 | 158.76 |
| 8 | 2.63 | 2.63 | 315 | 160.67 |
| 9 | 2.98 | 2.98 | 318 | 162.07 |
| 10 | 3.35 | 3.35 | 321 | 163.42 |
| 11 | 3.70 | 3.70 | 323 | 164.30 |
| 12 | 4.05 | 4.05 | 323 | 164.68 |
| 13 | 4.42 | 4.42 | 324 | 165.03 |
| 14 | 4.77 | 4.77 | 325 | 165.39 |
| 15 | 5.13 | 5.13 | 325 | 165.72 |
| 16 | 5.48 | 5.48 | 325 | 165.59 |
| 17 | 5.83 | 5.83 | 326 | 165.94 |
| 18 | 6.20 | 6.20 | 326 | 166.25 |
| 19 | 6.55 | 6.55 | 326 | 166.10 |
| 20 | 6.90 | 6.90 | 327 | 166.43 |
| 21 | 7.27 | 7.27 | 326 | 166.25 |
| 22 | 7.62 | 7.62 | 326 | 166.09 |
| 23 | 7.97 | 7.97 | 327 | 166.40 |
| 24 | 8.33 | 8.33 | 327 | 166.67 |
| 25 | 8.68 | 8.68 | 327 | 166.50 |
| 26 | 9.05 | 9.05 | 327 | 166.29 |
| 27 | 9.40 | 9.40 | 326 | 166.11 |
| 28 | 9.65 | 9.65 | 328 | 167.03 |
| 29 | 10.12 | 10.12 | 327 | 166.63 |

| | | | | |
|----|-------|-------|-----|--------|
| 30 | 10.47 | 10.47 | 327 | 166.44 |
| 31 | 10.83 | 10.83 | 326 | 166.21 |
| 32 | 11.18 | 11.18 | 325 | 165.56 |
| 33 | 11.53 | 11.53 | 326 | 165.81 |
| 34 | 11.90 | 11.90 | 325 | 165.57 |
| 35 | 12.25 | 12.25 | 325 | 165.36 |
| 36 | 12.60 | 12.60 | 324 | 165.14 |
| 37 | 12.97 | 12.97 | 324 | 164.89 |
| 38 | 13.32 | 13.32 | 322 | 164.23 |
| 39 | 13.68 | 13.68 | 322 | 163.97 |
| 40 | 14.03 | 14.03 | 321 | 163.31 |
| 41 | 14.38 | 14.38 | 320 | 163.08 |
| 42 | 14.75 | 14.75 | 321 | 163.25 |
| 43 | 15.10 | 15.10 | 320 | 163.01 |
| 44 | 15.47 | 15.47 | 319 | 162.31 |
| 45 | 15.82 | 15.82 | 318 | 162.07 |
| 46 | 16.17 | 16.17 | 318 | 161.82 |
| 47 | 16.53 | 16.53 | 316 | 161.11 |
| 48 | 16.88 | 16.88 | 316 | 160.86 |
| 49 | 17.25 | 17.25 | 315 | 160.57 |
| 50 | 17.60 | 17.60 | 314 | 159.89 |
| 51 | 17.95 | 17.95 | 313 | 159.63 |
| 52 | 18.32 | 18.32 | 313 | 159.33 |
| 53 | 18.67 | 18.67 | 312 | 159.06 |
| 54 | 19.02 | 19.02 | 312 | 158.79 |
| 55 | 19.38 | 19.38 | 311 | 158.48 |
| 56 | 19.73 | 19.73 | 311 | 158.61 |
| 57 | 19.98 | 19.98 | 311 | 158.53 |

Test name: Specimen 1

Borehole: S1680

TOTAL STRESS TRIAXIAL COMPRESSION

| No. | Strain (mm) | Strain, ϵ (%) | Load (N) | Deviator Stress (1-3) (kPa) |
|-----|-------------|------------------------|----------|-----------------------------|
| 1 | 0.32 | 0.32 | 150 | 76.15 |
| 2 | 0.68 | 0.68 | 244 | 124.43 |
| 3 | 1.03 | 1.03 | 312 | 158.77 |
| 4 | 1.38 | 1.38 | 364 | 185.33 |
| 5 | 1.75 | 1.75 | 405 | 206.16 |
| 6 | 2.10 | 2.10 | 435 | 221.38 |
| 7 | 2.45 | 2.45 | 458 | 233.50 |
| 8 | 2.82 | 2.82 | 479 | 244.01 |
| 9 | 3.17 | 3.17 | 495 | 252.01 |
| 10 | 3.53 | 3.53 | 506 | 257.93 |
| 11 | 3.88 | 3.88 | 516 | 262.87 |
| 12 | 4.23 | 4.23 | 523 | 266.30 |
| 13 | 4.60 | 4.60 | 529 | 269.66 |
| 14 | 4.95 | 4.95 | 533 | 271.57 |
| 15 | 5.30 | 5.30 | 537 | 273.47 |
| 16 | 5.67 | 5.67 | 539 | 274.33 |
| 17 | 6.02 | 6.02 | 541 | 275.70 |
| 18 | 6.33 | 6.33 | 541 | 275.73 |
| 19 | 6.73 | 6.73 | 540 | 275.03 |
| 20 | 7.08 | 7.08 | 540 | 274.94 |
| 21 | 7.45 | 7.45 | 540 | 274.80 |
| 22 | 7.80 | 7.80 | 538 | 273.76 |
| 23 | 8.15 | 8.15 | 536 | 273.19 |
| 24 | 8.52 | 8.52 | 533 | 271.63 |
| 25 | 8.87 | 8.87 | 531 | 270.59 |
| 26 | 9.22 | 9.22 | 529 | 269.56 |
| 27 | 9.58 | 9.58 | 526 | 268.01 |
| 28 | 9.93 | 9.93 | 524 | 266.97 |
| 29 | 10.30 | 10.30 | 521 | 265.42 |

| | | | | |
|----|-------|-------|-----|--------|
| 30 | 10.65 | 10.65 | 521 | 265.30 |
| 31 | 11.00 | 11.00 | 518 | 263.81 |
| 32 | 11.37 | 11.37 | 514 | 261.81 |
| 33 | 11.72 | 11.72 | 512 | 260.78 |
| 34 | 12.07 | 12.07 | 509 | 259.30 |
| 35 | 12.43 | 12.43 | 505 | 257.33 |
| 36 | 12.78 | 12.78 | 501 | 255.41 |
| 37 | 13.13 | 13.13 | 499 | 254.39 |
| 38 | 13.50 | 13.50 | 496 | 252.43 |
| 39 | 13.85 | 13.85 | 492 | 250.53 |
| 40 | 14.22 | 14.22 | 487 | 248.15 |
| 41 | 14.57 | 14.57 | 484 | 246.27 |
| 42 | 14.92 | 14.92 | 479 | 243.96 |
| 43 | 15.28 | 15.28 | 476 | 242.48 |
| 44 | 15.63 | 15.63 | 472 | 240.19 |
| 45 | 15.98 | 15.98 | 468 | 238.34 |
| 46 | 16.35 | 16.35 | 464 | 236.44 |
| 47 | 16.70 | 16.70 | 460 | 234.18 |
| 48 | 17.07 | 17.07 | 455 | 231.88 |
| 49 | 17.42 | 17.42 | 452 | 230.06 |
| 50 | 17.77 | 17.77 | 447 | 227.83 |
| 51 | 18.13 | 18.13 | 443 | 225.57 |
| 52 | 18.48 | 18.48 | 439 | 223.36 |
| 53 | 18.83 | 18.83 | 435 | 221.57 |
| 54 | 19.20 | 19.20 | 430 | 218.92 |
| 55 | 19.55 | 19.55 | 426 | 217.16 |
| 56 | 19.92 | 19.92 | 422 | 214.94 |
| 57 | 19.98 | 19.98 | 422 | 214.76 |

Test name: Specimen 2

Borehole: S1680

TOTAL STRESS TRIAXIAL COMPRESSION

| No. | Strain (mm) | Strain, ϵ (%) | Load (N) | Deviator Stress (1-3) (kPa) |
|-----|-------------|------------------------|----------|-----------------------------|
| 1 | 0.33 | 0.33 | 136 | 69.03 |
| 2 | 0.68 | 0.68 | 263 | 134.04 |
| 3 | 1.05 | 1.05 | 361 | 183.94 |
| 4 | 1.40 | 1.40 | 438 | 222.96 |
| 5 | 1.77 | 1.77 | 504 | 256.65 |
| 6 | 2.12 | 2.12 | 556 | 283.16 |
| 7 | 2.47 | 2.47 | 600 | 305.49 |
| 8 | 2.83 | 2.83 | 636 | 324.14 |
| 9 | 3.18 | 3.18 | 666 | 339.24 |
| 10 | 3.53 | 3.53 | 692 | 352.26 |
| 11 | 3.88 | 3.88 | 712 | 362.73 |
| 12 | 4.25 | 4.25 | 732 | 372.57 |
| 13 | 4.60 | 4.60 | 744 | 378.98 |
| 14 | 4.98 | 4.98 | 758 | 386.17 |
| 15 | 5.33 | 5.33 | 767 | 390.53 |
| 16 | 5.68 | 5.68 | 775 | 394.85 |
| 17 | 6.03 | 6.03 | 780 | 397.21 |
| 18 | 6.40 | 6.40 | 785 | 399.95 |
| 19 | 6.75 | 6.75 | 788 | 401.31 |
| 20 | 7.10 | 7.10 | 791 | 402.64 |
| 21 | 7.65 | 7.65 | 792 | 403.55 |
| 22 | 7.82 | 7.82 | 791 | 402.82 |
| 23 | 8.18 | 8.18 | 791 | 402.62 |
| 24 | 8.53 | 8.53 | 788 | 401.55 |
| 25 | 8.88 | 8.88 | 785 | 399.55 |
| 26 | 9.25 | 9.25 | 780 | 397.48 |
| 27 | 9.60 | 9.60 | 777 | 395.49 |
| 28 | 9.95 | 9.95 | 772 | 393.04 |
| 29 | 10.32 | 10.32 | 768 | 390.98 |

| | | | | |
|----|-------|-------|-----|--------|
| 30 | 10.67 | 10.67 | 763 | 388.54 |
| 31 | 11.03 | 11.03 | 759 | 386.50 |
| 32 | 11.38 | 11.38 | 754 | 384.08 |
| 33 | 11.73 | 11.73 | 749 | 381.21 |
| 34 | 12.10 | 12.10 | 745 | 379.18 |
| 35 | 12.45 | 12.45 | 738 | 375.88 |
| 36 | 12.82 | 12.82 | 734 | 373.86 |
| 37 | 13.17 | 13.17 | 727 | 370.15 |
| 38 | 13.52 | 13.52 | 721 | 367.34 |
| 39 | 13.88 | 13.88 | 716 | 364.47 |
| 40 | 14.23 | 14.23 | 709 | 361.24 |
| 41 | 14.58 | 14.58 | 704 | 358.46 |
| 42 | 14.95 | 14.95 | 697 | 355.19 |
| 43 | 15.30 | 15.30 | 693 | 352.86 |
| 44 | 15.67 | 15.67 | 687 | 350.05 |
| 45 | 16.02 | 16.02 | 681 | 346.88 |
| 46 | 16.37 | 16.37 | 676 | 344.16 |
| 47 | 16.73 | 16.73 | 669 | 340.96 |
| 48 | 17.08 | 17.08 | 664 | 338.26 |
| 49 | 17.45 | 17.45 | 659 | 335.50 |
| 50 | 17.80 | 17.80 | 653 | 332.40 |
| 51 | 18.15 | 18.15 | 647 | 329.74 |
| 52 | 18.52 | 18.52 | 641 | 326.60 |
| 53 | 18.87 | 18.87 | 636 | 323.95 |
| 54 | 19.22 | 19.22 | 631 | 321.32 |
| 55 | 19.58 | 19.58 | 626 | 318.64 |
| 56 | 19.93 | 19.93 | 620 | 315.62 |
| 57 | 19.97 | 19.97 | 619 | 315.49 |

Test name: Specimen 3

Borehole: S1680

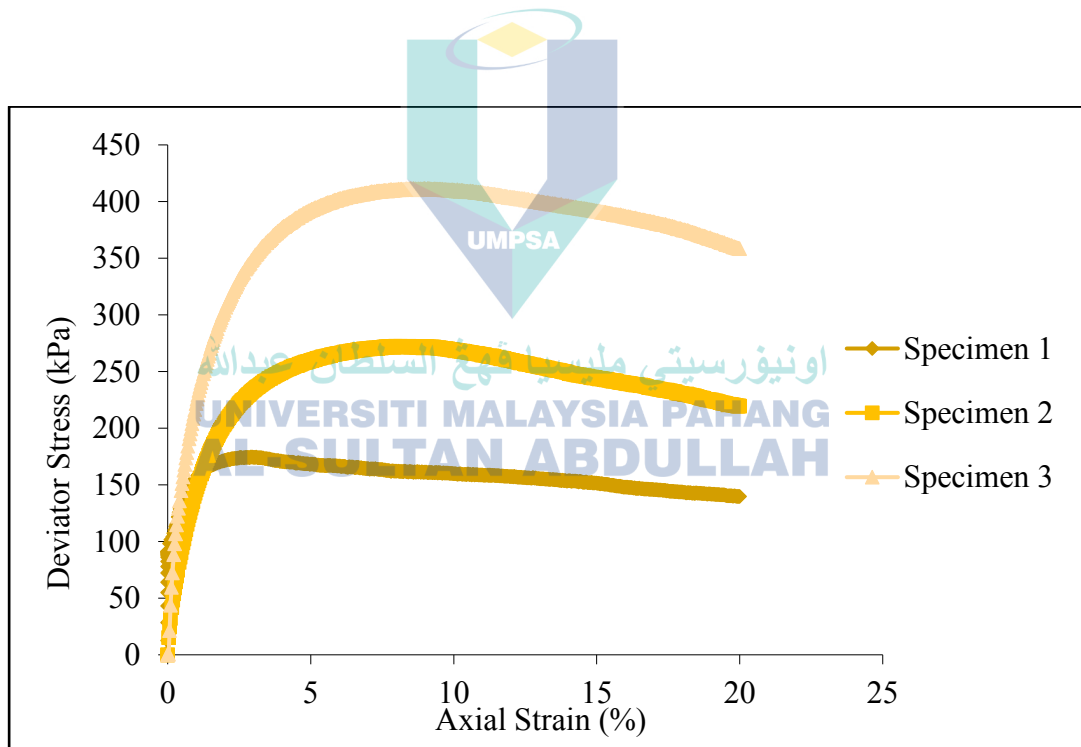
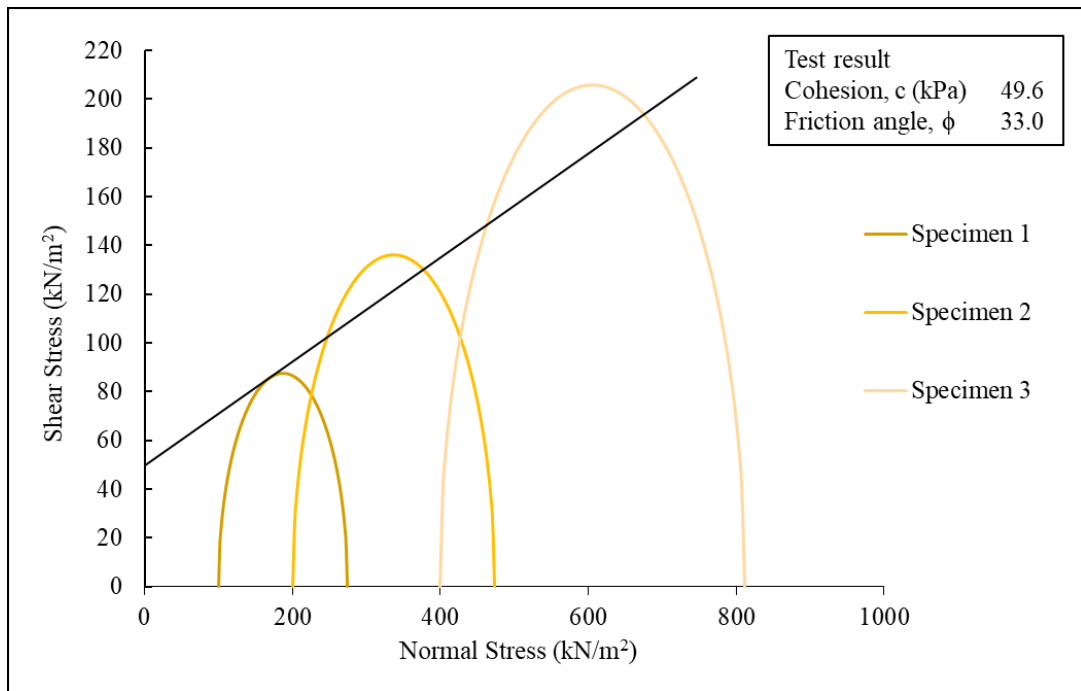
UNCONSOLIDATED UNDRAINED (UU) TRIAXIAL TEST

| | Specimen 1 | Specimen 2 | Specimen 3 |
|--|------------|------------|------------|
| Height (mm) | 100.00 | 100.00 | 100.00 |
| Diameter (mm) | 50.00 | 50.00 | 50.00 |
| Weight (g) | 350 | 350 | 350 |
| Particle Density, p_s | 2.62 | 2.62 | 2.62 |
| | | | |
| Specimen | Specimen 1 | Specimen 2 | Specimen 3 |
| Cell Pressure, σ_3 (kPa) | 100 | 200 | 400 |
| Moisture Content (%) | 20 | 20 | 20 |
| Bulk Density, (Mg/m ³) | 1.78 | 1.78 | 1.78 |
| Dry Density, (Mg/m ³) | 1.49 | 1.49 | 1.49 |
| Void Ratio | 0.76 | 0.76 | 0.76 |
| Deg of Saturation (%) | 68.95 | 68.95 | 68.95 |
| Strain at failure, ϵ_f (%) | 3.10 | 7.95 | 8.98 |
| Shear Strength, C_u (kPa) | 87.35 | 136.19 | 205.81 |
| Max Deviator Stress, (kPa) | 174.70 | 272.38 | 411.63 |
| Total Normal Stress ($\sigma_1 - \sigma_3$), (kPa) | 174.40 | 272.38 | 411.63 |

Test method: BS1377: Part 7: 1990

Borehole: S16100

(delete as appropriate)



TOTAL STRESS TRIAXIAL COMPRESSION

| No. | Strain (mm) | Strain, ϵ (%) | Load (N) | Deviator Stress (1-3) (kPa) |
|-----|-------------|------------------------|----------|-----------------------------|
| 1 | 0.067 | 0.067 | 193 | 98.23 |
| 2 | 0.12 | 0.12 | 200 | 101.74 |
| 3 | 0.47 | 0.47 | 257 | 130.78 |
| 4 | 0.82 | 0.82 | 295 | 150.03 |
| 5 | 1.18 | 1.18 | 316 | 161.05 |
| 6 | 1.53 | 1.53 | 329 | 167.50 |
| 7 | 1.90 | 1.90 | 336 | 170.87 |
| 8 | 2.25 | 2.25 | 340 | 173.25 |
| 9 | 2.60 | 2.60 | 342 | 174.11 |
| 10 | 2.97 | 2.97 | 343 | 174.45 |
| 11 | 3.10 | 3.10 | 343 | 174.70 |
| 12 | 3.68 | 3.68 | 337 | 171.69 |
| 13 | 4.03 | 4.03 | 335 | 170.58 |
| 14 | 4.38 | 4.38 | 334 | 169.95 |
| 15 | 4.75 | 4.75 | 331 | 168.82 |
| 16 | 5.10 | 5.10 | 330 | 168.20 |
| 17 | 5.45 | 5.45 | 328 | 167.09 |
| 18 | 5.82 | 5.82 | 328 | 166.93 |
| 19 | 6.17 | 6.17 | 327 | 166.30 |
| 20 | 6.53 | 6.53 | 324 | 165.18 |
| 21 | 6.88 | 6.88 | 323 | 164.56 |
| 22 | 7.23 | 7.23 | 322 | 163.94 |
| 23 | 7.60 | 7.60 | 321 | 163.29 |
| 24 | 7.95 | 7.95 | 318 | 162.21 |
| 25 | 8.30 | 8.30 | 318 | 162.06 |
| 26 | 8.67 | 8.67 | 317 | 161.41 |
| 27 | 9.02 | 9.02 | 317 | 161.25 |
| 28 | 9.38 | 9.38 | 316 | 161.07 |
| 29 | 9.73 | 9.73 | 315 | 160.44 |

| | | | | |
|----|-------|-------|-----|--------|
| 30 | 10.08 | 10.08 | 314 | 159.82 |
| 31 | 10.45 | 10.45 | 313 | 159.17 |
| 32 | 10.80 | 10.80 | 312 | 159.00 |
| 33 | 11.17 | 11.17 | 311 | 158.35 |
| 34 | 11.52 | 11.52 | 311 | 158.17 |
| 35 | 11.87 | 11.87 | 309 | 157.55 |
| 36 | 12.23 | 12.23 | 308 | 156.89 |
| 37 | 12.58 | 12.58 | 307 | 156.27 |
| 38 | 12.95 | 12.95 | 306 | 155.61 |
| 39 | 13.30 | 13.30 | 304 | 154.99 |
| 40 | 13.65 | 13.65 | 303 | 154.36 |
| 41 | 14.02 | 14.02 | 302 | 153.71 |
| 42 | 14.37 | 14.37 | 300 | 152.64 |
| 43 | 14.73 | 14.73 | 298 | 151.99 |
| 44 | 15.08 | 15.08 | 297 | 151.37 |
| 45 | 15.43 | 15.43 | 295 | 150.31 |
| 46 | 15.80 | 15.80 | 292 | 148.80 |
| 47 | 16.15 | 16.15 | 290 | 147.76 |
| 48 | 16.50 | 16.50 | 289 | 147.14 |
| 49 | 16.87 | 16.87 | 287 | 146.07 |
| 50 | 17.22 | 17.22 | 286 | 145.46 |
| 51 | 17.58 | 17.58 | 284 | 144.39 |
| 52 | 17.93 | 17.93 | 282 | 143.78 |
| 53 | 18.28 | 18.28 | 281 | 143.17 |
| 54 | 18.65 | 18.65 | 280 | 142.52 |
| 55 | 19.00 | 19.00 | 279 | 141.91 |
| 56 | 19.37 | 19.37 | 277 | 141.27 |
| 57 | 19.72 | 19.72 | 275 | 140.25 |
| 58 | 20.00 | 20.00 | 274 | 139.75 |

Test name: Specimen 1

Borehole: S16100

TOTAL STRESS TRIAXIAL COMPRESSION

| No. | Strain (mm) | Strain, ϵ (%) | Load (N) | Deviator Stress (1-3) (kPa) |
|-----|-------------|------------------------|----------|-----------------------------|
| 1 | 0.32 | 0.32 | 137 | 69.55 |
| 2 | 0.68 | 0.68 | 226 | 115.33 |
| 3 | 1.03 | 1.03 | 291 | 148.19 |
| 4 | 1.38 | 1.38 | 340 | 173.28 |
| 5 | 1.75 | 1.75 | 379 | 193.15 |
| 6 | 2.10 | 2.10 | 409 | 208.42 |
| 7 | 2.47 | 2.47 | 432 | 220.05 |
| 8 | 2.82 | 2.82 | 451 | 229.66 |
| 9 | 3.17 | 3.17 | 465 | 236.72 |
| 10 | 3.53 | 3.53 | 478 | 243.69 |
| 11 | 3.88 | 3.88 | 487 | 248.19 |
| 12 | 4.25 | 4.25 | 496 | 252.60 |
| 13 | 4.60 | 4.60 | 504 | 256.54 |
| 14 | 4.95 | 4.95 | 509 | 258.99 |
| 15 | 5.32 | 5.32 | 514 | 261.85 |
| 16 | 5.67 | 5.67 | 519 | 264.24 |
| 17 | 6.02 | 6.02 | 523 | 266.13 |
| 18 | 6.38 | 6.38 | 526 | 267.95 |
| 19 | 6.73 | 6.73 | 529 | 269.33 |
| 20 | 7.10 | 7.10 | 530 | 270.16 |
| 21 | 7.45 | 7.45 | 532 | 271.03 |
| 22 | 7.95 | 7.95 | 535 | 272.38 |
| 23 | 8.17 | 8.17 | 534 | 271.74 |
| 24 | 8.52 | 8.52 | 533 | 271.63 |
| 25 | 8.88 | 8.88 | 533 | 271.47 |
| 26 | 9.23 | 9.23 | 534 | 271.82 |
| 27 | 9.58 | 9.58 | 531 | 270.31 |
| 28 | 9.95 | 9.95 | 529 | 269.21 |
| 29 | 10.30 | 10.30 | 526 | 267.71 |

| | | | | |
|----|-------|-------|-----|--------|
| 30 | 10.65 | 10.65 | 524 | 266.66 |
| 31 | 11.02 | 11.02 | 520 | 264.66 |
| 32 | 11.37 | 11.37 | 517 | 263.17 |
| 33 | 11.73 | 11.73 | 513 | 261.18 |
| 34 | 12.08 | 12.08 | 509 | 259.25 |
| 35 | 12.43 | 12.43 | 506 | 257.77 |
| 36 | 12.80 | 12.80 | 502 | 255.81 |
| 37 | 13.15 | 13.15 | 499 | 253.89 |
| 38 | 13.52 | 13.52 | 494 | 251.50 |
| 39 | 13.87 | 13.87 | 490 | 249.60 |
| 40 | 14.22 | 14.22 | 486 | 247.72 |
| 41 | 14.58 | 14.58 | 483 | 246.22 |
| 42 | 14.93 | 14.93 | 481 | 244.78 |
| 43 | 15.30 | 15.30 | 477 | 242.86 |
| 44 | 15.65 | 15.65 | 474 | 241.43 |
| 45 | 16.02 | 16.02 | 470 | 239.52 |
| 46 | 16.37 | 16.37 | 468 | 238.10 |
| 47 | 16.72 | 16.72 | 466 | 237.11 |
| 48 | 17.08 | 17.08 | 462 | 235.22 |
| 49 | 17.43 | 17.43 | 458 | 233.38 |
| 50 | 17.80 | 17.80 | 454 | 231.09 |
| 51 | 18.15 | 18.15 | 452 | 230.11 |
| 52 | 18.50 | 18.50 | 447 | 227.88 |
| 53 | 18.87 | 18.87 | 442 | 225.20 |
| 54 | 19.22 | 19.22 | 439 | 223.40 |
| 55 | 19.58 | 19.58 | 433 | 220.75 |
| 56 | 19.93 | 19.93 | 431 | 219.38 |
| 57 | 20.00 | 20.00 | 431 | 219.61 |

Test name: Specimen 2

Borehole: S16100

TOTAL STRESS TRIAXIAL COMPRESSION

| No. | Strain (mm) | Strain, ϵ (%) | Load (N) | Deviator Stress (1-3) (kPa) |
|-----|-------------|------------------------|----------|-----------------------------|
| 1 | 0.32 | 0.32 | 225 | 114.74 |
| 2 | 0.67 | 0.67 | 351 | 178.58 |
| 3 | 1.03 | 1.03 | 443 | 225.81 |
| 4 | 1.38 | 1.38 | 512 | 260.67 |
| 5 | 1.73 | 1.73 | 565 | 287.77 |
| 6 | 2.10 | 2.10 | 611 | 311.13 |
| 7 | 2.45 | 2.45 | 646 | 328.89 |
| 8 | 2.82 | 2.82 | 675 | 343.99 |
| 9 | 3.18 | 3.18 | 699 | 356.01 |
| 10 | 3.53 | 3.53 | 718 | 365.53 |
| 11 | 3.88 | 3.88 | 734 | 373.99 |
| 12 | 4.25 | 4.25 | 749 | 381.34 |
| 13 | 4.60 | 4.60 | 760 | 387.24 |
| 14 | 4.95 | 4.95 | 770 | 392.11 |
| 15 | 5.32 | 5.32 | 777 | 395.90 |
| 16 | 5.67 | 5.67 | 784 | 399.24 |
| 17 | 6.03 | 6.03 | 791 | 402.96 |
| 18 | 6.38 | 6.38 | 795 | 404.79 |
| 19 | 6.73 | 6.73 | 798 | 406.60 |
| 20 | 7.10 | 7.10 | 802 | 408.32 |
| 21 | 7.45 | 7.45 | 803 | 409.13 |
| 22 | 7.82 | 7.82 | 807 | 410.80 |
| 23 | 8.17 | 8.17 | 807 | 411.11 |
| 24 | 8.52 | 8.52 | 808 | 411.41 |
| 25 | 8.98 | 8.98 | 808 | 411.63 |
| 26 | 9.23 | 9.23 | 807 | 410.96 |
| 27 | 9.60 | 9.60 | 807 | 411.14 |
| 28 | 9.95 | 9.95 | 806 | 410.47 |
| 29 | 10.30 | 10.30 | 805 | 409.78 |

| | | | | |
|----|-------|-------|-----|--------|
| 30 | 10.67 | 10.67 | 803 | 409.02 |
| 31 | 11.02 | 11.02 | 801 | 407.87 |
| 32 | 11.37 | 11.37 | 798 | 406.26 |
| 33 | 11.73 | 11.73 | 794 | 404.59 |
| 34 | 12.08 | 12.08 | 792 | 403.43 |
| 35 | 12.43 | 12.43 | 790 | 402.27 |
| 36 | 12.80 | 12.80 | 787 | 400.58 |
| 37 | 13.15 | 13.15 | 784 | 399.42 |
| 38 | 13.52 | 13.52 | 782 | 398.17 |
| 39 | 13.87 | 13.87 | 778 | 396.12 |
| 40 | 14.22 | 14.22 | 775 | 394.51 |
| 41 | 14.58 | 14.58 | 773 | 393.70 |
| 42 | 14.93 | 14.93 | 770 | 392.08 |
| 43 | 15.30 | 15.30 | 767 | 390.82 |
| 44 | 15.65 | 15.65 | 763 | 388.78 |
| 45 | 16.00 | 16.00 | 760 | 387.17 |
| 46 | 16.37 | 16.37 | 757 | 385.48 |
| 47 | 16.72 | 16.72 | 752 | 383.01 |
| 48 | 17.07 | 17.07 | 748 | 380.98 |
| 49 | 17.43 | 17.43 | 745 | 379.30 |
| 50 | 17.78 | 17.78 | 740 | 376.85 |
| 51 | 18.13 | 18.13 | 735 | 374.42 |
| 52 | 18.50 | 18.50 | 729 | 371.49 |
| 53 | 18.85 | 18.85 | 723 | 368.24 |
| 54 | 19.22 | 19.22 | 718 | 365.76 |
| 55 | 19.57 | 19.57 | 712 | 362.53 |
| 56 | 19.92 | 19.92 | 705 | 358.92 |
| 57 | 20.00 | 20.00 | 704 | 358.54 |

Test name: Specimen 3

Borehole: S16100

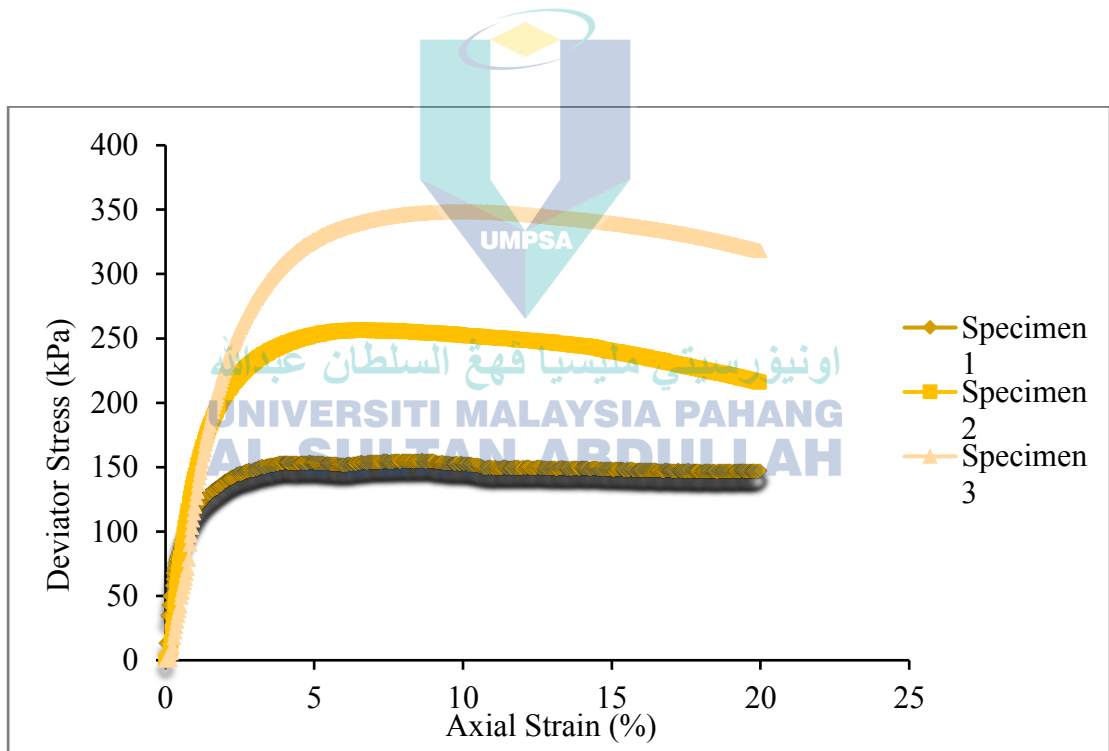
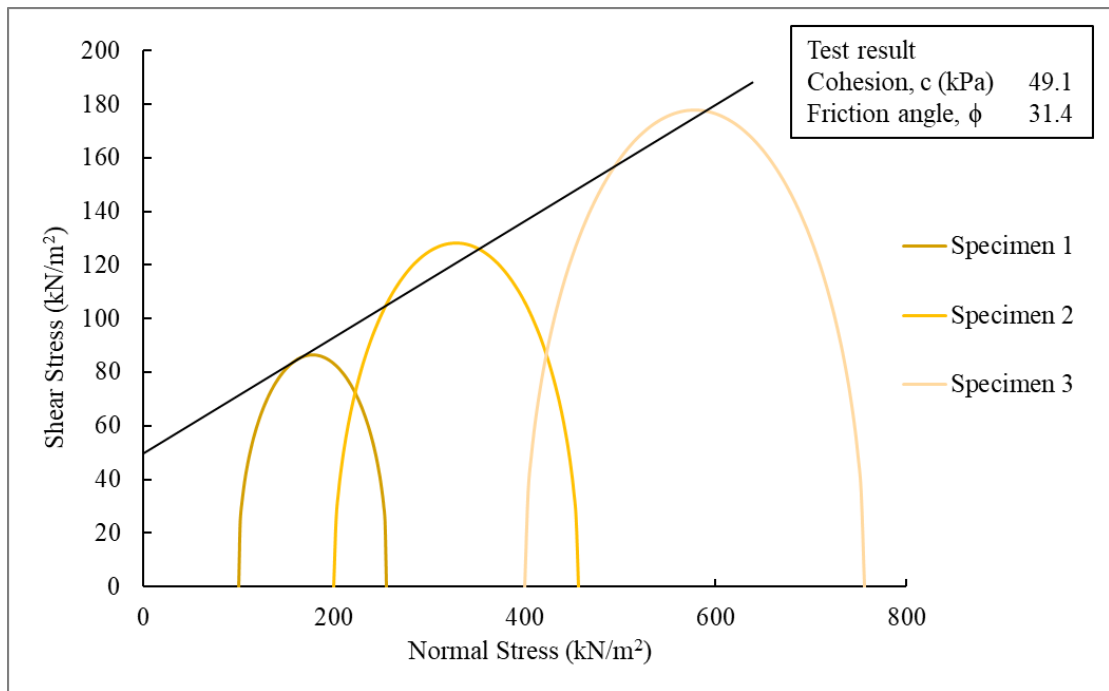
UNCONSOLIDATED UNDRAINED (UU) TRIAXIAL TEST

| | Specimen 1 | Specimen 2 | Specimen 3 |
|--|------------|------------|------------|
| Height (mm) | 100.00 | 100.00 | 100.00 |
| Diameter (mm) | 50.00 | 50.00 | 50.00 |
| Weight (g) | 350 | 350 | 350 |
| Particle Density, p_s | 2.62 | 2.62 | 2.62 |
| | | | |
| Specimen | Specimen 1 | Specimen 2 | Specimen 3 |
| Cell Pressure, σ_3 (kPa) | 100 | 200 | 400 |
| Moisture Content (%) | 20 | 20 | 20 |
| Bulk Density, (Mg/m ³) | 1.78 | 1.78 | 1.78 |
| Dry Density, (Mg/m ³) | 1.49 | 1.49 | 1.49 |
| Void Ratio | 0.76 | 0.76 | 0.76 |
| Deg of Saturation (%) | 68.95 | 68.95 | 68.95 |
| Strain at failure, ϵ_f (%) | 8.62 | 6.63 | 10.05 |
| Shear Strength, C_u (kPa) | 86.53 | 128.39 | 177.82 |
| Max Deviator Stress, (kPa) | 155.06 | 256.78 | 349.04 |
| Total Normal Stress ($\sigma_1 - \sigma_3$), (kPa) | 155.06 | 256.78 | 349.04 |

Test method: BS1377: Part 7: 1990

Borehole: G1060

(delete as appropriate)



TOTAL STRESS TRIAXIAL COMPRESSION

| No. | Strain (mm) | Strain, ϵ (%) | Load (N) | Deviator Stress (1-3) (kPa) |
|-----|-------------|------------------------|----------|-----------------------------|
| 1 | 0.32 | 0.34 | 148 | 75.16 |
| 2 | 0.68 | 0.69 | 199 | 101.11 |
| 3 | 1.03 | 1.06 | 231 | 117.90 |
| 4 | 1.40 | 1.41 | 251 | 127.89 |
| 5 | 1.75 | 1.76 | 265 | 134.85 |
| 6 | 2.10 | 2.12 | 275 | 140.25 |
| 7 | 2.47 | 2.47 | 283 | 144.16 |
| 8 | 2.82 | 2.82 | 289 | 147.31 |
| 9 | 3.17 | 3.19 | 294 | 149.67 |
| 10 | 3.53 | 3.54 | 297 | 151.31 |
| 11 | 3.88 | 3.89 | 300 | 152.94 |
| 12 | 4.25 | 4.24 | 301 | 153.11 |
| 13 | 4.60 | 4.61 | 301 | 153.24 |
| 14 | 4.95 | 4.96 | 301 | 153.39 |
| 15 | 5.32 | 5.31 | 300 | 152.83 |
| 16 | 5.67 | 5.67 | 299 | 152.24 |
| 17 | 6.02 | 6.02 | 298 | 151.67 |
| 18 | 6.38 | 6.37 | 299 | 152.52 |
| 19 | 6.73 | 6.74 | 301 | 153.33 |
| 20 | 7.10 | 7.09 | 303 | 154.15 |
| 21 | 7.45 | 7.44 | 303 | 154.27 |
| 22 | 7.80 | 7.81 | 303 | 154.36 |
| 23 | 8.17 | 8.16 | 303 | 154.46 |
| 24 | 8.62 | 8.62 | 304 | 155.06 |
| 25 | 8.87 | 8.87 | 304 | 154.63 |
| 26 | 9.23 | 9.22 | 301 | 153.35 |
| 27 | 9.58 | 9.57 | 300 | 152.76 |
| 28 | 9.93 | 9.94 | 300 | 152.82 |
| 29 | 10.30 | 10.29 | 299 | 152.23 |

| | | | | |
|----|-------|-------|-----|--------|
| 30 | 10.65 | 10.64 | 295 | 150.29 |
| 31 | 11.02 | 11.01 | 293 | 149.00 |
| 32 | 11.37 | 11.36 | 294 | 149.75 |
| 33 | 11.72 | 11.71 | 294 | 149.82 |
| 34 | 12.08 | 12.07 | 293 | 149.20 |
| 35 | 12.43 | 12.42 | 293 | 149.27 |
| 36 | 12.78 | 12.77 | 293 | 149.33 |
| 37 | 13.15 | 13.14 | 292 | 148.70 |
| 38 | 13.50 | 13.49 | 292 | 148.75 |
| 39 | 13.87 | 13.84 | 293 | 149.45 |
| 40 | 14.22 | 14.19 | 292 | 148.85 |
| 41 | 14.57 | 14.56 | 291 | 148.21 |
| 42 | 14.93 | 14.91 | 291 | 148.24 |
| 43 | 15.28 | 15.26 | 291 | 148.27 |
| 44 | 15.63 | 15.62 | 291 | 148.27 |
| 45 | 16.00 | 15.97 | 290 | 147.65 |
| 46 | 16.35 | 16.32 | 290 | 147.67 |
| 47 | 16.72 | 16.69 | 289 | 147.02 |
| 48 | 17.07 | 17.04 | 289 | 147.03 |
| 49 | 17.42 | 17.39 | 289 | 147.03 |
| 50 | 17.78 | 17.76 | 289 | 147.00 |
| 51 | 18.13 | 18.11 | 289 | 146.99 |
| 52 | 18.48 | 18.46 | 287 | 146.36 |
| 53 | 18.85 | 18.82 | 288 | 146.93 |
| 54 | 19.20 | 19.17 | 288 | 146.91 |
| 55 | 19.57 | 19.52 | 288 | 146.88 |
| 56 | 19.92 | 19.89 | 288 | 146.81 |
| 57 | 20.00 | 19.99 | 289 | 147.23 |

Test name: Specimen 1

Borehole: G1060

TOTAL STRESS TRIAXIAL COMPRESSION

| No. | Strain (mm) | Strain, ϵ (%) | Load (N) | Deviator Stress (1-3) (kPa) |
|-----|-------------|------------------------|----------|-----------------------------|
| 1 | 0.15 | 0.15 | 15 | 7.63 |
| 2 | 0.33 | 0.33 | 97 | 49.24 |
| 3 | 0.68 | 0.68 | 211 | 107.23 |
| 4 | 1.05 | 1.05 | 292 | 148.66 |
| 5 | 1.40 | 1.40 | 347 | 176.76 |
| 6 | 1.75 | 1.75 | 385 | 196.15 |
| 7 | 2.12 | 2.12 | 414 | 210.87 |
| 8 | 2.47 | 2.47 | 434 | 221.05 |
| 9 | 2.83 | 2.83 | 450 | 229.12 |
| 10 | 3.18 | 3.18 | 463 | 235.69 |
| 11 | 3.53 | 3.53 | 473 | 240.74 |
| 12 | 3.90 | 3.90 | 480 | 244.72 |
| 13 | 4.25 | 4.25 | 486 | 247.73 |
| 14 | 4.62 | 4.62 | 491 | 250.18 |
| 15 | 4.97 | 4.97 | 496 | 252.65 |
| 16 | 5.32 | 5.32 | 500 | 254.61 |
| 17 | 5.68 | 5.68 | 502 | 255.55 |
| 18 | 6.03 | 6.03 | 503 | 256.03 |
| 19 | 6.38 | 6.38 | 503 | 256.03 |
| 20 | 6.63 | 6.63 | 504 | 256.78 |
| 21 | 7.10 | 7.10 | 504 | 256.44 |
| 22 | 7.47 | 7.47 | 502 | 255.90 |
| 23 | 7.82 | 7.82 | 502 | 255.87 |
| 24 | 8.17 | 8.17 | 501 | 255.37 |
| 25 | 8.53 | 8.53 | 500 | 254.81 |
| 26 | 8.88 | 8.88 | 499 | 254.30 |
| 27 | 9.23 | 9.23 | 499 | 254.25 |
| 28 | 9.60 | 9.60 | 497 | 253.22 |
| 29 | 9.95 | 9.95 | 496 | 252.70 |

| | | | | |
|----|-------|-------|-----|--------|
| 30 | 10.32 | 10.32 | 495 | 252.13 |
| 31 | 10.67 | 10.67 | 494 | 251.60 |
| 32 | 11.02 | 11.02 | 492 | 250.61 |
| 33 | 11.38 | 11.38 | 491 | 250.03 |
| 34 | 11.73 | 11.73 | 489 | 249.05 |
| 35 | 12.10 | 12.10 | 488 | 248.46 |
| 36 | 12.45 | 12.45 | 487 | 247.91 |
| 37 | 12.80 | 12.80 | 486 | 247.37 |
| 38 | 13.17 | 13.17 | 484 | 246.33 |
| 39 | 13.52 | 13.52 | 482 | 245.33 |
| 40 | 13.88 | 13.88 | 481 | 244.73 |
| 41 | 14.23 | 14.23 | 479 | 243.74 |
| 42 | 14.58 | 14.58 | 476 | 242.31 |
| 43 | 14.95 | 14.95 | 472 | 240.40 |
| 44 | 15.30 | 15.30 | 469 | 238.98 |
| 45 | 15.67 | 15.67 | 466 | 237.52 |
| 46 | 16.02 | 16.02 | 464 | 236.10 |
| 47 | 16.37 | 16.37 | 460 | 234.27 |
| 48 | 16.73 | 16.73 | 456 | 232.39 |
| 49 | 17.08 | 17.08 | 453 | 230.57 |
| 50 | 17.45 | 17.45 | 450 | 229.13 |
| 51 | 17.80 | 17.80 | 446 | 227.32 |
| 52 | 18.15 | 18.15 | 443 | 225.52 |
| 53 | 18.52 | 18.52 | 439 | 223.68 |
| 54 | 18.87 | 18.87 | 436 | 221.89 |
| 55 | 19.22 | 19.22 | 433 | 220.52 |
| 56 | 19.58 | 19.58 | 429 | 218.30 |
| 57 | 19.93 | 19.93 | 424 | 216.12 |
| 58 | 20.00 | 19.99 | 289 | 147.23 |

Test name: Specimen 2

Borehole: G1060

TOTAL STRESS TRIAXIAL COMPRESSION

| No. | Strain (mm) | Strain, ϵ (%) | Load (N) | Deviator Stress (1-3) (kPa) |
|-----|-------------|------------------------|----------|-----------------------------|
| 1 | 0.17 | 0.17 | 1 | 0.50 |
| 2 | 0.20 | 0.20 | 11 | 5.58 |
| 3 | 0.57 | 0.57 | 103 | 52.67 |
| 4 | 0.92 | 0.92 | 214 | 108.88 |
| 5 | 1.28 | 1.28 | 313 | 159.66 |
| 6 | 1.63 | 1.63 | 387 | 197.01 |
| 7 | 1.98 | 1.98 | 442 | 225.33 |
| 8 | 2.35 | 2.35 | 488 | 248.68 |
| 9 | 2.70 | 2.70 | 524 | 266.91 |
| 10 | 3.07 | 3.07 | 553 | 281.74 |
| 11 | 3.42 | 3.42 | 577 | 293.79 |
| 12 | 3.78 | 3.78 | 597 | 303.99 |
| 13 | 4.13 | 4.13 | 613 | 312.16 |
| 14 | 4.48 | 4.48 | 626 | 318.82 |
| 15 | 4.85 | 4.85 | 637 | 324.42 |
| 16 | 5.20 | 5.20 | 647 | 329.28 |
| 17 | 5.55 | 5.55 | 654 | 333.11 |
| 18 | 5.92 | 5.92 | 660 | 335.92 |
| 19 | 6.27 | 6.27 | 665 | 338.51 |
| 20 | 6.62 | 6.62 | 670 | 341.06 |
| 21 | 6.98 | 6.98 | 673 | 342.58 |
| 22 | 7.33 | 7.33 | 676 | 344.37 |
| 23 | 7.70 | 7.70 | 678 | 345.39 |
| 24 | 8.05 | 8.05 | 680 | 346.20 |
| 25 | 8.40 | 8.40 | 682 | 347.20 |
| 26 | 8.77 | 8.77 | 683 | 347.70 |
| 27 | 9.12 | 9.12 | 683 | 348.00 |
| 28 | 9.47 | 9.47 | 685 | 348.73 |
| 29 | 9.83 | 9.83 | 685 | 348.72 |

| | | | | |
|----|-------|-------|-----|--------|
| 30 | 10.05 | 10.05 | 685 | 349.04 |
| 31 | 10.53 | 10.53 | 684 | 348.32 |
| 32 | 10.90 | 10.90 | 683 | 348.03 |
| 33 | 11.25 | 11.25 | 683 | 348.03 |
| 34 | 11.62 | 11.62 | 682 | 347.53 |
| 35 | 11.97 | 11.97 | 681 | 346.58 |
| 36 | 12.32 | 12.32 | 679 | 345.89 |
| 37 | 12.68 | 12.68 | 679 | 345.81 |
| 38 | 13.03 | 13.03 | 676 | 344.43 |
| 39 | 13.38 | 13.38 | 674 | 343.47 |
| 40 | 13.75 | 13.75 | 673 | 342.71 |
| 41 | 14.10 | 14.10 | 671 | 341.77 |
| 42 | 14.47 | 14.47 | 669 | 340.97 |
| 43 | 14.82 | 14.82 | 668 | 340.02 |
| 44 | 15.17 | 15.17 | 665 | 338.85 |
| 45 | 15.53 | 15.53 | 664 | 338.25 |
| 46 | 15.88 | 15.88 | 662 | 337.07 |
| 47 | 16.23 | 16.23 | 659 | 335.65 |
| 48 | 16.60 | 16.60 | 656 | 334.22 |
| 49 | 16.95 | 16.95 | 654 | 333.01 |
| 50 | 17.32 | 17.32 | 651 | 331.57 |
| 51 | 17.67 | 17.67 | 649 | 330.39 |
| 52 | 18.02 | 18.02 | 645 | 328.54 |
| 53 | 18.38 | 18.38 | 641 | 326.69 |
| 54 | 18.73 | 18.73 | 638 | 324.89 |
| 55 | 19.08 | 19.08 | 635 | 323.26 |
| 56 | 19.45 | 19.45 | 631 | 321.22 |
| 57 | 19.80 | 19.80 | 626 | 319.01 |
| 58 | 20.00 | 19.99 | 289 | 147.23 |

Test name: Specimen 3

Borehole: G1060

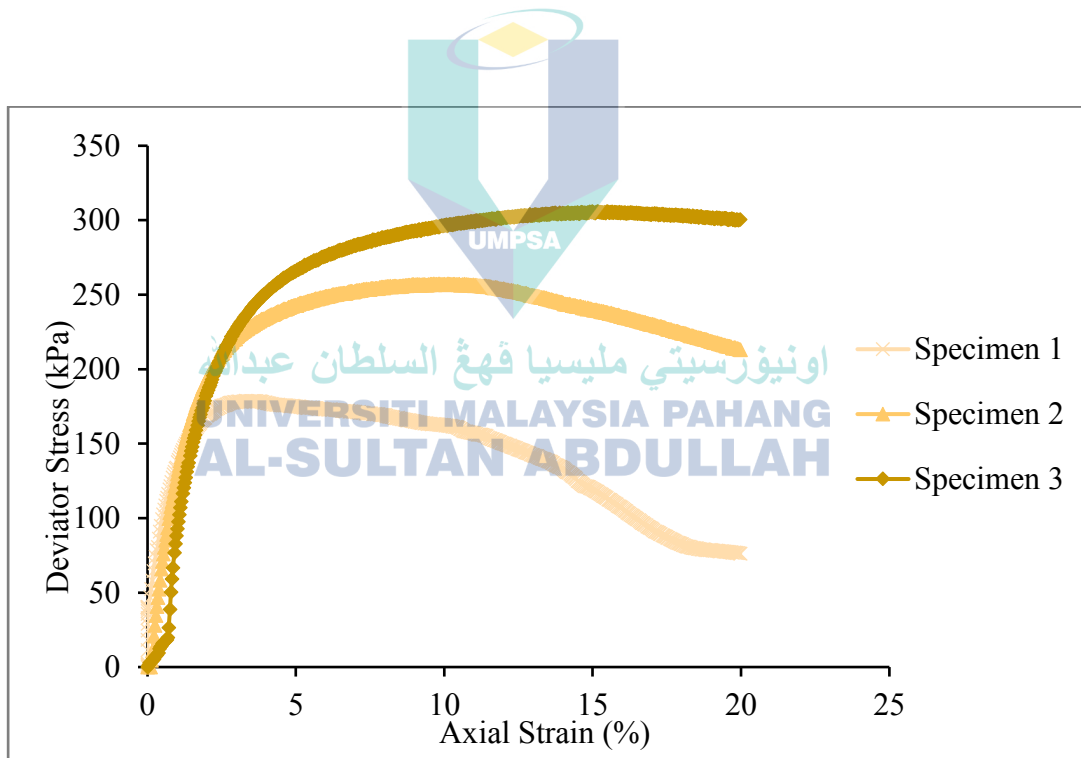
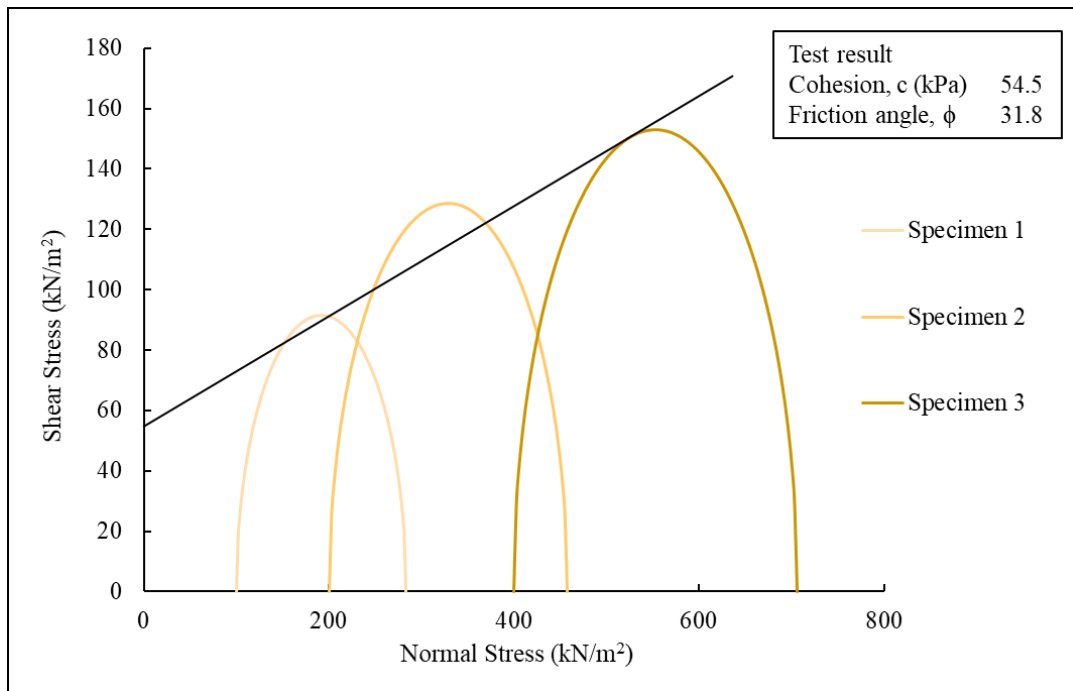
UNCONSOLIDATED UNDRAINED (UU) TRIAXIAL TEST

| | Specimen 1 | Specimen 2 | Specimen 3 |
|--|------------|------------|------------|
| Height (mm) | 100.00 | 100.00 | 100.00 |
| Diameter (mm) | 50.00 | 50.00 | 50.00 |
| Weight (g) | 350 | 350 | 350 |
| Particle Density, p_s | 2.62 | 2.62 | 2.62 |
| | | | |
| Specimen | Specimen 1 | Specimen 2 | Specimen 3 |
| Cell Pressure, σ_3 (kPa) | 100 | 200 | 400 |
| Moisture Content (%) | 20 | 20 | 20 |
| Bulk Density, (Mg/m ³) | 1.78 | 1.78 | 1.78 |
| Dry Density, (Mg/m ³) | 1.49 | 1.49 | 1.49 |
| Void Ratio | 0.76 | 0.76 | 0.76 |
| Deg of Saturation (%) | 68.95 | 68.95 | 68.95 |
| Strain at failure, ϵ_f (%) | 3.30 | 10.12 | 14.99 |
| Shear Strength, C_u (kPa) | 91.65 | 128.63 | 152.93 |
| Max Deviator Stress, (kPa) | 178.77 | 257.27 | 305.86 |
| Total Normal Stress ($\sigma_1 - \sigma_3$), (kPa) | 178.77 | 257.27 | 305.86 |

Test method: BS1377: Part 7: 1990

Borehole: G1080

(delete as appropriate)



TOTAL STRESS TRIAXIAL COMPRESSION

| No. | Strain (mm) | Strain, ϵ (%) | Load (N) | Deviator Stress (1-3) (kPa) |
|-----|-------------|------------------------|----------|-----------------------------|
| 1 | 0.09 | 0.09 | 92 | 46.82 |
| 2 | 0.16 | 0.16 | 114 | 57.97 |
| 3 | 0.52 | 0.52 | 201 | 102.60 |
| 4 | 0.88 | 0.88 | 254 | 129.49 |
| 5 | 1.23 | 1.23 | 289 | 147.38 |
| 6 | 1.59 | 1.59 | 313 | 159.38 |
| 7 | 1.94 | 1.94 | 329 | 167.55 |
| 8 | 2.30 | 2.30 | 340 | 173.41 |
| 9 | 2.66 | 2.66 | 346 | 176.24 |
| 10 | 3.02 | 3.02 | 350 | 178.31 |
| 11 | 3.30 | 3.30 | 351 | 178.77 |
| 12 | 3.73 | 3.73 | 350 | 178.23 |
| 13 | 4.08 | 4.08 | 348 | 177.08 |
| 14 | 4.44 | 4.44 | 345 | 175.93 |
| 15 | 4.80 | 4.80 | 344 | 175.27 |
| 16 | 5.15 | 5.15 | 343 | 174.62 |
| 17 | 5.51 | 5.51 | 342 | 173.97 |
| 18 | 5.87 | 5.87 | 341 | 173.54 |
| 19 | 6.22 | 6.22 | 339 | 172.66 |
| 20 | 6.58 | 6.58 | 338 | 171.98 |
| 21 | 6.93 | 6.93 | 337 | 171.58 |
| 22 | 7.28 | 7.28 | 335 | 170.70 |
| 23 | 7.65 | 7.65 | 333 | 169.78 |
| 24 | 8.00 | 8.00 | 332 | 169.14 |
| 25 | 8.37 | 8.37 | 328 | 167.30 |
| 26 | 8.72 | 8.72 | 326 | 165.96 |
| 27 | 9.08 | 9.08 | 323 | 164.61 |
| 28 | 9.43 | 9.43 | 321 | 163.28 |
| 29 | 9.78 | 9.78 | 320 | 162.87 |

| | | | | |
|----|-------|-------|-----|--------|
| 30 | 10.14 | 10.14 | 318 | 161.99 |
| 31 | 10.49 | 10.49 | 315 | 160.68 |
| 32 | 10.86 | 10.86 | 309 | 157.53 |
| 33 | 11.21 | 11.21 | 306 | 156.00 |
| 34 | 11.60 | 11.60 | 301 | 153.08 |
| 35 | 11.96 | 11.96 | 295 | 150.21 |
| 36 | 12.31 | 12.31 | 290 | 147.61 |
| 37 | 12.67 | 12.67 | 285 | 145.01 |
| 38 | 13.03 | 13.03 | 279 | 141.97 |
| 39 | 13.38 | 13.38 | 274 | 139.42 |
| 40 | 13.74 | 13.74 | 267 | 135.75 |
| 41 | 14.09 | 14.09 | 258 | 131.48 |
| 42 | 14.44 | 14.44 | 248 | 126.15 |
| 43 | 14.81 | 14.81 | 238 | 121.27 |
| 44 | 15.16 | 15.16 | 231 | 117.75 |
| 45 | 15.53 | 15.53 | 221 | 112.72 |
| 46 | 15.88 | 15.88 | 212 | 107.97 |
| 47 | 16.22 | 16.22 | 202 | 103.04 |
| 48 | 16.59 | 16.59 | 193 | 98.13 |
| 49 | 16.94 | 16.94 | 183 | 93.28 |
| 50 | 17.29 | 17.29 | 175 | 89.30 |
| 51 | 17.66 | 17.66 | 168 | 85.55 |
| 52 | 18.01 | 18.01 | 162 | 82.48 |
| 53 | 18.38 | 18.38 | 157 | 80.03 |
| 54 | 18.73 | 18.73 | 155 | 79.06 |
| 55 | 19.08 | 19.08 | 154 | 78.31 |
| 56 | 19.44 | 19.44 | 152 | 77.55 |
| 57 | 19.79 | 19.79 | 151 | 76.80 |
| 58 | 19.98 | 19.98 | 150 | 76.22 |

Test name: Specimen 1

Borehole: G1080

TOTAL STRESS TRIAXIAL COMPRESSION

| No. | Strain (mm) | Strain, ϵ (%) | Load (N) | Deviator Stress (1-3) (kPa) |
|-----|-------------|------------------------|----------|-----------------------------|
| 1 | 0.13 | 0.13 | 9 | 4.58 |
| 2 | 0.32 | 0.32 | 80 | 40.61 |
| 3 | 0.67 | 0.67 | 184 | 93.59 |
| 4 | 1.03 | 1.03 | 260 | 132.56 |
| 5 | 1.38 | 1.38 | 314 | 159.72 |
| 6 | 1.75 | 1.75 | 357 | 181.64 |
| 7 | 2.10 | 2.10 | 388 | 197.45 |
| 8 | 2.47 | 2.47 | 412 | 209.62 |
| 9 | 2.82 | 2.82 | 428 | 217.78 |
| 10 | 3.17 | 3.17 | 441 | 224.39 |
| 11 | 3.53 | 3.53 | 451 | 229.44 |
| 12 | 3.88 | 3.88 | 458 | 233.50 |
| 13 | 4.25 | 4.25 | 465 | 237.00 |
| 14 | 4.60 | 4.60 | 472 | 240.50 |
| 15 | 4.97 | 4.97 | 477 | 242.97 |
| 16 | 5.32 | 5.32 | 481 | 244.97 |
| 17 | 5.67 | 5.67 | 486 | 247.42 |
| 18 | 6.03 | 6.03 | 489 | 248.86 |
| 19 | 6.38 | 6.38 | 491 | 250.31 |
| 20 | 6.75 | 6.75 | 494 | 251.71 |
| 21 | 7.10 | 7.10 | 496 | 252.65 |
| 22 | 7.47 | 7.47 | 498 | 253.54 |
| 23 | 7.82 | 7.82 | 501 | 254.93 |
| 24 | 8.18 | 8.18 | 502 | 255.79 |
| 25 | 8.53 | 8.53 | 502 | 255.74 |
| 26 | 8.90 | 8.90 | 504 | 256.57 |
| 27 | 9.25 | 9.25 | 504 | 256.51 |
| 28 | 9.60 | 9.60 | 504 | 256.91 |
| 29 | 9.97 | 9.97 | 504 | 256.78 |

| | | | | |
|----|-------|-------|-----|--------|
| 30 | 10.12 | 10.12 | 505 | 257.27 |
| 31 | 10.68 | 10.68 | 505 | 257.01 |
| 32 | 11.03 | 11.03 | 504 | 256.46 |
| 33 | 11.40 | 11.40 | 502 | 255.85 |
| 34 | 11.75 | 11.75 | 500 | 254.84 |
| 35 | 12.12 | 12.12 | 497 | 253.33 |
| 36 | 12.47 | 12.47 | 495 | 252.32 |
| 37 | 12.82 | 12.82 | 492 | 250.43 |
| 38 | 13.18 | 13.18 | 489 | 248.93 |
| 39 | 13.53 | 13.53 | 485 | 247.05 |
| 40 | 13.90 | 13.90 | 481 | 245.12 |
| 41 | 14.25 | 14.25 | 478 | 243.25 |
| 42 | 14.62 | 14.62 | 475 | 241.78 |
| 43 | 14.97 | 14.97 | 472 | 240.35 |
| 44 | 15.33 | 15.33 | 468 | 238.46 |
| 45 | 15.68 | 15.68 | 465 | 237.04 |
| 46 | 16.05 | 16.05 | 461 | 234.73 |
| 47 | 16.40 | 16.40 | 458 | 233.32 |
| 48 | 16.77 | 16.77 | 454 | 231.45 |
| 49 | 17.12 | 17.12 | 450 | 229.21 |
| 50 | 17.47 | 17.47 | 447 | 227.40 |
| 51 | 17.83 | 17.83 | 443 | 225.56 |
| 52 | 18.18 | 18.18 | 439 | 223.35 |
| 53 | 18.55 | 18.55 | 434 | 221.10 |
| 54 | 18.90 | 18.90 | 431 | 219.32 |
| 55 | 19.27 | 19.27 | 426 | 217.10 |
| 56 | 19.62 | 19.62 | 423 | 215.34 |
| 57 | 19.98 | 19.98 | 418 | 213.13 |

Test name: Specimen 2

Borehole: G1080

TOTAL STRESS TRIAXIAL COMPRESSION

| No. | Strain (mm) | Strain, ϵ (%) | Load (N) | Deviator Stress (1-3) (kPa) |
|-----|-------------|------------------------|----------|-----------------------------|
| 1 | 0.13 | 0.07 | 5 | 2.74 |
| 2 | 0.35 | 0.29 | 15 | 7.52 |
| 3 | 0.72 | 0.65 | 36 | 18.38 |
| 4 | 1.07 | 1.00 | 182 | 92.94 |
| 5 | 1.42 | 1.35 | 264 | 134.53 |
| 6 | 1.78 | 1.72 | 324 | 165.01 |
| 7 | 2.13 | 2.07 | 369 | 187.91 |
| 8 | 2.48 | 2.42 | 403 | 205.29 |
| 9 | 2.85 | 2.79 | 432 | 219.84 |
| 10 | 3.20 | 3.14 | 455 | 231.66 |
| 11 | 3.57 | 3.50 | 474 | 241.36 |
| 12 | 3.92 | 3.85 | 489 | 249.05 |
| 13 | 4.28 | 4.22 | 501 | 255.33 |
| 14 | 4.63 | 4.57 | 512 | 260.93 |
| 15 | 4.98 | 4.92 | 521 | 265.19 |
| 16 | 5.35 | 5.29 | 530 | 270.01 |
| 17 | 5.70 | 5.64 | 536 | 272.89 |
| 18 | 6.05 | 5.99 | 541 | 275.74 |
| 19 | 6.40 | 6.34 | 547 | 278.57 |
| 20 | 6.77 | 6.70 | 552 | 281.31 |
| 21 | 7.12 | 7.05 | 557 | 283.44 |
| 22 | 7.47 | 7.40 | 561 | 285.55 |
| 23 | 7.83 | 7.77 | 565 | 287.58 |
| 24 | 8.18 | 8.12 | 567 | 289.01 |
| 25 | 8.53 | 8.47 | 570 | 290.41 |
| 26 | 8.90 | 8.84 | 574 | 292.37 |
| 27 | 9.25 | 9.19 | 576 | 293.12 |
| 28 | 9.60 | 9.54 | 578 | 294.47 |
| 29 | 9.97 | 9.90 | 582 | 296.36 |

| | | | | |
|----|-------|-------|-----|--------|
| 30 | 10.32 | 10.25 | 583 | 297.05 |
| 31 | 10.67 | 10.60 | 586 | 298.35 |
| 32 | 11.02 | 10.95 | 587 | 299.01 |
| 33 | 11.38 | 11.32 | 589 | 300.21 |
| 34 | 11.73 | 11.67 | 591 | 300.84 |
| 35 | 12.10 | 12.04 | 593 | 302.00 |
| 36 | 12.45 | 12.39 | 594 | 302.60 |
| 37 | 12.80 | 12.74 | 595 | 303.19 |
| 38 | 13.17 | 13.10 | 596 | 303.70 |
| 39 | 13.52 | 13.45 | 596 | 303.66 |
| 40 | 13.87 | 13.80 | 597 | 304.21 |
| 41 | 14.23 | 14.17 | 599 | 305.27 |
| 42 | 14.58 | 14.52 | 598 | 304.61 |
| 43 | 15.05 | 14.99 | 601 | 305.86 |
| 44 | 15.30 | 15.24 | 600 | 305.54 |
| 45 | 15.65 | 15.59 | 600 | 305.43 |
| 46 | 16.00 | 15.94 | 598 | 304.74 |
| 47 | 16.37 | 16.30 | 599 | 305.13 |
| 48 | 16.72 | 16.65 | 598 | 304.43 |
| 49 | 17.07 | 17.00 | 597 | 304.29 |
| 50 | 17.43 | 17.37 | 597 | 304.08 |
| 51 | 17.78 | 17.72 | 596 | 303.35 |
| 52 | 18.13 | 18.07 | 595 | 303.19 |
| 53 | 18.50 | 18.44 | 594 | 302.39 |
| 54 | 18.85 | 18.79 | 592 | 301.65 |
| 55 | 19.20 | 19.14 | 592 | 301.45 |
| 56 | 19.57 | 19.50 | 591 | 301.19 |
| 57 | 19.92 | 19.85 | 590 | 300.43 |
| 58 | 20.03 | 19.97 | 590 | 300.54 |

Test name: Specimen 3

Borehole: G1080

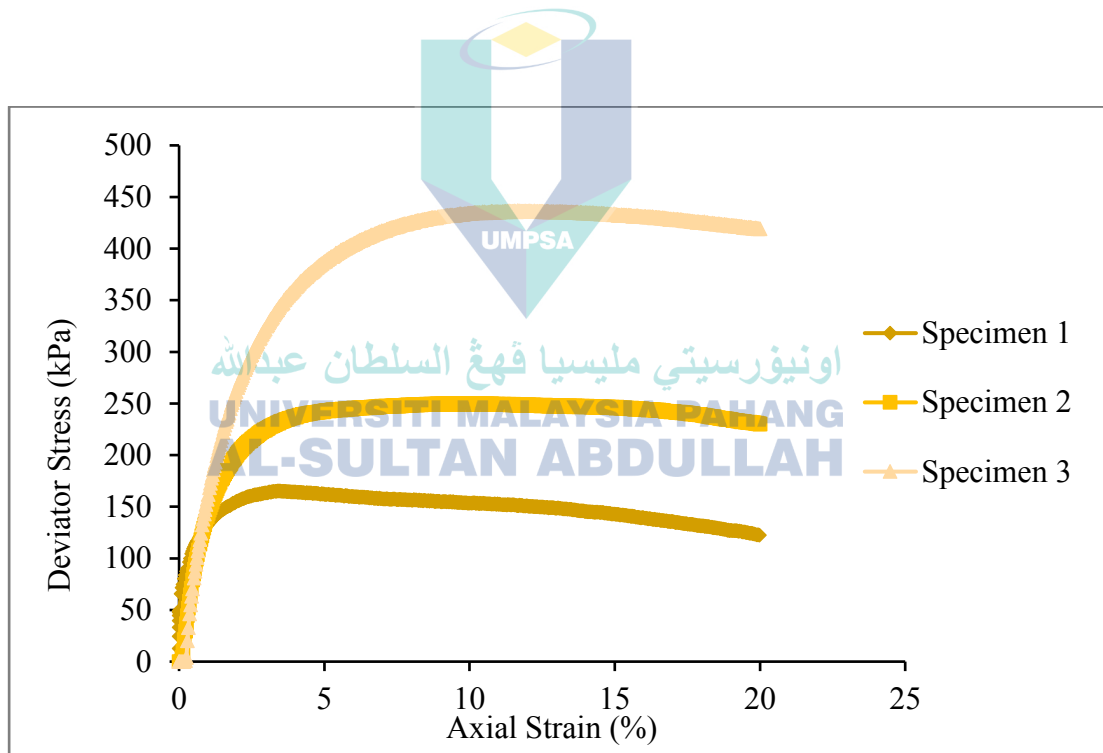
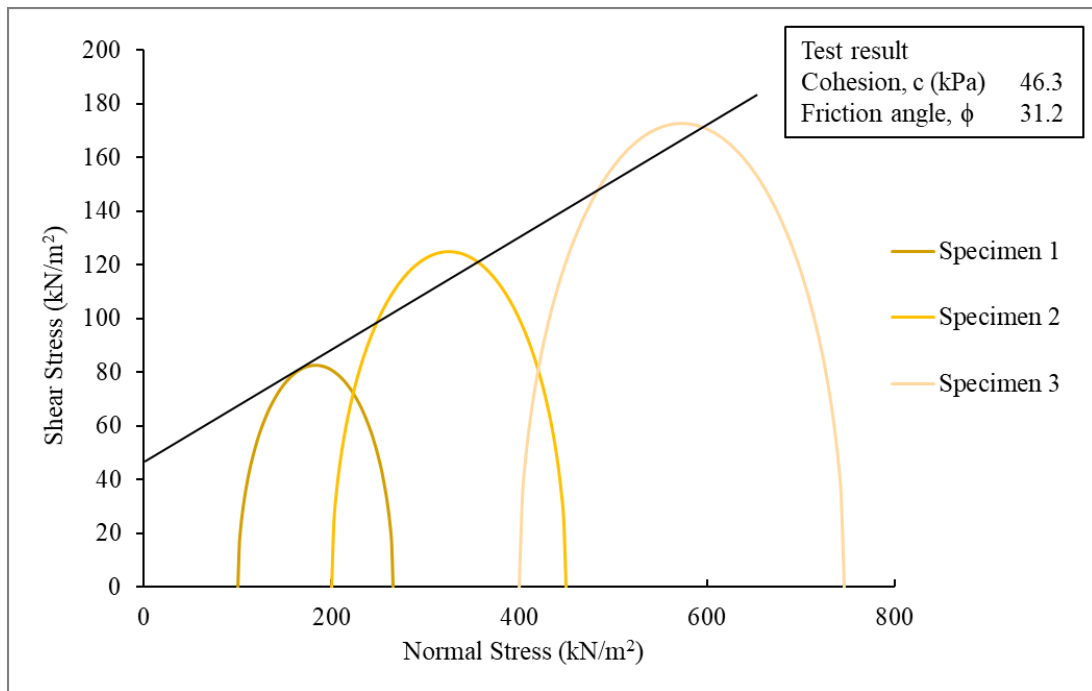
UNCONSOLIDATED UNDRAINED (UU) TRIAXIAL TEST

| | Specimen 1 | Specimen 2 | Specimen 3 |
|--|------------|------------|------------|
| Height (mm) | 100.00 | 100.00 | 100.00 |
| Diameter (mm) | 50.00 | 50.00 | 50.00 |
| Weight (g) | 350 | 350 | 350 |
| Particle Density, p_s | 2.62 | 2.62 | 2.62 |
| Specimen | Specimen 1 | Specimen 2 | Specimen 3 |
| Cell Pressure, σ_3 (kPa) | 100 | 200 | 400 |
| Moisture Content (%) | 20 | 20 | 20 |
| Bulk Density, (Mg/m ³) | 1.78 | 1.78 | 1.78 |
| Dry Density, (Mg/m ³) | 1.49 | 1.49 | 1.49 |
| Void Ratio | 0.76 | 0.76 | 0.76 |
| Deg of Saturation (%) | 68.95 | 68.95 | 68.95 |
| Strain at failure, ϵ_f (%) | 3.38 | 9.42 | 11.67 |
| Shear Strength, C_u (kPa) | 82.67 | 124.98 | 172.85 |
| Max Deviator Stress, (kPa) | 165.33 | 249.95 | 436.83 |
| Total Normal Stress ($\sigma_1 - \sigma_3$), (kPa) | 165.33 | 249.95 | 436.83 |

Test method: BS1377: Part 7: 1990

Borehole: G10100

(delete as appropriate)



TOTAL STRESS TRIAXIAL COMPRESSION

| No. | Strain (mm) | Strain, ϵ (%) | Load (N) | Deviator Stress (1-3) (kPa) |
|-----|-------------|------------------------|----------|-----------------------------|
| 1 | 0.13 | 0.13 | 147 | 74.77 |
| 2 | 0.50 | 0.50 | 215 | 109.46 |
| 3 | 0.85 | 0.85 | 251 | 127.76 |
| 4 | 1.22 | 1.22 | 275 | 139.86 |
| 5 | 1.57 | 1.57 | 291 | 148.39 |
| 6 | 1.92 | 1.92 | 302 | 153.86 |
| 7 | 2.28 | 2.28 | 312 | 158.76 |
| 8 | 2.63 | 2.63 | 317 | 161.66 |
| 9 | 2.98 | 2.98 | 321 | 163.55 |
| 10 | 3.38 | 3.38 | 325 | 165.33 |
| 11 | 3.70 | 3.70 | 324 | 164.79 |
| 12 | 4.07 | 4.07 | 322 | 164.16 |
| 13 | 4.42 | 4.42 | 321 | 163.56 |
| 14 | 4.77 | 4.77 | 320 | 162.97 |
| 15 | 5.13 | 5.13 | 319 | 162.34 |
| 16 | 5.48 | 5.48 | 317 | 161.26 |
| 17 | 5.83 | 5.83 | 315 | 160.18 |
| 18 | 6.20 | 6.20 | 312 | 159.08 |
| 19 | 6.55 | 6.55 | 311 | 158.49 |
| 20 | 6.90 | 6.90 | 311 | 158.37 |
| 21 | 7.27 | 7.27 | 309 | 157.27 |
| 22 | 7.62 | 7.62 | 309 | 157.15 |
| 23 | 7.98 | 7.98 | 307 | 156.53 |
| 24 | 8.33 | 8.33 | 307 | 156.40 |
| 25 | 8.68 | 8.68 | 306 | 155.80 |
| 26 | 9.05 | 9.05 | 304 | 154.71 |
| 27 | 9.40 | 9.40 | 304 | 154.58 |
| 28 | 9.75 | 9.75 | 302 | 153.98 |
| 29 | 10.12 | 10.12 | 302 | 153.81 |

| | | | | |
|----|-------|-------|-----|--------|
| 30 | 10.47 | 10.47 | 302 | 153.67 |
| 31 | 10.83 | 10.83 | 300 | 152.59 |
| 32 | 11.18 | 11.18 | 298 | 151.99 |
| 33 | 11.53 | 11.53 | 298 | 151.84 |
| 34 | 11.90 | 11.90 | 296 | 150.76 |
| 35 | 12.25 | 12.25 | 295 | 150.16 |
| 36 | 12.60 | 12.60 | 294 | 149.56 |
| 37 | 12.97 | 12.97 | 292 | 148.49 |
| 38 | 13.32 | 13.32 | 290 | 147.89 |
| 39 | 13.68 | 13.68 | 288 | 146.83 |
| 40 | 14.03 | 14.03 | 285 | 145.36 |
| 41 | 14.38 | 14.38 | 284 | 144.77 |
| 42 | 14.75 | 14.75 | 282 | 143.71 |
| 43 | 15.10 | 15.10 | 280 | 142.69 |
| 44 | 15.45 | 15.45 | 277 | 141.24 |
| 45 | 15.82 | 15.82 | 274 | 139.77 |
| 46 | 16.17 | 16.17 | 272 | 138.33 |
| 47 | 16.53 | 16.53 | 270 | 137.31 |
| 48 | 16.88 | 16.88 | 267 | 135.88 |
| 49 | 17.23 | 17.23 | 264 | 134.47 |
| 50 | 17.60 | 17.60 | 261 | 133.03 |
| 51 | 17.95 | 17.95 | 258 | 131.63 |
| 52 | 18.32 | 18.32 | 256 | 130.21 |
| 53 | 18.67 | 18.67 | 253 | 128.82 |
| 54 | 19.02 | 19.02 | 249 | 127.03 |
| 55 | 19.38 | 19.38 | 247 | 125.64 |
| 56 | 19.73 | 19.73 | 244 | 124.27 |
| 57 | 19.98 | 19.98 | 241 | 122.66 |

Test name: Specimen 1

Borehole: G10100

TOTAL STRESS TRIAXIAL COMPRESSION

| No. | Strain (mm) | Strain, ϵ (%) | Load (N) | Deviator Stress (1-3) (kPa) |
|-----|-------------|------------------------|----------|-----------------------------|
| 1 | 0.32 | 0.32 | 102 | 58.36 |
| 2 | 0.67 | 0.67 | 213 | 113.77 |
| 3 | 1.03 | 1.03 | 288 | 149.14 |
| 4 | 1.38 | 1.38 | 337 | 173.72 |
| 5 | 1.75 | 1.75 | 374 | 192.08 |
| 6 | 2.10 | 2.10 | 400 | 205.35 |
| 7 | 2.47 | 2.47 | 420 | 215.51 |
| 8 | 2.82 | 2.82 | 436 | 222.65 |
| 9 | 3.18 | 3.18 | 448 | 228.71 |
| 10 | 3.53 | 3.53 | 457 | 232.80 |
| 11 | 3.90 | 3.90 | 464 | 236.80 |
| 12 | 4.25 | 4.25 | 470 | 239.35 |
| 13 | 4.62 | 4.62 | 473 | 241.35 |
| 14 | 4.97 | 4.97 | 475 | 242.88 |
| 15 | 5.32 | 5.32 | 479 | 243.43 |
| 16 | 5.68 | 5.68 | 480 | 244.89 |
| 17 | 6.03 | 6.03 | 482 | 245.42 |
| 18 | 6.38 | 6.38 | 483 | 245.89 |
| 19 | 6.75 | 6.75 | 484 | 246.87 |
| 20 | 7.10 | 7.10 | 486 | 247.36 |
| 21 | 7.45 | 7.45 | 487 | 247.80 |
| 22 | 7.82 | 7.82 | 488 | 248.27 |
| 23 | 8.17 | 8.17 | 489 | 248.73 |
| 24 | 8.53 | 8.53 | 489 | 249.13 |
| 25 | 8.88 | 8.88 | 490 | 249.57 |
| 26 | 9.42 | 9.42 | 490 | 249.95 |
| 27 | 9.60 | 9.60 | 490 | 249.91 |
| 28 | 9.95 | 9.95 | 491 | 249.40 |
| 29 | 10.32 | 10.32 | 491 | 249.29 |

| | | | | |
|----|-------|-------|-----|--------|
| 30 | 10.67 | 10.67 | 490 | 249.23 |
| 31 | 11.02 | 11.02 | 489 | 249.16 |
| 32 | 11.38 | 11.38 | 488 | 249.04 |
| 33 | 11.73 | 11.73 | 488 | 248.50 |
| 34 | 12.08 | 12.08 | 488 | 248.36 |
| 35 | 12.45 | 12.45 | 487 | 247.82 |
| 36 | 12.80 | 12.80 | 487 | 247.72 |
| 37 | 13.17 | 13.17 | 485 | 248.00 |
| 38 | 13.52 | 13.52 | 485 | 247.44 |
| 39 | 13.88 | 13.88 | 486 | 247.27 |
| 40 | 14.23 | 14.23 | 485 | 246.70 |
| 41 | 14.58 | 14.58 | 484 | 246.56 |
| 42 | 14.95 | 14.95 | 483 | 246.37 |
| 43 | 15.30 | 15.30 | 482 | 245.79 |
| 44 | 15.67 | 15.67 | 481 | 244.72 |
| 45 | 16.02 | 16.02 | 480 | 244.13 |
| 46 | 16.37 | 16.37 | 478 | 243.54 |
| 47 | 16.73 | 16.73 | 476 | 242.47 |
| 48 | 17.08 | 17.08 | 474 | 241.45 |
| 49 | 17.43 | 17.43 | 473 | 240.85 |
| 50 | 17.80 | 17.80 | 470 | 239.37 |
| 51 | 18.15 | 18.15 | 467 | 237.93 |
| 52 | 18.50 | 18.50 | 464 | 236.45 |
| 53 | 18.87 | 18.87 | 462 | 234.61 |
| 54 | 19.22 | 19.22 | 458 | 233.18 |
| 55 | 19.58 | 19.58 | 455 | 231.71 |
| 56 | 19.93 | 19.93 | 452 | 230.30 |
| 57 | 19.97 | 19.97 | 452 | 230.20 |

Test name: Specimen 2

Borehole: G10100

TOTAL STRESS TRIAXIAL COMPRESSION

| No. | Strain (mm) | Strain, ϵ (%) | Load (N) | Deviator Stress (1-3) (kPa) |
|-----|-------------|------------------------|----------|-----------------------------|
| 1 | 0.32 | -0.29 | 65 | 33.00 |
| 2 | 0.68 | 0.06 | 221 | 112.80 |
| 3 | 1.05 | 0.43 | 330 | 168.32 |
| 4 | 1.40 | 0.78 | 413 | 210.41 |
| 5 | 1.77 | 1.13 | 481 | 245.15 |
| 6 | 2.12 | 1.50 | 536 | 273.19 |
| 7 | 2.47 | 1.85 | 581 | 296.06 |
| 8 | 2.83 | 2.20 | 621 | 316.22 |
| 9 | 3.18 | 2.56 | 653 | 332.34 |
| 10 | 3.55 | 2.91 | 681 | 346.80 |
| 11 | 3.90 | 3.26 | 704 | 358.75 |
| 12 | 4.27 | 3.63 | 726 | 369.58 |
| 13 | 4.62 | 3.98 | 743 | 378.42 |
| 14 | 4.98 | 4.33 | 760 | 387.13 |
| 15 | 5.33 | 4.68 | 772 | 393.42 |
| 16 | 5.68 | 5.05 | 785 | 399.65 |
| 17 | 6.05 | 5.40 | 796 | 405.28 |
| 18 | 6.40 | 5.76 | 806 | 410.44 |
| 19 | 6.77 | 6.11 | 814 | 414.53 |
| 20 | 7.12 | 6.46 | 820 | 417.71 |
| 21 | 7.48 | 6.83 | 827 | 421.24 |
| 22 | 7.83 | 7.18 | 832 | 423.87 |
| 23 | 8.20 | 7.53 | 839 | 427.33 |
| 24 | 8.55 | 7.90 | 842 | 428.96 |
| 25 | 8.92 | 8.25 | 846 | 430.95 |
| 26 | 9.27 | 8.60 | 848 | 432.06 |
| 27 | 9.62 | 8.96 | 851 | 433.16 |
| 28 | 9.98 | 9.31 | 852 | 434.15 |
| 29 | 10.33 | 9.66 | 855 | 435.21 |

| | | | | |
|----|-------|-------|-----|--------|
| 30 | 10.70 | 10.03 | 855 | 435.24 |
| 31 | 11.05 | 10.38 | 856 | 435.80 |
| 32 | 11.42 | 10.75 | 857 | 436.26 |
| 33 | 11.67 | 11.00 | 858 | 436.83 |
| 34 | 12.12 | 11.45 | 856 | 435.95 |
| 35 | 12.48 | 11.81 | 857 | 436.36 |
| 36 | 12.83 | 12.16 | 856 | 435.95 |
| 37 | 13.20 | 12.51 | 856 | 435.88 |
| 38 | 13.55 | 12.88 | 855 | 435.44 |
| 39 | 13.90 | 13.23 | 853 | 434.56 |
| 40 | 14.27 | 13.60 | 854 | 434.89 |
| 41 | 14.62 | 13.95 | 852 | 433.98 |
| 42 | 14.98 | 14.30 | 852 | 433.85 |
| 43 | 15.33 | 14.65 | 849 | 432.50 |
| 44 | 15.68 | 15.01 | 847 | 431.57 |
| 45 | 16.05 | 15.36 | 847 | 431.40 |
| 46 | 16.40 | 15.73 | 845 | 430.45 |
| 47 | 16.77 | 16.08 | 843 | 429.41 |
| 48 | 17.12 | 16.43 | 840 | 428.03 |
| 49 | 17.47 | 16.80 | 839 | 427.06 |
| 50 | 17.83 | 17.15 | 836 | 425.59 |
| 51 | 18.18 | 17.50 | 835 | 425.44 |
| 52 | 18.53 | 17.86 | 833 | 424.04 |
| 53 | 18.90 | 18.21 | 830 | 422.54 |
| 54 | 19.25 | 18.56 | 828 | 421.54 |
| 55 | 19.62 | 18.93 | 826 | 420.85 |
| 56 | 19.97 | 19.28 | 824 | 419.43 |
| 57 | 20.00 | 19.31 | 823 | 419.25 |

Test name: Specimen 3

Borehole: G10100

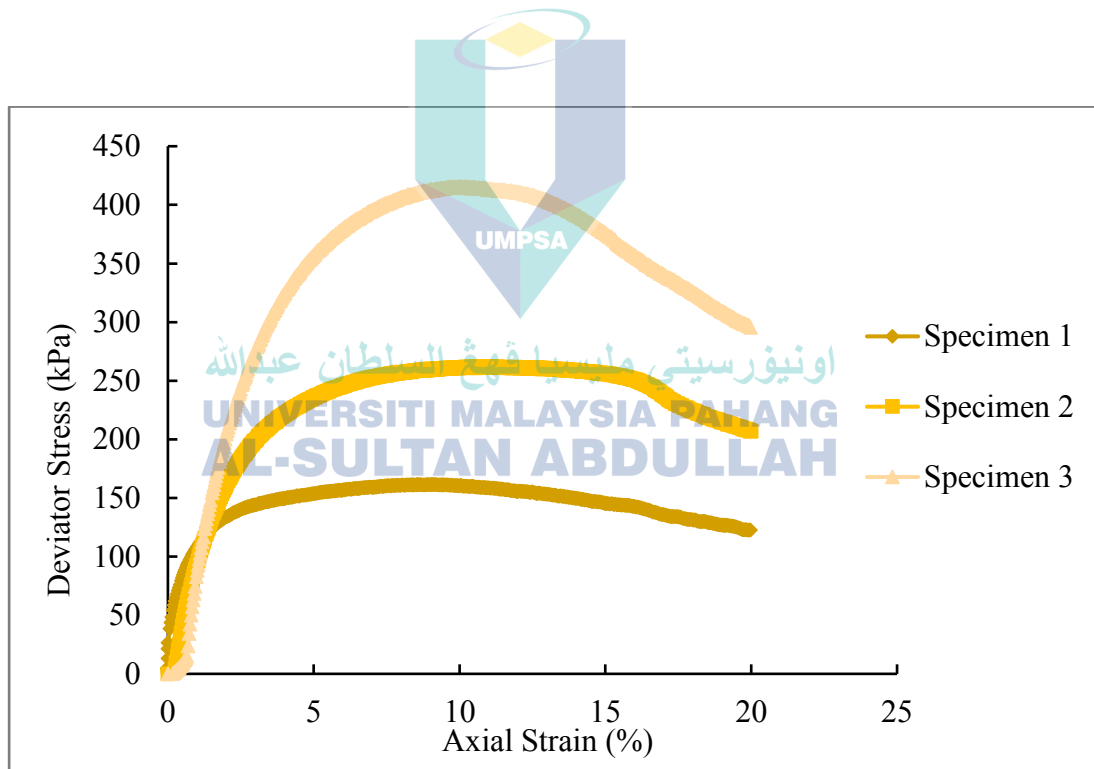
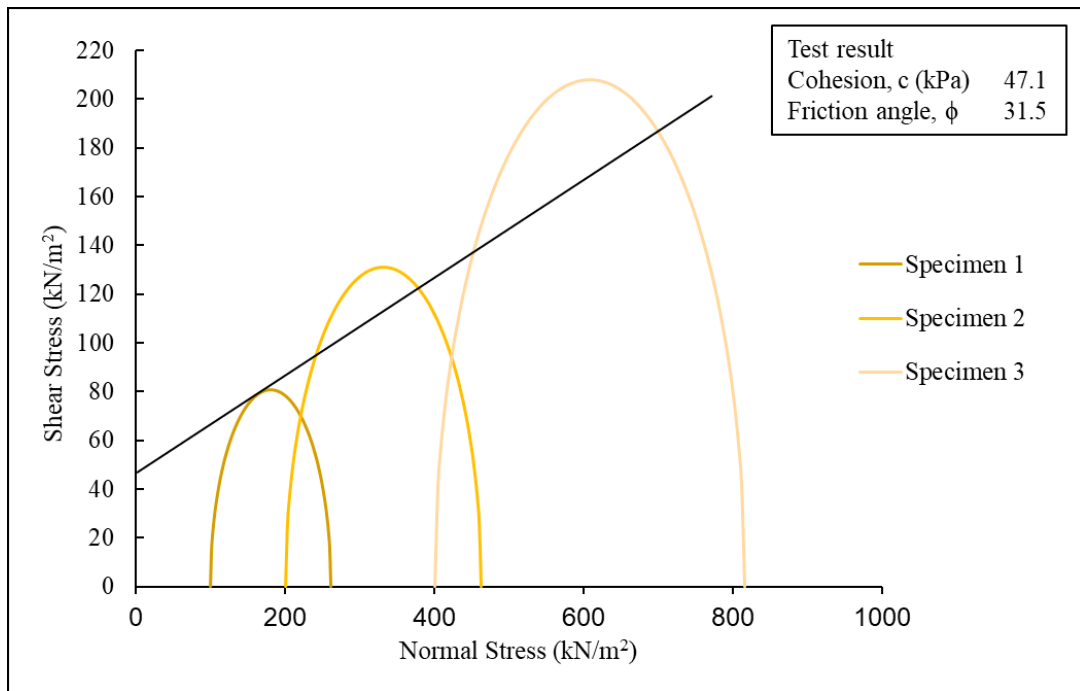
UNCONSOLIDATED UNDRAINED (UU) TRIAXIAL TEST

| | Specimen 1 | Specimen 2 | Specimen 3 |
|--|------------|------------|------------|
| Height (mm) | 100.00 | 100.00 | 100.00 |
| Diameter (mm) | 50.00 | 50.00 | 50.00 |
| Weight (g) | 350 | 350 | 350 |
| Particle Density, p_s | 2.62 | 2.62 | 2.62 |
| Specimen | Specimen 1 | Specimen 2 | Specimen 3 |
| Cell Pressure, σ_3 (kPa) | 100 | 200 | 400 |
| Moisture Content (%) | 20 | 20 | 20 |
| Bulk Density, (Mg/m ³) | 1.78 | 1.78 | 1.78 |
| Dry Density, (Mg/m ³) | 1.49 | 1.49 | 1.49 |
| Void Ratio | 0.76 | 0.76 | 0.76 |
| Deg of Saturation (%) | 68.95 | 68.95 | 68.95 |
| Strain at failure, ϵ_f (%) | 9.05 | 11.12 | 10.03 |
| Shear Strength, C_u (kPa) | 80.83 | 131.05 | 207.79 |
| Max Deviator Stress, (kPa) | 161.66 | 262.10 | 415.59 |
| Total Normal Stress ($\sigma_1 - \sigma_3$), (kPa) | 161.66 | 262.10 | 415.59 |

Test method: BS1377: Part 7: 1990

Borehole: G1660

(delete as appropriate)



TOTAL STRESS TRIAXIAL COMPRESSION

| No. | Strain (mm) | Strain, ϵ (%) | Load (N) | Deviator Stress (1-3) (kPa) |
|-----|-------------|------------------------|----------|-----------------------------|
| 1 | 0.07 | 0.07 | 76 | 38.68 |
| 2 | 0.10 | 0.10 | 86 | 43.76 |
| 3 | 0.47 | 0.47 | 156 | 79.59 |
| 4 | 0.82 | 0.82 | 196 | 100.02 |
| 5 | 1.17 | 1.17 | 223 | 113.76 |
| 6 | 1.53 | 1.53 | 245 | 124.87 |
| 7 | 1.88 | 1.88 | 259 | 131.92 |
| 8 | 2.23 | 2.23 | 270 | 137.43 |
| 9 | 2.60 | 2.60 | 278 | 141.38 |
| 10 | 2.95 | 2.95 | 282 | 143.83 |
| 11 | 3.30 | 3.30 | 287 | 146.27 |
| 12 | 3.67 | 3.67 | 291 | 148.17 |
| 13 | 4.02 | 4.02 | 294 | 149.59 |
| 14 | 4.38 | 4.38 | 297 | 151.45 |
| 15 | 4.73 | 4.73 | 300 | 152.84 |
| 16 | 5.08 | 5.08 | 303 | 154.21 |
| 17 | 5.45 | 5.45 | 305 | 155.54 |
| 18 | 5.80 | 5.80 | 307 | 156.40 |
| 19 | 6.15 | 6.15 | 309 | 157.25 |
| 20 | 6.52 | 6.52 | 310 | 158.07 |
| 21 | 6.87 | 6.87 | 312 | 158.90 |
| 22 | 7.23 | 7.23 | 314 | 159.69 |
| 23 | 7.58 | 7.58 | 315 | 160.50 |
| 24 | 7.93 | 7.93 | 316 | 160.83 |
| 25 | 8.30 | 8.30 | 316 | 161.12 |
| 26 | 8.65 | 8.65 | 317 | 161.44 |
| 27 | 9.05 | 9.05 | 317 | 161.66 |
| 28 | 9.37 | 9.37 | 316 | 161.10 |
| 29 | 9.72 | 9.72 | 316 | 160.93 |

| | | | | |
|----|-------|-------|-----|--------|
| 30 | 10.08 | 10.08 | 315 | 160.28 |
| 31 | 10.43 | 10.43 | 314 | 160.11 |
| 32 | 10.80 | 10.80 | 312 | 159.00 |
| 33 | 11.15 | 11.15 | 311 | 158.38 |
| 34 | 11.50 | 11.50 | 310 | 157.75 |
| 35 | 11.87 | 11.87 | 307 | 156.20 |
| 36 | 12.22 | 12.22 | 305 | 155.58 |
| 37 | 12.58 | 12.58 | 303 | 154.49 |
| 38 | 12.93 | 12.93 | 301 | 153.43 |
| 39 | 13.28 | 13.28 | 299 | 152.37 |
| 40 | 13.65 | 13.65 | 296 | 150.84 |
| 41 | 14.00 | 14.00 | 294 | 149.79 |
| 42 | 14.37 | 14.37 | 291 | 148.28 |
| 43 | 14.72 | 14.72 | 288 | 146.81 |
| 44 | 15.07 | 15.07 | 285 | 145.34 |
| 45 | 15.43 | 15.43 | 283 | 144.28 |
| 46 | 15.78 | 15.78 | 282 | 143.69 |
| 47 | 16.15 | 16.15 | 279 | 142.21 |
| 48 | 16.50 | 16.50 | 274 | 139.49 |
| 49 | 16.85 | 16.85 | 268 | 136.36 |
| 50 | 17.22 | 17.22 | 264 | 134.49 |
| 51 | 17.57 | 17.57 | 263 | 133.93 |
| 52 | 17.92 | 17.92 | 259 | 131.68 |
| 53 | 18.28 | 18.28 | 255 | 129.85 |
| 54 | 18.63 | 18.63 | 253 | 128.88 |
| 55 | 19.00 | 19.00 | 249 | 127.06 |
| 56 | 19.35 | 19.35 | 248 | 126.10 |
| 57 | 19.98 | 19.98 | 241 | 122.66 |

Test name: Specimen 1

Borehole: G1660

TOTAL STRESS TRIAXIAL COMPRESSION

| No. | Strain (mm) | Strain, ϵ (%) | Load (N) | Deviator Stress (1-3) (kPa) |
|-----|-------------|------------------------|----------|-----------------------------|
| 1 | 0.25 | 0.25 | 8 | 4.06 |
| 2 | 0.32 | 0.32 | 30 | 15.23 |
| 3 | 0.67 | 0.67 | 120 | 61.21 |
| 4 | 1.03 | 1.03 | 189 | 96.27 |
| 5 | 1.38 | 1.38 | 244 | 124.06 |
| 6 | 1.73 | 1.73 | 289 | 147.14 |
| 7 | 2.10 | 2.10 | 327 | 166.53 |
| 8 | 2.45 | 2.45 | 356 | 181.34 |
| 9 | 2.80 | 2.80 | 380 | 193.56 |
| 10 | 3.17 | 3.17 | 400 | 203.68 |
| 11 | 3.52 | 3.52 | 416 | 211.79 |
| 12 | 3.88 | 3.88 | 431 | 219.30 |
| 13 | 4.23 | 4.23 | 442 | 225.33 |
| 14 | 4.58 | 4.58 | 452 | 230.34 |
| 15 | 4.95 | 4.95 | 462 | 235.27 |
| 16 | 5.30 | 5.30 | 470 | 239.22 |
| 17 | 5.67 | 5.67 | 477 | 243.10 |
| 18 | 6.02 | 6.02 | 483 | 246.03 |
| 19 | 6.37 | 6.37 | 488 | 248.45 |
| 20 | 6.73 | 6.73 | 493 | 251.28 |
| 21 | 7.08 | 7.08 | 497 | 253.17 |
| 22 | 7.45 | 7.45 | 501 | 255.00 |
| 23 | 7.80 | 7.80 | 503 | 256.39 |
| 24 | 8.15 | 8.15 | 505 | 257.28 |
| 25 | 8.52 | 8.52 | 508 | 258.59 |
| 26 | 8.87 | 8.87 | 509 | 258.99 |
| 27 | 9.23 | 9.23 | 510 | 259.80 |
| 28 | 9.58 | 9.58 | 512 | 260.64 |
| 29 | 9.93 | 9.93 | 512 | 261.00 |

| | | | | |
|----|-------|-------|-----|--------|
| 30 | 10.30 | 10.30 | 514 | 261.77 |
| 31 | 10.65 | 10.65 | 513 | 261.20 |
| 32 | 11.12 | 11.12 | 515 | 262.10 |
| 33 | 11.37 | 11.37 | 513 | 261.36 |
| 34 | 11.72 | 11.72 | 513 | 261.23 |
| 35 | 12.08 | 12.08 | 513 | 261.04 |
| 36 | 12.43 | 12.43 | 513 | 261.34 |
| 37 | 12.80 | 12.80 | 512 | 260.69 |
| 38 | 13.15 | 13.15 | 511 | 260.09 |
| 39 | 13.50 | 13.50 | 510 | 259.92 |
| 40 | 13.87 | 13.87 | 509 | 259.26 |
| 41 | 14.22 | 14.22 | 507 | 258.20 |
| 42 | 14.58 | 14.58 | 506 | 257.53 |
| 43 | 14.93 | 14.93 | 503 | 256.05 |
| 44 | 15.28 | 15.28 | 501 | 254.99 |
| 45 | 15.65 | 15.65 | 497 | 253.03 |
| 46 | 16.00 | 16.00 | 493 | 251.12 |
| 47 | 16.35 | 16.35 | 486 | 247.52 |
| 48 | 16.72 | 16.72 | 476 | 242.19 |
| 49 | 17.07 | 17.07 | 464 | 236.53 |
| 50 | 17.43 | 17.43 | 452 | 230.44 |
| 51 | 17.78 | 17.78 | 446 | 226.95 |
| 52 | 18.13 | 18.13 | 438 | 223.07 |
| 53 | 18.50 | 18.50 | 430 | 219.16 |
| 54 | 18.85 | 18.85 | 425 | 216.57 |
| 55 | 19.22 | 19.22 | 418 | 213.12 |
| 56 | 19.57 | 19.57 | 413 | 210.56 |
| 57 | 19.92 | 19.92 | 408 | 208.01 |
| 58 | 20.00 | 20.00 | 406 | 206.98 |

Test name: Specimen 2

Borehole: G1660

TOTAL STRESS TRIAXIAL COMPRESSION

| No. | Strain (mm) | Strain, ϵ (%) | Load (N) | Deviator Stress (1-3) (kPa) |
|-----|-------------|------------------------|----------|-----------------------------|
| 1 | 0.17 | 0.17 | 1 | 0.51 |
| 2 | 0.52 | 0.52 | 18 | 9.12 |
| 3 | 0.87 | 0.87 | 124 | 63.11 |
| 4 | 1.22 | 1.22 | 229 | 116.72 |
| 5 | 1.58 | 1.58 | 317 | 161.40 |
| 6 | 1.93 | 1.93 | 387 | 197.28 |
| 7 | 2.30 | 2.30 | 448 | 228.39 |
| 8 | 2.65 | 2.65 | 497 | 253.35 |
| 9 | 3.00 | 3.00 | 541 | 275.66 |
| 10 | 3.37 | 3.37 | 582 | 296.28 |
| 11 | 3.72 | 3.72 | 614 | 312.85 |
| 12 | 4.08 | 4.08 | 644 | 327.78 |
| 13 | 4.43 | 4.43 | 668 | 340.22 |
| 14 | 4.78 | 4.78 | 689 | 351.09 |
| 15 | 5.15 | 5.15 | 709 | 361.33 |
| 16 | 5.50 | 5.50 | 725 | 369.15 |
| 17 | 5.87 | 5.87 | 741 | 377.30 |
| 18 | 6.22 | 6.22 | 753 | 383.54 |
| 19 | 6.57 | 6.57 | 763 | 388.77 |
| 20 | 6.93 | 6.93 | 775 | 394.83 |
| 21 | 7.28 | 7.28 | 783 | 399.01 |
| 22 | 7.63 | 7.63 | 791 | 402.68 |
| 23 | 8.00 | 8.00 | 798 | 406.23 |
| 24 | 8.35 | 8.35 | 802 | 408.42 |
| 25 | 8.70 | 8.70 | 807 | 411.05 |
| 26 | 9.07 | 9.07 | 810 | 412.64 |
| 27 | 9.42 | 9.42 | 813 | 414.28 |
| 28 | 9.78 | 9.78 | 816 | 415.36 |
| 29 | 10.03 | 10.03 | 816 | 415.59 |

| | | | | |
|----|-------|-------|-----|--------|
| 30 | 10.48 | 10.48 | 815 | 414.87 |
| 31 | 10.85 | 10.85 | 813 | 414.08 |
| 32 | 11.20 | 11.20 | 811 | 412.91 |
| 33 | 11.57 | 11.57 | 809 | 412.10 |
| 34 | 11.92 | 11.92 | 807 | 410.92 |
| 35 | 12.27 | 12.27 | 805 | 409.73 |
| 36 | 12.63 | 12.63 | 799 | 406.69 |
| 37 | 12.98 | 12.98 | 794 | 404.17 |
| 38 | 13.35 | 13.35 | 786 | 400.26 |
| 39 | 13.70 | 13.70 | 777 | 395.57 |
| 40 | 14.05 | 14.05 | 768 | 391.34 |
| 41 | 14.42 | 14.42 | 757 | 385.31 |
| 42 | 14.77 | 14.77 | 746 | 379.83 |
| 43 | 15.13 | 15.13 | 733 | 373.44 |
| 44 | 15.48 | 15.48 | 718 | 365.88 |
| 45 | 15.83 | 15.83 | 707 | 360.07 |
| 46 | 16.20 | 16.20 | 695 | 353.81 |
| 47 | 16.55 | 16.55 | 683 | 347.66 |
| 48 | 16.92 | 16.92 | 670 | 341.47 |
| 49 | 17.27 | 17.27 | 661 | 336.66 |
| 50 | 17.62 | 17.62 | 650 | 331.04 |
| 51 | 17.98 | 17.98 | 641 | 326.23 |
| 52 | 18.33 | 18.33 | 630 | 320.68 |
| 53 | 18.70 | 18.70 | 616 | 313.86 |
| 54 | 19.05 | 19.05 | 606 | 308.79 |
| 55 | 19.40 | 19.40 | 596 | 303.76 |
| 56 | 19.77 | 19.77 | 587 | 298.70 |
| 57 | 19.83 | 19.83 | 585 | 298.05 |

Test name: Specimen 3

Borehole: G1660

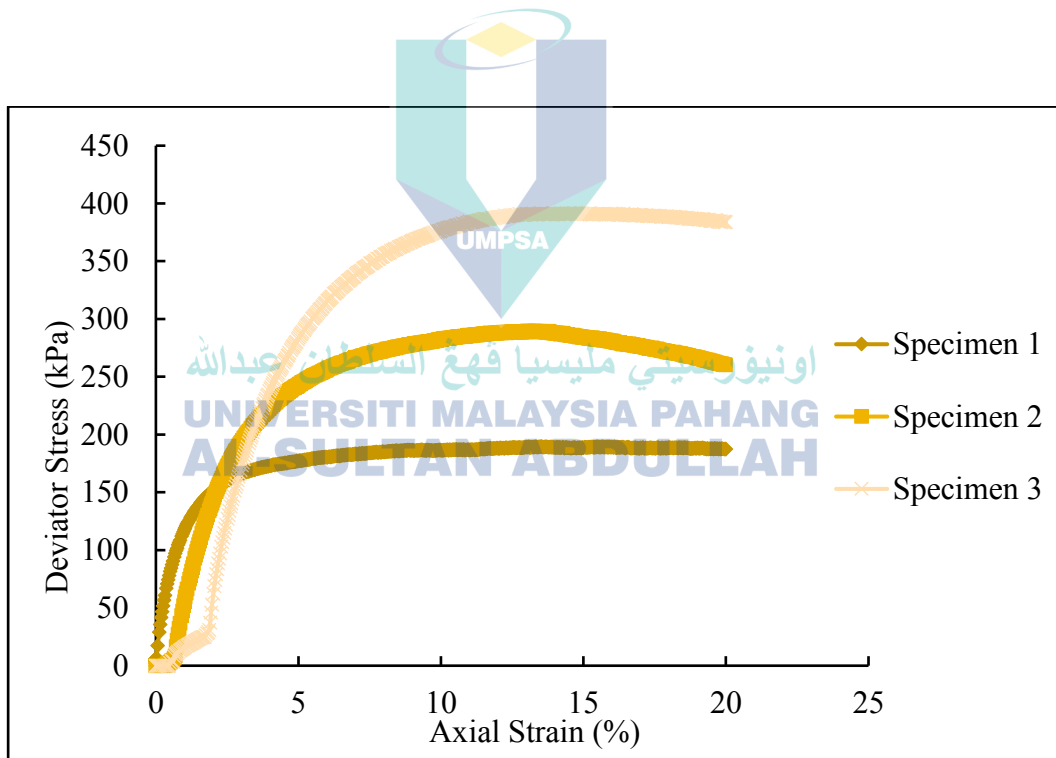
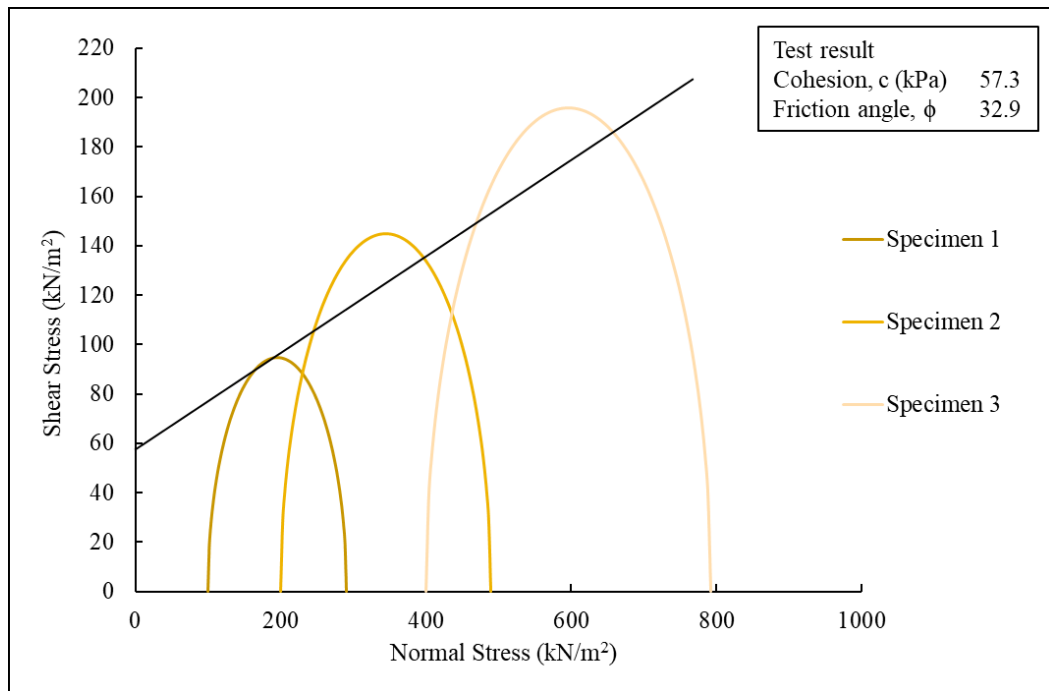
UNCONSOLIDATED UNDRAINED (UU) TRIAXIAL TEST

| | Specimen 1 | Specimen 2 | Specimen 3 |
|--|------------|------------|------------|
| Height (mm) | 100.00 | 100.00 | 100.00 |
| Diameter (mm) | 50.00 | 50.00 | 50.00 |
| Weight (g) | 350 | 350 | 350 |
| Particle Density, p_s | 2.62 | 2.62 | 2.62 |
| Specimen | Specimen 1 | Specimen 2 | Specimen 3 |
| Cell Pressure, σ_3 (kPa) | 100 | 200 | 400 |
| Moisture Content (%) | 20 | 20 | 20 |
| Bulk Density, (Mg/m ³) | 1.78 | 1.78 | 1.78 |
| Dry Density, (Mg/m ³) | 1.49 | 1.49 | 1.49 |
| Void Ratio | 0.76 | 0.76 | 0.76 |
| Deg of Saturation (%) | 68.95 | 68.95 | 68.95 |
| Strain at failure, ϵ_f (%) | 13.52 | 13.28 | 15.18 |
| Shear Strength, C_u (kPa) | 94.92 | 144.86 | 195.90 |
| Max Deviator Stress, (kPa) | 189.84 | 289.72 | 391.80 |
| Total Normal Stress ($\sigma_1 - \sigma_3$), (kPa) | 189.94 | 289.72 | 391.80 |

Test method: BS1377: Part 7: 1990

Borehole: G1680

(delete as appropriate)



TOTAL STRESS TRIAXIAL COMPRESSION

| No. | Strain (mm) | Strain, ϵ (%) | Load (N) | Deviator Stress (1-3) (kPa) |
|-----|-------------|------------------------|----------|-----------------------------|
| 1 | 0.12 | 0.12 | 57 | 29.00 |
| 2 | 0.47 | 0.47 | 153 | 78.07 |
| 3 | 0.82 | 0.82 | 209 | 106.58 |
| 4 | 1.18 | 1.18 | 248 | 126.32 |
| 5 | 1.53 | 1.53 | 274 | 139.41 |
| 6 | 1.88 | 1.88 | 293 | 149.41 |
| 7 | 2.25 | 2.25 | 307 | 156.32 |
| 8 | 2.60 | 2.60 | 317 | 161.22 |
| 9 | 2.97 | 2.97 | 325 | 165.55 |
| 10 | 3.32 | 3.32 | 332 | 168.89 |
| 11 | 3.67 | 3.67 | 336 | 171.23 |
| 12 | 4.03 | 4.03 | 340 | 173.02 |
| 13 | 4.38 | 4.38 | 343 | 174.82 |
| 14 | 4.75 | 4.75 | 346 | 176.09 |
| 15 | 5.10 | 5.10 | 348 | 177.38 |
| 16 | 5.45 | 5.45 | 352 | 179.13 |
| 17 | 5.82 | 5.82 | 354 | 180.36 |
| 18 | 6.17 | 6.17 | 356 | 181.12 |
| 19 | 6.52 | 6.52 | 357 | 181.87 |
| 20 | 6.88 | 6.88 | 359 | 182.58 |
| 21 | 7.23 | 7.23 | 361 | 183.79 |
| 22 | 7.60 | 7.60 | 362 | 184.47 |
| 23 | 7.95 | 7.95 | 364 | 185.18 |
| 24 | 8.30 | 8.30 | 365 | 185.88 |
| 25 | 8.67 | 8.67 | 365 | 186.06 |
| 26 | 9.02 | 9.02 | 367 | 186.74 |
| 27 | 9.37 | 9.37 | 366 | 186.48 |
| 28 | 9.73 | 9.73 | 366 | 186.19 |
| 29 | 10.08 | 10.08 | 366 | 186.38 |

| | | | | |
|----|-------|-------|-----|--------|
| 30 | 10.45 | 10.45 | 367 | 186.99 |
| 31 | 10.80 | 10.80 | 368 | 187.17 |
| 32 | 11.17 | 11.17 | 367 | 186.85 |
| 33 | 11.52 | 11.52 | 368 | 187.47 |
| 34 | 11.87 | 11.87 | 369 | 188.07 |
| 35 | 12.23 | 12.23 | 369 | 188.18 |
| 36 | 12.58 | 12.58 | 371 | 188.77 |
| 37 | 12.93 | 12.93 | 371 | 188.90 |
| 38 | 13.30 | 13.30 | 372 | 189.43 |
| 39 | 13.52 | 13.52 | 373 | 189.84 |
| 40 | 14.02 | 14.02 | 371 | 188.74 |
| 41 | 14.37 | 14.37 | 371 | 188.84 |
| 42 | 14.72 | 14.72 | 370 | 188.50 |
| 43 | 15.08 | 15.08 | 371 | 188.99 |
| 44 | 15.43 | 15.43 | 371 | 189.08 |
| 45 | 15.80 | 15.80 | 371 | 189.11 |
| 46 | 16.15 | 16.15 | 371 | 188.75 |
| 47 | 16.50 | 16.50 | 371 | 188.82 |
| 48 | 16.87 | 16.87 | 370 | 188.41 |
| 49 | 17.22 | 17.22 | 369 | 188.04 |
| 50 | 17.57 | 17.57 | 370 | 188.50 |
| 51 | 17.93 | 17.93 | 370 | 188.50 |
| 52 | 18.28 | 18.28 | 370 | 188.53 |
| 53 | 18.65 | 18.65 | 370 | 188.51 |
| 54 | 19.00 | 19.00 | 370 | 188.53 |
| 55 | 19.38 | 19.38 | 368 | 187.63 |
| 56 | 19.72 | 19.72 | 368 | 187.67 |
| 57 | 20.00 | 20.00 | 368 | 187.42 |

Test name: Specimen 1

Borehole: G1680

TOTAL STRESS TRIAXIAL COMPRESSION

| No. | Strain (mm) | Strain, ϵ (%) | Load (N) | Deviator Stress (1-3) (kPa) |
|-----|-------------|------------------------|----------|-----------------------------|
| 1 | 0.35 | 0.35 | 1 | 0.51 |
| 2 | 0.68 | 0.68 | 17 | 8.60 |
| 3 | 1.03 | 1.03 | 117 | 59.48 |
| 4 | 1.40 | 1.40 | 188 | 95.91 |
| 5 | 1.75 | 1.75 | 246 | 125.10 |
| 6 | 2.12 | 2.12 | 296 | 150.55 |
| 7 | 2.47 | 2.47 | 335 | 170.38 |
| 8 | 2.82 | 2.82 | 366 | 186.60 |
| 9 | 3.18 | 3.18 | 393 | 200.19 |
| 10 | 3.53 | 3.53 | 415 | 211.26 |
| 11 | 3.90 | 3.90 | 433 | 220.73 |
| 12 | 4.25 | 4.25 | 451 | 229.68 |
| 13 | 4.62 | 4.62 | 465 | 236.58 |
| 14 | 4.97 | 4.97 | 476 | 242.48 |
| 15 | 5.33 | 5.33 | 488 | 248.30 |
| 16 | 5.68 | 5.68 | 496 | 252.67 |
| 17 | 6.03 | 6.03 | 505 | 256.99 |
| 18 | 6.40 | 6.40 | 512 | 260.76 |
| 19 | 6.75 | 6.75 | 518 | 264.05 |
| 20 | 7.12 | 7.12 | 524 | 266.80 |
| 21 | 7.47 | 7.47 | 529 | 269.56 |
| 22 | 7.82 | 7.82 | 534 | 271.83 |
| 23 | 8.18 | 8.18 | 538 | 274.03 |
| 24 | 8.53 | 8.53 | 541 | 275.78 |
| 25 | 8.90 | 8.90 | 545 | 277.45 |
| 26 | 9.25 | 9.25 | 548 | 279.16 |
| 27 | 9.60 | 9.60 | 551 | 280.39 |
| 28 | 9.97 | 9.97 | 555 | 282.46 |
| 29 | 10.32 | 10.32 | 557 | 283.64 |

| | | | | |
|----|-------|-------|-----|--------|
| 30 | 10.68 | 10.68 | 559 | 284.76 |
| 31 | 11.03 | 11.03 | 560 | 285.46 |
| 32 | 11.38 | 11.38 | 563 | 286.59 |
| 33 | 11.75 | 11.75 | 565 | 287.65 |
| 34 | 12.10 | 12.10 | 566 | 288.30 |
| 35 | 12.45 | 12.45 | 566 | 288.49 |
| 36 | 12.82 | 12.82 | 567 | 288.61 |
| 37 | 13.28 | 13.28 | 569 | 289.72 |
| 38 | 13.53 | 13.53 | 568 | 289.32 |
| 39 | 13.88 | 13.88 | 566 | 288.15 |
| 40 | 14.23 | 14.23 | 564 | 287.42 |
| 41 | 14.60 | 14.60 | 561 | 285.75 |
| 42 | 14.95 | 14.95 | 558 | 284.15 |
| 43 | 15.32 | 15.32 | 557 | 283.79 |
| 44 | 15.67 | 15.67 | 554 | 282.18 |
| 45 | 16.02 | 16.02 | 551 | 280.59 |
| 46 | 16.38 | 16.38 | 547 | 278.51 |
| 47 | 16.73 | 16.73 | 545 | 277.77 |
| 48 | 17.08 | 17.08 | 542 | 276.18 |
| 49 | 17.45 | 17.45 | 539 | 274.54 |
| 50 | 17.80 | 17.80 | 535 | 272.54 |
| 51 | 18.17 | 18.17 | 533 | 271.32 |
| 52 | 18.52 | 18.52 | 529 | 269.33 |
| 53 | 18.87 | 18.87 | 525 | 267.34 |
| 54 | 19.23 | 19.23 | 520 | 264.90 |
| 55 | 19.58 | 19.58 | 515 | 262.53 |
| 56 | 19.98 | 19.98 | 511 | 260.41 |

Test name: Specimen 2

Borehole: G1680

TOTAL STRESS TRIAXIAL COMPRESSION

| No. | Strain (mm) | Strain, ϵ (%) | Load (N) | Deviator Stress (1-3) (kPa) |
|-----|-------------|------------------------|----------|-----------------------------|
| 1 | 0.50 | 0.50 | 5 | 2.53 |
| 2 | 0.72 | 0.72 | 20 | 10.11 |
| 3 | 1.08 | 1.08 | 34 | 17.13 |
| 4 | 1.43 | 1.43 | 43 | 22.09 |
| 5 | 1.80 | 1.80 | 55 | 28.01 |
| 6 | 2.15 | 2.15 | 164 | 83.72 |
| 7 | 2.52 | 2.52 | 250 | 127.10 |
| 8 | 2.87 | 2.87 | 316 | 160.78 |
| 9 | 3.22 | 3.22 | 372 | 189.28 |
| 10 | 3.58 | 3.58 | 420 | 214.10 |
| 11 | 3.93 | 3.93 | 461 | 234.85 |
| 12 | 4.30 | 4.30 | 498 | 253.45 |
| 13 | 4.65 | 4.65 | 528 | 269.03 |
| 14 | 5.02 | 5.02 | 558 | 283.96 |
| 15 | 5.37 | 5.37 | 581 | 295.92 |
| 16 | 5.73 | 5.73 | 604 | 307.74 |
| 17 | 6.08 | 6.08 | 623 | 317.12 |
| 18 | 6.43 | 6.43 | 640 | 325.95 |
| 19 | 6.80 | 6.80 | 655 | 333.69 |
| 20 | 7.15 | 7.15 | 669 | 340.95 |
| 21 | 7.52 | 7.52 | 683 | 348.08 |
| 22 | 7.87 | 7.87 | 694 | 353.33 |
| 23 | 8.22 | 8.22 | 702 | 357.60 |
| 24 | 8.58 | 8.58 | 712 | 362.69 |
| 25 | 8.95 | 8.95 | 720 | 366.80 |
| 26 | 9.30 | 9.30 | 727 | 370.47 |
| 27 | 9.67 | 9.67 | 734 | 374.03 |
| 28 | 10.02 | 10.02 | 740 | 376.71 |
| 29 | 10.38 | 10.38 | 745 | 379.28 |

| | | | | |
|----|-------|-------|-----|--------|
| 30 | 10.75 | 10.75 | 751 | 382.73 |
| 31 | 11.10 | 11.10 | 754 | 383.94 |
| 32 | 11.45 | 11.45 | 757 | 385.59 |
| 33 | 11.82 | 11.82 | 760 | 387.13 |
| 34 | 12.17 | 12.17 | 762 | 388.28 |
| 35 | 12.53 | 12.53 | 764 | 389.34 |
| 36 | 12.88 | 12.88 | 767 | 390.44 |
| 37 | 13.25 | 13.25 | 768 | 391.01 |
| 38 | 13.60 | 13.60 | 767 | 390.75 |
| 39 | 13.97 | 13.97 | 769 | 391.72 |
| 40 | 14.32 | 14.32 | 768 | 391.00 |
| 41 | 14.68 | 14.68 | 769 | 391.50 |
| 42 | 15.18 | 15.18 | 769 | 391.80 |
| 43 | 15.38 | 15.38 | 767 | 390.44 |
| 44 | 15.75 | 15.75 | 767 | 390.46 |
| 45 | 16.10 | 16.10 | 768 | 390.98 |
| 46 | 16.47 | 16.47 | 766 | 390.12 |
| 47 | 16.82 | 16.82 | 766 | 390.18 |
| 48 | 17.18 | 17.18 | 766 | 390.15 |
| 49 | 17.53 | 17.53 | 764 | 388.92 |
| 50 | 17.88 | 17.88 | 763 | 388.52 |
| 51 | 18.25 | 18.25 | 762 | 388.04 |
| 52 | 18.60 | 18.60 | 761 | 387.62 |
| 53 | 18.97 | 18.97 | 759 | 386.70 |
| 54 | 19.32 | 19.32 | 758 | 385.85 |
| 55 | 19.68 | 19.68 | 756 | 384.92 |
| 56 | 20.00 | 20.00 | 754 | 383.81 |

Test name: Specimen 3

Borehole: G1680

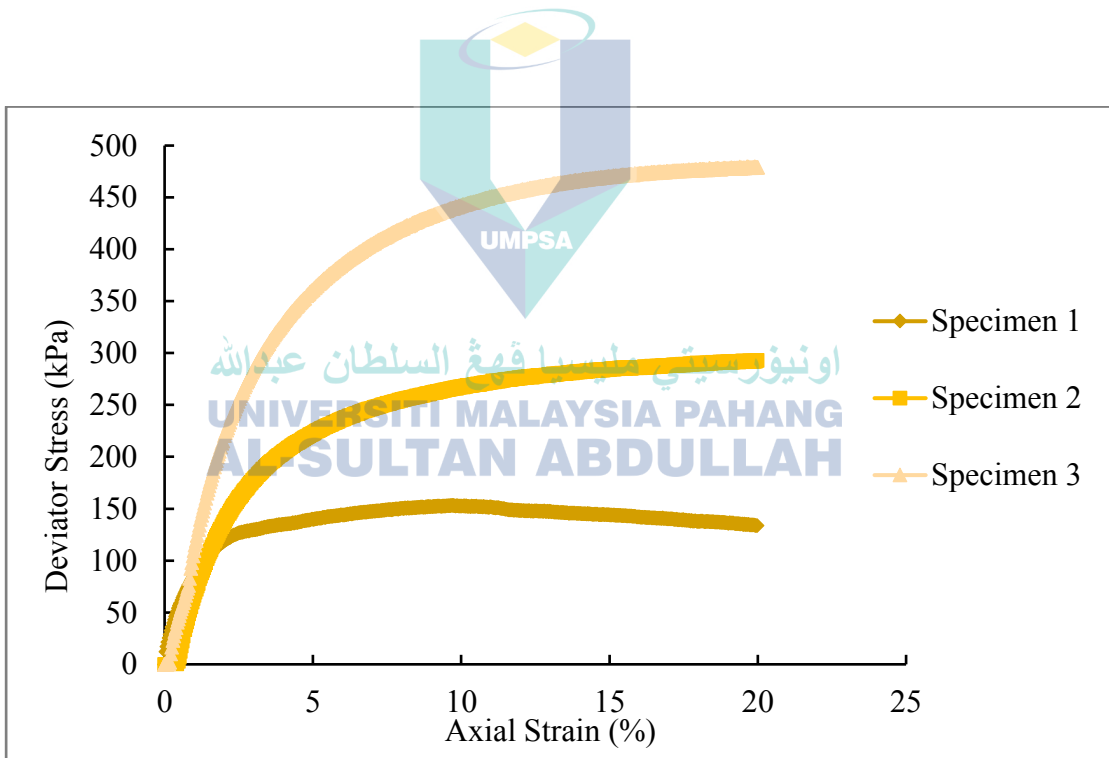
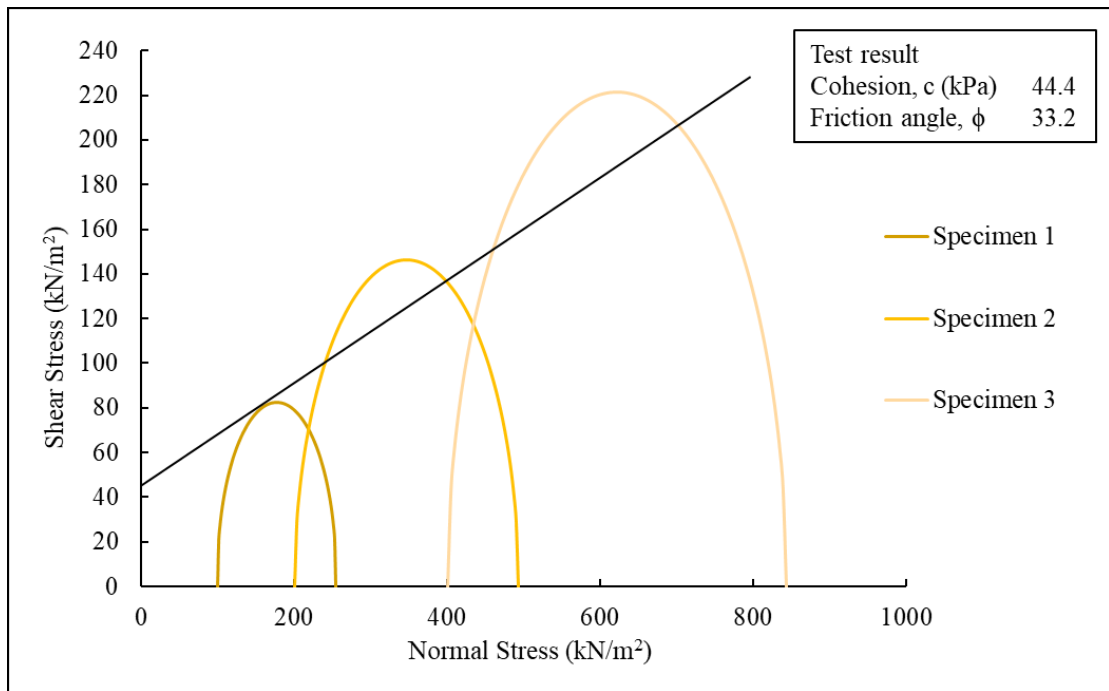
UNCONSOLIDATED UNDRAINED (UU) TRIAXIAL TEST

| | Specimen 1 | Specimen 2 | Specimen 3 |
|--|------------|------------|------------|
| Height (mm) | 100.00 | 100.00 | 100.00 |
| Diameter (mm) | 50.00 | 50.00 | 50.00 |
| Weight (g) | 350 | 350 | 350 |
| Particle Density, p_s | 2.62 | 2.62 | 2.62 |
| | | | |
| Specimen | Specimen 1 | Specimen 2 | Specimen 3 |
| Cell Pressure, σ_3 (kPa) | 100 | 200 | 400 |
| Moisture Content (%) | 20 | 20 | 20 |
| Bulk Density, (Mg/m ³) | 1.78 | 1.78 | 1.78 |
| Dry Density, (Mg/m ³) | 1.49 | 1.49 | 1.49 |
| Void Ratio | 0.76 | 0.76 | 0.76 |
| Deg of Saturation (%) | 68.95 | 68.95 | 68.95 |
| Strain at failure, ϵ_f (%) | 9.67 | 19.98 | 19.90 |
| Shear Strength, C_u (kPa) | 82.60 | 146.50 | 221.35 |
| Max Deviator Stress, (kPa) | 153.20 | 293.01 | 479.74 |
| Total Normal Stress ($\sigma_1 - \sigma_3$), (kPa) | 153.20 | 293.01 | 479.74 |

Test method: BS1377: Part 7: 1990

Borehole: G16100

(delete as appropriate)



TOTAL STRESS TRIAXIAL COMPRESSION

| No. | Strain (mm) | Strain, ϵ (%) | Load (N) | Deviator Stress (1-3) (kPa) |
|-----|-------------|------------------------|----------|-----------------------------|
| 1 | 0.05 | 0.05 | 24 | 12.22 |
| 2 | 0.33 | 0.33 | 85 | 43.15 |
| 3 | 0.68 | 0.68 | 134 | 68.29 |
| 4 | 1.03 | 1.03 | 171 | 87.20 |
| 5 | 1.40 | 1.40 | 201 | 102.44 |
| 6 | 1.75 | 1.75 | 221 | 112.59 |
| 7 | 2.10 | 2.10 | 237 | 120.66 |
| 8 | 2.47 | 2.47 | 248 | 126.17 |
| 9 | 2.82 | 2.82 | 253 | 128.69 |
| 10 | 3.18 | 3.18 | 257 | 130.67 |
| 11 | 3.53 | 3.53 | 261 | 133.14 |
| 12 | 3.88 | 3.88 | 264 | 134.62 |
| 13 | 4.25 | 4.25 | 266 | 135.57 |
| 14 | 4.60 | 4.60 | 270 | 137.50 |
| 15 | 4.97 | 4.97 | 275 | 139.88 |
| 16 | 5.32 | 5.32 | 277 | 141.29 |
| 17 | 5.67 | 5.67 | 280 | 142.69 |
| 18 | 6.03 | 6.03 | 283 | 144.05 |
| 19 | 6.38 | 6.38 | 286 | 145.42 |
| 20 | 6.75 | 6.75 | 288 | 146.75 |
| 21 | 7.10 | 7.10 | 290 | 147.62 |
| 22 | 7.45 | 7.45 | 292 | 148.95 |
| 23 | 7.82 | 7.82 | 294 | 149.77 |
| 24 | 8.17 | 8.17 | 296 | 150.60 |
| 25 | 8.52 | 8.52 | 297 | 151.42 |
| 26 | 8.88 | 8.88 | 299 | 152.21 |
| 27 | 9.23 | 9.23 | 300 | 152.55 |
| 28 | 9.67 | 9.67 | 301 | 153.20 |
| 29 | 9.95 | 9.95 | 300 | 152.72 |

| | | | | |
|----|-------|-------|-----|--------|
| 30 | 10.32 | 10.32 | 299 | 152.10 |
| 31 | 10.67 | 10.67 | 298 | 151.96 |
| 32 | 11.02 | 11.02 | 298 | 151.82 |
| 33 | 11.38 | 11.38 | 295 | 150.29 |
| 34 | 11.73 | 11.73 | 292 | 148.80 |
| 35 | 12.10 | 12.10 | 291 | 148.18 |
| 36 | 12.45 | 12.45 | 290 | 147.59 |
| 37 | 12.80 | 12.80 | 290 | 147.89 |
| 38 | 13.17 | 13.17 | 288 | 146.82 |
| 39 | 13.52 | 13.52 | 287 | 146.23 |
| 40 | 13.88 | 13.88 | 286 | 145.61 |
| 41 | 14.23 | 14.23 | 285 | 145.02 |
| 42 | 14.58 | 14.58 | 284 | 144.86 |
| 43 | 14.95 | 14.95 | 283 | 144.24 |
| 44 | 15.30 | 15.30 | 282 | 143.65 |
| 45 | 15.67 | 15.67 | 281 | 143.02 |
| 46 | 16.02 | 16.02 | 279 | 142.00 |
| 47 | 16.37 | 16.37 | 278 | 141.41 |
| 48 | 16.73 | 16.73 | 276 | 140.79 |
| 49 | 17.08 | 17.08 | 275 | 140.20 |
| 50 | 17.45 | 17.45 | 273 | 139.16 |
| 51 | 17.80 | 17.80 | 271 | 138.15 |
| 52 | 18.15 | 18.15 | 271 | 137.98 |
| 53 | 18.52 | 18.52 | 270 | 137.36 |
| 54 | 18.87 | 18.87 | 269 | 136.77 |
| 55 | 19.23 | 19.23 | 267 | 135.74 |
| 56 | 19.58 | 19.58 | 265 | 134.75 |
| 57 | 19.98 | 19.98 | 262 | 133.67 |

Test name: Specimen 1

Borehole: G16100

TOTAL STRESS TRIAXIAL COMPRESSION

| No. | Strain (mm) | Strain, ϵ (%) | Load (N) | Deviator Stress (1-3) (kPa) |
|-----|-------------|------------------------|----------|-----------------------------|
| 1 | 0.32 | 0.32 | -4 | -2.03 |
| 2 | 0.68 | 0.68 | 66 | 33.38 |
| 3 | 1.03 | 1.03 | 137 | 69.56 |
| 4 | 1.38 | 1.38 | 192 | 97.94 |
| 5 | 1.75 | 1.75 | 242 | 123.09 |
| 6 | 2.10 | 2.10 | 279 | 142.10 |
| 7 | 2.47 | 2.47 | 311 | 158.46 |
| 8 | 2.82 | 2.82 | 337 | 171.75 |
| 9 | 3.18 | 3.18 | 361 | 183.92 |
| 10 | 3.53 | 3.53 | 380 | 193.57 |
| 11 | 3.90 | 3.90 | 397 | 202.14 |
| 12 | 4.25 | 4.25 | 412 | 209.69 |
| 13 | 4.62 | 4.62 | 424 | 216.17 |
| 14 | 4.97 | 4.97 | 436 | 222.16 |
| 15 | 5.32 | 5.32 | 447 | 227.61 |
| 16 | 5.68 | 5.68 | 456 | 232.49 |
| 17 | 6.03 | 6.03 | 464 | 236.41 |
| 18 | 6.38 | 6.38 | 473 | 240.78 |
| 19 | 6.75 | 6.75 | 480 | 244.58 |
| 20 | 7.10 | 7.10 | 487 | 247.92 |
| 21 | 7.47 | 7.47 | 492 | 250.71 |
| 22 | 7.82 | 7.82 | 498 | 253.52 |
| 23 | 8.17 | 8.17 | 503 | 256.30 |
| 24 | 8.53 | 8.53 | 508 | 258.54 |
| 25 | 8.88 | 8.88 | 512 | 260.80 |
| 26 | 9.25 | 9.25 | 516 | 262.98 |
| 27 | 9.60 | 9.60 | 521 | 265.19 |
| 28 | 9.95 | 9.95 | 525 | 267.38 |
| 29 | 10.32 | 10.32 | 528 | 269.03 |

| | | | | |
|----|-------|-------|-----|--------|
| 30 | 10.67 | 10.67 | 532 | 270.71 |
| 31 | 11.02 | 11.02 | 534 | 271.91 |
| 32 | 11.38 | 11.38 | 538 | 273.95 |
| 33 | 11.73 | 11.73 | 540 | 275.12 |
| 34 | 12.10 | 12.10 | 543 | 276.66 |
| 35 | 12.45 | 12.45 | 545 | 277.79 |
| 36 | 12.82 | 12.82 | 547 | 278.40 |
| 37 | 13.17 | 13.17 | 549 | 279.49 |
| 38 | 13.52 | 13.52 | 551 | 280.57 |
| 39 | 13.88 | 13.88 | 554 | 282.01 |
| 40 | 14.23 | 14.23 | 556 | 283.05 |
| 41 | 14.60 | 14.60 | 557 | 283.58 |
| 42 | 14.95 | 14.95 | 558 | 284.15 |
| 43 | 15.30 | 15.30 | 560 | 285.14 |
| 44 | 15.67 | 15.67 | 562 | 286.05 |
| 45 | 16.02 | 16.02 | 562 | 286.15 |
| 46 | 16.37 | 16.37 | 563 | 286.66 |
| 47 | 16.73 | 16.73 | 564 | 287.10 |
| 48 | 17.08 | 17.08 | 565 | 288.00 |
| 49 | 17.45 | 17.45 | 568 | 289.25 |
| 50 | 17.80 | 17.80 | 568 | 289.28 |
| 51 | 18.15 | 18.15 | 570 | 290.13 |
| 52 | 18.52 | 18.52 | 571 | 290.91 |
| 53 | 18.87 | 18.87 | 572 | 291.31 |
| 54 | 19.23 | 19.23 | 573 | 292.05 |
| 55 | 19.58 | 19.58 | 573 | 292.02 |
| 56 | 19.98 | 19.98 | 575 | 293.01 |

Test name: Specimen 2

Borehole: G16100

TOTAL STRESS TRIAXIAL COMPRESSION

| No. | Strain (mm) | Strain, ϵ (%) | Load (N) | Deviator Stress (1-3) (kPa) |
|-----|-------------|------------------------|----------|-----------------------------|
| 1 | 0.10 | 0.18 | 4 | 2.03 |
| 2 | 0.17 | 0.24 | 32 | 16.50 |
| 3 | 0.52 | 0.60 | 111 | 56.40 |
| 4 | 0.88 | 0.97 | 205 | 104.60 |
| 5 | 1.23 | 1.32 | 297 | 151.48 |
| 6 | 1.60 | 1.68 | 374 | 190.23 |
| 7 | 2.00 | 2.06 | 438 | 223.19 |
| 8 | 2.35 | 2.41 | 489 | 248.98 |
| 9 | 2.72 | 2.77 | 534 | 272.07 |
| 10 | 3.07 | 3.13 | 571 | 290.82 |
| 11 | 3.42 | 3.48 | 604 | 307.69 |
| 12 | 3.78 | 3.84 | 634 | 322.96 |
| 13 | 4.13 | 4.20 | 660 | 336.15 |
| 14 | 4.50 | 4.56 | 684 | 348.26 |
| 15 | 4.90 | 4.94 | 706 | 359.70 |
| 16 | 5.27 | 5.30 | 725 | 369.19 |
| 17 | 5.62 | 5.65 | 742 | 377.68 |
| 18 | 5.98 | 6.02 | 758 | 386.27 |
| 19 | 6.33 | 6.37 | 772 | 393.41 |
| 20 | 6.68 | 6.73 | 785 | 399.98 |
| 21 | 7.05 | 7.08 | 797 | 406.02 |
| 22 | 7.42 | 7.45 | 808 | 411.72 |
| 23 | 7.77 | 7.80 | 819 | 417.21 |
| 24 | 8.13 | 8.17 | 830 | 422.80 |
| 25 | 8.48 | 8.52 | 838 | 426.78 |
| 26 | 8.85 | 8.88 | 846 | 431.10 |
| 27 | 9.20 | 9.23 | 854 | 434.77 |
| 28 | 9.57 | 9.59 | 861 | 438.57 |
| 29 | 9.92 | 9.95 | 867 | 441.65 |

| | | | | |
|----|-------|-------|-----|--------|
| 30 | 10.28 | 10.31 | 874 | 445.15 |
| 31 | 10.63 | 10.67 | 879 | 447.47 |
| 32 | 11.02 | 11.03 | 885 | 450.84 |
| 33 | 11.37 | 11.39 | 890 | 453.09 |
| 34 | 11.72 | 11.74 | 894 | 455.12 |
| 35 | 12.08 | 12.10 | 898 | 457.30 |
| 36 | 12.43 | 12.46 | 902 | 459.45 |
| 37 | 12.78 | 12.81 | 905 | 460.95 |
| 38 | 13.15 | 13.18 | 910 | 463.21 |
| 39 | 13.50 | 13.53 | 912 | 464.64 |
| 40 | 13.87 | 13.88 | 915 | 466.22 |
| 41 | 14.22 | 14.24 | 918 | 467.56 |
| 42 | 14.57 | 14.59 | 920 | 468.70 |
| 43 | 14.93 | 14.96 | 924 | 470.37 |
| 44 | 15.28 | 15.31 | 924 | 470.81 |
| 45 | 15.65 | 15.67 | 927 | 472.25 |
| 46 | 16.03 | 16.04 | 929 | 473.14 |
| 47 | 16.38 | 16.39 | 930 | 473.72 |
| 48 | 16.75 | 16.76 | 931 | 474.40 |
| 49 | 17.10 | 17.11 | 933 | 474.94 |
| 50 | 17.47 | 17.47 | 934 | 475.61 |
| 51 | 17.82 | 17.83 | 935 | 476.06 |
| 52 | 18.18 | 18.18 | 937 | 477.11 |
| 53 | 18.53 | 18.53 | 937 | 477.35 |
| 54 | 18.90 | 18.90 | 939 | 478.09 |
| 55 | 19.25 | 19.25 | 939 | 478.09 |
| 56 | 19.90 | 19.90 | 942 | 479.74 |
| 57 | 20.00 | 20.00 | 940 | 478.94 |

Test name: Specimen 3

Borehole: G16100